CONTROL OF ACID ROCK DRAINAGE FROM MINE TAILINGS THROUGH THE ADDITION OF DISSOLVED ORGANIC CARBON

by

Paul John Sturman

A dissertation submitted in partial fulfillment
of the requirements for the degree

of

Doctor of Philosophy

in

Engineering

MONTANA STATE UNIVERSITY
Bozeman, Montana

November 2004

APPROVAL

of a dissertation submitted by

Paul John Sturman

This thesis has been read by each member of the thesis committee and has been found to be satisfactory regarding content, English usage, format, citations, bibliographic style, and consistency, and is ready for submission to the College of Graduate Studies.

Dr. Alfred B. Cunningham

Approved for the Department of Civil Engineering

Dr. Brett Gunnink

Approved for the College of Graduate Studies

Dr. Bruce McLeod

STATEMENT OF PERMISSION TO USE

TABLE OF CONTENTS

TABLE OF CONTENTS - Continued

Page

TABLE OF CONTENTS - Continued

LIST OF TABLES

LIST OF TABLES – Continued

Table Page

LIST OF FIGURES

LIST OF FIGURES – Continued

Figure Page

LIST OF FIGURES – Continued

Figure Page

LIST OF FIGURES – Continued

Figure Page

ABSTRACT

Acid mine drainage detrimentally affects thousands of surface watercourses throughout the world and costs tens of millions of dollars annually in site remediation expenditures. This process is accelerated by the activity of iron- and sulfur-oxidizing bacteria which grow chemolithotrophically in mine tailings. Low cost, environmentally acceptable, and low maintenance treatment technologies are needed to both treat acid mine drainage and prevent its occurrence. The addition of dissolved organic carbon to mine tailings has the potential to stimulate beneficial heterotrophic populations of bacteria at the expense of iron and sulfur oxidizers. These experiments investigated the use of three organic carbon sources: molasses, cheese whey and methanol in controlling acid mine drainage from two tailings sources. All three organic carbon sources are easily dissolved in water, relatively inexpensive, and easily transported to remote locations. Mine tailings were acquired from the Fox Lake Mine (Manitoba) and the Mammoth Mine (Montana) and were packed into columns. Columns were watered on a weekly basis and dissolved organic carbon was periodically applied. The treatments increased pH up to 3 units over untreated controls, while simultaneously decreasing oxidation-reduction potential over 300 mV. Sulfate reducing bacteria were stimulated in columns treated with organic carbon, as were heterotrophic populations. Some iron- and sulfur-oxidizing organisms were found to be capable of heterotrophic growth, a condition which compromised treatment effectiveness. Individual organic carbon treatments were found to vary in pH/ORP effect from several months to over 2 years. Phylogenetic analysis of column samples suggests both a robust population of bacteria in untreated mine tailings and the growth of SRB resulting from treatment.

CHAPTER 1

INTRODUCTION

General

Acid mine drainage (AMD) from currently operating and abandoned hard-rock mine lands is a major environmental problem that impacts both ground- and surface water throughout the Western United States and is a major contributor to loss of habitat for fisheries. AMD refers to acidic, metals-laden water that results from contact with mining wastes. Mining activity typically involves at least two steps that generate solid waste materials, i) the removal of overburden soil and rock (waste rock) to access the ore-bearing strata, and ii) the separation of high value minerals from closely associated non-commercial minerals. This separation process was historically accomplished by crushing ore-bearing minerals to the texture of fine grain sand and using water floatation to remove non-commercial "tailings" from the heavier commercial metals, a process which often creates literally tons of waste material for each ounce of commercial metal. Tailings were typically deposited in low-lying areas, often stream beds, where accumulations may vary in depth from several meters to over 20 meters. Mined lands therefore contain waste rock piles, mine tailings heaps, and unmined (yet disturbed) mineral deposits, all of which may contain high concentrations of metals in the form of metal sulfides. When oxygen-containing rainwater, streamwater, and/or groundwater comes into contact with these materials, chemical and biocatalyzed oxidation reactions occur which liberate the bound metals into solution and may radically lower the pH of the receiving water.

Many abandoned mine lands are located on public land (State, US Forest Service, or US Bureau of Land Management) or on patented parcels enclosed by public lands. It is therefore in the public interest to foster innovative, cost-effective solutions to AMD. Mine waste remediation has historically sought to either prevent tailings and waste rock oxidation through physical means by inhibiting the movement of oxygen into the wastes or to neutralize the wastes through chemical additions. Soil covers, geomembranes, and water flooding have been used with some success, albeit often at very high cost. Likewise, high alkalinity materials, such as lime, have been added either directly to tailings or to acidic waste streams, also typically a high cost solution.

Beginning in the 1970s, bioreactors were often used to treat the drainage streams from tailings heaps or mine adits, a process which established the potential for microorganisms that can cause the precipitation of dissolved metals, such as sulfate-reducing bacteria (SRB), to affect low-cost solutions to liquid waste streams. More recently, microbial ecologists have identified populations of potentially beneficial bacteria, including SRB, in mine tailings. Past work sought to both establish exogenous populations of these beneficial organisms (bioaugmentation) and to enhance naturally occurring populations through the addition of solid substrates mixed with tailings in bioreactors. The purpose of this research was to investigate the effectiveness of an inexpensive and potentially widely applicable treatment technology to utilize indigenous microorganisms within mine tailings to abate AMD at its source. It has long been recognized that the activity of iron- and sulfur-oxidizing microbial populations (IOB/SOB) within mine tailings accelerate the production of AMD. It may be possible to

control these detrimental microbial populations through the stimulation of competing microorganisms, such as heterotrophic bacteria (GHB), and SRB. This research investigates the potential for the control of AMD from tailings through the stimulation of beneficial microbial populations by adding easily assimilable, dissolved organic carbon to the surface of the tailings.

Research Goal and Objectives

The goal of this research was to assess the effects of easily assimilable organic compounds on the generation of acid mine drainage from tailings. Specific objectives were as follows:

1. Compare the effectiveness of several sources of inexpensive dissolved organic carbon in reducing AMD (i.e., acidity and dissolved metals) from tailings columns.
2. Determine the effects of organic carbon addition on the indigenous microbial consortium within tailings columns.
3. Determine optimum organic carbon sources for use at abandoned mine sites and assess the efficacy of concurrent treatment with organic carbon and neutralization agents (e.g., lime).
4. Develop a conceptual understanding of the interdependencies of individual microbial populations in mine tailings such that further treatments can be more effectively designed.

Research Approach

This research was undertaken using mine tailings from two sites: the Fox Lake Mine (Manitoba, Canada), and the abandoned Mammoth Mine, South Boulder River, Montana. Experiments were conducted using column reactors open to the atmosphere. Tailings bioreactors were operated in an unsaturated flow condition, with regular (weekly) water additions and periodic additions of dissolved organic carbon substrates. Baseline conditions for acid generation, metals production, microbial colonization, and tailings mineralogy were determined prior to the addition of organic carbon. These parameters were measured regularly following treatment as well. Effluent from the tailings columns was sampled on a weekly basis for pH and oxidation-reduction potential (ORP), and on a monthly basis for microbiology (IOB/SOB, SRB, and GHB), dissolved metals, and other inorganic ions. Solid phase samples were taken from the tailings columns on a periodic basis over the course of the experiments to determine biofilm microbial colonization (IOB/SOB, SRB, and GHB) and tailings mineralogy. Details of column set-up, sampling, and analysis are described in Chapter 3, MATERIALS AND METHODS.

Data collected from the reactors were utilized to determine rates of metals dissolution and acid production both in the presence and absence of organic carbon addition. Microbial activity, as determined via water and tailings sampling, was correlated with subsurface oxygen (O_2) and carbon dioxide (CO_2) measurements. Likewise, subsurface O_2 and CO_2 observations were correlated with oxygen flux calculations and dissolved metals measurements to assess the rate of pyrite (FeS_2)

oxidation under various conditions. Measurement techniques and methods of analysis are further described in Chapter 3, MATERIALS AND METHODS.

Results of the column sampling and data correlation exercises are reported in Chapter 4, RESULTS. Experimental results are reported separately for Fox Lake tailings column experiments and Mammoth tailings column experiments. Results for each set of column experiments are further subdivided by the type of substrate added and timing of substrate addition.

Experimental results are interpreted, compared to relevant literature accounts of similar work, and further analyzed in Chapter 5, DISCUSSION. Also discussed in Chapter 5 are the implications of this work for field application of this and similar treatment technologies. A summary of the results, conclusions and implications is presented in Chapter 6, CONCLUSIONS AND IMPLICATIONS.

CHAPTER 2

LITERATURE REVIEW

Background

There are over 500,000 abandoned mines in the United States, approximately half of which are owned by an agency of the federal government (Fortin et al., 1995). Most of these sites, some dating as far back as the mid 19th century, have mine tailings and/or waste rock impoundments associated with them. Drainage from these sites can result in the most acidic conditions known on Earth (Nordstrom et al., 2000) and adversely impacts tens of thousands of miles of surface watercourses, with remediation costs estimated to be in excess of US$50 billion (US Water Reports, 1993). In the US alone, an estimated $1 million per day is spent on AMD treatment (Evangelou, 1995). The US is not unique in this regard; virtually every nation in which hard-rock or coal mining takes place is faced with similar challenges. In many developing nations, the expense of remedial efforts often precludes their use, and regulations requiring mine reclamation are often lacking.

Mineral Dissolution Processes in Acid Mine Drainage

Many commercially important minerals exist either as metal sulfides or in combination with metal sulfides (Johnson, 1998). AMD arises from waste rock and mine tailings containing sulfide minerals that lack adequate acid-consuming carbonate minerals to neutralize runoff water. Sulfide minerals such as pyrite (FeS_2) are oxidized to

form ferrous iron (Fe^{2+}) and sulfate when oxygenated water infiltrates tailings. This process is described by the following reaction (Sand et al., 2001):

$$4FeS_2 + 14O_2 + 4H_2O \rightarrow 4Fe^{2+} + 8SO_4^{2-} + 8H^+ \quad (1)$$

This reaction generates ferrous iron and some acidity. As conditions become more acidic, growth conditions for acidophillic iron- and sulfur-oxidizing microorganisms become more favorable. Populations of these naturally occurring and environmentally ubiquitous chemolithotrophs colonize open tailings after placement and accelerate acid production through the cycling of ferrous to ferric iron (Brierley and Brierley, 1996):

$$4Fe^{2+} + O_2 + 4H^+ \rightarrow 4Fe^{3+} + 2H_2O \quad (2)$$

The role of these bacteria (such as *Acidithiobacillus ferrooxidans*) in accelerating the production of acidic drainage from sulfide-containing mine tailings has been known for decades (Silverman and Lundgren, 1959). The ferric iron produced in reaction (2) is a strong oxidant, which further abiotically oxidizes pyrite (or other mineral sulfides) as follows:

$$FeS_2 + 14Fe^{3+} + 8H_2O \rightarrow 15Fe^{2+} + 2SO_4^{2-} + 16H^+ \quad (3)$$

Though reaction (2) consumes some acidity, the overall effect is the regeneration of ferric iron, which can then oxidize more pyrite and generate much more acidity (via reaction 3). It has been estimated that an active population of *At. ferrooxidans* increases the rate of pyrite oxidation up to 6 orders of magnitude over simple abiotic oxidation (Brierley, 1978; Singer and Stumm, 1970). The acidity generated in these reactions further assists the growth and downward migration of acidophilic iron- and sulfur-

oxidizers through the tailings column by providing the low pH conditions (<3.5) necessary for their growth. Many acidophiles (including *At. ferrooxidans*) are also capable of oxidizing reduced sulfur species to sulfate, a process which also accelerates AMD through the removal of sulfur compounds from the reaction site (Hansford and Vargas, 2001; Fowler and Crundwell, 1999):

$$H_2S + 2O_2 \rightarrow SO_4^{2-} + 2H^+ \quad (4)$$

$$S_o + H_2O + 1.5\ O_2 \rightarrow SO_4^{2-} + 2H^+ \quad (5)$$

$$S_2O_3^{2-} + H_2O + 2O_2 \rightarrow 2SO_4^{2-} + 2H^+ \quad (6)$$

As mineral dissolution and acidophilic bacterial growth proceeds, acidic conditions extend with depth into the tailings profile. The rate of this process is influenced by temperature, infiltration rate, mineralogy, organic carbon condition, site microbial colonization, and the presence of neutralizing minerals. It is, therefore, highly site dependent. The processes controlling AMD (biotic and abiotic) as well as efforts to mitigate AMD through engineered solutions will be discussed in detail in the remainder of this review.

Mineral Dissolution via Ferric Iron and Protons

Sulfide mineral dissolution in a mine tailings environment has been noted to proceed via either proton attack (acid dissolution) or oxidation (Schippers and Sand, 1999). While many sulfide minerals of commercial or environmental importance, notably sphalerite (ZnS), chalcopyrite ($CuFeS_2$), galena (PbS), hauerite (MnS_2), orpiment (As_2S_3), and realgar (As_4S_4) are susceptible to acid dissolution, the most common mineral found in mine tailings, pyrite (FeS_2), is not. Though not unique to pyrite, this

characteristic is found only in disulfide minerals and results from the configuration of bonding orbitals in the crystal lattice. In pyrite (as well as MoS_2 and WS_2) the valence bands (outer electrons) belong only to the metal (Fe, Mo, etc.) and are not shared with the sulfur moiety. Attraction between solution-phase protons and these outer shell electrons does not result in a loss of integrity of the crystal lattice, as is the case where valence bands are part of the metal-sulfur bond (Crundwell, 1988). In the case of pyrite and molybdenite, oxidizing attack is necessary for dissolution, this typically results from either O_2 or Fe^{3+} (Schippers, 1999; Guevremont et al., 1998). This distinction is important because it determines whether mineral dissolution will proceed with thiosulfate ($S_2O_3^{2-}$) or a polysulfide (H_2S_n) as the intermediate sulfur compound (Schippers and Sand, 1999). In the presence of ferric iron, pyrite dissolution proceeds via the reaction shown in Equation 3, which is a composite of two reactions with thiosulfate as the intermediate:

$$FeS_2 + 6\,Fe^{3+} + 3\,H_2O \rightarrow S_2O_3^{2-} + 7\,Fe^{2+} + 6\,H^+ \qquad (7)$$

$$S_2O_3^{2-} + 8\,Fe^{3+} + 5\,H_2O \rightarrow 2SO_4^{2-} + 8\,Fe^{2+} + 10\,H^+ \qquad (8)$$

In the case of the polysulfide mechanism, metal sulfide dissolution proceeds via a combination of proton and ferric iron attack, as shown by the following reactions (valid for ZnS, $CuFeS_2$, and PbS):

$$MS + Fe^{3+} + H^+ \rightarrow M^{2+} + 0.5\,H_2S_n + Fe^{2+} \quad (n\geq 2) \qquad (9)$$

$$0.5\,H_2S_n + Fe^{3+} \rightarrow 0.125\,S_8 + Fe^{2+} + H^+ \qquad (10)$$

$$0.125\,S_8 + 1.5\,O_2 + H_2O \rightarrow SO_4^{2-} + 2\,H^+ \qquad (11)$$

The importance of distinguishing between these mechanisms is that the polysulfide pathway results in significantly less acid production than the thiosulfate pathway (Schippers and Sand, 1999).

Although not susceptible to proton attack, pyrite dissolution via oxidizing attack is effected by pH. Bossinssel-Gissinger et al. (1998) noted that pyrite oxidation under basic conditions proceeds much more rapidly than at low pH, probably as a direct result of abiotic Fe^{2+} oxidation to Fe^{3+} at high pH.

Direct vs. Indirect Bacterial Leaching

The close association of acidophilic iron- and sulfur-oxidizing bacteria and AMD has been noted for over 50 years (Leathen et al., 1953) and the importance of the most intensively studied species, *Acidithiobacillus* (*At.*) *ferrooxidans* (formerly *Thiobacillus ferrooxidans*) was noted very early in this research (Silverman and Lundgren, 1959). Speculation regarding the basic processes at work in the mineral leaching environment lead to the development of two primary conceptual models: direct and indirect mineral leaching by bacteria (Fowler and Crundwell, 1998). Proponents of the direct leaching model have suggested that bacteria are able to directly interact with the mineral surface to increase the rate of leaching over that achievable by ferric ions alone (Free et al., 1991; Lizama et al., 1991; Silverman and Ehrlich, 1964). Alternatively, proponents of the indirect mechanism have claimed that mineral leaching in the presence of microorganisms is accelerated only because iron-oxidizing bacteria regenerate ferric iron from ferrous, and because sulfur-oxidizers clear reduced sulfur compounds from the reaction site (Boon et al., 1998; Sand et al., 1995; Fowler and Crundwell, 1998). In

addition, iron oxidizing bacteria increase the pH in close proximity to the pyrite surface, a condition which accelerates leaching rates (Fowler et al., 1999; Holmes and Crundwell, 1999) Recent work (Fowler et. al., 2001; Sand et al., 2001) supports the indirect leaching mechanism and furthermore suggests that prior work which supported the direct mechanism was incorrect due to many experimenter's failure to carefully control the Fe^{2+}/Fe^{3+} ratio, a condition which could lead to higher measured leaching in bacterial cultures.

Importance of Extracellular Polymer in Bacterial Leaching

Although there is now general agreement that bacteria play an indirect role in the leaching process, ongoing work confirms the importance of close association between bacteria and mineral surfaces for rapid bioleaching. Gehrke et al., (1998) found that the attachment of *At. ferrooxidans* to pyrite was mediated by extracellular polymeric substances (EPS), and that EPS is necessary both for bacterial attachment and rapid mineral leaching. Gehrke et al., (1998) and Edwards et al., (2000a) also noted that *At. ferrooxidans* and *Thiobacillus caldus*, respectively, attached preferentially to surface imperfections in the pyrite grains, such as cracks and grain boundaries and Fletcher (1996) observed that the expression of genes which control EPS composition is influenced by substratum composition. For rapid pyrite oxidation, ferric iron is complexed into the exopolymer of iron-oxidizers, providing the necessary close proximity to the mineral surface (Geesey and Lang, 1989).

Microbial Ecology of Mine Tailings

It has long been recognized that acidic environments, both natural and anthropogenic, may present a robust growth medium for acidophilic microorganisms. Among the earliest acidophiles isolated and characterized were chemolithotrophs of the genus *Thiobacillus* (Waksman and Joffe, 1921). Since then, our understanding of the microbial ecology of mineral leaching environments, mainly heap leach pads and mine tailings, has steadily increased. Although concern about the environmental impacts of AMD is a relatively new phenomena (starting circa 1970), attempts to maximize microbial leaching of mineral bodies for economic recovery of metals has a more robust publication record in the literature (Johnson, 1991). Indeed, until relatively recently, the majority of research regarding acidophilic microorganisms has been in the development of new technologies for minerals extraction and recovery (Johnson, 2001a). Fortunately, this body of research has been helpful in fostering an understanding of the microbial ecology of mine tailings and has facilitated progress in the abatement of AMD (Brierley and Brierley, 1997).

Biodiversity of Acidophilic Microorganisms

Mine tailings are inhabited by a broad range of chemolithotrophic and heterotrophic prokaryotes, as well as by acidophilic eukaryotes such as fungi, yeasts, algae, and protozoa. In the past, most acidophiles were considered to be obligately aerobic. Increasing evidence suggests that many acidophilic prokaryotes, including some of the most commonly studied and cultured iron- and sulfur-oxidizers (such as *At.*

ferrooxidans), are facultative aerobes capable of coupling the oxidation of organic or inorganic electron donors to the reduction of ferric iron (Johnson, 1998). In addition to metabolic diversity, tailings microbiota also exhibit incredible acid tolerance and temperature tolerance ranging from psychrophilic to thermophilic. Edwards et al., (2000b) isolated an iron-oxidizing archaea growing at pH 0 in AMD from the Iron Mountain mine (California). Heterotrophic acidophiles have been noted in mine tailings for decades. These organisms were thought to grow principally on organic carbon resulting from primary producers (chemolithotrophs and autotrophs). Recent work (Johnson, 2001b) indicates that many of these organisms are also capable of CO_2 fixation, ferrous iron oxidation, and ferric iron reduction. Although conditions within tailings piles would seem too hostile for their survival, viable populations of SRB have also been isolated from acid producing tailings (Fortin and Beveridge, 1997). Each of these phylogenetic groups will be discussed in detail in the following sections.

Iron-Oxidizing Bacteria

Iron-oxidizing bacteria (IOB) are a metabolically diverse group that includes autotrophs, mixotrophs, and heterotrophs (Johnson, 1998). Most IOB have traditionally been considered chemolithotrophic, gaining energy from the transfer of electrons from ferrous iron to oxygen under aerobic conditions while carbon for cell growth is fixed from CO_2. Because mine tailings are typically oligotrophic environments, with ferrous iron and oxygen readily available, chemolithotrophy has distinct competitive advantages over heterotrophy under carbon-limited conditions. However, where organic carbon is available, some IOB have been observed to assimilate it for cell mass, while still

oxidizing ferrous iron for energy (mixotrophy) (Pronk et al., 1991a). These organisms do not require organic carbon for growth, but will utilize it if available. Members of this group include mesophiles such as *At. ferrooxidans* and moderate thermophiles such as the Gram-positive *Sulfobacillus acidophilus* and *S. thermosulfidooxidans* as well as members of *Acidimicrobium* (Johnson, 1998; Johnson, 2001b). Some acidophilic iron oxidizers are obligate heterotrophs, being unable to fix CO_2. *Ferrimicrobium acidiphilum*, a Gram-positive IOB and *Sphaerotilus sp.* are representative of this group (Johnson et al., 1992; Johnson, 2001b). Some obligately heterotrophic iron-oxidizers are relatively sensitive to high concentrations of organic carbon, and may be inhibited under carbon-rich conditions (Bacelar-Nicolau and Johnson, 1999)

Many IOB, such as *At. ferrooxidans*, are also capable of oxidizing reduced sulfur compounds, including elemental sulfur, thiosulfate, and tetrathionate (Harrison, 1984). In addition to the obvious advantages this lends such bacteria in a pyrite leaching environment, it also provides a potential mechanism for energy transduction under anaerobic conditions. Sugio et al., (1985) first noted that *T. ferrooxidans* was capable of ferric iron reduction coupled with sulfur oxidation through the enzyme ferric ion reductase. Subsequently, Sugio et. at., (1992) determined this enzyme was widely distributed among iron oxidizing bacteria. Pronk et al., (1991b) demonstrated that *T. ferrooxidans* could grow anaerobically using ferric iron as electron acceptor and elemental sulfur as the electron donor. Furthermore, this process was postulated to occur as a result of the same oxidoreductase enzyme that is involved in ferrous iron oxidation

under aerobic conditions, further suggesting that this capability may be widespread among iron-oxidizers.

Acidic conditions may not be necessary for the activity of IOB from a physiological standpoint, but because ferrous iron readily oxidizes in solution abiotically above pH 5, acidic conditions are necessary from a practical standpoint (Walsh and Mitchell, 1972). Not surprisingly, bacterial succession in tailings proceeds from initial colonization and growth on freshly placed, slightly acidic tailings to mature, typically highly acidophilic microbial communities in older placements. This progression may start in the meso-acidic range with filamentous IOB, such as *Metallogenium* (Walsh and Mitchell, 1972) and progress to the more acid-tolerant Gram-negative IOB, such as the *Thiobacilli and Acidithiobacilli* (Johnson, 2001a), and progress to the archaea under highly acidic conditions. The rate of this progression is dependent on the mineral character and texture of the tailings, temperature, water infiltration, and site biota. In studying an AMD stream from the Iron Mountain Mine (CA), Edwards et al., (1999) found high temporal and spatial variation in iron-oxidizing microbial populations, with cycling among bacteria and archaea for predominance, depending on influent rainfall, temperature and distance from source.

Because of its ubiquity in mine tailings and in AMD streams and its high culturability, *At. ferrooxidans* is the best studied of the IOB. Prior to the common use of molecular techniques to identify individual species in the AMD mix, *At. ferrooxidans* was also thought to be responsible for the majority of acid production from exposed minerals (Harrison, 1984). Recent work (Schrenk et al., 1998; Bond et al., 2000a)

suggests that IOB of the genus *Leptospirillum* are both more abundant at low pH, and more efficient at iron oxidation than *At. ferrooxidans*. Whereas *At. ferrooxidans* was active downstream in the AMD, *Leptospirillum* was responsible for the initial pyrite oxidation. Furthermore, *L. ferrooxidans* has been observed to oxidize ferrous iron under both aerobic and anaerobic conditions, using other metals as electron acceptors (Gonzalez-Toril et al., 2003). Taken together with the recent discovery of novel acidophilic bacteria and archaea from environmental samples, these findings further indicate the importance of understanding the microbial ecology of the mine waste environment in formulating engineered solutions.

Sulfur-Oxidizing Bacteria

As indicated in the above discussion, many sulfur-oxidizing bacteria (SOB) are also capable of iron oxidation. In fact, overlap between these groups is extensive enough that they are often enumerated concurrently (Eaton et al., 1995). SOB have been postulated to be among the most primitive life forms on Earth (Kelly, 1987), and are extremely diverse phylogenetically, with members in the alpha, beta, and gamma subdivisions of proteobacteria as well as Gram-positive bacteria (Lane et al., 1992). Apart from the iron-oxidation function many sulfur oxidizers also perform, the most important reaction they catalyze is the transformation of thiosulfate ($S_2O_3^{2-}$), elemental sulfur (S^0) or polysulfide (H_2S_n) from the immediate vicinity of active pyrite (or other metal sulfide) dissolution (Johnson, 1998; Fowler and Crundwell, 1999). SOB have been observed to grow synergistically with heterotrophic IOB. Bacelar-Nicolau and Johnson (1999) found that various species of heterotrophic IOB isolated from mine waste, some of

which were capable of pyrite oxidation in pure culture, oxidized pyrite much more rapidly when grown in mixed cultures with *Thiobacillus thiooxidans*, a SOB that cannot oxidize iron. These finding suggest that, while perhaps not necessary for mineral oxidation, isolates specializing in sulfur oxidation nonetheless may greatly accelerate the process.

Capabilities for iron- and sulfur-oxidation, iron-reduction and heterotrophy exist (and co-exist) in many acidophilic organisms. These capabilities, as well as Gram-stain designation, are listed in Table 1 for some commonly studied acidophiles found in mineral leaching environments. As indicated by the recent citations for many of the isolates listed in Table 1, particularly the Gram-positive bacteria, the identification and classification of new species from mineral leaching environments is a robust area of current research. Among the most interesting physiologically is the obligately heterotrophic *Ferrimicrobium acidophilum*. This Gram-positive isolate is capable of both iron oxidation and reduction, depending on site conditions, while requiring an organic carbon source (Johnson, 1998). An important point to note from Table 1 is the occurrence of facultative anaerobes among the acidophilic bacteria. These species are typically able to oxidize or reduce iron, in the latter case using reduced sulfur compounds as the electron donor.

Species	Fe^{2+} Ox	S Ox	Fe^{3+} Red	Growth Pattern[a]	Source
Gram negative					
Acidithiobacillus ferrooxidans	+	+	+	f-Ar, M	Pronk and Johnson, 1992 Barros et al., 1984 Brock and Gustafson, 1976
A. thiooxidans	-	+	+	f-Ar	Johnson, 1998
Acidiphilium acidophilum		+	+	M, f-Ar	Johnson, 1998 Pronk and Johnson, 1992
Leptospirillum ferrooxidans	+	-	-	A f-Ar	Johnson, 1998 Gonzalez-Toril et al., 2003
Gram positive					
Sulfobacillus thermosulfidooxidans	+	+	+	A,M,H f-Ar	Johnson, 1998
S. acidophilus	+	+	+	A,M,H, f-Ar	Johnson, 1998
S. montserratensis	+	+	+	A,M,H	Johnson, 2001b
S. ambivalens	+	+	+	A,M,H	Johnson, 2001b
S. yellowstonensis	+	+	+	A,M,H	Johnson, 2001b
S. disulfidooxidans	-	+	-	M	Johnson, 1998
Ferromicrobium acidophilum	+	-	+	ob-H	Johnson, 2001b
Acidimicrobium ferrooxidans	+	-	+	A,M,H f-Ar	Johnson, 1998
Caldibacillus ferrovorus	+	+	+	A,M,H,	Johnson, 2001b

Table 1. Metabolic processes of selected acidophilic bacteria. [a] A = autotrophic growth, M = mixotrophic growth, H = heterotrophic growth, Ar = aerobic growth, f = facultative growth, ob = obligate.

Heterotrophic Bacteria

As indicated in Table 1, many recently identified acidophilic organisms, particularly the Gram positive isolates of the genus *Sulfobacillus* can grow autotrophically, heterotrophically, and mixotrophically. In fact, the majority of heterotrophs isolated from tailings are also capable of iron- and/or sulfur oxidation (Harrison, 1984) Although mine tailings are normally oligotrophic environments, adequate organic carbon is typically present to sustain populations of obligately

heterotrophic bacteria, sulfate reducers being an obvious example (this group is considered separately in the following section). In most exposed tailings, the source of this organic carbon is the cell detritus from dead chemolithotrophic bacteria. Because organic carbon is often inhibitory to iron- and sulfur-oxidizing bacteria, heterotrophs can enhance mineral oxidation through their consumption of organic carbon (Pronk and Johnson, 1992; Frattini et al., 2000). Heterotrophic bacteria, apart from those also capable of iron or sulfur oxidation, may account for only a small fraction of the biomass active in tailings (Johnson and Roberto, 1997), but are difficult to enumerate separately from these other populations (Leduc et al., 2002). Schippers et al. (1995) found that chemoorganotrophic organisms outnumbered chemolithotrophs in both uncovered and covered tailings piles; however heterotrophs were not further characterized in terms of their ability to oxidize iron and/or sulfur. Significant concentrations of anaerobic heterotrophic bacteria (non-SRB) have been enumerated from tailings deposits (Wielenga et al., 1999), although, again it is difficult to determine whether these populations may also be capable of iron/sulfur oxidation activity in aerobic conditions.

Sulfate Reducing Bacteria

SRB have been widely used for the treatment of AMD in engineered bioreactors, where influent organic carbon, pH, and oxidation-reduction (redox) potential can ostensibly be controlled to the benefit of SRB populations. The oxidized and acidic conditions present in most sulfidic mineral tailings would seem prohibitive to SRB, which are generally obligate anaerobes and are typically considered acid intolerant (Postgate, 1984). Nonetheless, SRB have been isolated from tailings piles (Fortin et al.,

1995; Fortin et al., 1996; Fortin and Beveridge, 1997). In addition, SRB have been recovered from sediments deposited from mine waste effluent streams (Wielinga et al., 1999; Gyure et al., 1990; Herlihy and Mills, 1985) and their presence has been inferred from genetic sequencing of some of the most acidic drainage streams on Earth (Bond et al., 2000b). Detailed study of pore-water chemistry and mineralogy in mine tailings at an abandoned Cu Zn mine in Ontario, Canada (Fortin et al., 1996) indicated that bulk water Eh and pH should not have been conducive to SRB growth (minimum Eh > 100, maximum pH < 4). Yet intact cores removed from the tailings indicated a color transition from bright orange to gray as depth increased, suggesting a significant change in chemical conditions. Further analysis indicated almost the complete removal of the mobile iron phase as well as a significant drop in sulfate, suggesting SRB may be active. Culturing SRBs was attempted on Postgate's Medium B at pH 3.5, 5.5, and 7.5. Interestingly, SRB growth was observed only at pH 7.5. SRB were evidently active in the tailings based on bulk water chemistry measurements, but they could only be enumerated under conditions which were not apparent in the field. This finding suggests that SRB were not adapted to the low pH conditions in the field, but perhaps were capable of altering their microsite water chemistry to allow them to survive under these harsh conditions. Kolmert and Johnson (2001) have isolated SRB capable of growth in AMD at pH 3 using ethanol and glycerol as carbon sources.

The conditions necessary for SRB growth are generally considered to be a reducing environment, available sulfate, and a volatile fatty acid (VFA) carbon source such as formate, butyrate, lactate, etc. The conditions created by the growth of *T.*

ferrooxidans and other acidophillic organisms in the surface layers of a tailings pile would seem to provide only the sulfate necessary for SRB growth. Influent water to tailings piles is typically either rainwater or oligotrophic surface water, neither of which contains appreciable concentrations of VFAs. Very low concentrations of formate and acetate were found by Fortin et al. (1996) in the pore water of the tailings pile. These organic acids were either metabolic excretions or decay products of iron-oxidizing bacteria living upgradient in the tailings. Thus, iron-oxidizing bacteria provided both the necessary electron donor and carbon source for downstream SRB. This still leaves SRB with the issues of very low pH and oxidized conditions to overcome, however, high concentrations of mobile iron in pore water entering the SRB zone may help explain their ability to overcome these adversities. Whether bacteria are Gram-positive or Gram-negative, they typically contain a negative surface charge due to the presence of anionic surface structures such as carboxyl, phosphoryl, and amino groups (Beveridge, 1981). Mineral deposition initially occurs on the bacterial cell surface to satisfy this charge imbalance based on the stoichiometric interaction of cations (such as metal species) in solution. The binding of metals to the cell surface lowers the total free energy of the system, which subsequently initiates further metal deposition (Douglas and Beveridge, 1998). Though the specific mineral phases formed are in response to the anions present on the cell surface, mineral formation is not controlled by the cell, but rather by the chemistry of the cell's environment (Beveridge et al., 1983). It has been noted, however, that bacteria in a highly active metabolic state can inhibit the formation of metallic

complexes because their cell wall is highly energized and is proton rich (Urrutia Mera et al., 1992).

In the case of SRB growing in an acidic, iron-rich environment such as mine tailings, cell surface reactions which precipitate metals are enhanced by the production of hydrogen sulfide, which readily reacts with iron in solution to form insoluble iron sulfides on both SRB cell surfaces and on the surrounding mineral surfaces (Fortin and Beveridge, 1997). Likewise, other metallic species (Cu, Zn, Pb, Cd) can precipitate as sulfides in close proximity to active SRB, and can result in detoxification of the medium and significant secondary mineral formation (Beveridge et al., 1997). These precipitates may have a beneficial effect for the SRB growing in an environment that could potentially become oxic in that the precipitated metal sulfides readily react with oxygen in solution and thereby act to keep the cell's immediate environment at a low redox potential. Even in oxic zones within mine tailings, SRB have been found to be active, presumably in microsites created by precipitated solids. In these zones, amorphous iron-oxide precipitates provide the necessary diffusion barrier to dissolved oxygen to allow SRB to remain active (Fortin and Beveridge, 1997).

The generation of alkalinity by SRB is also well documented, which helps explain their survival in low pH environments, particularly where a cell-precipitated diffusion barrier exists. This alkalinity may also cause the precipitation of carbonates within the tailings matrix (Douglas and Beveridge, 1998) which further protects SRB from toxic levels of acidity.

Fortin and Beveridge (1997) noted that precipitated iron sulfides in the SRB-active anoxic zone of mine tailings mimicked the size and shape of bacterial cells when viewed by transmission electron microscopy (TEM) and chemically analyzed by EDS. They suggest that these precipitates are the remains of individual SRB which had been completely encased in iron-monosulfides. Such encasements could act as a protective coat, allowing a single bacterium to alter its microenvironment to exist under hostile low pH, or high Eh conditions.

Fungi

Fungi, including both yeasts (unicellular) and molds (multicellular filamentous), may be active in mineral leaching environments. The genera *Aspergillus* and *Penicillium* have been noted for their tolerance to high metals concentrations, particularly copper (Wenberg et al., 1971). In studying the ability of members of these genera to leach a variety of metals (Cu, Sn, Al, Ni, Pb and Zn) into solution, Brandl et al. (2001) determined that their leaching efficiency was of the same order as cultures of *At. ferrooxidans*. In a sucrose amended media containing solid phase metals, these fungi catalyzed a decrease in pH from 6.5 to <4 in two weeks of exposure. Yeasts such as *Saccharomyces cerevisiae* have been used to leach lead and copper (Hahn, et al., 1993), and it has been observed that in some AMD streams, yeasts and molds are the dominant heterotrophic life form (Leduc et al., 2002).

Mineral Precipitation in Mine Tailings

Secondary mineral precipitation is readily apparent in AMD streams downgradient from tailings impoundments, such as in the deposition of the mineral ferric hydroxide ($Fe(OH)_3$), commonly referred to as "yellow-boy". This occurs as a result of redox and pH changes as AMD is exposed to the environment. Such environmental changes can also occur within the tailings piles, also leading to secondary mineral formation. As discussed in the preceding sections, mine tailings are geochemically dynamic environments. Frequently, conditions leading to the mineral dissolution processes discussed above are altered with depth in the tailings pile. Changes in pH, redox potential, available neutralizing minerals, organic carbon, and site microbiology often lead to secondary mineral precipitation within the tailings pile. This process can occur abiotically as a result of insoluble complexes being formed from neutralization reactions, or, more commonly, it can occur as a direct consequence of the activity of microbial populations. Secondary minerals can form as a result of oxidation or reduction reactions. Each situation is presented separately below.

Oxidized Mineral Precipitation

Microbially catalyzed mineral precipitation (biomineralization) can occur either as a result of active metabolism or passively as a result of the inherent metal binding capacity of cell wall constituents (Fortin et al., 1995). In open environments, these processes may not be easily distinguished (Ferris, 1993). In the oxidized zone, these precipitates are typically iron-oxides or iron-oxyhydroxides that precipitate as a result of

supersaturated conditions with respect to ferric iron, a direct result of the activity of iron-oxidizing bacteria. *At. ferrooxidans* and other IOB generate a pH gradient between the cell surface/mineral interface and the surrounding fluid such that metals are maintained in solution at the bacteria-mineral interface (low pH) and precipitated on cell surfaces exposed to the bulk fluid (Southam and Beveridge, 1992). The resulting precipitates depend on the tailings composition and have been noted to include schwertmannite ($Fe_8O_8(OH)_6(SO_4)_2$), jarosite ($KFe_3(SO_4)_2(OH)_6$), goethite (FeOOH), ferrihydrite ($Fe(OH)_3$), gypsum ($CaSO_4 \bullet 2H_2O$) and oxidized phases containing lead, zinc, copper, and nickel (Southam and Beveridge, 1992; Blowes et al., 1991; Ferris et al., 1991; Bigham et al., 1996). The precipitation of hydroxide, oxyhydroxide and sulfate minerals can result in the formation of a "hardpan" layer at the depth of active tailings oxidation. In this layer, tailings grains are cemented together, severely reducing air and water permeability. Blowes et al. (1991) noted the formation of a ferric iron mineral hardpan layer only 1-5 cm thick, occurring at a depth of 10-100 cm that resulted in the complete exclusion of oxygen from pores in the unsaturated zone below the hardpan. Hardpan layers such as this do not develop in all cases, but may result from a combination of biotic and abiotic factors, such as a decrease in the activity of IOB due to oxygen becoming unavailable, and a pH buffering effect at depth within the tailings (Blowes et al., 1991). Bigham et al. (1996) noted that system pH influenced the oxidized iron phase that precipitated in bioreactors with active *At. ferrooxidans* populations. At low pH (<2.5) jarosite was the predominant precipitate, while schwertmannite predominated at pH 3 and goethite predominated at pH 3.5.

Reduced Mineral Precipitation

Oxygen consuming reactions in the near-surface zone of mine tailings may result in reducing conditions at depth. Where and if this occurs is a function of the degree of saturation of the tailings, the oxygen demand exerted by biotic and abiotic reactions occurring in the tailings, and physical characteristics of the tailings such as porosity and permeability (Reardon and Moddle, 1985). Like the oxidized mineral precipitation discussed above, reduced minerals can precipitate as a result of either biotic or abiotic processes. Hardpan layers such as that described in the preceding section can also form in reducing zones of the tailings as a result of the combination of anoxic conditions and pH buffering from the tailings solid phase (Blowes et al., 1991). The mineralogy in this case is typified by ferrous iron precipitates such as melanterite ($FeSO_4 \bullet 7H_2O$), with similar reductions to air and water permeability.

More commonly, metals precipitate in the anoxic zone as sulfides, which result directly from the activity of SRB (Fortin and Beveridge, 1997). Because of the preponderance of iron in solution, metal sulfide precipitates are typically dominated by iron monosulfides, which often contain significant concentrations of copper, lead, cadmium and zinc (Fortin and Beveridge, 1997; Morse and Arakaki, 1993). These monosulfides are metastable as solid phases, and are reported to be precursors to pyrite (FeS_2) formation (Schoonen and Barnes, 1991).

Methods of Preventing Acid Mine Drainage

Land managers and miners have been aware of the toxicity problems associated with mine tailings and AMD for well over 100 years (Shea, 2000). Efforts to control and mitigate this toxicity include physical, chemical, and microbiological control measures. An overview of various techniques and the theory behind them is presented in the following sections.

Physical Means of Preventing AMD

AMD abatement through physical means has centered on two basic processes, submergence of the tailings underwater or the use of solid cover materials (soil, geotextiles, etc.). Both processes attempt to control the rate of tailings oxidation by limiting the availability of oxygen. Water submergence is one of the oldest methods of tailings treatment/disposal, and can be very effective in controlling AMD. Historic use of this treatment method typically involved tailings disposal in natural lakes or marine environments (Robertson et al., 1997). Tailings disposal under natural waters is now precluded in most countries by environmental regulations, although disposal in engineered water cover systems is commonly practiced (Dave et al., 1997; Vigneault et al., 2001). Ironically, long-term studies of historic disposal sites have shown that they are typically more effective in preventing AMD and metals release than engineered water cover systems, mainly because they have a deeper water cover, more biological productivity, and are less exposed to wind-related oxygenation (Li et al., 2000; Elberling and Damgaard, 2001). Complete submergence of the tailing may not be necessary for

substantial reduction in oxidation rates, however. In investigating bacterial and chemical oxidation rates of tailings on Baffin Island, Elberling et al, (2000) found that oxygen penetrated to 30 cm under well drained conditions but only to 2 cm under pore saturation conditions (no standing water).

Although maintenance costs for subaqueous tailings disposal are very low, initial construction costs are sometime prohibitive. In addition, mines are frequently located in areas where site topography prevents the construction of a tailings dam and pond. Furthermore, abandoned tailings are usually not amenable to submergence because of the high costs of relocating the wastes.

Oxygen movement into tailings can also be inhibited through the use of a soil cover layer. The critical parameters for soil covers are those that influence oxygen flux, such as depth, water saturation, permeability, and organic matter content (Gatzweiler et al., 2000). Oxygen flux occurs either by way of infiltrating water (dissolved phase), or through unsaturated pore spaces. In the latter case, diffusion, barometric pumping, and thermal convection are the causative mechanisms. For partially saturated soils, oxygen flux due to diffusion is the most important transport mechanism. The effective diffusivity can vary over 4 orders of magnitude from full water saturation to dry conditions (Nicholson et al., 1989). Maintaining moisture is therefore very important in soil covers. Moisture retention may be confounded by heat generated by exothermic oxidation reactions within the tailings, which leads to thermal gradients and convective flow (Lefebvre et al, 2001), or by evapotranspiration by vegetation. Innovative methods of retaining moisture in tailings covers take advantage of the capillary barrier effects of

placing a low permeability cover in contact with high permeability materials, such as a clay layer covering a coarse sand layer (Bussiere et al., 2000).

Geomembranes have gained acceptance in recent years as a method to prevent water infiltration into sensitive materials. These membranes are typically constructed from high density polyethylene, and are covered by a protective soil layer (Lewis et al., 2000). Advantages of a geomembrane are complete water impermeability, assuming leaks can be prevented, and the ability to install the system under any topographic conditions. A distinct disadvantage, one that is shared with soil covers in general, is high expense.

Chemical Means of Preventing AMD

Chemical methods of preventing and/or treating AMD can be divided into 1) neutralization methods, 2) bacterial inhibitors, and 3) surface coatings to retard mineral dissolution. Early chemical methods employed to treat tailings and AMD relied mainly on the addition of alkaline compounds to raise the pH to levels where precipitation of metal hydroxides occurs. Alkaline compounds, such as CaO (quicklime), $Ca(OH)_2$ (hydrated lime), limestone ($CaCO_3$), NaOH (caustic soda), and Na_2CO_3 (soda ash) have been used extensively both as conditioners to solid tailings and as treatments for liquid AMD. For liquid treatment, neutralizing solids are typically placed in a bioreactor with a controlled residence time, or they may simply be dumped into the AMD stream, depending on the sophistication of the installation. Although some alkalinity-containing minerals (such as limestone) may be relatively inexpensive, their use results in the generation of significant quantities of metal-hydroxide sludge, which is a hazardous

waste (El-Ammouri et al., 2000). When used as a conditioner for tailings piles, neutralizing materials can prevent the conditions necessary for AMD generation (i.e., acidification), and can provide a more hospitable environment for the growth of non-acidogenic bacteria, such as SRB (Brierley and Brierley, 1997). Where tailings or AMD contain arsenic, neutralization through liming has been noted to result in increased As mobility both as a function of increased pH and higher bacterial activity (Macur et al., 2001).

Scrap iron has also been successfully used as a neutralizing agent for AMD (Shokes and Moller, 1999; Shelp et al., 1995). Under acidic conditions, iron hydrolyzes water, producing hydroxide ion, thus increasing the pH and reducing the ORP of the solution. This process has been most successful in enclosed reactors treating AMD, rather than in tailings. If oxygen can be excluded, scrap iron can facilitate anoxic conditions and enhance SRB growth (Shokes and Moller, 1999).

Although the role of iron- and sulfur-oxidizing bacteria in accelerated mineral dissolution has long been recognized, the use of biocides to control these processes has not been widely investigated. The detergent sodium dodecylsulfate (SDS) has been found to selectively inhibit iron- and sulfur-oxidizing bacteria in mine tailings environments (Schippers et al., 1998; Schippers et al., 2001). SDS effectiveness has been found to be highly concentration dependent, ranging from biocidal (at 1 mM) to temporarily inhibitory (at 0.1 mM) to the iron-oxidizing chemolithotroph *At. ferrooxidans*. SDS was found to have little effect on chemo-organotrophic organisms (Schippers et al., 2001) however, these bacteria were enumerated on nutrient agar so

overlap between heterotrophs and iron-oxidizers cannot be ruled out. Recent work has shown that the cyanide leaching by-product thiocyanate exhibits selective toxicity to iron- and sulfur oxidizing bacteria (Suzuki et al., 1999; Olson et al., 2003). Thiocyanate is produced as a detoxification by-product by bacteria present in cyanide heap-leach environments, principally iron- and sulfur-oxidizers. In a bioleaching environment, thiocyanate production results in reduced leaching efficiency. However, when added to mine tailings, it can reduce acid production 90% or more through the same toxicity mechanism (Olsen et al., 2003).

Surface coatings or micro-encapsulation methods have been used to inhibit both biotic and abiotic tailings oxidation. The addition of phosphate in solution has been found to inhibit pyrite oxidation. Phosphate binds to Fe^{3+} and forms a protective coating on the mineral surface, inhibiting further oxidation by chemical agents (Huang and Evangelou, 1994; Lan et al., 1999). Elsetinow et al. (2001) found this process to be pH sensitive; showing effectiveness only at pH 4 and above. Unfortunately, phosphate is also an essential nutrient which could lead to enhanced microbial growth in open tailings applications, and its use has not been extensively studied where iron- and sulfur-oxidzing bacteria are present. More recently, the use of 8-hydroxyquinoline has shown promise in suppression of both chemical and biological leaching of pyrite (Lan et al., 2002). In this case, a coating of iron 8-hydroxyquinoline forms on the surface of the pyrite grains, preventing dissolution by oxygen attack and in the presence of a mixed culture of iron- and sulfur oxidizing bacteria.

Microbiological Means of Preventing AMD

Microbiological processes can be used both to prevent AMD generation in the tailings pile and to treat AMD in surface waters or groundwater. Prevention measures involve the manipulation of microorganisms within the tailings pile prior to the release of AMD to receiving waters, whereas treatment typically involves the stimulation of beneficial microorganisms either in the receiving water or in an engineered system (bioreactor) which treats this water.

Effluent waters from mine tailings and waste rock piles are typically saturated with respect to iron and at a relatively low pH (<3). When mixed with higher pH receiving waters, precipitation of iron hydroxide readily occurs according to the following reaction:

$$Fe^{3+} + 3\ H_2O \rightarrow Fe(OH)_{3(s)} + 3\ H^+ \qquad (12)$$

This precipitate, termed "yellow boy" by early miners, chokes aquatic vegetation and re-acidifies the receiving stream. In-stream bioreactors have sought to alter stream conditions to promote the growth of beneficial microorganisms, principally SRB. Engineered systems to promote metals removal and pH control include enclosed bioreactors and constructed wetlands. Experimentation with and application of both technologies has been widespread.

In its simplest form, an engineered system to promote SRB growth requires an active biological system (or some other means) to consume available oxygen, a source of organic carbon for SRB growth, a solid phase for attachment of SRB, and sulfate in solution. Various configurations have been used to create conditions favorable for SRB

growth in bioreactors, the simplest (from an operational standpoint) uses a support media which also acts as a source of reducing power for biological growth. Various types of inexpensive and readily available solid-phase organic matter have been used, including compost (Benner et al., 1997), manure (Zaluski et al., 2000), sawdust and wood chips (Waybrant et al., 2002), paper pulp (Johnson et al., 2000) and various combinations of these materials (Cocos et al., 2002; Benner et al., 1999). The reactor systems are enclosed to prevent atmospheric oxygen influx, and can be operated under either upflow or downflow conditions. A critical factor in the design of support media mix is balancing the need for reducing power (organic matter), which is typically amorphous and of low permeability, with the inorganic bulking agent (gravel, sand, etc.) which is necessary to maintain adequate permeability and throughput. Cellulose-based substrates are popular field choices due to their low cost and bulking properties, but SRB cannot directly utilize cellulose as a carbon source. Initial degradation of these materials necessitates a population of fermentative anaerobes, which produce fatty acids and alcohols necessary for the growth of SRB (Chang et al., 2000). The SRB inoculum source for passive bioreactors is usually the organic matter. While manure-based sources have much higher initial SRB counts than compost or wood-based sources, subsequent bioreactor performance is influenced more by the conditions within the reactor than the initial SRB counts. Lyew and Sheppard (1997) found that SRB activity was directly correlated to the surface area available for colonization in a packed gravel reactor. Obviously, an optimum permeability and surface area:volume ratio must be determined for maximum reactor performance.

A variation of the passive bioreactor approach is the in-place biobarrier designed to treat groundwater impacted by AMD. Design considerations for in-place biobarriers are similar to above-ground bioreactors (carbon/SRB source, bulking agent, adequate residence time, etc.), although engineering controls are significantly more difficult. In-place barriers have been successfully used to treat acidic metal-laden groundwater resulting from AMD using a phased approach wherein groundwater passes sequentially through sand, an organic mixture containing compost and wood wastes, and gravel (Benner et al., 1997; Benner et al., 1999). Initial performance of in-place systems suggests an active life of at least 15 years under tested conditions (Benner et al., 1997).

Although the beneficial effects of wetlands in treating AMD have been noted for over 100 years, the use of constructed wetlands for AMD treatment has received attention only in the last 20 years (Brenner, 2001). Constructed wetlands offer a compromise between the greater control (and expense) of an engineered bioreactor and unamended stream disposal. Constructed wetlands utilize a gravel or coarse sand matrix on which vegetative aquatic plants are grown. Plant exudates and decay products provide organic matter necessary to develop anaerobic conditions in the lower layers of the wetlands system. Cattails have been utilized extensively for wetlands vegetation due to their acid tolerance (Samuel et al., 1988). Maintaining the levels of dissolved organic carbon necessary to insure anaerobic conditions and subsequent SRB activity has been a primary challenge, particularly since organic carbon demand may exceed supply in some systems (Sharp, 1999). Metals precipitation in wetlands is primarily through SRB activity, although some researchers have noted that metals removal is associated with a highly

organic environment rather than sulfide generation (Webb et al., 1998). Biomass sorption of heavy metals has been noted under more controlled conditions as well. Non-SRB bacterial cells (Mullen et al., 1989) and ground plant matter such as corn-cobs (Schneegurt et al., 2001) have both been noted to bind toxic metals such as Cd, Cu, and Pb when exposed to AMD solutions.

Above-ground bioreactors and in-place barriers that depend on substratum materials for their organic carbon supply are subject to a loss of reducing power and concomitant metal removal and pH neutralization efficiency over time. A step up in design complexity, cost, and process control involves the use of largely inert substratum materials in bioreactors that are continuously fed a source of dissolved organic carbon (DOC) with the AMD influent. Laboratory and field scale systems have demonstrated the effectiveness of fed systems using a variety of DOC sources including whey (Christensen et al., 1996), lactate (Elliott et al., 1998), and methanol (Tsukamoto and Miller, 1999). An advantage to these systems is that the carbon supply can be tailored to ephemeral conditions in the AMD stream, and other nutrients can be added if necessary. Where totally inert substrata materials are used, problems can arise with the loss of SRB populations following upset conditions or shock doses of acidity or metals. Johnson et al. (2000) found that inoculated SRB populations were incapable of sustained activity in mixed culture, glass bead bioreactors when fed a paper pulp energy source. This implies that, under adverse conditions, SRB populations may be out-competed or that this energy source was simply incapable of sustaining SRB growth. Available literature suggests that performance of fed bioreactors may be enhanced by using an organic-based substratum

(such as compost or manure) in addition to an influent DOC source. Additionally, influent DOC has been used to revitalize organic carbon substratum-based bioreactors near the end of their useful life, despite being depleted of substratum organic carbon (Tsukamoto and Miller; 1999).

An AMD treatment scheme which utilizes iron-reducing bacteria instead of SRB was tested by Marchland and Silverstein (2000). In dual species tests in laboratory shake flasks, iron oxidation by *At. ferrooxidans* was reported to be inhibited by the addition of glucose and subsequent oxygen consumption by *A. acidophilum*. Unfortunately, both these species have been observed to exhibit mixotrophic growth (Table 1), which suggests that either species could have coupled glucose oxidation to Fe^{3+} reduction, thus it is inconclusive whether *At. ferrooxidans* was indeed inhibited. The use of dissimilatory iron reduction to inhibit iron oxidizers under oxygen limited conditions is a potential research area that has not been fully explored in the literature.

Although they have potential to prevent AMD at its source, treatment schemes aimed at manipulation of microbiology within the tailings pile have received much less research attention than reactor-based systems treating AMD streams. Potential tailings treatments include both the addition of biocidal agents to control or prevent the activity of iron- and sulfur-oxidizing bacteria and the addition of various sources of organic carbon to stimulate beneficial microbial populations. Biocides investigated for use in controlling iron- and sulfur-oxidizing bacteria include sodium lauryl sulfate and benzoic acid (Dugan, 1987), the surfactant sodium dodecyl sulfate (Schippers et al., 2001), and halogen-containing calcium fluoride (Schippers et al., 1998). These compounds have

been successfully used in laboratory experiments, but field use has not been reported. Biocide use is problematic in field application because toxicity may persist into receiving waters and because beneficial populations of microorganisms (principally SRB) may also be inhibited.

The addition of organic carbon directly to the surface of mine tailings has been recognized as a potentially effective means of excluding oxygen from the tailings and thereby preventing both biotic and abiotic oxidation reactions. Two methods of organic carbon addition are the surface application of solid and semi-solid phase materials such as compost, municipal sewage sludge, manure, and various agricultural wastes and the aqueous application of dissolved organic carbon. Solid phase materials tend to be more often utilized due to ease of handling and application, ready availability and low cost. Elliott et al. (1997) noted that solid phase organic matter application to tailings surfaces can mitigate AMD in five ways: 1) As a physical oxygen barrier (lower gas-phase permeability); 2) As an oxygen-consuming barrier, due to microbial oxygen demand in the solid; 3) Chemical leachate from the barrier may inhibit the growth of iron- and sulfur-oxidizing bacteria; 4) Leachate may stimulate the growth of SRB or other beneficial bacteria; and 5) The organic matter may inhibit water infiltration. Manure and compost additions have proven beneficial to tailings revegetation efforts (Ye et al., 2000), and municipal compost additions have increased pH and moisture retention better than lime/fertilizer treatments at field sites (Bagatto and Shorthouse, 2000). The application of a green manure/sewage sludge mixture was observed to both significantly increase tailings organic matter, and to decrease water infiltration capacity at the tailings surface

(Harris and Megharaj, 2001). The latter property was seen as a disadvantage by the authors, who were more concerned with physical properties than microbial, but the decreased infiltration rate would serve to increase surface saturation and thereby reduce gas-phase oxygen transport, the primary means of oxygen movement into tailings (Nicholson et al., 1989). In side by side comparisons of various organic solids applied to tailings surfaces, Elliott et al. (1997) found that application of lime stabilized sewage sludge resulted in much higher pH and dissolved organic carbon, and much lower dissolved iron and sulfate than municipal compost or peat moss over a one year period in pilot scale laboratory tests.

The application of dissolved organic carbon (DOC) directly to the tailings surface as an aqueous solution has received less research attention than solid phase application. Blenkinsopp et al. (1992) "top dressed" columns filled with mine tailings with a mixture of brain-heart infusion and a known slime producing bacterium, *Klebsiella* sp. These workers observed that the added nutrient and bacteria mixture was more effective in fresh (unoxidized) tailings than in older (oxidized) tailings, and that the added bacteria had little beneficial effect over nutrient alone. In continuous flow studies using saturated mine tailings columns fed with high concentrations of citrate and yeast extract, Kim et al. (1999) reported a pH increase from 3-7 in the treated column. An active SRB population was present in the treated column and was postulated to be responsible for the robust performance.

Data Gaps

Although the addition of solid phase materials to tailings surfaces has received significant research attention, little is known about the effects of the treatments on microbial populations within tailings. Metals and sulfate removal results (Elliott et al., 1997; Benner et al., 1999) suggest robust activity of SRB within treated columns and field systems, yet little is known about the impact of carbon additions on other important populations, such as iron- and sulfur-oxidizers. Longer term studies which track these populations are necessary to determine their response to carbon addition, and their potential for growth after the treatment effectiveness subsides.

The addition of dissolved organic carbon to tailings surfaces is a promising technology for application in remote field locations. To date, few organic carbon sources have been studied and virtually no work has highlighted field-relevant moisture and application conditions. At field sites, unsaturated conditions are typically present (saturated tailings generally remain anoxic naturally) and continuous DOC addition is usually not feasible. Prior to field application of this technology, further studies are therefore needed to determine the effectiveness of various organic carbon sources, the temporal effects on various important microbial populations, and the longevity of treatment effectiveness. As outlined in Chapter 1, Research Goals and Objectives, the work described in the following pages addresses these issues for dissolved organic carbon addition to mine tailings to prevent acid rock drainage.

CHAPTER 3

MATERIALS AND METHODS

General

The research approach was designed to evaluate the effects of dissolved organic carbon additions to mine tailings in a laboratory environment. The specific effects monitored were changes in tailings microbiology, mineralogy, acid production, and oxidation-reduction potential. Acid producing mine tailings typically exist as a vertically stratified deposit, open to the atmosphere at the top surface and in contact with natural soil or rock at the bottom surface. The reactor systems were chosen to emulate the natural condition of in-place tailings. Column reactors were constructed open to the atmosphere at the top and intermittently dosed with both water and organic carbon, as described in detail in later sections. Mine tailings were acquired from two sources, the Fox Lake Mine (Fox Lake, Manitoba) and the Mammoth Mine (South Boulder River, Montana). The Fox Lake tailings are representative of recently placed tailings while the Mammoth tailings are representative of historically placed mine tailings.

Under natural conditions, influent water into mine tailings is either surface runoff or precipitation. Because these sources are typically deficient in organic carbon, the microbial ecology of mine tailings represents an oligotrophic community. The periodic addition of dissolved organic carbon in tailings column influent was expected to significantly alter this ecology, creating a more robust community which would effectively reduce acid and metals production. For field applicability, organic carbon

sources must be easily dissolved, easily transported, widely available, relatively inexpensive, and highly energetic. The sources chosen for investigation in this study were molasses, whey, and methanol.

The experimental strategy was to periodically dose "test" columns with the selected nutrient, and then measure the effects of treatment on column microbiology, chemistry, and mineralogy over the ensuing weeks. The details of each nutrient addition and methods of analysis are discussed in the following sections.

Mine Tailings Acquisition and Initial Testing

Mine tailings were selected based on availability, acid production, degree of oxidation, and landowner permission. Tailings from the Mammoth Mine were collected in 5 gallon buckets using a backhoe. Tailings from the Fox Lake Mine were shipped in palletized crates. Tailings from both mines were dry when received.

Following receipt, tailings from both mines were tested for acid production potential and mineral composition. Acid production potential was determined by EPA Method 670/2-74-070. This method utilizes an acid-base accounting technique wherein the propensity for a material to produce acid mine drainage is predicted by quantitatively determining the total amount of acidity and alkalinity the tailings can potentially produce. The potential acidity is calculated stoichiometrically based on the percent of non-sulfate sulfur in the tailings. This quantity is assigned a negative value and summed with the total potential alkalinity (termed neutralization potential), which is determined through acid digestion of the sample and subsequent titration with NaOH. This sum is the

acid/base potential and indicates whether the tailings should produce alkaline water (positive result) or acidic water (negative result) following an extended period of leaching (Smith et al., 1974).

The elemental composition of both sets of mine tailings was determined by energy dispersive X-ray spectroscopy (EDS) using a Jeol 6100 scanning electron microscope. Tailings samples were carbon sputter coated prior to analysis and elemental composition was recorded as atomic percent and weight percent for each element present at greater than 0.2%.

Tailings Column Set-up

Fox Lake Tailings Columns

Three 12 inch diameter (30.5 cm) polyvinylchloride (PVC) pipes were cut to 40" length and capped on one end. An effluent port was installed approximately 1" from the bottom of the column, and soil gas monitoring ports were installed at approximately 6", 18", and 30" from the eventual surface of the tailings and were then capped. The bottom 2" of the column was filled with pea gravel. Unamended tailings were then filled to a depth of 36" in the columns. Physical specification for Fox Lake tailings columns are shown in Table 2. After filling, the columns were flooded from the bottom up, to expel excess air from the tailings. The tailings were then allowed to drain under gravity. This flooding procedure was repeated 3 times for each column to approximate field deposition conditions. The effluent line from each column was fitted with an in-line silver-silver chloride oxidation-reduction (ORP) probe (Cole Parmer, Vernon Hills, IL). Columns

were labeled test column 1 (TC1), test column 2 (TC2), and control column (CC). Test columns 1 and 2 were to receive dissolved organic carbon amendments while the control column would receive only tap water.

To facilitate the stabilization of chemical and biological parameters within the columns prior to the addition of organic carbon, columns were operated with a daily application of tap water at a rate of 30 ml/min for 25 min/day (total volume added: 750 ml/day). Influent water was pH 7.5-8.0. Effluent pH was monitored on a daily basis using a pH probe and meter (VWR Scientific). When effluent pH and ORP stabilized (after approximately 3 weeks of operation), baseline conditions of effluent metals and microbiology were assessed as described below.

Mammoth Tailings Columns

The columns used for this work were 3" inch (7.6 cm) diameter PVC, 12 inches in length. Each experimental set-up consisted of 3 columns plumbed vertically in series such that infiltrating water could be easily sampled between the columns. Six such 3-column sets were constructed, 5 to receive periodic dissolved organic carbon additions and one control which received only tap water as influent. Columns were packed with raw tailings and were subsequently flooded with tap water from the bottom up and then allowed to drain under gravity as described above. Physical specifications for Mammoth tailings columns are shown in Table 2. The effluent line from each 3-column apparatus was fitted with an in-line ORP probe. ORP probes were also inserted between each of the 3 individual columns in the apparatus. The columns were labeled 1 through 6.

To facilitate the stabilization of chemical and biological parameters within the columns prior to the addition of organic carbon, columns were operated with a weekly application of tap water at a rate of 200 ml/week. When effluent pH and ORP stabilized (after approximately 3 weeks of operation), baseline conditions of effluent metals and microbiology were established.

Property	Fox Lake	Mammoth
Total column volume (L)	67	4.2
Column top area (cm^2)	729	45.6
Column depth (cm)	92	92
Tailings specific gravity (g/cm^3)	1.25	1.2
Tailings total mass (kg)	84	5.3
Pore volume (L)	20	1.3

Table 2. Physical specifications for Fox Lake and Mammoth tailings columns.

Tailings Column Operation

Both Fox Lake and Mammoth tailings columns were operated under gravity drainage conditions with tap water influent. To facilitate effluent sample collection, the effluent line on each column was closed for a 24 hour period each week to allow accumulation of sufficient fluid for sampling purposes. Influent water flowrates varied over the course of operation of the Fox Lake columns, as indicated in Table 3. Mammoth column influent flowrate remained stable at 200 mL/week throughout the experiment.

Date	Day of Operation	Influent Flowrate	Loading Rate
10/99 – 11/10/99	0	750 ml/day	1.02 cm/day
11/10/99 – 2/11/00	0-93	375 ml/day	0.51 cm/day
2/11/00 – 3/24/00	93-135	1000 ml/day	1.37 cm/day
3/24/00 – 4/17/00	135-159	375 ml/day	0.51 cm/day
4/17/00 – 10/6/03	159-1426	2L/week	2.7 cm/week

Table 3. Fox Lake column influent flowrates.

For each column set, several separate organic carbon addition experiments were performed. These experiments are described in detail in the section titled Organic Carbon Addition Experiments below.

Microbiological Assessment

The microbiological condition of the tailings columns was assessed on a regular basis throughout both sets of column experiments. Bacteria were enumerated from liquid effluent from the columns as well as from periodic solid phase sampling. The presence of bacterial genetic material (DNA) was also assessed via molecular techniques. Detailed description of each method is presented below.

Column Effluent Microbiology

Liquid effluent samples were collected on a monthly basis for enumeration of total heterotrophic bacteria (THB), sulfate reducing bacteria (SRB) and iron/sulfur-oxidizing bacteria (IOB/SOB). THB were enumerated via serial dilution and plating on R2A agar (Standard Method SM 9215C, Standard Methods for the Examination of Water and Wastewater). IOB/SOB were enumerated using the most-probable number (MPN) technique (SM 9240 D.1F) and SRB were enumerated using API recommended practice 38/SRB MPN.

Solid Phase Microbiology

Solid phase samples were periodically collected from both the Fox Lake and Mammoth tailings columns for microbial and metals analysis. Solid phase samples were

obtained from the Fox Lake columns by advancing a 3/8" diameter hollow stainless steel rod into the tailings from the surface. The rod was advanced to the desired depth then extracted and the tailings contained within were removed to a sterile 20 ml centrifuge tube. Samples were collected from 3-4 depth intervals within the tailings, typically 4"-8", 10"-14", 22"-26" and 32"-36". The sample was designated as the mean depth from the sampled interval. Following sampling, the sample hole was filled with fresh slurried tailings to prevent channeling. For microbial assessment, a 1 g aliquot of tailings was combined with 10 ml of buffer solution containing 4.3 g/L $(NH_4)_2SO_4$, 142 mg/L KCl, 714 mg/L K_2HPO_4, 714 mg/L $MgSO_4$-$7H_2O$, and 14 mg/L $Ca(NO_3)_2$. The tailings slurry was placed on a shaker table for 30 minutes, and then allowed to settle for 5 minutes. 5 mL of the supernatant was removed and placed in a new sample tube. Following this, normal procedures (cited above) for THB, IOB/SOB, and SRB were followed.

Genetic Assessment

Genetic assessment was performed on solid phase tailings samples from the Fox Lake columns. Nucleic acids were extracted and purified using a FastDNA Spin Kit for Soil and a FastPrep FP120 beadbeater (BIO101 Systems; Qbiogene, Inc, Carlsbad, CA). For tailings samples, 5 g tailings were suspended in 30 mL desorption buffer (Camper et al., 1985) and votexed for 30 seconds. Following settling, the supernatant was passed through a 0.22 μm filter. The filter was placed into FastDNA SPIN Kit and DNA was extracted as per instructions.

DNA was subsequently amplified using polymerase chain reaction (PCR). Complimentary regions of the 16S rDNA were amplified using 1μL each of 5' and 3'

primer sets mixed with 25 µL Accuprime SuperMix II, 23 µL nuclease-free water (Sigma Chemical, St. Louis, MO) and 1 µL sample. Reagents were mixed in a 0.2 mL Thermowell tube and transferred to a programmable Thermal Blok II thermocycler (Lab-Line, Melrose Park, IL) for replication.

PCR products were separated using denaturing gradient gel electrophoresis (DGGE), which was performed using a Bio-Rad DCode universal mutation detection system and PowerPac 300, 100V power supply (Bio-Rad Laboratories, Hercules, CA). Acrylamide gradient gels (40%-70%) were poured using a Bio-Rad Model 485 Gradient Former and allowed to set up for 1 hour. Wells were loaded with PCR product (approximately 10 µL) and run for 17 hr at 100V. The gel was then stained with SYBR Green for 30 minutes and gel images were recorded using a FluorChem 8800 imaging system (Alpha Innotech, San Leandro, CA). Prominent DGGE bands were harvested from the gels and sent to the Thermal Lab (Montana State University) for sequencing. Phylogenetic analysis was performed using a BLAST search.

Metals Assessment

Dissolved phase and sorbed metals analyses were performed on effluent from both column sets on a periodic basis. Each is described in detail below.

Column Effluent Metals

Fox Lake and Mammoth column effluent samples were collected in a similar manner to the microbiological samples described above. 20 mL liquid samples were preserved in nitric acid at pH<2 and were then filter sterilized using a glass syringe and a

0.2 μM sterile nylon filter. Samples were then analyzed via inductively coupled plasma emission spectrophotometry using an Accuris ICP (Fisons Instruments, Beverly MA). Samples were analyzed for aluminum, arsenic, cadmium, cobalt, copper, iron, lead, magnesium, manganese, zinc and total sulfur. Sulfate was analyzed via ion chromatography (Dionex Model DX500) equipped with an ion conductivity detector, electrochemical suppressor and Anion-IonPac AS4A-SC column (Dionex Corp., Sunnyvale, CA).

Solid Phase Metals

Samples for solid phase metals were collected in a similar manner to the solid phase microbial samples described above. 200 mg samples were extracted with hydrochloric acid using the method of Briggs (1996) and metals were quantified using a Perkins Elmer Elan 6000 inductively coupled plasma mass spectrometer (Boston, MA)

Vadose Zone Gas Analyses

Oxygen and carbon dioxide as a percent of total atmospheric gas were quantified on a weekly basis using a portable LMS-40 Landfill Gas Analyzer (CEA Instruments, Emerson, NJ). The instrument was affixed to soil gas monitoring ports on the Fox Lake columns until readings stabilized (10-15 seconds). The instrument was calibrated on a monthly basis using a calibration gas consisting of 0% O_2, CO_2 and 40% O_2, CO_2. Vadose zone gas was monitored at ports 1 and 2 only due to consistent water saturation in the deepest port in all columns.

The diffusive flux of oxygen and carbon dioxide across the surface of the Fox Lake tailings was determined by capping the headspace of the columns and measuring the disappearance of O_2 and accumulation of CO_2 over a period of 10-15 hours. Oxidation rates of tailings minerals can be estimated based on the decrease in oxygen concentration with time in the tailings headspace. Under steady-state conditions, the flux of oxygen across the tailings/atmosphere interface can be measured and related to the rate of oxygen consumption within the tailings (Elberling and Nicholson, 1996). In this method, Fick's Second Law is combined with a kinetic reaction term to give:

$$D_e \frac{\delta^2 C}{\delta z^2} - KC = \frac{\delta C}{\delta t} \qquad (12)$$

where D_e is the effective diffusion coefficient of oxygen in air ($L^2 \bullet t^{-1}$), C is the concentration of oxygen in air ($M \bullet L^{-3}$), z is the depth (L), K is the first-order reaction rate constant for mineral oxidation (T^{-1}), and t is time. The effective diffusion coefficient is based on the diffusion coefficient (D_0), but also takes into account porosity, the tortuosity of the medium and the percentage of gas filled (as opposed to water filled) pore space. D_e is always less than D_0, and can vary up to 4 orders of magnitude from dry conditions to complete saturation (Nicholson et al., 1989). At steady state ($dC/dt = 0$) and when $C(0) = C_0$ and $C(\infty) = 0$ equation 12 reduces to:

$$C = C_0 \exp\left[-z \left(\frac{K}{D_e} \right)^{0.5} \right] \qquad (13)$$

Fick's First Law calculates mass flux (F) as a function of the diffusivity and first derivative of the concentration in the z direction:

$$F = D_e \frac{dC}{dz} \tag{14}$$

where F has units of $M \bullet L^{-2} \bullet T^{-1}$. Combining equations 13 and 14 yields:

$$F = C_0 \left(KD_e\right)^{0.5} \tag{15}$$

When a gas reservoir of known volume is placed over the tailings surface, as was the case with the Fox Lake column flux measurements, the change in oxygen concentration with time is expressed as (Elberling and Nicholas, 1996):

$$\frac{dC}{dt} = \frac{A}{V} C\left(KD_e\right)^{0.5} \tag{16}$$

where *A* is the area of the tailings surface exposed to the atmosphere and *V* is the volume of the gas reservoir above the tailings. For initial conditions $C = C_0$ and $t = 0$, this equation simplifies to:

$$\ln\left(\frac{C}{C_0}\right) = -t\left(KD_e\right)^{0.5} \frac{A}{V} \tag{17}$$

When A and V are known, the slope of the linear plot of $\ln(C/C_0)$ over time gives $(KD_e)^{0.5}$, which was then substituted into equation 15 to calculate the flux of oxygen into (and carbon dioxide from) the columns.

As discussed above, the effective diffusivity (D_e) is influenced by porosity, tortuosity, and water saturation. D_e is difficult to determine independently, but can be estimated using either the method of Elberling et al. (1996) or Collin and Rasmuson (1988). The method of Elberling uses tailings tortuosity (τ), water saturation (S), air and water diffusion coefficients (D^o_a, and D^o_w, respectively), a modified dimensionless Henry's law coefficient (H), and a fitting parameter (α) as follows:

$$D_e = \tau D_a^o (1-S)^\alpha + \frac{\tau S D_w^o}{H} \tag{18}$$

The fitting parameter α was found to be 3.28 ± 0.4 for sandy tailings (Elberling et al., 1996). Within this range of variation, α has little effect on D_e variability. The method of Collin and Rasmuson uses air and water diffusivity, porosity, saturation and a dimensionless Henry's law coefficient (as above) with two fitting parameters, X_a and X_w as shown below:

$$D_e = D_a^o (1-S)^2 \left[n(1-S)\right]^{2Xa} + \frac{D_w^o S^2 (nS)^{2Xw}}{H} \tag{19}$$

The fitting parameters X_a and X_w are found through two additional equations as follows:

$$\left[n(1-S)\right]^{2Xa} + \left[1-n(1-S)\right]^{Xa} = 1 \tag{20}$$

$$(nS)^{2Xw} + (1-nS)^{Xw} = 1 \tag{21}$$

Porosity was approximately 25% for both Fox Lake and Mammoth tailings, allowing solution of equations 20 and 21 for X_a and X_w, respectively based on S. Saturation varies with time based on water application, infiltration and evaporation. However this variation is limited; as S varies from 30% to 95%, X_a varies from 0.625 – 0.565 and X_w varies from 0.595 – 0.64.

Calculations of D_e for oxygen using equations 18 and 19 as well as the parameter values used in the calculations are shown in Table 4. Effective diffusivity calculated via equation 18 is approximately twice that calculated via equation 19. This difference does not significantly alter estimates of oxygen influx, as will be shown in later discussion.

Parameter	Value	unit	Description
D^o_a	2.06 e-5	m^2s^{-1}	Diffusion coefficient of oxygen in air
D^o_w	1.80 e-9	m^2s^{-1}	Diffusion coefficient of oxygen in water
S	0.5	(-)	Saturation
τ	0.333	(-)	Tortuosity
α	3.28	(-)	Fitting parameter (Elberling et al., 1996)
H	29.875	(-)	Modified Henry's Law coefficient
n	0.25	(-)	Porosity
X_a	0.615	(-)	Fitting parameter (Collin and Rasmuson, 1988)
X_w	0.615	(-)	Fitting parameter (Collin and Rasmuson, 1988)
D_e	7.06 e-7	m^2s^{-1}	Effective diffusivity (Equation 18)
D_e	3.91 e-7	m^2s^{-1}	Effective diffusivity (Equation 19)

Table 4. Parameters and values used for effective diffusivity calculations.

Organic Carbon Addition Experiments

Organic carbon in the form of molasses, whey, and methanol were added to the Fox Lake columns over the course of these experiments. The Mammoth columns received exogenous organic carbon only in the form of whey. The overall strategy for organic carbon addition was to fully dissolve the carbon source in tap water at the target concentration, then immediately add this solution to the tailings surface. This addition method was chosen because dissolution in water and mass addition is the most practical addition method for remote field sites. Each group of addition experiments is described separately below.

Fox Lake Column Molasses Addition

Molasses was chosen for initial experimentation due to its high aqueous solubility, low expense, and ready availability. Molasses is a by-product of both cane and beet sugar refining. Typical physical and chemical properties of cane molasses are shown in Table 5.

For the first 2 molasses addition events, 3 l of molasses was added to both TC1 and TC2 at a concentration of 10 g/l. Three liters of water was added to the control column during these events. The first molasses addition was performed after the columns had been operational for approximately 6 weeks and pH had stabilized between 3.9 and 4.3 for all columns and ORP readings had stabilized between +140 and +200. The second molasses addition event was performed 56 days later. Because the first two molasses additions did not result in significant changes in pH in the treated columns, an extended period of molasses addition was conducted for a period of 42 days beginning on day 93. During this period, a 1 l molasses solution was added daily to the test columns at a concentration of 10 g/l. One liter water was added daily to the control column. From day 135 to day 159, 1 l of water was added to each of the 3 columns per day. On Day 167, the operation of the effluent ports of the columns was changed such that the ports were closed for a 24 hour period prior to sampling. Prior to this, the ports remained open at all times, a condition which made sample collection difficult in some cases. This operational condition was maintained throughout subsequent operation of the columns. On day 177, 10 l molasses at 10 g/l were added to TC1 and TC2. The control column received 10 L water. The final molasses dose (10 l at 10 g/l) was applied to TC1 and TC2 on day 238. During the molasses addition period, a total of 680 g molasses was added to the columns. This rate of application translates to 0.0081 g molasses per gram tailings.

Fox Lake Column Whey Addition

Cheese whey was chosen as an alternative carbon source to molasses because, in contrast to molasses, whey is relatively protein rich (Table 5). Like molasses, it is highly soluble, inexpensive, and easily transported.

Property	Molasses	Cheese Whey
Energy (kcal/g)	2.2	3.5
Carbohydrate (%)	59-69	63-75
Protein (%)	0	11-15
Fat (%)	0.01	1.5
Ash (%)	5-9	8-9
Moisture (%)	19-25	5

Table 5. Typical physical and chemical properties of molasses and cheese whey.

For whey addition, powdered whey was mixed with tap water at a concentration of 68 g/L. For each addition event, 10 L of this solution was added to the surface of the tailings in a slug dose. The total mass of whey added per addition was 680 g. This whey addition rate translates to 0.0081 g whey per gram tailings. Thus, the test columns received the same mass of whey during a single treatment as they had received molasses during the entire molasses addition period. Whey alone was added to TC1 and TC2 at days 288, 505, 673, 1503 and again at day 1710. Table 6 shows the timing, quantity and carbon source of all organic carbon additions to TC1 and TC2. During all organic carbon addition events to the test columns, the control column received an equal volume of tap water. Whey additions were not rigidly timed, but were performed in response to pH shifts in one or both test columns which suggested the diminishing effectiveness of the previous treatment.

Addition Number	Timing (Day #)	Carbon Source	Total Mass per Column (g)	Water Volume Added per Column (L)
1	0	Molasses	30	3
2	56	Molasses	30	3
3	93-135	Molasses	10 g/day (420 g total)	1 L/day (42 L total)
4	177	Molasses	100	10
5	238	Molasses	100	10
6	288	Whey	680	10
7	505	Whey	680	10
8	673	Whey	680	10
9	1072	Methanol*	70	10
10/11	1232/1246	Whey/Methanol*	680/70	10/10
12	1503	Whey	680	10
13	1710	Whey	680	5

Table 6. Timing, carbon source, and mass of organic carbon additions to test columns. *SRB were concurrently added with methanol, as described below.

Fox Lake Column SRB/Methanol Addition

In an attempt to directly stimulate SRB within the test columns, a culture of SRB was isolated from TC1 effluent and enriched on Postgate C media augmented with 1% methanol as an additional carbon source. Three liters of this culture broth, containing 10^6-10^7 SRB/ml, was mixed with 7 L of fresh 1% methanol solution and added to both TC1 and TC2 on day 1072. The final added volume was 10 L at a methanol concentration of 0.7%. Methanol is 100% carbohydrate and has been utilized in acid mine drainage field situations as a preferential carbon source for SRB growth (Tsukamoto and Miller, 1999). Although it is not a waste product per se, it is readily available and relatively inexpensive for field use. Methanol also has a very low freezing point, and is therefore a candidate for use at field sites which may experience sub-freezing temperatures. A concern with methanol application, however, is bacterial toxicity. The threshold of toxicity (LD_0) to *Pseudomonas sp*. is reported to be 600 mg/L,

however algal species such as *Chlorella pyrenoidosa* are reported to have much higher tolerance, up to 3% methanol in solution (Dakota Gasification Co., 2003).

Fox Lake Column Whey/Methanol Addition

Approximately 6 months following the methanol/SRB addition, a more robust organic carbon addition was initiated in an attempt to stimulate SRB with the intention of increasing effluent pH in both test columns. On day 1232, a methanol/SRB mixture (similar to that added on day 1072) was again added to TC1 and TC2. Two weeks following, on day 1246, a whey solution containing 680 g whey in 10 L water was added to both test columns. The purpose of this dual addition was to both directly stimulate SRB and provide a more long-lasting carbon source than was possible using methanol alone. Because of the expected toxicity of methanol concentrations higher than 1%, simply increasing the concentration of methanol in a 10 L water addition was not considered a workable option.

Mammoth Column Whey/Lime Addition

The six Mammoth columns were labeled 1-6. In addition to weekly addition of 200 mL tap water, columns 1, 3, 4, 5, and 6 received either whey alone, whey plus lime, or lime alone, as indicated in Table 7. Column 2 was designated the control column and received tap water only. Columns 1 and 2 were put into operation approximately 8 months prior to columns 3-6. All columns were operated with only water influent for 6 weeks to allow equilibration of chemical parameters. Columns that received only whey addition (columns 1 and 6) were treated with a slug dose of 16.25 g whey dissolved in

250 mL water (65 g/L). This is equal to a whey addition rate of 0.0031 g whey per g tailings. Columns that received lime treatment (columns 4, 5, and 6) were top dressed with powdered CaO in the following manner. After the tailings surface was leveled, a 70 mm Whatman filter (#4) containing 114 mg CaO was placed atop the tailings and secured with a small stone weight. This method was used to emulate the field method wherein lime would be applied to the tailings surface. The mass of CaO was calculated as the amount necessary to neutralize potential acidity in the top 10 cm of tailings, thus providing a neutral zone more conducive to heterotrophic bacterial growth. The mass of CaO necessary for neutralization was determined experimentally by analysis of slurries containing 5 g dry weight aliquots of Mammoth tailings with various mass additions of lime. An application rate of 1 mg CaO per 5 g tailings was observed to increase slurry pH from 4 to 6 in a 5 day dosing experiment. This application rate is close to that calculated via an active acidity analysis using the Shoemaker, McLean and Pratt (SMP) method (Shoemaker et al., 1961). This widely used method predicts the mass of calcium carbonate addition necessary to bring soil (tailings) pH from ambient to 6.4. This analysis predicted a $CaCO_3$ addition rate of 0.3 mg $CaCO_3$/g tailings. This translates into a lime addition rate of 96 mg CaO to neutralize the top 10 cm of tailings.

Column	Treatment
1	Whey (two additions)
2	Control (water only)
3	Whey (one addition)
4	Lime + Whey (one addition)
5	Lime + Whey (one addition)
6	Lime only

Table 7. Mammoth tailings columns treatments.

CHAPTER 4

RESULTS

General

Experimental results are divided into those that assist understanding of the initial conditions of the tailings and the baseline conditions of the bioreactor columns, experimental results from the various organic carbon addition experiments, and column sampling results that provide insight into the processes at work within the columns as they are exposed to organic carbon.

Initial Physical Testing of Mine Tailings

The physical composition and condition of mine tailings in large measure determines their potential for acid production. The propensity for acid production of both tailings sets was determined through direct measurement of neutralization potential and determination of the mineral make up of the tailings.

Acid Generating Capacity of Fox Lake and Mammoth Mine Tailings

Analysis of the acid generating potential of both tailings materials, as determined via EPA Method 670/2-74-070, indicated that neutralization of Fox Lake tailings would require 469 kg $CaCO_3$ per 1000 kg tailings. Mammoth tailings required only 3 kg $CaCO_3$ per 1000 kg tailings for neutralization. Clearly, the Mammoth tailings represent a more highly weathered environment, as would be expected since they have been subject to

leaching for 80-100 years, while the Fox Lake tailing have been weathered for only 15-30 years.

Elemental Composition of Fox Lake and Mammoth Mine Tailings

Elemental composition, as determined via energy dispersive X-ray spectroscopy (EDS) for Fox Lake and Mammoth tailings is shown in Table 8. These data clearly

Element	Fox Lake		Mammoth	
	Weight %	Atomic %	Weight %	Atomic %
Oxygen	36	59	48	65
Silicon	3.6	3.7	31	23
Sulfur	21	18	1.8	1.1
Calcium	1.4	1	-	-
Iron	37	17	11	4.1
Aluminum	0.8	0.9	5.0	4.8
Magnesium	0.2	0.3	-	-
Potassium	-		3.2	2.0

Table 8. Elemental composition of mine tailings.

indicate the more sulfidic nature of the Fox Lake tailings relative to Mammoth. Although the oxidation state of the minerals present cannot be determined through EDS, the preponderance of oxygen and silica suggests that the Mammoth tailings are composed predominantly of oxidized silica minerals (silicates and alumino-silicates) with oxidized iron species (ferric oxy-hydroxides) also present. EDS analysis of multiple fields of the Fox Lake tailings under high magnification indicated that sulfur present is in the form of pyrite (FeS_2). Approximately half the iron present would therefore also exists as pyrite. The remaining iron likely exists as oxidized Fe species such as FeOOH (goethite), and ferric hydroxide ($Fe(OH)_3$). Assuming iron in the original tailings deposited at Fox Lake was primarily present as pyrite, these data suggest a leaching "half-life" of approximately 30 years at this site.

Fox Lake Column Baseline Conditions

Baseline conditions for pH, ORP, effluent metals, and effluent microbiology were determined after approximately 6 weeks of accelerated weathering at an influent flowrate of 750 mL/day, prior to organic carbon addition. These data are shown in Table 9.

	TC1	**TC2**	**Control**
pH	3.96	4.25	4.05
ORP (mV)	+164	+137	+198
Microbiology			
Heterotrophic bacteria (CFU/mL)	4.7×10^1	1.6×10^2	4.5×10^0
Sulfur/Iron-oxidizing bacteria (MPN/mL)	1.4×10^4	1.7×10^4	6.8×10^3
Sulfate-reducing bacteria (MPN/mL)	ND	ND	ND
Metals (mg/L)			
Aluminum	11.2	1.96	4.89
Arsenic	0.09	0.08	0.039
Cadmium	0.386	0.094	0.128
Cobalt	0.639	0.381	0.449
Copper	19.1	8.2	78
Iron	6910	4580	5110
Lead	0.1	0.02	0.02
Magnesium	57.8	42.9	44.9
Manganese	3.82	2.21	2.87
Zinc	22	11.7	15.1
Sulfur (mg/L as S)	9700	8030	8170

Table 9. Baseline effluent conditions for Fox Lake tailings columns. ND: not detected.

In all columns, effluent pH dropped over 2 units in the first weeks of operation to approximately 4. Effluent ORP remained relatively stable in the range of +100 to +200 mV. Further evidence of acidification of the columns is suggested by SOB/IOB numbers in the range of 10^3 to 10^4 MPN/ml in column effluent. GHB were sparingly present at less than 200 CFU/ml while SRB were not detected in effluent from any of the columns. Effluent dissolved metals showed the same basic trends between columns. Dissolved

sulfur and iron were present at a S:Fe mass ratio of 1.4:1, 1.7:1, and 1.6:1 respectively, for TC1, TC2, and the control column. For comparison, the S:Fe mass ratio of pyrite dissolution would be 1.14:1, indicating that less iron was leaching from the columns than would be expected from stoichiometric pyrite dissolution alone. Stability diagrams were developed for Fox Lake tailings initial conditions using effluent metals, sulfur, pH and ORP data as inputs to the chemical stability computer program STABCAL (Montana Tech., Butte, Montana). Examination of a simplified stability diagram (considering only Fe and S) for pH 4 and Eh 350-400 mV (this correlates with an ORP of 150-200 mV as measured by the Ag-AgCl electrodes used) indicates that the initial conditions are very near the boundary of FeOOH (solid) and aqueous $FeSO_4$, which would exist as dissociated Fe^{2+} and SO_4^{2-} (Figure 1). Other metals present at significant concentrations were Al, Mg, Cu, and Zn. Inclusion of aqueous and solid phases represented by these metals with Fe and S are shown in Figures 2 and 3, respectively. These figures suggest that only two solid phases are stable at pH and ORP conditions close to those initially measured in the columns, namely $CuFeO_2$ and $Zn_3(AsO_4)$-$2.5H_2O$. Of course, significant concentrations of other solid phases may be present based on their occurrence in the original tailings. Stable aqueous phases close to the observed conditions include SO_4^{2-} and $Al(SO_4)_2^-$. Because solid phase iron in the tailings exists as both FeS_2 and oxidized species (such as FeOOH), it is apparent that initial conditions were conducive to dissolution of the reduced solid phase (pyrite), and subsequent mobilization through the tailings.

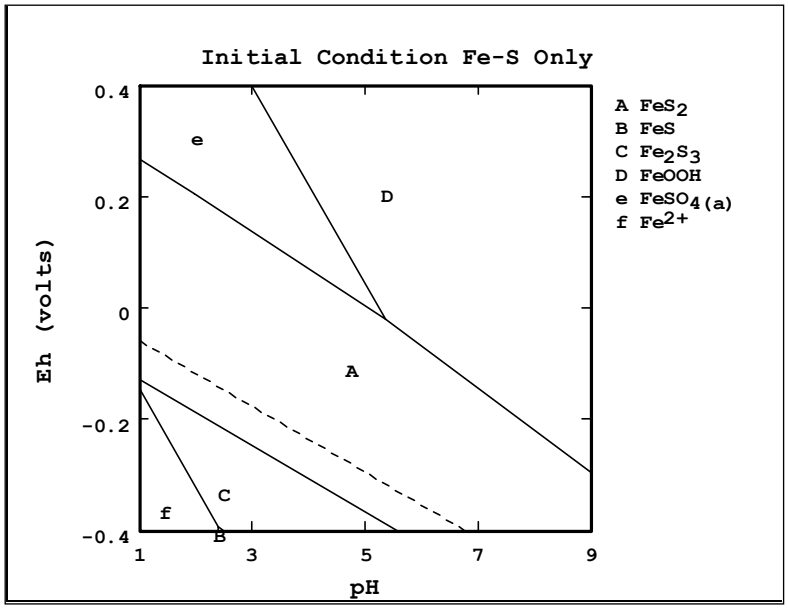

Figure 1. Simplified stability diagram for Fox Lake column initial conditions. Only Fe and S species are considered. Solid phases are represented by uppercase characters; aqueous phases are represented by lowercase characters.

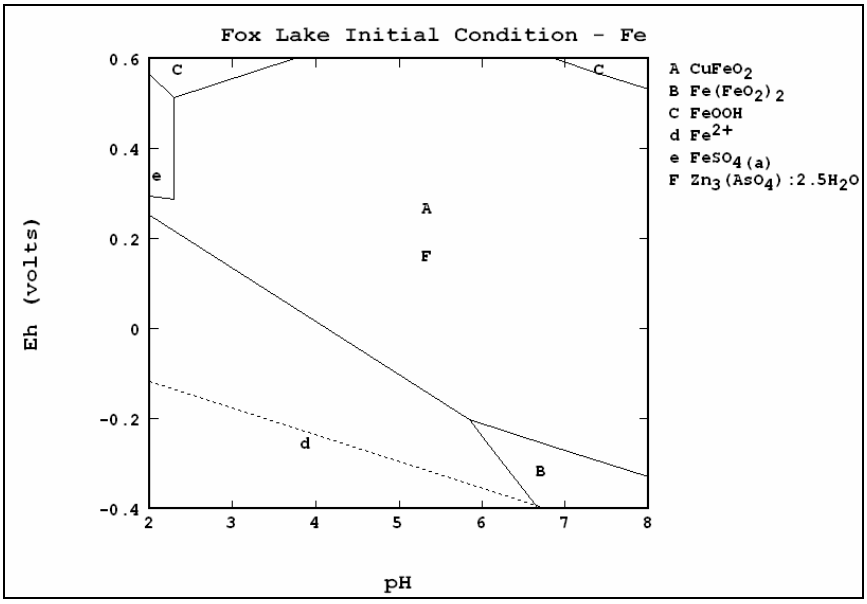

Figure 2. Initial condition stability diagram of Fox Lake columns with major metals and S complexed with Fe.

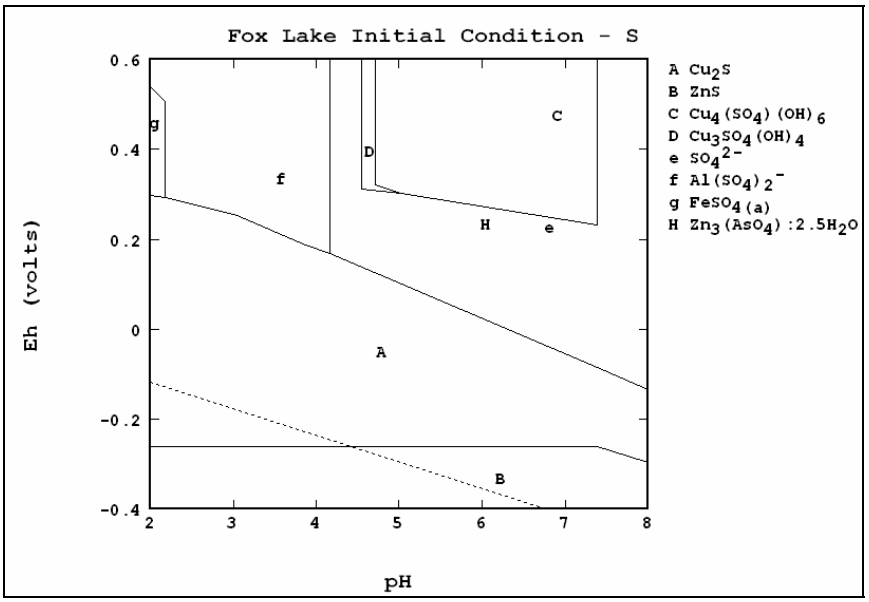

Figure 3. Initial condition stability diagram of Fox Lake columns with major metals complexed with S.

Distribution diagrams for all major elements occurring in effluent from the Fox Lake columns were also calculated using STABCAL. These diagrams plot the occurrence of various elements in compounds as a function of pH or Eh. At pH 4 and Eh +375 mV, the major elements in Fox Lake column effluent were predicted to distribute into the compounds shown in Table 10.

Element	Primary Phase	Secondary Phase
Aluminum	$Al(SO_4)_2$ (a) (95%)	$AlSO_4^+$ (a)(5%)
Arsenic	$Zn_3(AsO_4)$(s) (100%)	
Carbon	H_2CO_3 (100%)	
Copper	$CuFeO_2$ (s) (100%)	
Iron	$CuFeO_2$ (s) (95%)	Fe^{2+} (4%)
Magnesium	$MgSO_4$ (a) (98%)	Mg^{2+} (2%)
Manganese	MnO_2 (s) (100%)	
Sulfur	SO_4^{2-} (a) (99%)	$FeSO_4^-$ (1%)
Zinc	$ZnSO_4$(a) (95%)	$Zn_3(AsO_4)$(s) (3%)

Table 10. Occurrence of major compounds in Fox Lake column effluent as determined through distribution diagram analysis using STABCAL.

Atmospheric levels of CO_2 in equilibrium with influent water were assumed for generation of the distribution diagrams (Appendix A). CO_2 was not predicted to participate in any complexation reactions, but rather to remain dissolved as H_2CO_3. There is generally good agreement between those phases predicted in the distribution diagrams and the predominance (Eh/pH) diagrams (Figures 2 and 3). The majority of iron and copper is predicted to be in form of solid $CuFeO_2$. Since effluent Fe from the columns was measured at 4000-7000 mg/l and Cu was measured at 8-80 mg/l, clearly significant dissolved phases of these elements exist. It is likely that solution phase iron and copper are transitory between reduced phases (such as pyrite and chalcopyrite) and the oxidized stable phases.

Fox Lake Column Molasses Addition Experiments

Five molasses addition experiments were conducted over the first 250 days of operation of the columns. The first, second, fourth and fifth molasses addition events (occurring at days 0, 56, 177 and 238) consisted of single molasses additions, while the third addition event (occurring from day 96 to day 135) consisted of daily molasses additions (as described in Table 3).

First Molasses Addition

The first molasses addition consisted of 30 g molasses dissolved in 3 L water. In the weeks following this treatment, the pH of test columns 1 and 2 (TC1, TC2) increased approximately three quarters of a pH unit in both columns, while increasing less than half a pH unit in the control column (Figure 4). The treatment's effect on effluent pH in both

test columns was ephemeral, however, as pH dropped to pre-treatment conditions approximately 50 days following molasses addition in both test columns. During this period, effluent ORP dropped approximately 150 mV in both test columns (to 0 mV) while dropping approximately 50 mV in the control column (to +100 mV) (Figure 5). The effect on ORP was also ephemeral, as test column ORP increased to the level of the control column 50 days following treatment.

Second Molasses Addition

The second molasses treatment was identical to the first, with 3L molasses added (at 10 g/l) to TC1 and TC2 on day 56. Immediately following this addition, effluent pH increased 1 unit in TC1 but only 0.1 unit in TC2, while that in the control column increased 0.4 units, probably as a result of the slug of higher pH water added (without organic carbon) during the treatment. During this period (day 56 – 95) effluent ORP dropped 80 mV in TC1 (to -18 mV), while that in TC2 increased 20 mV to +90 mV. Control column effluent ORP increased slightly to +125 mV and stabilized.

During the 30 days prior to molasses addition, and the first 100 days following the first addition (day -30 to +100), dissolved effluent metals were tested on a bi-weekly basis. Effluent aluminum dropped significantly for the first 50 days of operation, then rebounded to initial levels between day 50 and100 (Figure 6). No differences in effluent aluminum were evident between the test columns and the control column during this period. Similarly, the first molasses treatment had no discernable effect on dissolved arsenic, copper, iron, lead, or zinc levels in column effluent. It is interesting to note that levels of several metals, most notably Al, dropped initially in all columns (from 30 days

before treatment to approximately 20 days following the first treatment) then increased again to initial levels. This is probably a result of the initial dissolution of more soluble minerals prior to more active leaching facilitated by microbially catalyzed reactions. Effluent sulfur was initially measured at 8000-10,000 mg/l in all columns. Corroborating the more active metal leaching measured in all columns following initial treatment, sulfur increased to 16,000 mg/l in the control column and to 20,000-23,000 in the test columns within the first 90 days following treatment (Figure 7).

The first two molasses additions had no apparent effect on heterotrophic bacterial populations in either of the test columns (Figure 8). IOB/SOB populations in all columns increased slightly over the course of the treatment period, from 10^2 to 10^4 MPN/ml, the treated columns showing no greater increase than the control. SRB, however, were only stimulated in TC1, from less than detection limits to 10^3 MPN/ml over the first 100 days following treatment. SRB remained undetectable in both TC2 and the control column.

Daily Molasses Addition

Due to the ephemeral effects of the first two molasses addition events, a more substantive organic carbon addition was conducted between days 95 and 135. This addition consisted of daily doses of 1 L molasses solution at a concentration of 10 g/L. The control column received 1 L tap water daily during this period, which is labeled in Figures 4-8 as “daily”. It was anticipated that this high dose rate would have a rapid and sustained effect on column effluent pH and ORP in the test columns. This was the case in TC1, which showed an increase in pH of approximately one unit (to 5.5) and a decrease in ORP of over 250 mV (to -180 mV). Surprisingly, over the first two weeks of

this treatment, TC2 initially reacted in an opposite manner, decreasing in pH to 3.2 and increasing in ORP over 200 mV (to +290 mV). During the final 3 weeks of daily molasses addition, pH increased rapidly in TC2, recovering to levels observed prior to daily treatment. Concurrently, ORP dropped significantly, to -150 mV. pH and ORP in the control column remained relatively stable during the daily addition period, at approximately 4.5 and +100 mV, respectively (Figures 4 and 5).

Effluent dissolved metals Al, Pb, and Zn decreased in TC1 as a result of daily treatment (compared to the control column), while As, Cu, and Fe tracked closely with the control (Figure 6). In TC2, Al, Pb, and Zn were relatively unchanged compared to the control while As, Cu, Fe increased as a result of daily treatment. Effluent S remained stable in TC2 during daily treatment, while decreasing approximately 25% in TC1 (Figure 7). Distribution diagrams (Appendix A) drawn for day 110 (the low point in TC2 pH) corroborate the differences in effluent As and Cu between TC1 and TC2. The sensitivity of As solubility to pH and Eh is illustrated by the phase differences shown in these diagrams; whereas in the control column and TC1 all As is in the form of solid zinc arsenate, 90% is predicted to be mobile as aqueous $H_2AsO_4^-$ in TC2. With Cu, the Eh shift between the test columns is largely responsible for aqueous $CuSO_4$ stability in TC2 versus solid $CuFeO_2$ in TC1.

Effluent cell counts taken during and after daily treatment indicate the continued increase of SRB populations in TC1, but still no measurable SRB in either TC2 or the control column (Figure 8). Iron- and sulfur-oxidizing bacteria (IOB/SOB) in column effluent were evidently not affected by daily molasses treatment, while heterotrophic

bacteria were evidently slightly inhibited by the treatment relative to the untreated control.

In the weeks following the cessation of the daily treatment (days 150-180), effluent pH decreased to pre-treatment levels in TC1 (to 4.5) while dropping significantly below these levels in TC2 (to 2.6) (Figure 4). During this period, the water flow regime was altered from daily addition of 375 mL to weekly addition of 2 L. This change likely caused some of the pH drop, as suggested by the drop in control column pH, but it cannot completely account for the additional acid production in TC2. The trend of increasing acid production in TC2 is supported by ORP data which indicates a spike from -50 mV at day 150 to +275 mV at day 180. During the 5 week period following continuous molasses addition to the test columns, levels of dissolved effluent metals rose as pH dropped, particularly in TC2 (Figure 6). In all cases, metals production was highest in TC2, followed by the control, and then TC1. The metals Al, As, Cu, and Zn were several orders of magnitude more concentrated in TC2 effluent than TC1. Between days 135-180, effluent S dropped in all columns but remained highest in TC2, followed closely by TC1 (Figure 7). Based on the dissolution of metal sulfides, effluent concentrations of S and metals, particularly iron, would be expected to be correlated. TC1 effluent was lower than the control in all metals except iron, but the predominance of Fe in the system accounts for the higher effluent S in TC1 versus the control. Distribution diagrams (Appendix A, day 110 diagrams) drawn for effluent conditions during this period indicate goethite (FeOOH) is the favored equilibrium Fe phase in all columns, yet conditions are very close to the soluble iron phase $FeSO_4$ in all columns. Fe initially present as iron

sulfide would presumably leach to the aqueous phase and precipitate as the secondary mineral goethite. The extent to which this happens is dependent on the proximity of the effluent pH-Eh condition in each column to the equipotential line between the solid and solution phase iron, and on the kinetics of goethite formation from solution.

Fourth Molasses Addition

Following the rapid drop in pH between days 160-175 in both test columns, a fourth molasses addition was made on day 177. This addition consisted of a single treatment of 10 L molasses at a concentration of 10 g/L (with the control column receiving 10 L water). This represents a greater mass of molasses (100 g) than was added in previous single point additions. Both TC1 and TC2 responded favorably to this treatment. Between days 180-220, effluent pH increased approximately one unit in both test columns, however TC2 was approximately 1.5 pH units below TC1. These data are corroborated by ORP measurements, which show both the same moderating trend and the enhanced oxidation of TC2 (Figures 4 and 5). Al, As, and Cu were evidently positively affected by this treatment in TC2, although other TC2 metals were unaffected. In TC1, all metals except Fe increased approximately 1 order of magnitude following this treatment, although all were present at less than 1 mg/l.

Effluent pH data from both test columns indicated stabilization at approximately day 220, followed by a slow downward trend. Another addition of molasses at high application rate was therefore implemented in an attempt to reverse falling pH trends in the test columns.

Fifth Molasses Addition

The fifth molasses addition was conducted on day 238. Like the previous treatment, this consisted of a single application of 10 L molasses at a concentration of 10 g/L (the control column received 10 L water). Following treatment, effluent pH in TC1 remained relatively stable for approximately 3 weeks, and then dropped from 5.1 to 4.3 over the next 20 days (Figure 4). This unexpected drop in pH was accompanied by a concomitant drop in ORP from -100 mV to -240 mV in TC1 (Figure 5). TC2 experienced a similar period of stability followed by a marked pH drop from 3.6 to 2.6 in this case. In TC2, however, the pH drop was accompanied by an increase in ORP, from +60 mV to +130 mV. Dissolved metals continued to be well correlated with effluent pH during the period following this treatment. Effluent Al, As, Fe, and Zn remained lower in TC1 than either TC2 or the control, while Cu and Pb were uniformly low in all columns. Generally, levels of dissolved metals were slightly higher in TC2 than in the control column (Figure 6). Effluent S was also highest in TC2 and the control column (Figure 7). Microbial trends described above continued during and after this molasses addition (Figure 8).

At day 272, approximately one month following the fifth molasses addition, solid phase samples were taken from each of the columns and were enumerated for attached heterotrophic bacteria, IOB/SOB, and SRB at depths of 9”, 18” and 30” below the tailings surface. Comparison of attached bacterial numbers at this time with similar samples taken immediately prior to the first molasses treatment (day 0) indicate increases in heterotrophic bacteria (GHB) in both test columns, while the control column showed

little change (Table 11). Neither IOB/SOB nor SRB numbers changed appreciably in any columns during the period of molasses addition. Comparison of these data with effluent microbial counts over the same time period (Figure 8) highlights the differences in these enumeration methods. Whereas GHB were most numerous in solid phase samples, IOB/SOB were found to be most abundant in effluent samples. Furthermore, while SRB were enumerated at 10^2 MPN/ml in effluent samples from TC1, and were absent from TC2 and the control column, attached SRB were enumerated at similar (albeit low) concentrations at all depths in all columns. Direct comparison of these methods is difficult because of potential problems with cell culturability, efficiency of removal of attached cells from tailings during sampling, and survival of detached cells as they flow through the column. Because of this, the data are most useful as a means to determine relative changes over time within each method.

Fox Lake Column Whey and Methanol Addition Experiments

Because molasses was not successful in uniformly increasing column effluent pH and decreasing ORP, an alternative was sought which would be lower in simple sugars and higher in complex carbohydrates and protein. Cheese whey was chosen due to its low cost, ease of handling, and ready availability. In later carbon additions, methanol was also added both alone and in combination with whey. Although not a waste product, methanol is inexpensive, resistant to freezing (an advantage for remote locations), and has been shown to stimulate SRB in bioreactors fed mine waste (Tsukamoto and Miller, 1999). Powdered cheese whey alone was mixed in solution with 10 L tap water and

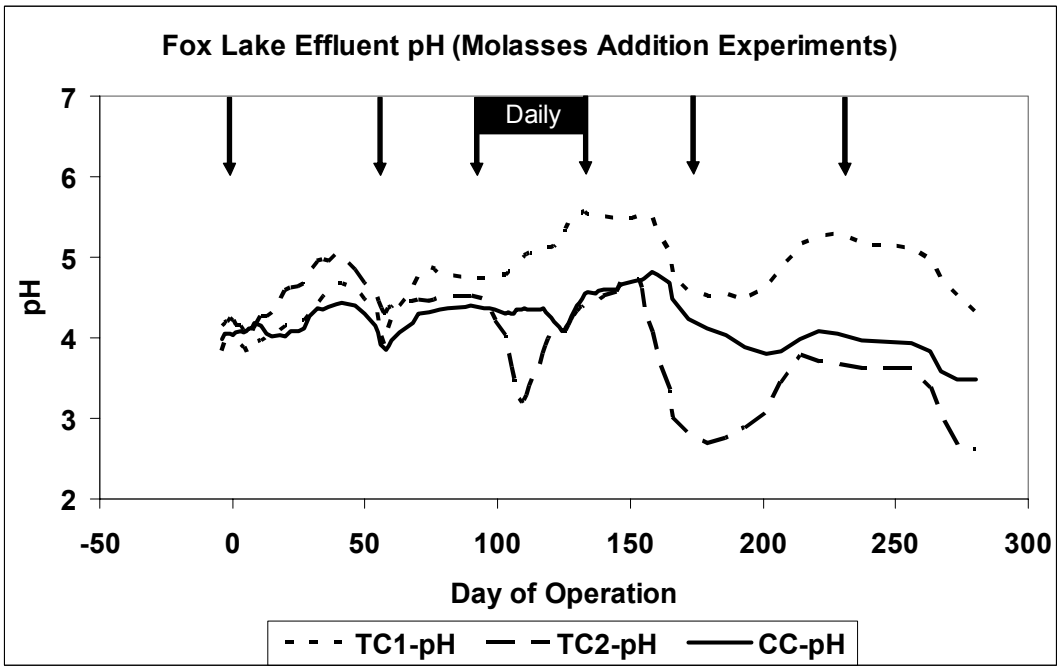

Figure 4. Fox Lake column effluent pH during molasses addition experiments. Arrows at top of chart indicate molasses addition events.

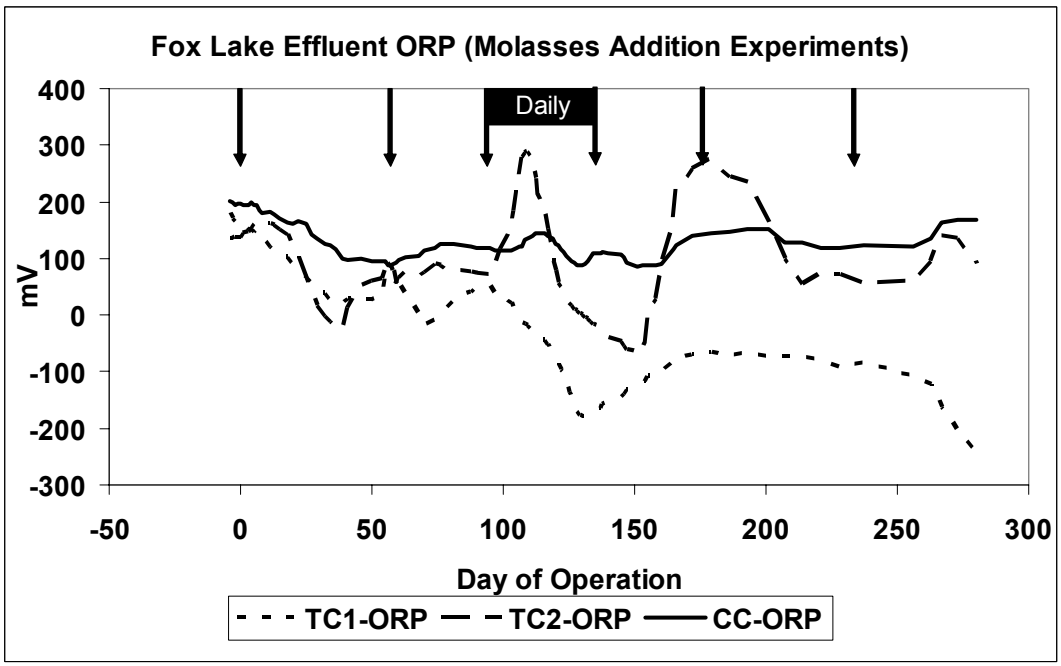

Figure 5. Fox Lake column effluent ORP during molasses addition experiments. Arrows at top of chart indicate molasses addition events.

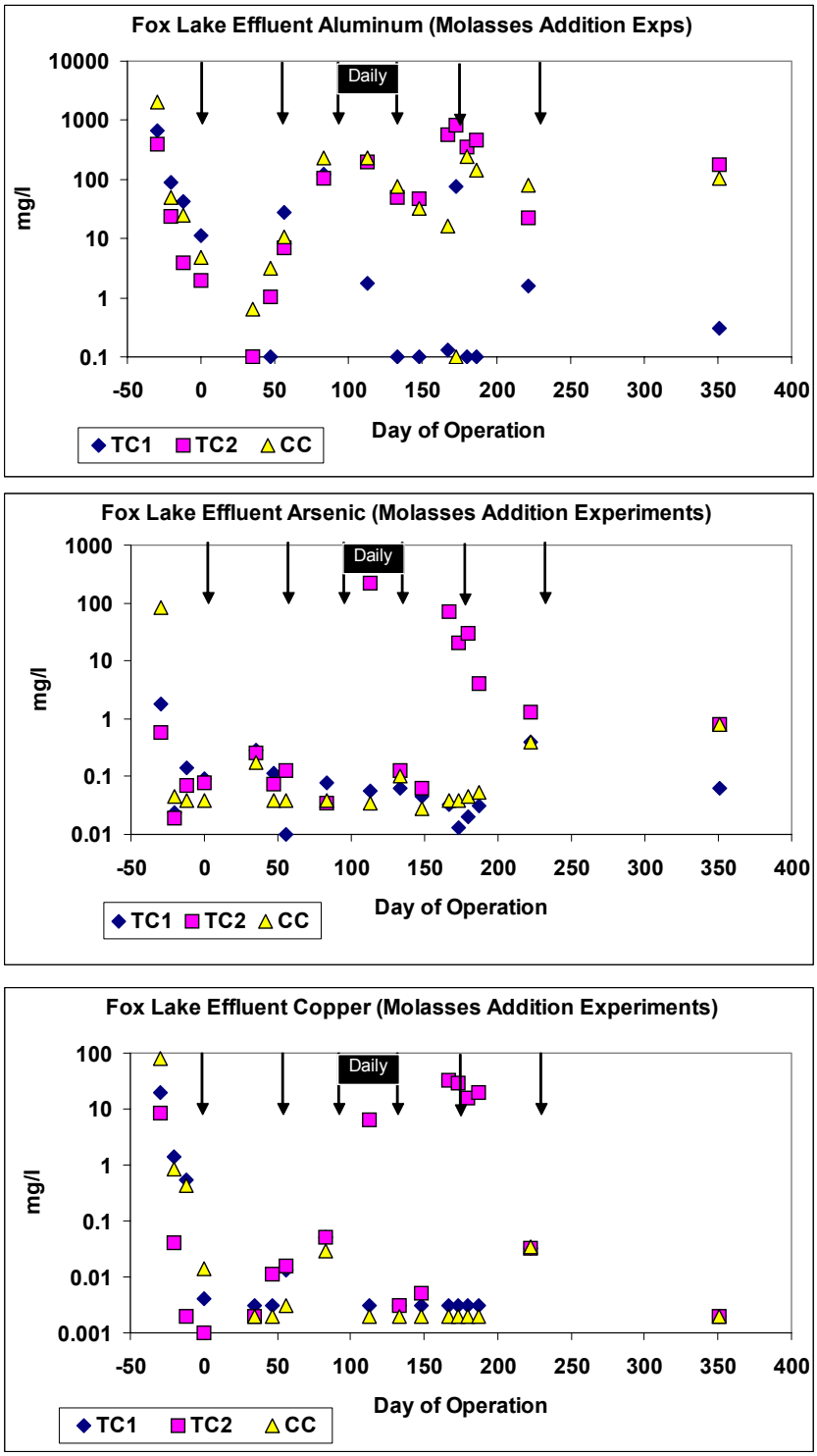

Figure 6. Dissolved metals in Fox Lake column effluent during molasses addition experiments. Molasses addition points are represented by arrows.

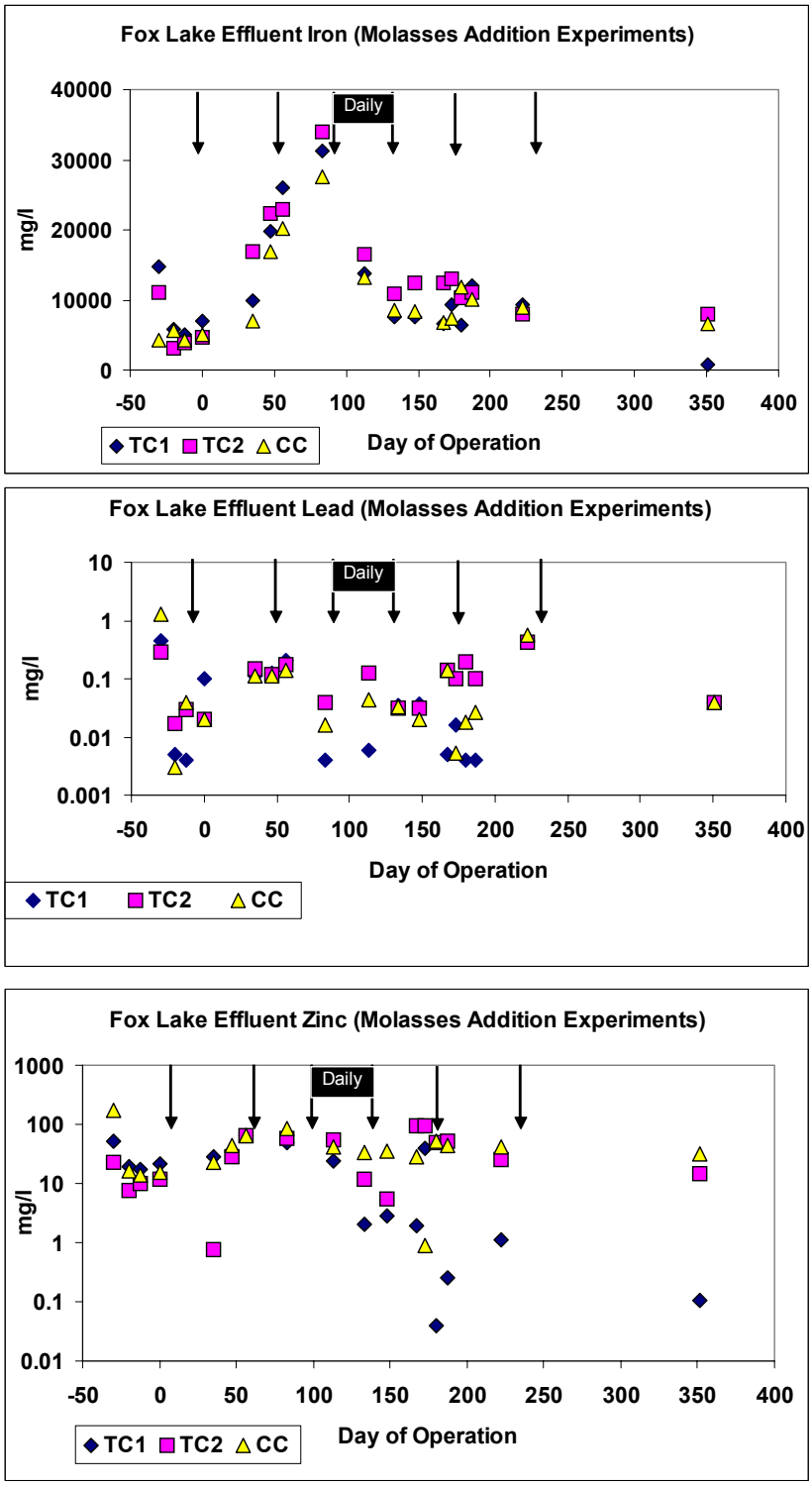

Figure 6 (continued). Dissolved metals in Fox Lake column effluent during molasses addition experiments. Molasses addition points are represented by arrows.

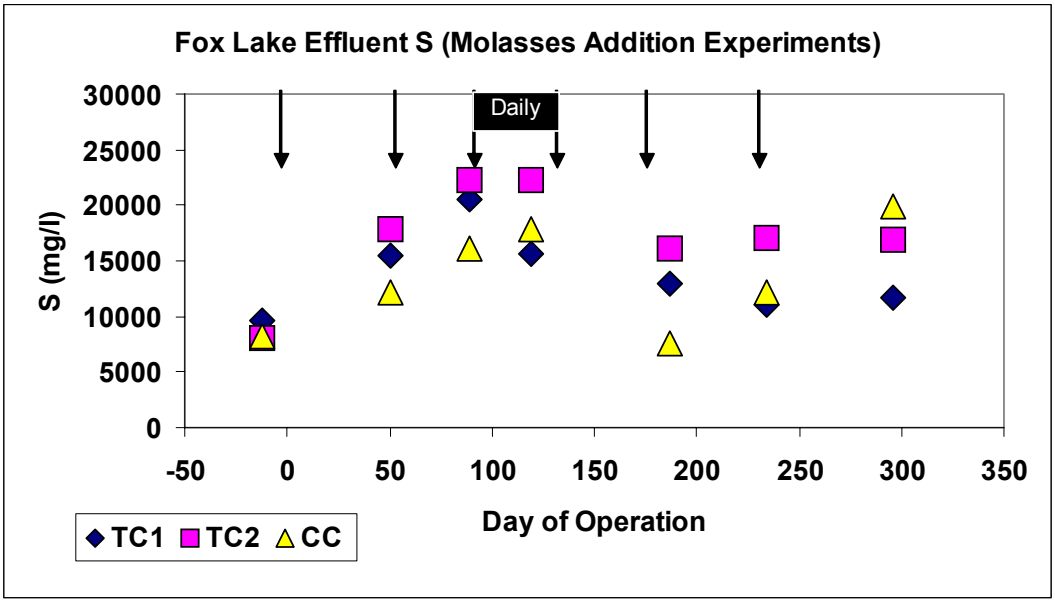

Figure 7. Dissolved sulfur in Fox Lake column effluent during molasses addition experiments. Molasses addition points are represented by arrows.

added to the test columns at a concentration of 68 g/L at days 288, 505, and 673 (Table 6). This concentration represents the whey's original condition prior to dehydration. On day 1072, a 10 L methanol solution was added to the test columns at a concentration of 7 g/L methanol. A combined treatment of whey (day 1232) and methanol (day 1246) was added to determine what, if any, synergistic effect this would have. A 10 L solution of whey was again added on day 1503 at a concentration of 68 g/L, and a final whey treatment was made on day 1710, using a 5 L solution of 136 g/L (half the water volume of previous additions but twice the whey concentration). In this final treatment, whey was applied to all 3 columns (both test columns and the heretofore control column). During all whey and methanol treatments, the control column received an equal quantity of unamended tap water (with the exception of the final whey treatment).

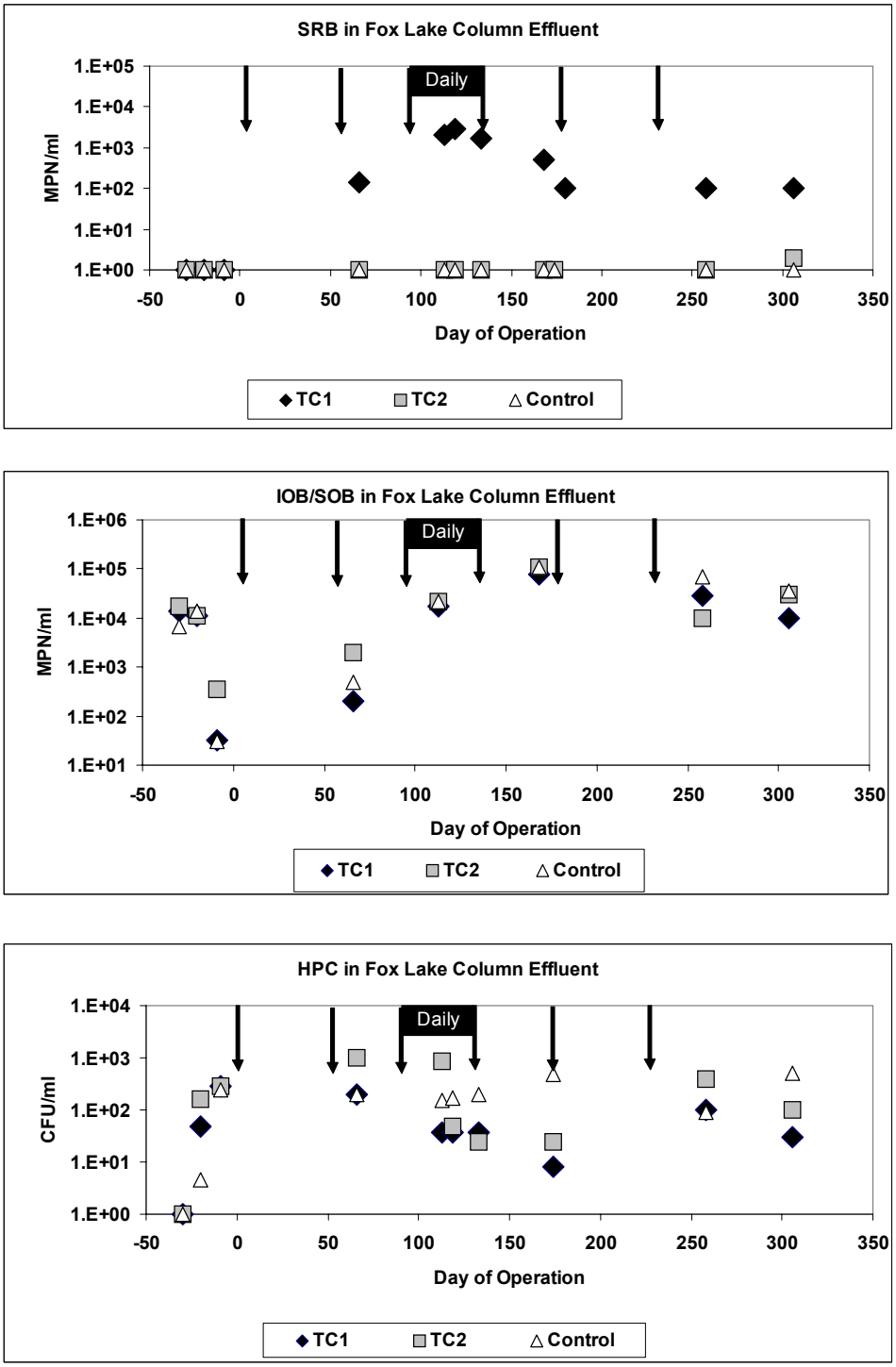

Figure 8. SRB, IOB/SOB, and HPC in Fox Lake column effluent during molasses addition experiments. Molasses addition points are represented by arrows.

Heterotrophic Bacteria												
	TC1				TC2				CC			
Day	3"	9"	18"	30"	3"	9"	18"	30"	3"	9"	18"	30"
0		100	400	1000		100	1000	1200		1200	800	2500
272		1000	39000	80000		270	80000	80000		1000	1000	1900
846		1500	1000	2000		8000	20000	20000		1000	9000	1500
1213	1900	100	3100	200	64000	4400	3400	9400	47000	9100	150	2500
1237	130	250	1500	100	22150	13000	490	160	150	20	ND	2500
1310	9450	1650	355	2560	12700	2300	6700	190	285	15	10	15
1483	18150	505	160	190	350950	29550	1010	113300	170	30	90	150
1701	1365	230	4050	55	21100	258000	155	1250	550	100	165	20

Iron/Sulfur Oxidizing Bacteria												
	TC1				TC2				CC			
Day	3"	9"	18"	30"	3"	9"	18"	30"	3"	9"	18"	30"
0		100	50	10		10	8	20		50	20	50
272		28	28	28		28	28	28		28	28	28
846		12	10	5		15	10	3		15	12	15
1213	4	4	2	ND	5	5	3	ND	4	4	2	ND
1237	17	11	ND	200	17	14	17	ND	17	14	200	450
1310	ND	ND	ND	9.3	ND	ND	ND	2	28	7.8	ND	ND
1483	1.8	24	17	7.8	17	1.8	1.8	1.8	280	24	17	1.8
1701	ND	ND	ND	ND	8	8	ND	ND	24	5	8	ND

Sulfate Reducing Bacteria												
	TC1				TC2				CC			
Day	3"	9"	18"	30"	3"	9"	18"	30"	3"	9"	18"	30"
0		10	5	20		28	18	18		18	1	5
272		28	28	28		28	28	28		17	11	7.8
846		200	610	45000		28	280	2400		14	17	11
1213	450	ND	7800	300	11	2	2	4500	ND	ND	ND	ND
1237	17	ND	ND	32	17	200	930	17	ND	ND	ND	ND
1310	7.8	ND	ND	24	ND	7.8	7.8	28	ND	ND	ND	ND
1483	1.8	1.8	1.8	170	ND	ND	ND	60	ND	ND	ND	ND
1701	ND	ND	11	780	5	7	2	1100	ND	ND	ND	ND

Table 11. Bacteria enumerated from Fox Lake tailings solid phase at various depths. All figures expressed in CFU/g (dry weight). ND = not detected.

First Whey Addition Day 288

Although the first whey addition (day 288) had a rapid effect on pH in both TC1 and TC2 (Figure 9), the previously established trend of higher acid generation in TC2

relative to TC1 continued. In the 3 month period following the initial whey treatment, pH increased from 4.4 to 5.6 in TC1 and from 2.6 to 4.5 in TC2. During this period, the control column also increased in pH, but to a lesser extent, from 3.5 to 4.1. The effectiveness of this whey addition was ephemeral, however, with pH dropping to below pre-whey treatment levels again approximately 7 months following treatment (circa day 500). Effluent ORP data was consistent with pH readings from day 280-500, with TC1 dropping from -100 to -350 mV and TC2 dropping from +100 to -100 mV (the control column concurrently increased from +100 to +250 mV) (Figure 10). Following the initial whey treatment, effluent Al, As, Fe, and Zn were lower in TC1 compared to TC2 and the control whereas Cu and Pb were similar in all three columns. During this period, effluent metals in TC2 were very similar to levels in the control column (Figure 11). Effluent S followed a similar pattern, with TC1 producing significantly less sulfur than either TC2 or the control column (Figure 12). Effluent microbial trends measured following molasses treatment continued through the first whey treatment, with two notable exceptions; SRB were evidently stimulated in TC2 following whey treatment and HPC were cultured in greater numbers from all three columns during this period (Figure 13). The presence of SRB in TC2 effluent at approximately day 300 marks the first detection of these organisms in effluent from this column.

Second Whey Addition Day 505

At the time of the second whey addition (day 505), pH readings were 3.9, 3.1, and 3.0 in TC1, TC2 and the control column, respectively. The response of the test columns following this addition was again rapid and significant, with pH increasing to 5.5 in TC1,

and 4.3 in TC2. The control column also increased slightly to 3.6 (Figure 9). In TC1, ORP initially dropped approximately 30 mV to -350 mV, and then increased to -200 mV over the next 150 days. In TC2, ORP increased immediately in the month following treatment from -50 mV to +180 mV, and then dropped to -150 mV over the next 50 days. Following this period, ORP in TC2 again increased to +150 mV (day 670) (Figure 10). Concurrently, ORP dropped approximately 100 mV in the control column (from +300 to +200 mV). Effluent Al and As remained low in TC1 but were evidently unaffected by the treatment in TC2. Iron and Zn were lower in both test columns following this addition, while effluent Cu dropped in all three columns (Figure 11). With the exception of Cu, all metals increased during this period (day 500-650) in the control column effluent, with Fe, Pb, and Zn increasing most significantly. Metals production was mirrored by effluent S in the control column (Figure 12) during this period, increasing from 21,000-26,000 mg/l. Effluent S dropped in both test columns following the second whey addition, probably a result of increased SRB activity (Figure 13). SRB populations increased from 10^2 to 10^5 MPN/ml and 10^1 to 10^2 MPN/ml in TC1 and TC2, respectively; while IOB/SOB decreased approximately 2 orders of magnitude in both test columns. General heterotrophic bacteria were evidently unaffected by the whey addition.

Third Whey Addition Day 673

On day 673, a third whey addition was made to both test columns (Table 6). The timing of additions had been approximately semi-annually up to this point, however, the goal of this addition was to test the performance of the treatment for an extended time period (400 days). Effluent pH levels were 5.5 in TC1, and 3.6 in both TC2 and the

control column at the time of the treatment (Figure 9). Concurrently, ORP was -200 mV in TC1 and +160 mV in both TC2 and the control (Figure 10). This whey addition did not have an immediate effect on pH in TC1, but, like the previous treatment, pH decreased rapidly in TC2 for approximately 30 days following treatment, to a low of 2.8 (day 700). Likewise, ORP remained stable in TC1 following treatment, but increased to a high of +200 mV in TC2 (day 700). In a similar pattern with the previous treatment, rapid pH increase and ORP decrease occurred in TC2 from 30-120 days after treatment.

Over the year of operation following the third whey treatment, pH in TC1 gradually dropped from 5.4 to 3.8, a rate of 1.5 pH units in 20 months. This drop started at day 820, approximately 5 months following treatment. During this pH drop in TC1, ORP increased from -230 to -85 mV. Following the rise in pH mentioned above, TC2 also dropped consistently, from 4.9 to 2.4, a rate of 2.5 pH units in 20 months. Unlike the gradual increase in ORP measured in TC1, TC2 increased rapidly, from -90 to +320 mV beginning approximately 5 months following treatment. During the year following the third whey treatment, effluent pH in the control column dropped slowly but consistently from 3.6 to 3.0 (with some fluctuation) and ORP increased from +190 to +300 mV. From the standpoint of effluent pH, the longevity of whey treatment under these conditions is less than 1 year, depending on the acceptable level to which pH can drop.

Immediately following the third whey treatment, effluent Al in TC1 was less than 1 mg/l, more than 3 orders of magnitude below the control column at 2000 mg/l. Effluent Al remained at approximately 1 mg/l for approximately 6 months then increased steadily for 8 months to 1200 mg/l. Although increases were not as dramatic for other metals, As,

Cu, Fe, Pb, and Zn exhibited similar behavior in TC1, suggesting an effective period of metal suppression of 6-8 months following treatment (Figure 11). Because metals suppression was not as successful in TC2 during the first two whey addition events (with the exception of Cu and Zn) levels of effluent metals were higher than those in TC1 at the start of this treatment. While the treatment did not reduce effluent dissolved metals in TC2, it did evidently prevent increases that were observed in the control column for As, Cu, Fe, and Zn (Figure 11). Like TC1, this prevention lasted 6-8 months, whereupon levels of all metals increased to levels approaching that of the control column.

Increases in dissolved metals were mirrored by effluent S following the third whey treatment (Figure 12). In TC1, effluent S was 3,500 mg/l before treatment. This remained low for 6 months then increased gradually to 20,000 mg/l. Similar behavior was observed in TC2; with S increasing from 12,000 mg/l to 20,000 mg/l.

Effluent metals and sulfur data suggest waning activity of SRB 6-8 months following this whey addition. Effluent SRB counts did not indicate this, however, remaining relatively stable from day 650 to 900 (Figure 13). SRB were enumerated at approximately 10^4 MPN/ml and 10^2 MPN/ml in TC1 and TC2, respectively, during this period. IOB/SOB dropped slightly in effluent from both test columns following this treatment; however significant scatter in TC2 data suggests unstable conditions. Interestingly, effluent IOB/SOB from the control column dropped gradually during this period from a high of 10^4 MPN/ml to 10^2 MPN/ml. Effluent HPC remained at $>10^3$ CFU/ml in both test columns, evidently neither stimulated nor inhibited by the treatment.

Six months after this whey addition (day 875), gas monitoring ports were installed on the columns, allowing measurement of vadose zone O_2 and CO_2 partial pressure at the depths shown in Table 12. Vadose zone gases were measured weekly thereafter. The deepest port in each column (port 3) was found to be submerged in all cases, preventing gas measurement at these depths. Six months following the third whey addition, oxygen levels in port 1 were 12% in the control column and 2-4% in the test columns (Figure 14). At the port 2 depths, oxygen was measured sporadically for several weeks, and then was found to be absent in all columns. These data suggest greater oxygen consumption in the test columns during this period than in the control. Carbon dioxide was measured at less than 2% in port 1 and 2-3% in port 2 in the test columns. CO_2 was generally absent in the control column at both depths. Carbon dioxide data collected between days 875-1072 suggest the production of CO_2 at depth in the test columns and diffusion upward in the profile. Also evident is a slow drop in CO_2 at both port depths over this time period, indicating a decrease in production over time. This decrease is concurrent with the drop in SRB numbers in both test columns circa day 1000.

Column	Port 1 depth	Port 2 depth	Port 3 depth
TC1	6 in.	18 in.	30 in.
TC2	4 in.	16 in.	28 in.
Control	4 in.	16 in.	28 in.

Table 12. Depth of vadose zone gas monitoring ports in Fox Lake columns.

Approximately six months after the third whey addition (day 846), bacteria were again enumerated from the solid phase of the tailings at various depths. This enumeration was performed previously at day 272, approximately one month after the final molasses addition. Results from this sampling indicate a small drop in IOB/SOB

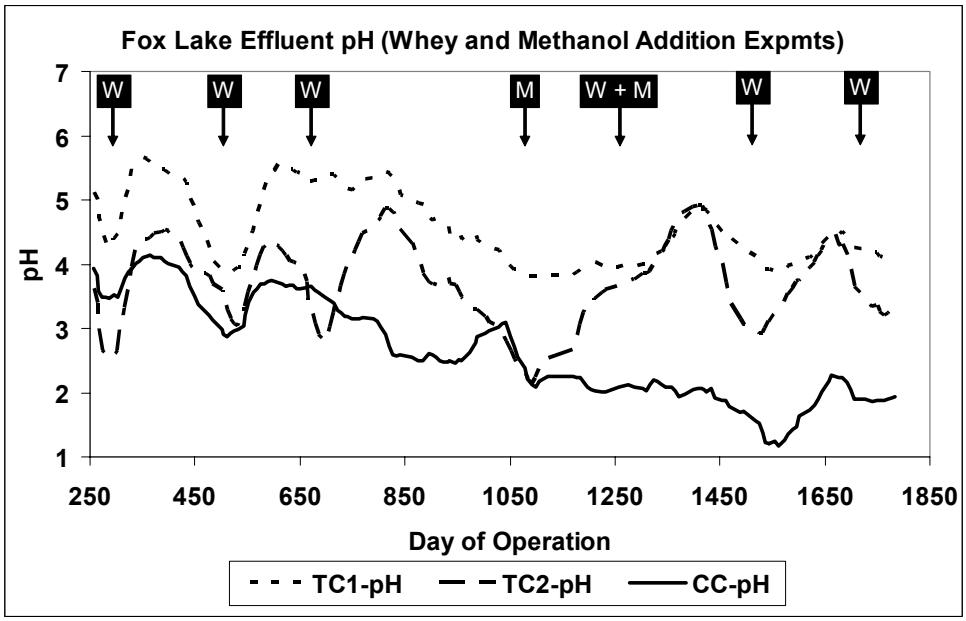

Figure 9. Fox Lake column effluent pH during whey and methanol addition experiments. Arrows at top of chart indicate addition events and carbon source (W = whey, M = methanol).

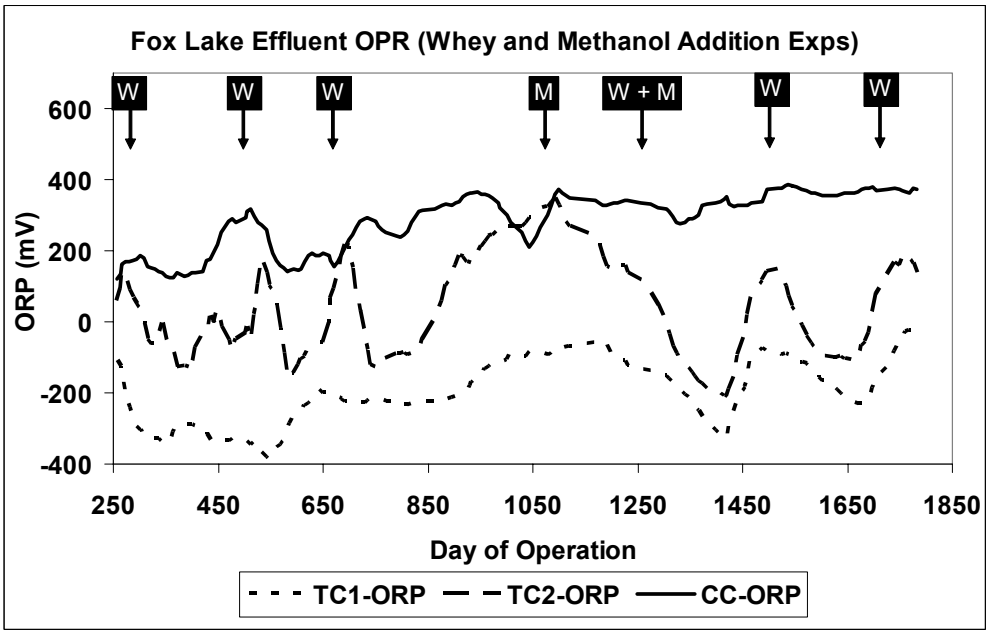

Figure 10. Fox Lake column effluent ORP during whey and methanol addition experiments. Arrows at top of chart indicate addition events and carbon source (W = whey, M = methanol).

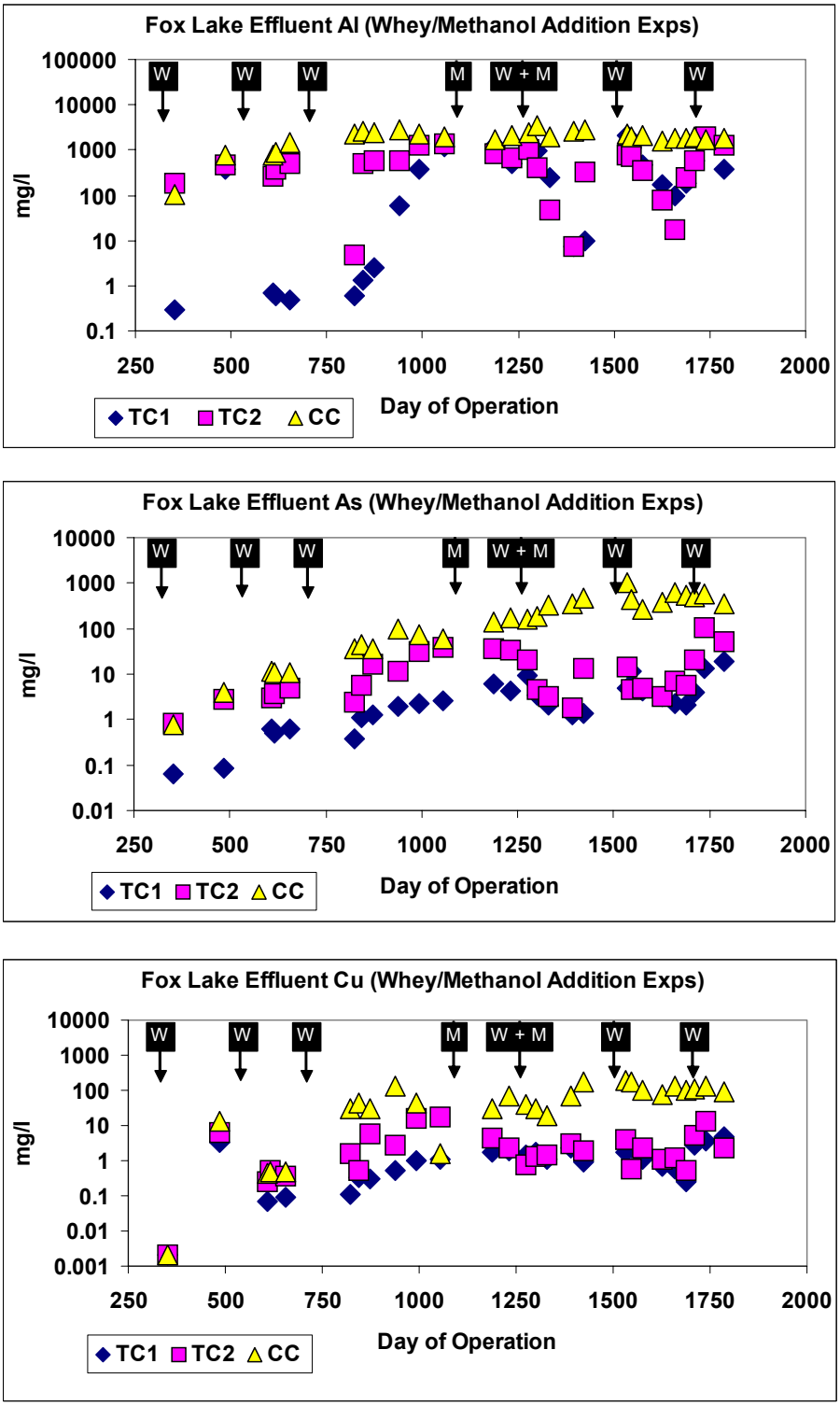

Figure 11. Dissolved metals in Fox Lake column effluent during whey and methanol addition experiments (addition points are represented by arrows).

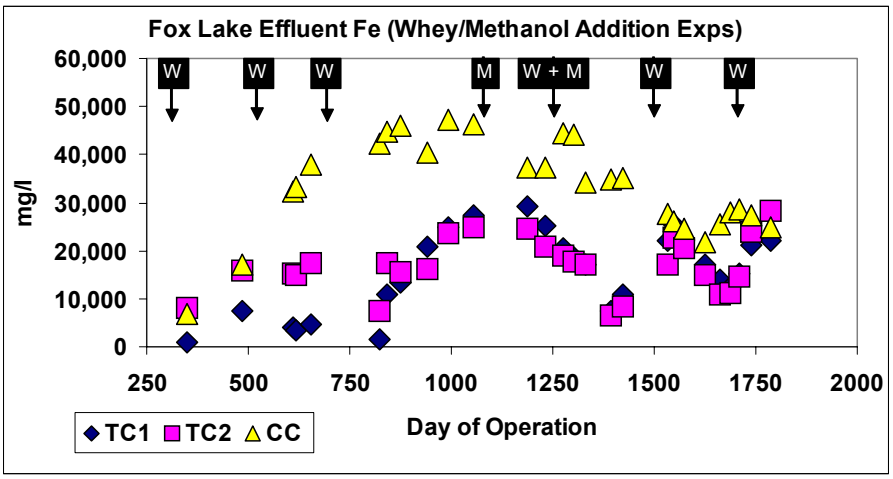

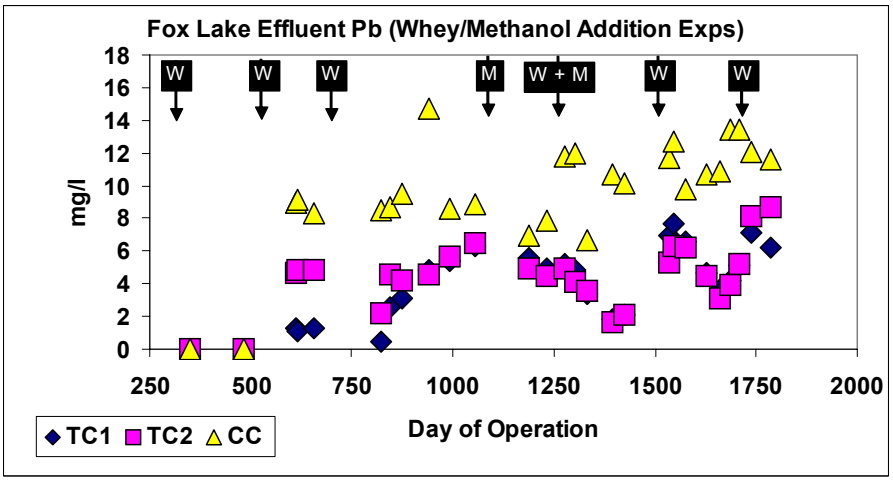

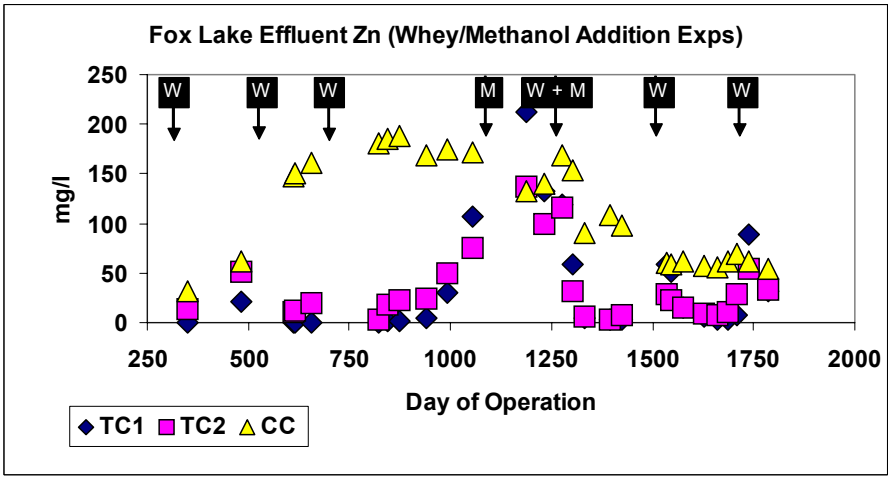

Figure 11 (continued). Dissolved metals in Fox Lake column effluent during whey and methanol addition experiments (addition points are represented by arrows).

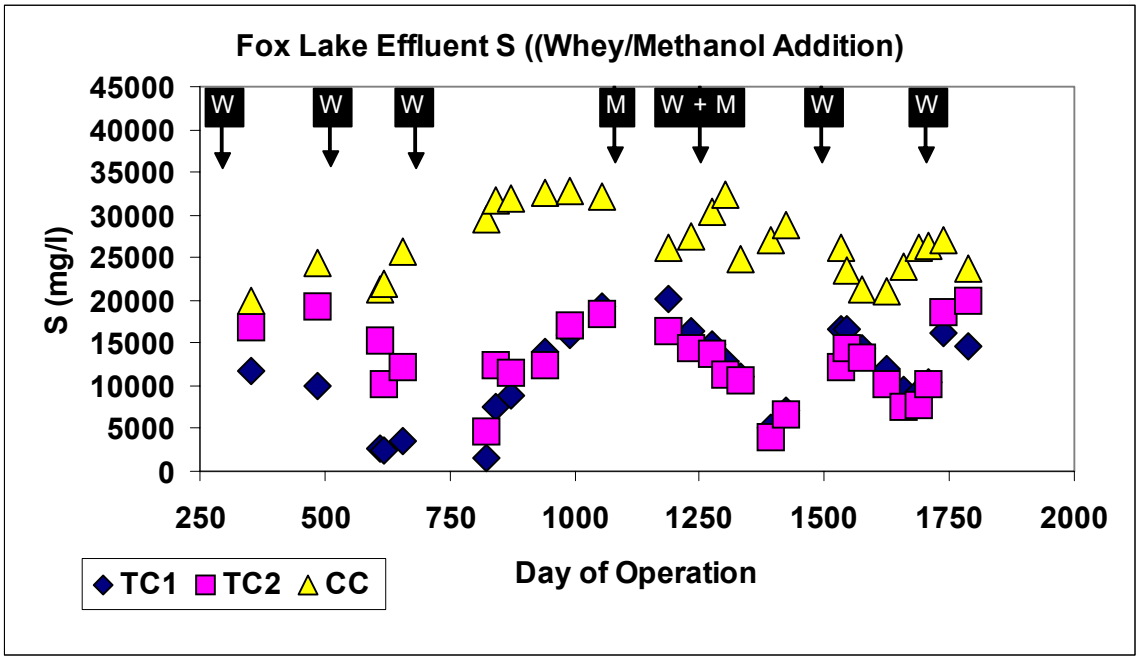

Figure 12. Dissolved sulfur in Fox Lake column effluent during whey and methanol addition experiments (addition points are represented by arrows).

numbers over the previous 19 months and three whey treatments (Table 11). Heterotrophic counts remained relatively stable in TC2 and the control column, while dropping approximately an order of magnitude at the lower depths in TC1. Interestingly, SRB increased over 20-fold in TC1 at 18" and over 1000-fold at 30". TC2 also exhibited SRB increases at these depths of 10- and 100-fold, respectively. No SRB increases were observed in the control column. These SRB data corroborate the effluent SRB measurements (Figure 13), indicating significantly more SRB in TC1 and TC2 than in the control, as well as the increase in SRB observed over the previous 19 months. Solid phase HPC data also follow a similar pattern with effluent HPC, suggesting a decrease in these populations in the test columns over the period of whey addition.

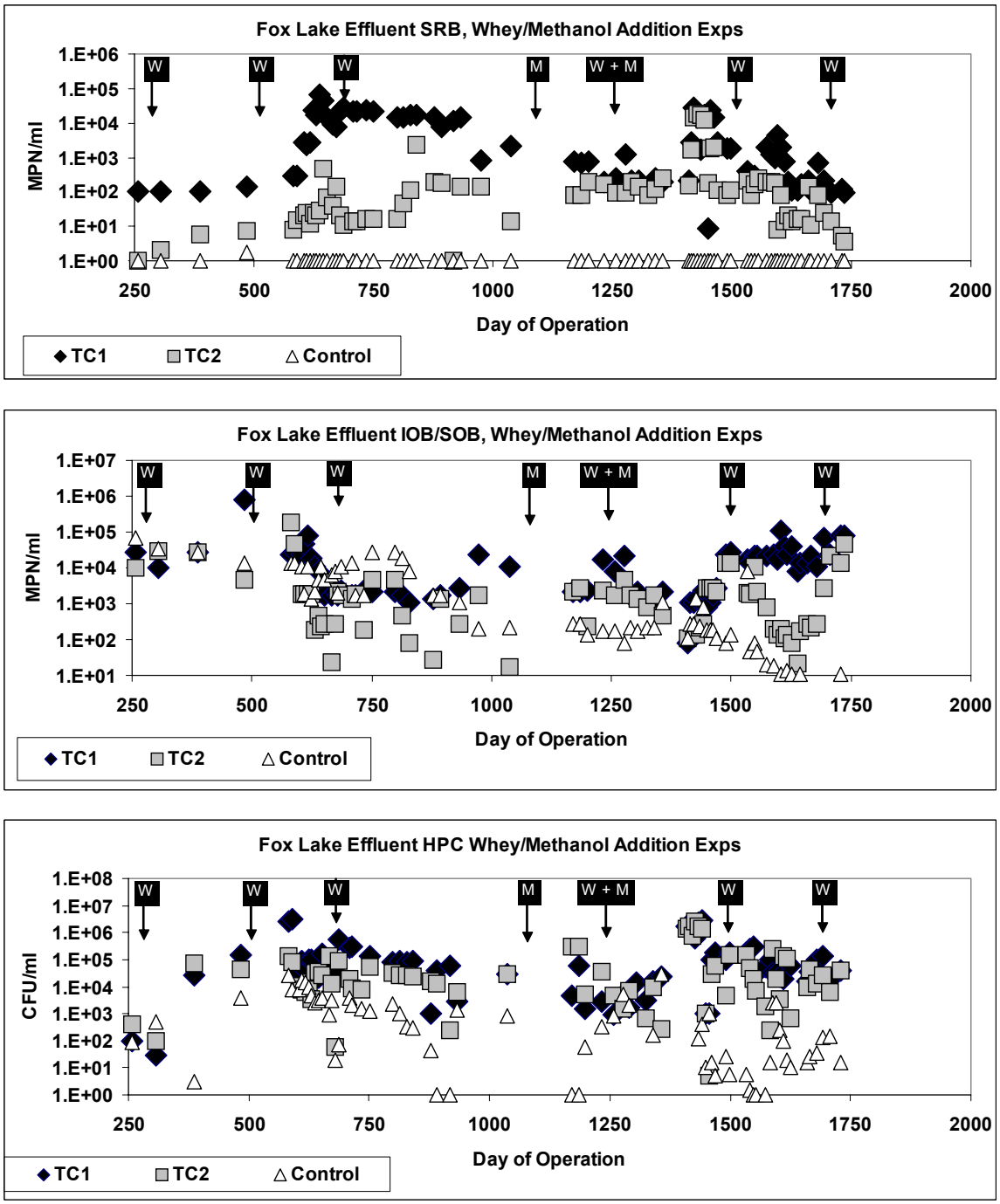

Figure 13. SRB, IOB/SOB, and HPC in Fox Lake column effluent during whey and methanol addition experiments (addition points are represented by arrows).

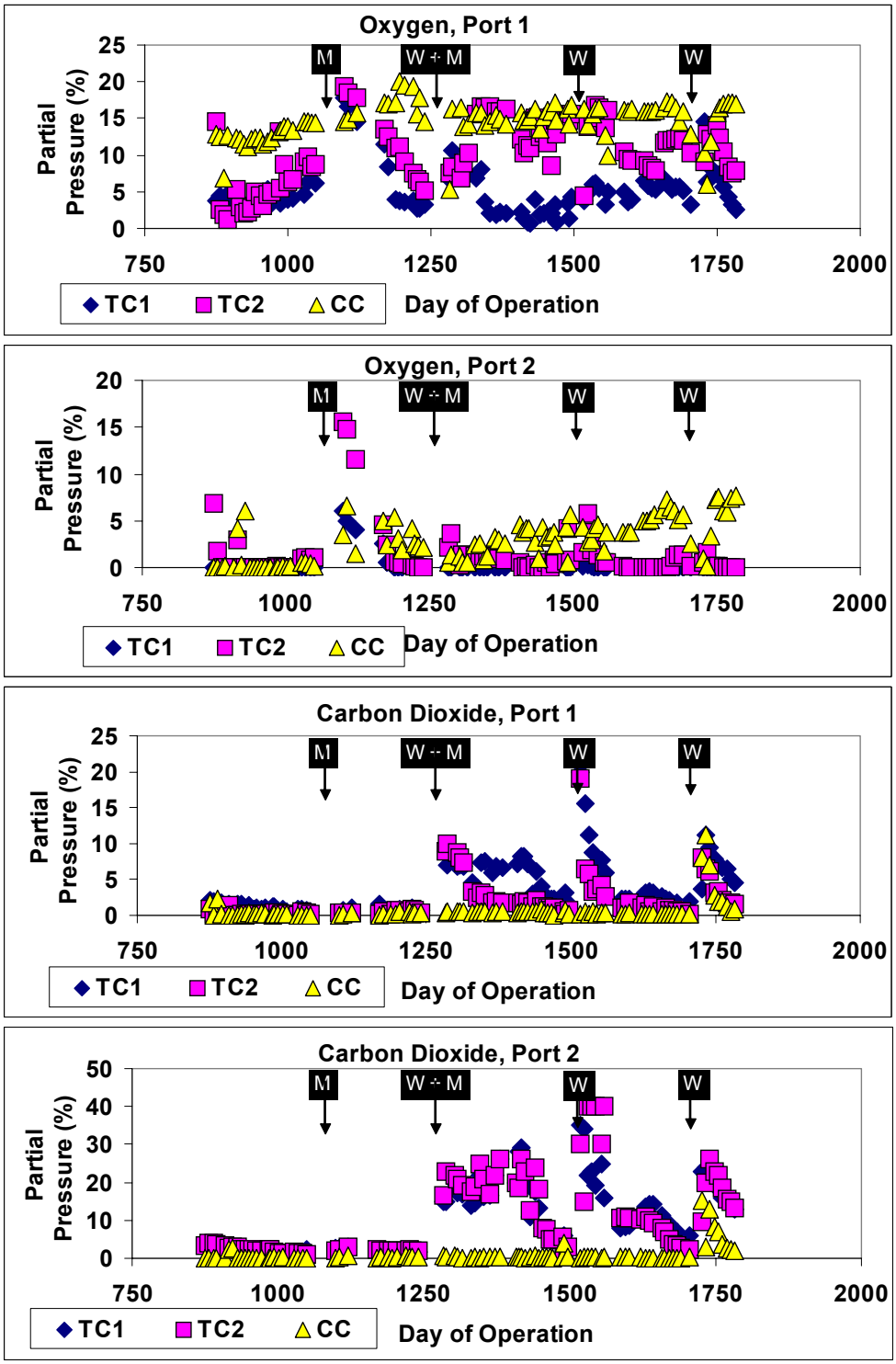

Figure 14. Oxygen and carbon dioxide measurements from vadose zone gas monitoring ports. Methanol and whey addition points are noted.

Methanol Addition Day 1072

On day 1072, a 10 L methanol solution was added to the test columns at a concentration of 7 g/L methanol. The success of other workers in stimulating SRB bioreactors with added methanol as the primary carbon source demonstrated its ability to promote sulfate reduction and subsequent metals precipitation in an acidic mine waste stream (Tsukamoto and Miller, 1999). It's efficacy in an open system has not been demonstrated, however. Prior to treatment, effluent pH was 3.9, 2.2, and 2.1 in TC1, TC2 and the control column, respectively (Figure 9). Effluent ORP was -74, +350 and +360 mV, respectively in TC1, TC2, and the control column (Figure 10). Methanol treatment had little effect on either pH or ORP in TC1. However, in TC2, increasing pH and falling ORP were immediately apparent following treatment. pH increased for approximately 6 months, then leveled off at 3.7. ORP dropped steadily during this period as well, also stabilizing at approximately day 1240. Methanol treatment had little effect on effluent dissolved metals, even in TC2, where favorable pH and ORP effects were noted (Figure 11). Effluent S also remained stable at approximately 20,000 mg/l in both test columns following methanol treatment (Figure 12). Effluent SRB remained stable following treatment in TC2 while dropping one-half log in TC1 (Figure 13). Both IOB/SOB and HPC remained stable in effluent from both test columns following methanol treatment.

Immediately following methanol treatment, oxygen levels in TC1 and TC2 increased from <10% to approximately atmospheric (20.7%) in port 1 while remaining at 15% in the control column (Figure 14) at this depth. In port 2, oxygen increased from

<2% to 15% in TC2 but only to 6% in TC1. At port 2 in the control column, the slug-dose water addition caused an increase in pO_2 from 0 to 3-5%. This was similar to the increase measured in TC1 at this depth. Methanol addition evidently reduced oxygen demand in the unsaturated zone of both test columns, allowing greater accumulation of oxygen through diffusive flux. Over the 5 month period following methanol treatment (days 1072 – 1230), oxygen levels in the test columns gradually decreased back to pre-treatment conditions in both measurement ports, suggesting increased microbial consumption.

CO_2 levels in both ports of the test columns remained stable at under 2% following methanol treatment. CO_2 is generated by heterotrophic bacteria and SRB as a product of metabolism and is consumed by lithotrophic growth. During this period, CO_2 levels were slightly higher in the test columns at port 2 than in the control column, suggesting some net generation in the test columns (Figure 14). Evidently, methanol addition did little to stimulate CO_2 generation, however.

Oxygen and carbon dioxide flux measurements were initially taken on day 1245, approximately 6 months following methanol treatment and 2 weeks prior to whey + methanol treatment. Oxygen diffused into the test columns at a rate of approximately 0.4 $mg/cm^2/hr$ and into the control column at 0.5 $mg/cm^2/hr$. CO_2 efflux from the test columns was measured at 0.01 $mg/cm^2/hr$. A similar rate of CO_2 influx was measured in the control column (Figure 15). The greater oxygen influx in the control column is unexpected based on the soil gas monitoring data (Figure 14), which suggests a higher oxygen gradient (between the column surface and port 1) in the test columns at this time

(circa day 1245), a condition which would cause a larger driving force for oxygen diffusion. It is likely that this condition results from partially occluded pore spaces in the test columns impeding gas diffusion. Enhanced attached bacterial growth has been shown to be capable of reducing hydraulic conductivity and permeability in laboratory and field studies (Cunningham et al., 2003). In this case, gas permeability reductions would result from both effective porosity reduction and increased water saturation resulting from enhanced bacterial growth in the test columns (see equations 18 and 19).

Solid phase microbial enumeration was performed on day 1213, approximately 5 months following methanol addition. Samples were collected from depths of 3", 9", 18", and 30" in each column, whereas in previous solid phase sampling events 3" depth samples were not collected. Heterotrophic bacteria were found to be relatively abundant at the 3" depth in all columns (Table 11), however overall HPC numbers evidently dropped as a result of methanol treatment, with the exception of 18" in TC1. IOB/SOB evidently decreased to very low levels over this period as they were enumerated at less than 10 cells/g in all samples. SRB also decreased in all samples except 18" in TC1 and 30" in TC2. In the control column, SRB were not detected in any samples.

Whey and Methanol Addition Day 1232, 1246

Because methanol treatment proved to be less successful than anticipated, a combined treatment of whey followed two weeks later by methanol was applied on days 1232 and 1246, respectively, approximately 6 months after the methanol addition described above. Beginning approximately 2 months following this combined treatment, effluent pH increased from 3.9 to 4.9 in TC1 and from 3.6 to 4.9 in TC2. This period of

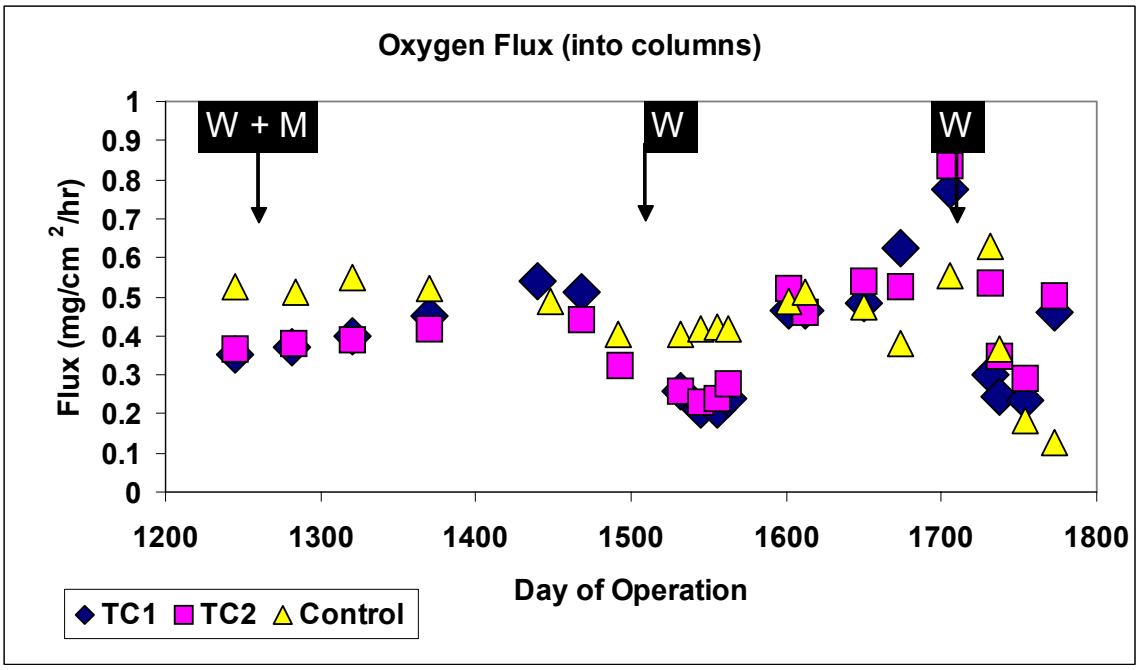

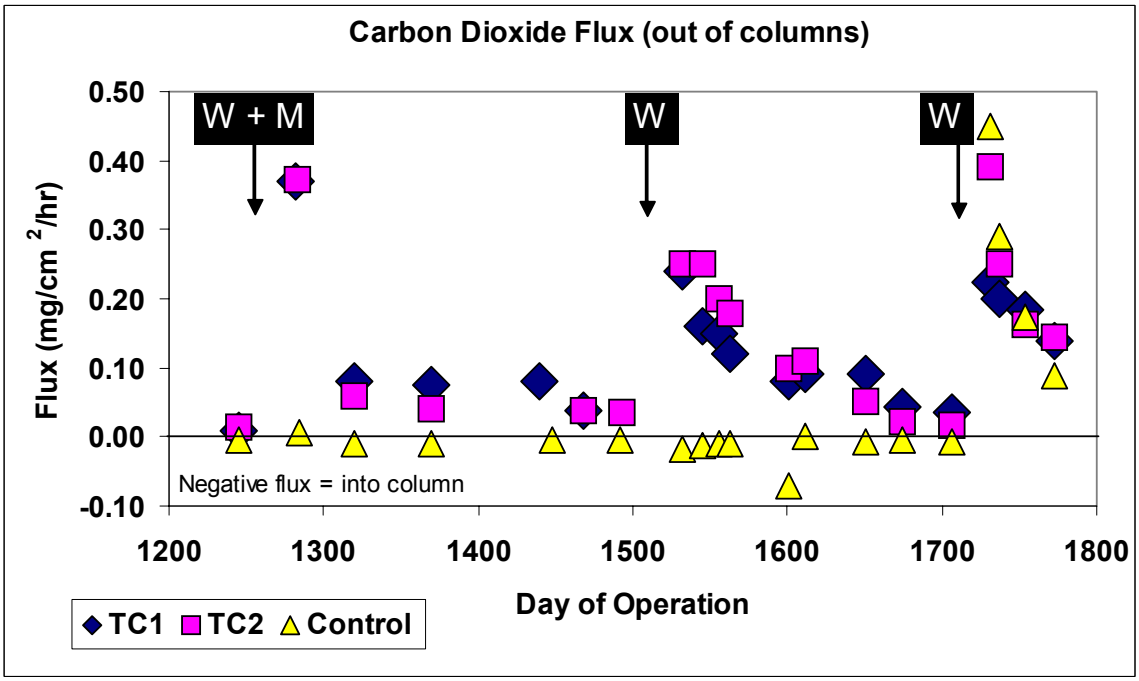

Figure 15. Oxygen and carbon dioxide flux in Fox Lake columns. Whey and methanol addition points are noted.

pH increase lasted for only approximately 100 days, however, whereupon pH began to drop in both test columns (Figure 9). Control column effluent pH remained stable at approximately 2.0 over this period. Concurrently, effluent ORP also remained stable in the control column (at approximately +300 mV) while dropping from -100 to -330 mV in TC1 and from +150 to -210 mV in TC2 (Figure 10). At approximately day 1420, ORP began to increase in both test columns, coinciding with the pH drop described above.

Effluent dissolved metals measured following the combined treatment suggest a more efficacious treatment than methanol alone. Effluent Al, As, Fe, Pb, and Zn dropped following the combined treatment (Figure 11). Only Cu (already at a relatively low concentration) remained stable. Effluent S dropped almost 3-fold in the test columns following the combined treatment, from 25,000 mg/L to less than 10,000 mg/L.

Initially, concurrent whey and methanol addition had no apparent effect on effluent microbial numbers (Figure 13). However, after approximately day 1400, both SRB and HPC increased approximately 2 orders of magnitude in the test columns. It is interesting to note that this increase was coincident with decreasing pH and increasing ORP. Solid phase microbial enumeration supports these data in the case of HPC in TC2, showing large increases in heterotrophic bacteria between the day 1310 and day 1483. In TC1, HPC were found to increase at a depth of 3”, but drop at 9”, 18” and 30” depths (Table 11). Small increases in SRB were measured in both test columns at 30” depths, however, the greatest concentration measured was 170 MPN/g, significantly below what would be expected based on the concurrently measured effluent concentration of over 10^4 MPN/ml (Figure 13).

In contrast to the vadose zone gas data collected immediately following methanol treatment alone, the combined whey/methanol treatment caused an immediate and sharp increase in CO_2 in both ports in the test columns (Figure 14). At port 2 depths (18" and 16" in TC1 and TC2, respectively), CO_2 was measured at 20-25% from treatment until approximately day 1400. At port 1 depths (6" and 4" in TC1 and TC2, respectively), CO_2 was initially measured at 7-10% in both columns. However, this measurement dropped to under 3% in TC2 by day 1350, while remaining at 7-8% until day 1400 in TC1. These data suggest CO_2 generation at depths of >18" in both test columns and diffusion of CO_2 to the upper reaches of the columns. Furthermore, the differences in port 1 between TC1 and TC2 indicate less CO_2 in TC2 at shallow depths, possibly indicating greater consumption by autotrophic bacteria (greater CO_2 flux out of TC2 could also account for lower pCO_2 readings at port 1, but measured fluxes were similar between the columns at this time). By day 1500 (8 months following treatment), CO_2 levels had dropped to under 5% at both ports in both test columns.

Oxygen levels in port 1 of TC1 and TC2 rose from 3% to 10% immediately following the combined treatment (Figure 14). This increase was significantly less than that observed following methanol treatment alone. In TC1, the increase was short-lived, as O_2 levels dropped to pre-treatment levels by day 1350. In TC2, however, oxygen levels continued to climb, stabilizing at approximately 15% by day 1350. In port 2, oxygen was measured ephemerally in TC2, but was generally absent from both test columns following treatment. At port 1 depths, oxygen levels remained <5% in TC1, but >10% in TC2 from day 1350 to 1500.

Gas flux data collected immediately before the combined treatment indicates similar levels of oxygen influx for all three columns (Figure 15). CO_2 efflux from both TC1 and TC2 was 0.01 mg/cm^2/hr, and CO_2 influx into the control column was 0.01 mg/cm^2/hr. While oxygen influx did not change significantly as a result of combined whey and methanol treatment, CO_2 efflux increased to 0.37 mg/cm^2/hr in the test columns, indicating much greater net production within the columns. CO_2 influx into the control column remained stable during this period. In the six months following the combined treatment, O_2 influx remained stable in all columns, while CO_2 efflux decreased in the test columns to 0.05 mg/cm^2/hr.

Whey Addition Day 1503

Whey was again added to the test columns on day 1503, approximately 9 months following the combined whey/methanol treatment. At this time, effluent pH had dropped to 4.1 and 3.0 in TC1 and TC2, respectively (Figure 9). ORP was concurrently measured at -80 and +150 mV, in TC1 and TC2, respectively (Figure 10). In the control column, pH and ORP were 1.5 and +400, respectively. As with previous whey treatments, this whey addition caused effluent pH to increase and ORP to decrease in the test columns, although this effect was more pronounced in TC2, which was both more acidic and more oxidized than TC1 at the time of treatment. In the 6 months following treatment, pH in both test columns increased to 4.3, an increase of 0.2 units in TC1 and 1.3 units in TC2. Concurrently, effluent pH in the control column increased to 2.1. Effluent ORP dropped 140 mV in TC1 and 250 mV in TC2, while remaining stable in the control column.

Effluent dissolved metals generally decreased in both test columns following treatment, but the magnitude of this drop was significant only in the case of Al, which fell from 800 mg/l to approximately 100 mg/l in both test columns (Figure 11). Concurrently, effluent S dropped from approximately 25,000 mg/l to 5,000 and 11,000 mg/l in TC1 and TC2, respectively (Figure 12).

This whey treatment did not have a profound effect on effluent microbiology. Effluent SRB dropped one order of magnitude in both test columns following treatment, but were within the range of variation observed historically through column operation (Figure 13). IOB/SOB remained stable in TC1 at 10^4 MPN/ml, but dropped in TC2 from 10^3 to 10^2 MPN/ml. HPC were highly variable in effluent from TC2 and the control column, while remaining stable in TC1.

Core samples were taken from each of the columns on day 1710 (approximately 7 months following the whey treatment on day 1503) and analyzed for attached HPC, IOB/SOB, and SRB at various depths. As with previous core samples, very few IOB/SOB were enumerated from any level in any column (Table 11). HPC were abundant in the test columns, as with previous solid-phase microbial analyses. SRB were abundant only at the 30" depth in the test columns, and were absent from the control at all depths.

Prior to whey treatment on day 1503, oxygen levels at port 1 were 1-5% in TC1 and approximately 15% in TC2 and the control column (Figure 14). Oxygen was not present in either test column at port 2 depth. Prior to treatment, CO_2 levels were very low at both measurement depths in all three columns. Vadose zone gas analyses indicated a

very different response to whey treatment when compared to previous methanol and methanol + whey treatment. Oxygen partial pressure did not change dramatically immediately following whey treatment in either test column, as had occurred with both previous methanol and methanol + whey treatments and CO_2 levels increased immediately and to a greater extent than observed following the previous whey and/or methanol treatments. Approximately 2 months following whey treatment, O_2 levels at port 1 in TC2 (which had been much higher than in TC1 prior to treatment) decreased from 15% to 9%, indicating greater aerobic bacterial growth, while levels in TC1 remained constant at 5%. After reaching a peak of over 40% in port 2 of both test columns immediately after treatment, CO_2 levels dropped back to pre-treatment levels after approximately 60 days. Elevated concentrations of CO_2 persisted longer at all depths following the whey + methanol treatment than the whey treatment alone.

Gas flux measurements indicated decreased O_2 flux into the test columns and increased CO_2 flux out of the columns (Figure 15). The increase in CO_2 efflux is expected based on the production of CO_2 via heterotrophic bacterial growth following whey addition to the test columns, but this conceptual model would also suggest that O_2 movement into the fed columns would increase. The decrease in oxygen flux is probably a result of decreased gas permeability following whey addition both as a result of biomass occlusion of pore spaces and due to a thin coating on the surface of the treated columns, which was noted for approximately one month following whey addition events.

During sampling for phylogenetic analysis on day 1700, tailings pH was measured as a function of depth within the columns. These data indicate that all three

columns were highly acidic throughout most of their depth, but the treated columns had a thin layer (<6”) at the bottom where pH increased approximately 3 units (Figure 16). Samples taken from the columns were uniformly orange-brown in color, with the exception of the 33” and 36” depth samples from TC1 and TC2, which were black.

Final Whey Addition Day 1710

A final whey addition was performed on day 1710 to determine the immediate effects of whey treatment on attached microbial populations through phylogenetic analysis. Pre- and post-treatment core samples were taken approximately 1 week before treatment and three weeks following treatment, respectively. All three columns received whey addition during this treatment. This is the only time the control column received organic carbon during these experiments. Four depths were sampled in each of the columns (6”, 12”, 24”, and 36”). Column core pH was also measured during this sampling, as described above for the pre-treatment sample. This sampling indicated similar conditions to the pre-treatment sample with two notable exceptions. First, the whey addition the control column, which received no organic carbon heretofore, caused an increase in shallow zone pH from less than 2 to almost neutral conditions; and second, the higher pH zone at greater than 30” depths in the test columns evidently expanded as a result of treatment (Figure 16).

Genetic material extracted from tailings samples was amplified via polymerase chain reaction (PCR) and amplified product from each sample was analyzed via denaturing gradient gel electrophoresis (DGGE). DGGE results from the pre-treatment tailings samples are shown in Figure 17. Prominent bands (labeled 1-20 in Figure 17)

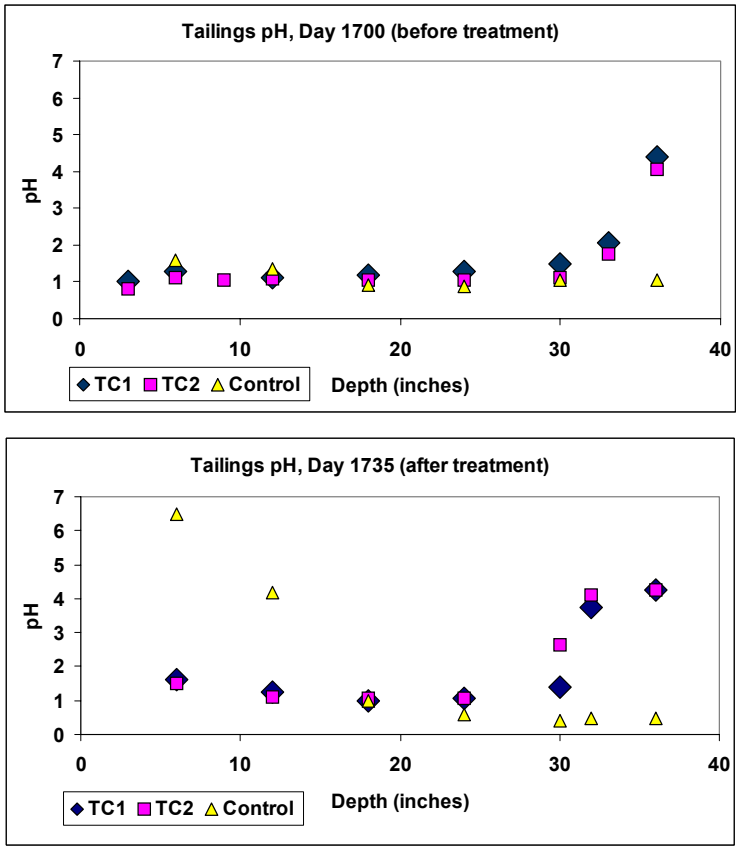

Figure 16. Tailings pH measured in core samples on days 1700 and 1735, immediately before and 3 weeks following the final whey addition to all columns (including the control column).

were selected from the DGGE gel and were harvested for sequencing and phylogenetic analysis via BLAST search techniques. Results of this analysis are shown in Table 13, with genus and, where appropriate, species identification. The DGGE banding pattern illustrates the differences between the test columns and the control, particularly at the 24" and 36" depths. Homology with identified species varied from 93-98%, sequence length varied from 150-300 base pairs. Eight unique genera were identified among the BLAST search results shown in Table 13. The occurrence of these bands among the Fox Lake samples is shown in Table 14.

The most prominent band which could be identified (band 5 in Figure 17) best matched the genus *Pantoea*, a group of facultatively anaerobic, heterotrophic, dissimilatory metal-reducing organisms within the γ-subdivision of *Proteobacteria* (Francis et al., 2000). While the conditions in the test columns clearly offer this bacterium the organic carbon, solution phase metals, and generally anoxic conditions which favor its growth, its abundance in the control column (which, at the time of this sampling had received no organic carbon) is less expected. SRB were identified in all three columns, as members of the genera *Desulfotomaculum* and *Desulfosporosinus* (bands 10 and 3). Members of both closely related, gram-positive genera have been found in mine tailings environments (Suzuki et al., 2003). The DGGE band signature for SRB was clearly strongest at the 36" depth in both test columns, although a faint SRB band signature could be identified at all levels even in the control column. Bands representing iron- and sulfur oxidizing autotrophs and mixotrophs were clearly present, but were not as ubiquitous as would be expected based on column conditions. *L. ferrooxidans* (band 1) and *At. ferrooxidans* (band 2) appeared most prominent in the upper levels of TC1, while the ecologically flexible *Sulfobacillus ambivalens* was present, although evidently not prominent, in most tailings samples. This organism has been noted to require both elevated levels of CO_2 and organic carbon for optimal growth (Rawlings, 2002). Many bands were identified as members of the genus *Alicyclobacillus*, a group of obligately aerobic and heterotrophic gram-positive organisms often found in acidic environments (Bridge and Johnson, 1998; Simbahan et al., 2004). A band most closely identified with *Ferroplasma acidiphilum* was harvested from only from the 36"

depth in TC1 (band 4). As an obligately aerobic, acidophilic archaea and Fe^{2+} oxidizer, *F. acidiphilum* would be expected to thrive in zones of very low pH (1.7 optimum for growth) and abundant oxygen (Rawlings 2002). Its presence only in the most anaerobic and least acidic zone of TC1 is therefore anomalous. A single band found in the 36" sample from TC2 was identified as *Bacteroides*, a fermentative *Enterobacteria*. Members of this genus are used as indicators of fecal contamination, particularly from livestock (Labrenz and Banfield, 2004). The use of cheese whey in as the primary carbon source may explain the presence of this bacterium. Interestingly, the treatment did not cause an increase in the near-surface pH in either of the test columns.

Vadose zone gas data collected following treatment indicated almost no change in pO_2 in either of the test columns at either measurement port, but an ephemeral decrease in pO_2 in the "control" column at both ports (Figure 14). All columns experienced an increase in subsurface CO_2 as result of treatment, although this increase was shorter-lived in the "control" column. Gas flux data collected following the final whey treatment indicated that O_2 flux into the "control" column decreased by approximately 60%, while CO_2 efflux from this column increased to similar levels measured in the test columns (Figure 15). Together these data indicate that the addition of whey to the highly acidic control column rapidly altered the oxygen flux characteristics and thereby prevented near-surface acid generation whereas it had no clear near-surface pH or O_2 flux effect in either of the test columns. The effectiveness of the treatment in the "control" column is likely due to occlusion of the pore spaces and subsequent prevention of oxygen diffusion.

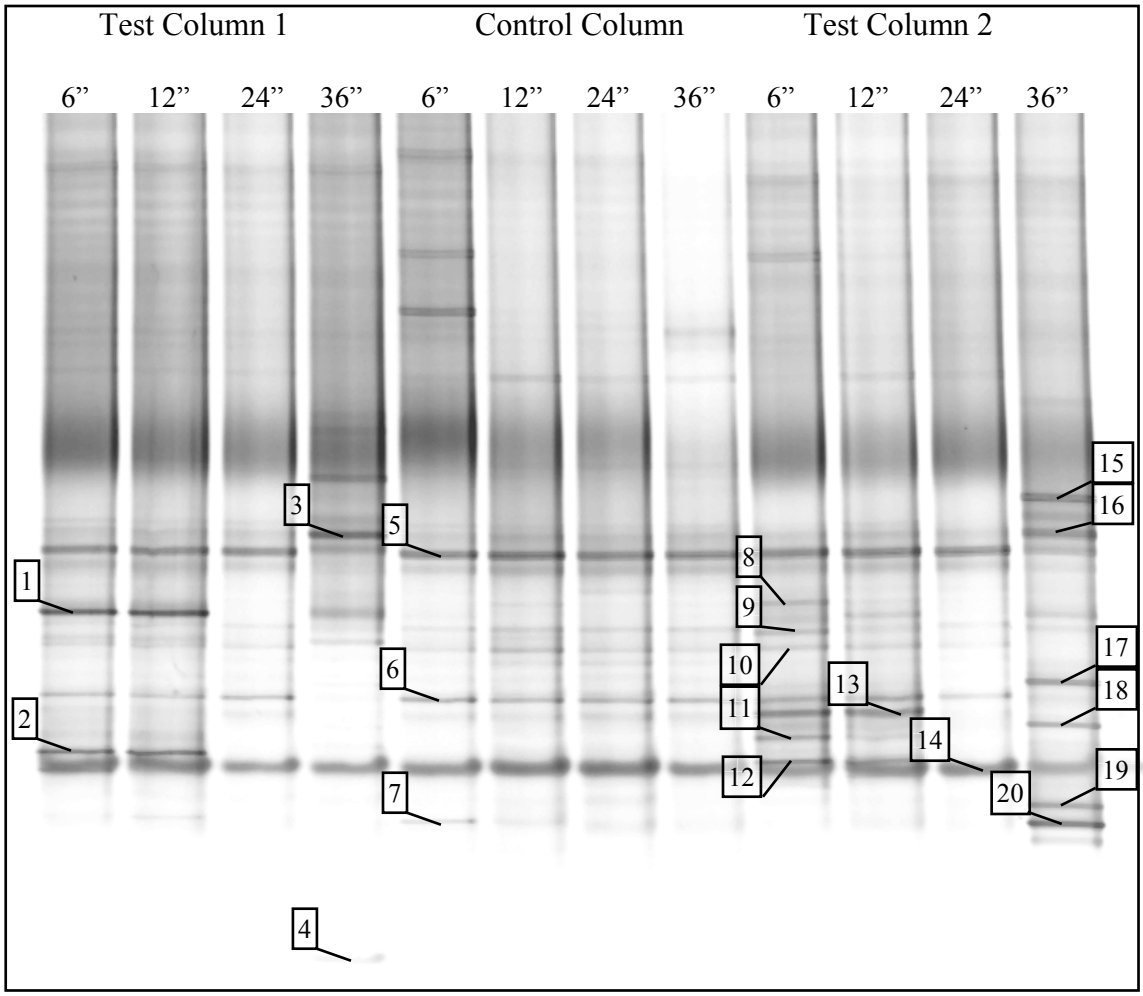

Figure 17. Denaturing gradient gel electrophoresis analysis of Fox Lake columns tailings samples prior to final whey treatment. Numbered bands were selected for sequencing and phylogenic analysis.

Infiltration rate measurements taken before and after treatment indicate no appreciable change in water infiltration rate in the test columns, but a 6 fold decrease in “control” column water infiltration rate, from 12 cm/hr to 2 cm/hr. This could be due to either biomass accumulation or the precipitation of whey solids in the near surface pore spaces. The near surface pH moderating effect in the control column suggests that the heterotrophic bacteria stimulated here were not also capable of iron- and/or sulfur-

Band	Species	Homology
1	*Leptospirillum ferroxidans*	94% match; 293 bases
2	*Acidithiobacillus ferrooxidans*	96% match; 292 bases
3	*Desulfotomaculum* or *Desulfosporosinus*	93% match; 305 bases
4	*Ferroplasma acidiphilum*	97% match; 154 bases
5	*Pantoea*	98% match; 306 bases
6	Unidentifiable	
7	*Sulfobacillus ambivalens*	98% match; 356 bases
8	Unidentifiable	
9	Unidentifiable	
10	*Desulfotomaculum* sp.	94% match; 149 bases
11	*Alicyclobacillus* (*acidocaldarius*)	96% (95%) match; 104 bases
12	*Alicyclobacillus cycloheptanicus*	98% match; 264 bases
13	*Alicyclobacillaceae*	96% match; 227 bases
14	Unidentifiable	
15	*Bacteroides* or (*Acetivibrio*)	96% (94%) match; 305 bases
16	Unidentifiable	
17	Unidentifiable	
18	*Alicyclobacillus*	96% match; 290 bases
19	*Alicyclobacillus*	97% match; 267 bases
20	*Alicyclobacillus*	96% match; 296 bases

Table 13. Band identification for DGGE bands harvested from Fox Lake tailings samples before day 1710 whey treatment.

oxidation, as is likely in the test columns. This pH effect did not translate through to the column effluent, as no pH moderation effect was noted here (Figure 9).

Genetic material extracted from tailings samples following organic carbon treatment in all columns illustrates both some similarities with pre-treatment conditions and changes resulting from carbon addition. DGGE results from post-treatment sampling are shown in Figure 18. As in the pretreatment sampling, prominent bands were selected for sequencing and phylogenetic analysis via BLAST search (labeled 1-21, B, & C in Figure 18). Results of band sequencing are shown in Table 15, and the occurrence of

Species	*L. ferrooxidans*	*At. ferrooxidans*	*Desulfotomaculum* or *Desulfosporosinus*	*Ferroplasma acidiphilum*	*Pantoea.*	*Sulfobacillus ambivalens*	*Alicyclobacillus*	*Bacteroides*
Growth Pattern	Fe^{2+} oxidizer f-Ar	Fe^{2+} ox., S ox., Fe^{3+} red., M, f-Ar	SRB	Fe^{2+} ox., A	f – Ar., H	Fe^{2+} ox., S ox., Fe^{3+} red., A, M, H	Ar, H	An. F.
TC1 – 6”	X	X			X	x	x	
– 12”	X	X			X	x	x	
– 24”			x		X		x	
– 36”	x		X	x	x			
TC2 – 6”			x		X	x	X	
– 12”	x		x		X	x	X	
– 24”			x		X			
– 36”	x		X		x		X	X
CC – 6”			x		X	X	x	
– 12”			x		X	x	x	
– 24”			x		X	x	x	
– 36”			x		X		x	

Table 14. Identification of organisms from bands harvested from DGGE gel before whey treatment and occurrence in column samples. X = abundant (strong band signature), x = present but not abundant (weak band signature). Growth pattern codes: A = autotrophic growth, An = anaerobic growth, Ar = aerobic growth, f-Ar = facultative growth, F = fermentative growth, H = heterotrophic growth, M = mixotrophic growth.

these bands is among the post-treatment samples is shown in Table 16. The most prominent band, visible in all column samples, was most closely matched with a gram positive, iron-oxidizing a member of *Alicyclobacillaceae*. Several bands were identified as acidophilic pseudomonads, but otherwise obligately heterotrophic organisms, other than SRB did not appear prominent. The occurrence of bands identified as SRB (*Desulfosporosinus*, *Desulfitobacterium*, or *Desulfotomaculum*) increased following organic carbon treatment, and were clearly more prominent at the 24" and 36" depths of TC1 and TC2. Despite whey treatment during this period, the "control" column did not contain SRB bands. The appearance of bands 11, 12, 20 and 21 at the 6" depth in the "control" column probably resulted from treatment (Figure 18). Bands 11, 12 and 21 were identified as most closely matching two gram positive, iron-oxidizing acidophiles also capable of Fe^{3+} reduction, heterotrophic growth, and sulfur oxidation (Johnson et al., 2003). Band 20 was most closely matched with a *Pseudomonas* strain recently identified from deep-sea sediments which also contained members of *Shewanella* (Wang et al., 2004). Comparison of the pre- and post-treatment DGGE gels suggests increased diversity as a result of treatment in the deeper zones of TC1 and TC2. Additionally, no evidence of increased non- Fe-oxidizing heterotrophic organism presence was noted in the "control" column, despite whey addition.

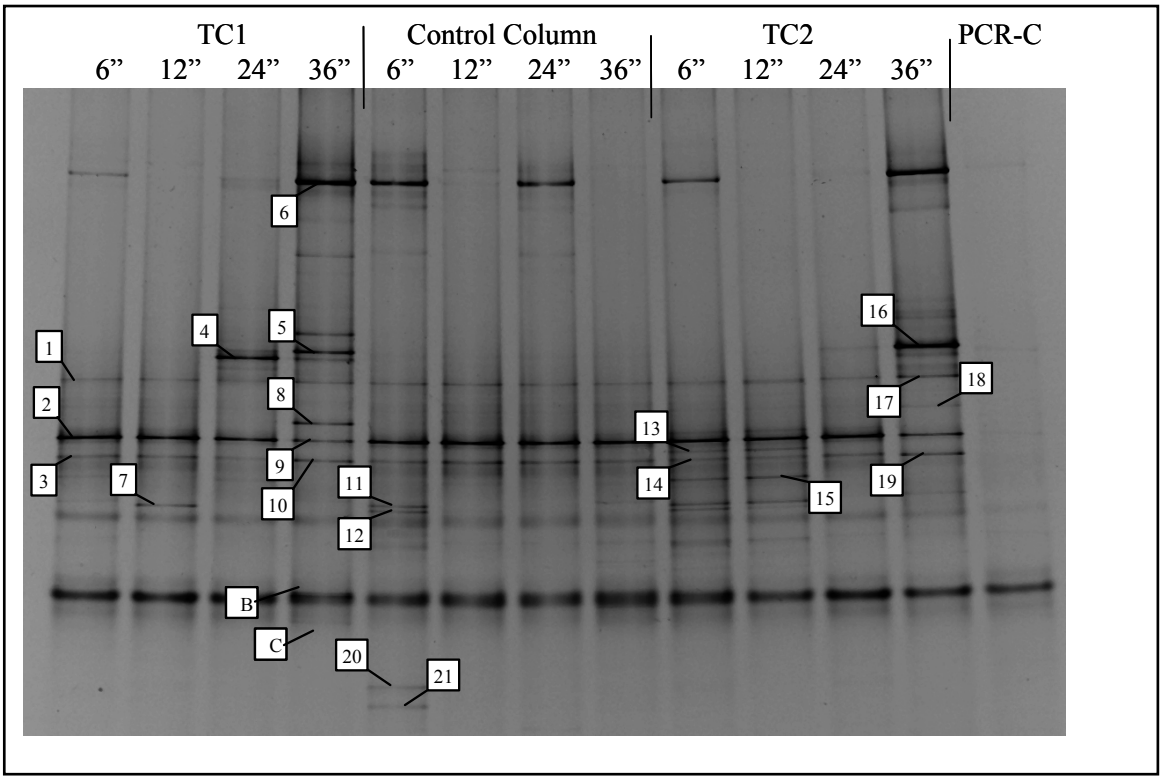

Figure 18. Denaturing gradient gel electrophoresis analysis of Fox Lake columns tailings samples after final whey treatment. Numbered bands were selected for sequencing and phylogenic analysis.

Mammoth Column Baseline Conditions

A total of six Mammoth tailings columns were operated during this experiment. The first two Mammoth columns were started in October 2000 (designated Day 0). One of these columns received two whey treatments (“whey 2X”) and the other was kept as the control column and received only water (“water only”). Baseline conditions for pH, ORP, effluent metals and effluent microbiology were determined for these two columns after approximately one month of accelerated weathering at an influent flowrate of 200 mL/week and prior to the addition of organic carbon to the whey 2X column. These data are shown in Table 17.

Band	Species	Homology
1	Unidentifiable (similar to Band 17)	
2	Gram-positive iron-oxidizing acidophile G1 Bacteria; Firmicutes; Bacillales; *Alicyclobacillaceae*	88% match; 285 bases
3	uncultured gamma proteobacterium Bacteria; Proteobacteria; Gammaproteobacteria;	85% match; 129 bases
4	*Desulfitobacterium metallireducens*	94% match; 238 bases
5	*Desulfitobacterium metallireducens* or *Desulfosporosinus orientis*	85% match; 168 bases 84% match; 167 bases
6	Unidentifiable	
7	*Pseudomonas* sp.	94% match; 311 bases
8	*Desulfosporosinus* sp.	84% match; 145 bases
9	*Desulfosporosinus* sp.	86% match; 256 bases
10	*Desulfosporosinus orientis*	86% match; 165 bases
11	Gram-positive iron-oxidizing acidophile Y0010 Bacteria; Firmicutes; Bacillales; *Alicyclobacillaceae*	90% match; 301 bases
12	Gram-positive iron-oxidizing acidophile Y0010 Bacteria; Firmicutes; Bacillales; *Alicyclobacillaceae*	82% match; 90 bases
13	Unidentifiable	
14	Unidentifiable	
15	*Desulfotomaculum auripigmentum* or *Desulfosporosinus* sp.	91% match; 349 bases 91% match; 349 bases
16	*Pseudomonas* sp.	89% match; 268 bases
17	*Desulfosporosinus* sp. or *Desulfitobacterium metallireducens*	92% match; 242 bases 91% match; 170 bases
18	*Desulfosporosinus* sp.	91% match; 200 bases
19	*Thermoactinomyces peptonophilus* or *Alicyclobacillus* sp.	91% match; 163 bases 90% match; 128 bases
20	*Pseudomonas* sp. An20	92% match; 295 bases
21	Sulfobacillus sp. YTH2 or *Alicyclobacillus tolerans*	86% match; 48 bases 86% match; 48 bases
B	*Desulfosporosinus* sp.	83% match; 135 bases
C	*Desulfosporosinus* sp.	83% match; 135 bases

Table 15. Band identification for DGGE bands harvested from Fox Lake tailings samples after day 1710 whey treatment.

Species	*Alicyclobacil -laceae*	*Desulfito- bacterium*	*Pseudomonas*	*Desulfosporo -sinus*	*Desulfoto- maculum*	*Thermoacti- nomyces*	*Sulfobacillus* or *Sulfo-bacillus*-like
Growth Pattern	Gram +, Fe^{2+} Ox.,	SRB	H	SRB	SRB	AR,H	Fe^{2+} ox., S ox, Fe^{3+} red., A,M,H
TC1 – 6”	X						
–12”	X		x				
–24”	X	X		x			
–36”	x	X		X	x		
TC2 – 6”	X				x		X
–12”	X				x		x
–24”	X	x		x		x	
–36”	x	x	X	X		X	
CC – 6”	X		x				X
–12”	X						X
–24”	X						
–36”	X						

Table 16. Identification of organisms from bands harvested from DGGE gel after whey treatment and occurrence in column samples. X = abundant (strong band signature), x = present but not abundant (weak band signature). Growth pattern codes: A = autotrophic growth, An = anaerobic growth, Ar = aerobic growth, f-Ar = facultative growth, F = fermentative growth, H = heterotrophic growth, M = mixotrophic growth.

	Whey (2X)	Water Only
pH	3.49	3.54
ORP (mV)	+364	+396
Microbiology		
Heterotrophic bacteria (CFU/mL)	2.8×10^2	2.1×10^2
Sulfur/Iron-oxidizing bacteria (MPN/mL)	1.0×10^2	1.4×10^2
Sulfate-reducing bacteria (MPN/mL)	1.7×10^1	1.0×10^1
Metals (mg/L)		
Aluminum	2.8	2.6
Arsenic	0.03	0.03
Cadmium	BDL	BDL
Cobalt	BDL	BDL
Copper	4.2	4.1
Iron	21.4	20.3
Lead	BDL	BDL
Magnesium	2.0	2.5
Manganese	0.09	0.11
Zinc	4.3	2.9
Sulfur (mg/L as S)	81	62

Table 17. Baseline effluent conditions for Mammoth tailings columns prior to whey addition. BDL: below detection limits.

Within a month of the beginning of operation, acidic conditions developed in both columns and ORP stabilized at 350-400 mV. HPC and IOB/SOB were present in effluent from both columns at approximately 10^2 CFU/mL. With the exception of iron, effluent metals from both columns were below 5 mg/L. Interestingly sulfur was present at 3-4 times the concentration of Fe in pre-treatment column effluent. Under similar pH but 200 mV lower ORP conditions, Fox Lake columns produced only 1.4 – 1.7 times as much S as Fe (Table 9). The elemental composition of the tailings as determined via EDS (Table 8) indicated S comprised less than 2% of the total Mammoth tailings mass, in contrast to the Fox Lake tailings, wherein S comprised over 20% of the mass. The dissolved phase

Fe:S ratio differences are explained by the STABCAL predominance diagrams, which indicate Fe was much more likely to be soluble under the Fox Lake initial conditions than Mammoth (see below). An iron-controlled predominance diagram calculated using STABCAL for pH 3.5 and Eh 550-600 mV (this correlates with an ORP of 350-400 mV as measured by the Ag-AgCl electrodes used) indicates that the initial conditions are near the boundary of FeOOH (solid) and $CuFeO_2$ (solid) (Figure 19). A similar diagram including S species is shown in Figure 20, while a larger scale diagram showing stability regions for other prominent dissolved and solid species is shown in Figure 21. These diagrams show the predominant S phase as SO_4^{2-} (aqueous). Distribution diagrams for effluent from the Mammoth columns were also calculated using STABCAL. At pH 3.5, column effluent was predicted to form the compounds shown in Table 18. Individual distribution diagrams for major elements are shown in the Appendix A.

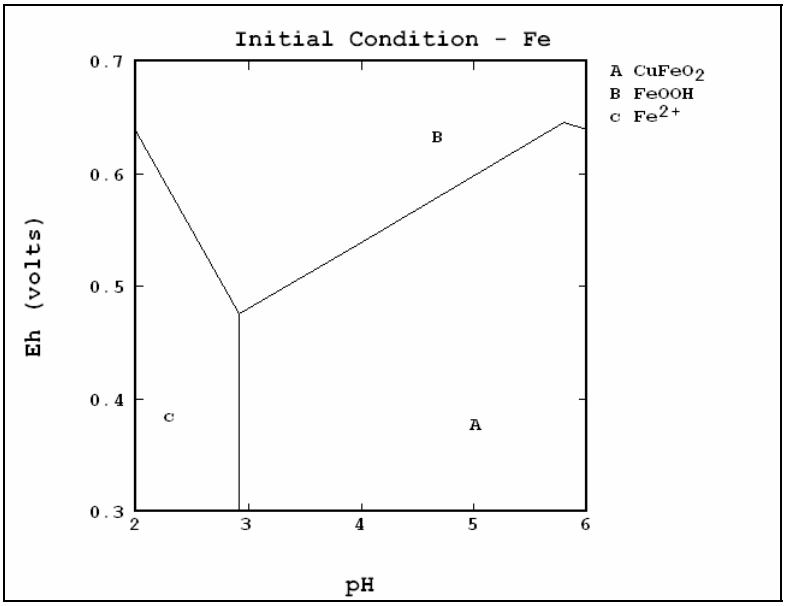

Figure 19. Initial condition stability diagram for Mammoth column effluent considering only Fe species.

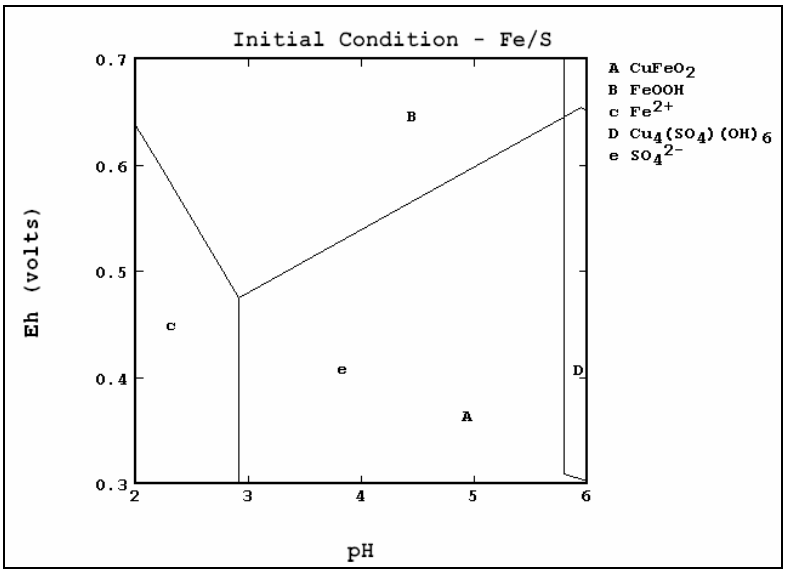

Figure 20. Initial condition stability diagram for Mammoth column effluent considering Fe and S species.

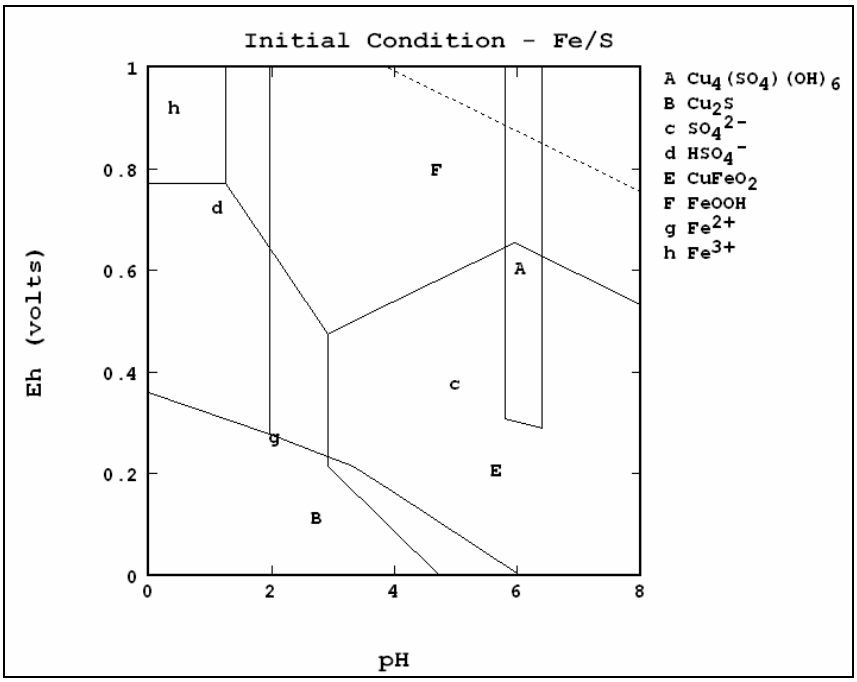

Figure 21. Initial condition stability diagram for Mammoth column effluent showing stability regions of major metals and sulfur.

Element	Major Phase	Secondary Phase	Tertiary Phase
Aluminum	$AlSO_4^+$ (a) (60%)	Al^{3+} (a) (30%)	$Al(SO_4)_2^-$ (a) (10%)
Carbon	H_2CO_3 (100%)		
Copper	Cu^{2+} (a) (75%)	$CuSO_4$ (a) (25%)	
Iron	FeOOH (s) (100%)		
Sulfur	SO_4^{2-} (a) (90%)	HSO_4^- (a) (5%)	$FeSO_4^+$ (a) (5%)
Zinc	Zn^{2+} (a) (70%)	$ZnSO_4$ (a) (30%)	

Table 18. Occurrence of major compounds in Mammoth column effluent as determined through distribution diagram analysis using STABCAL.

Similar to the Fox Lake column distribution diagram analysis, CO_2 in Mammoth column effluent was predicted to remain as H_2CO_3 rather than participating in any complexation reactions. The distribution analysis confirmed the predominant sulfur phase as aqueous SO_4^{2-} and iron phase as the solid FeOOH.

Mammoth Column Whey/Lime Addition Experiments

Effects of Treatment on Effluent pH and ORP

Whey was added to column 1 on days 56 and 119 of operation (Table 7). Whey and/or lime was added to columns 3-6 on day 301 (these columns began operation on day 253). The response of pH to these additions is shown in Figure 22. pH increased immediately after the first whey treatment in column 1 from approximately 3.5 to 5, upon which time the second whey treatment was applied. pH continued to increase to approximately 6 after 200 days of operation. pH fluctuated between 3.5 and 4.0 in the water-only control column (column 2) during this period. The two whey treatments effectively increased effluent pH in column 1 for approximately 2 years. After 700 days of operation, pH dropped from 6 to 5.5 and stabilized for another 6 months until the end

of the experiment at 900 days (Figure 22). Beginning approximately 1 month following the first whey addition, and continuing approximately 2 months after the second treatment, ORP dropped from +450 mV to -300 mV in column 1. ORP gradually increased throughout the remainder of the experiment, staying significantly below the control column (Figure 23), which remained in the +300 to +500 range throughout the experiment.

Columns 3-6, which began operation on day 253, were treated with whey and/or lime on day 301. Column 3 received a single whey treatment, and did not respond as rapidly or to the same extent as column 1, which received 2 whey treatments (Figure 22). After treatment, column 3 effluent pH increased 1.3 units over the next 8 months. In contrast to column 1, pH did not stabilize in column 3, but began a steady drop over the next 8 months, back to pre-test levels. ORP did not decrease significantly in column 3 following treatment (Figure 23).

Column 4 and column 5 each received a single whey treatment combined with a concurrently applied top-dressing of powdered lime. Following treatment, effluent pH in both columns increased approximately 2 units from 4 to 6 over 300 days. Like column 3, the effect of the combined treatment did not persist beyond this point in either column 4 or 5. After the high point was reached at approximately day 600, pH dropped approximately 1 unit and stabilized in the 5-5.5 range in column 4 but continued to drop to approximately 4.5 in column 5 (Figure 22). Effluent ORP in columns 4 and 5 dropped sharply in the 3 months following treatment to -100 to -150 mV in both columns. In column 5, however, ORP increased to above pretreatment levels from day 425 to 500,

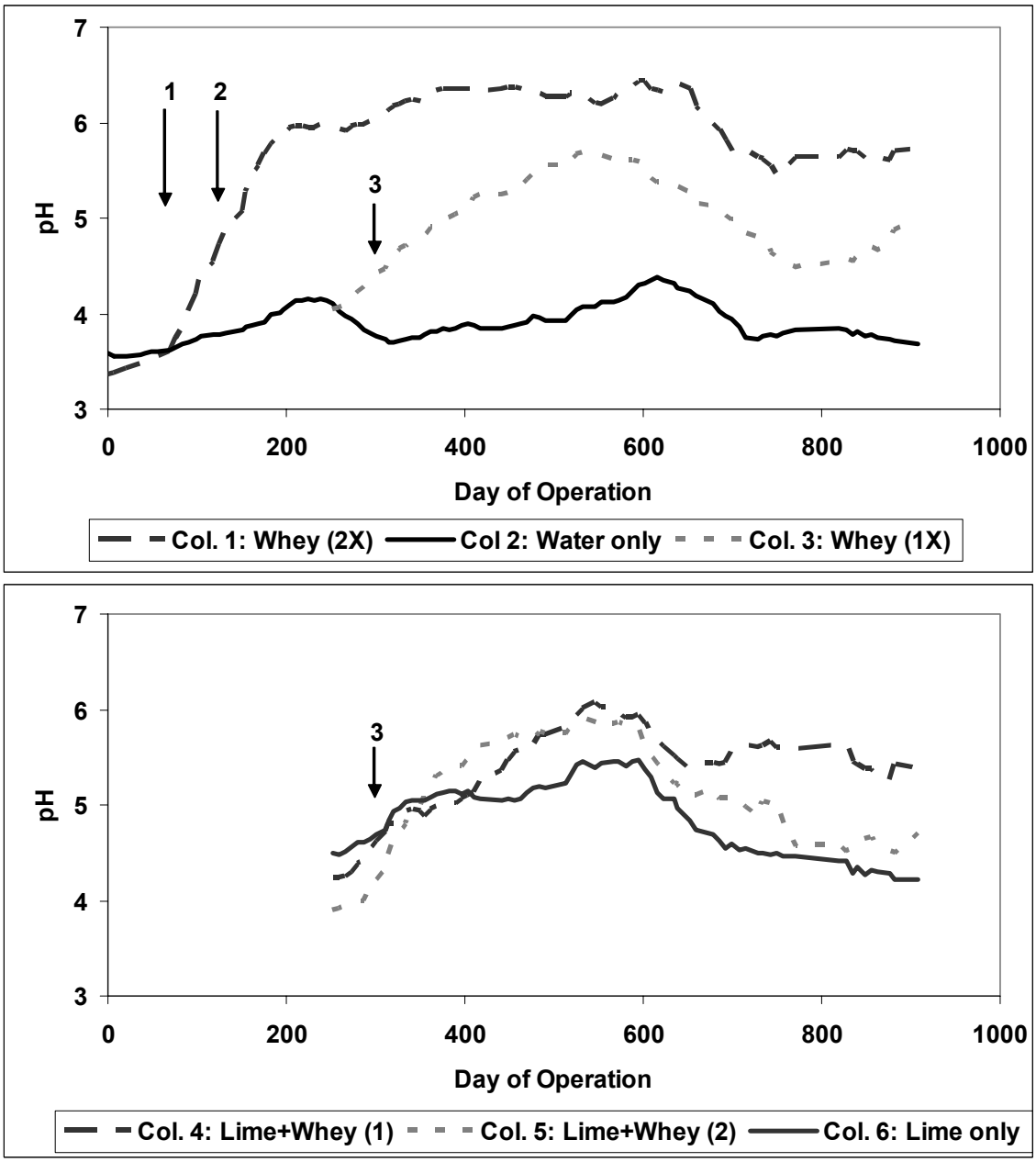

Figure 22. Mammoth columns effluent pH during whey and lime addition experiments. 1: First whey addition to column 1 at day 56. 2: Second whey addition to column 1 at day 119. 3: Whey and/or lime addition to columns 3-6 at day 301.

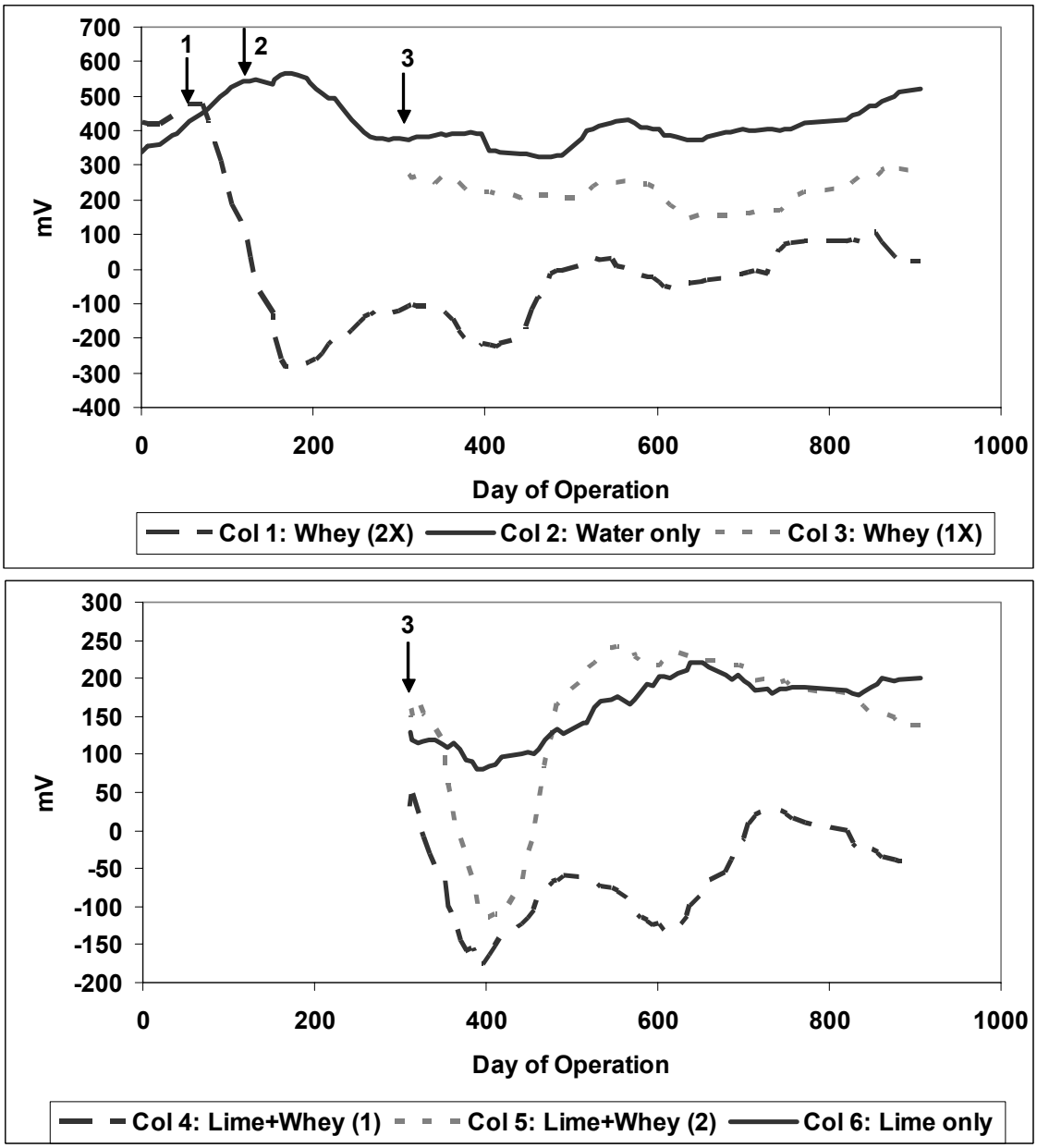

Figure 23. Mammoth columns effluent ORP during whey and lime addition experiments. 1: First whey addition to column 1 at day 56. 2: Second whey addition to column 1 at day 119. 3: Whey and/or lime addition to columns 3-6 at day 301.

while it remained under 0 mV in column 4 for approximately 1 year (Figure 23). In column 5, ORP remained high until the end of the experiment. OPR values collected at intermediate points in column 5 suggest that a leak occurred in this column, allowing atmospheric oxygen to infiltrate and causing effluent ORP values to be unrealistically high.

In column 6, which received only a lime top-dressing, effluent pH increased 1 unit in the year following treatment, then dropped to pre-treatment levels over the next year (Figure 22). Effluent ORP generally remained between +100 and +200 mV throughout the experiment (Figure 23).

The dual whey treatment in column 1 was clearly the most effective in both increasing effluent pH and decreasing ORP for an extended period of time – over 2 years. Concurrent application of dissolved whey with a top dressing of powdered lime did not increase effluent pH appreciably more than whey alone, however it did evidently increase treatment longevity in column 4 (similarly treated column 5 is inappropriate for comparison due to the suspected air leak). The combined treatment was much more effective in reducing ORP than whey treatment alone. Lime treatment alone did increase effluent pH, but was not as effective as the single whey treatment in this regard. Neither the single whey treatment nor the lime alone treatment had an appreciable effect on effluent ORP.

Effects of Treatment on Dissolved Effluent Metals

Dissolved effluent metals were quantified on a monthly to quarterly basis for all columns. Prior to treatment, dissolved Al was measured at 2.6 mg/l in columns 1 and 2

(Figure 24). Dissolved Al in column 1 dropped to below detection limits (0.1 mg/l) within 200 days following treatment whereas column 2 (control) effluent Al remained in the 1-2 mg/l range throughout the experiment. Over the following 2 years of operation, dissolved Al in the twice treated column 1 remained significantly below the control. All other treatments (Columns 3-6) also reduced dissolved Al to below detection limits approximately 1 year following treatment, although the rate of decrease was less for columns 3-6 than for column 1.

Whey and/or lime treatment had a stimulating effect on As production from most treated columns (Figure 25). Arsenic is generally mobilized by reductions in ORP, as it forms a more soluble As (III) under reducing conditions. While As remained below detection limits (0.05 mg/l) in the control, column 1 As increased over 40-fold to 2.2 mg/l. All other treatments also resulted in increased As relative to the control. The treated column showing the least As increase was column 5, the duplicate lime + whey column in which an air leak is suspected.

Prior to treatment, effluent copper was present in columns 1 and 2 at 4-5 mg/l. While remaining at this level in the control column, effluent Cu dropped almost 100-fold in column 1 following both whey additions (Figure 26). Columns 3-5 responded similarly, while column 6 (lime only) produced slightly more Cu during most sample events.

Like arsenic, dissolved iron generally increased following both the whey and lime treatments (Figure 27). In column 1, Fe increased from 27 mg/l to 1460 mg/l following the second whey treatment. The single whey treatment in column 3 caused iron to

increase from 28 mg/l to 140 mg/l. Lime + whey treatment resulted in Fe increasing from 20 to 200 mg/l in column 4 and from 28 to 150 mg/l in column 5 (immediately following treatment). Lime only treatment had the least effect causing an increase from 49 to 90 mg/l. Like arsenic, Fe is more soluble under reducing conditions, where it is more likely to be present as ferrous (Fe^{2+}) than ferric (Fe^{3+}) iron. Effluent Fe remained elevated in columns 1, 3, 4 and 6, but dropped significantly in column 5 at approximately day 425-450, when the air leak is suspected to have begun. This corresponds to relatively high ORP readings in column 5 (Figure 23).

Effluent zinc followed the typical pattern for non-ferrous metals of stability in the control column and significant reduction in the whey and/or lime treated columns (Figure 28), with the familiar exception of column 5, which after an initial reduction in Zn, increased to levels similar to those in the control column. The double whey treatment was evidently the most effective, resulting in Zn levels below the detection limit between days 500 and 700 (Figure 28).

While effluent sulfur remained at approximately 50 mg/l in the control column, increases of varying magnitude were measured in all treated columns (Figure 29). Immediately following the two whey treatments in column 1, effluent S increased over 10-fold to 1010 mg/l. In columns receiving a single whey treatment, S increased to approximately 200 – 250 mg/l (Figure 29) and then returned to pre-treatment levels from 300-400 days following treatment. A slight increase in S was measured in column 6, which received only lime treatment.

Comparison of total Fe produced, total S produced, and the daily production rates of both helps illustrate overall performance of the various treatments with regard to iron dissolution and re-precipitation. In the water only control (column 2), total Fe and S production were lowest, and the Fe:S ratio was 0.2. At the other extreme was the twice-treated column, which produced over 30 times as much Fe and 5 times as much S and had a Fe:S ratio of 1.27 (Table 19). All treatments evidently increased the dissolution of Fe and S from solid phases, and increased the mass of Fe produced relative to S.

Column #: treatment	Total Fe produced (mg)	Mean Fe production rate (mg/d)	Total S produced (mg)	Mean S production rate (mg/d)	Ratio Fe:S (mg/mg)
1: Whey 2X	7268	7.86	5702	6.27	1.27
2: Water	227	0.25	1133	1.25	0.20
3: Whey 1X	1440	2.30	1927	3.08	0.75
4: L+W (1)	1619	2.59	1876	3.00	0.86
5: L+W (2)	690	1.10	1381	2.21	0.50
6: Lime	1172	1.88	1253	2.01	0.94

Table 19. Iron and sulfur production from Mammoth tailings columns for whey/lime treatment experiments.

Initial analysis of the Mammoth tailings via energy dispersive x-ray spectroscopy (EDS) prior to treatment indicated low levels of sulfur (~ 2% by mass) relative to iron (11% by mass), but stability diagrams indicated that sulfur would be present as soluble SO_4^{2-} and iron as solid FeOOH, therefore sulfur should be present in column effluent at concentrations greater than would be predicted by mass percentages alone. EDS observation indicated that Fe was present primarily as ferric oxy-hydroxides but, while S was stable as aqueous sulfate under pre-treatment conditions, the columns' acid generating capability suggests that reduced sulfur was also present, probably as pyrite and chalcopyrite ($FeCuS_2$). If conditions become sufficiently reducing, Fe that was

present as FeOOH could be reduced and mobilized as Fe^{2+}, or mobilization could result from reduced Fe-mineral oxidation and subsequent transport. Even under conditions of stability for FeOOH, the kinetics of goethite formation may not be rapid enough within the columns to completely remove solution phase Fe. The more reducing conditions caused by the whey and lime treatments increased Fe and As solubility and discharge, however, the effect on other metals was an overall decrease in effluent concentrations.

Effects of Treatment on Effluent and Core Microbiology

Viable microbial counts for HPC, IOB/SOB and SRB from Mammoth column effluents were determined on a monthly basis. The two whey treatments had no evident effect on effluent HPC in column 1 compared to the water only control (column 2), whereas effluent HPC were an order of magnitude higher in column 3, which received a single whey treatment (Figure 30). HPC counts were similar in both columns 4 and 5, which received identical whey treatments, while counts were generally lower in column 6, which received only lime treatment. These data do not indicate that either whey and/or lime treatment had a significant effect on effluent HPC.

In contrast to HPC, IOB/SOB evidently were stimulated by the addition of organic carbon in Mammoth columns (Figure 31). Columns 1, 3, 4 and 5 indicated effluent IOB/SOB in the range of 10^2-10^3 MPN/ml whereas the columns receiving either only water or lime generally contained fewer than 10^1 MPN/ml. In whey treated columns, effluent IOB/SOB counts were highest approximately 100 days following treatment, after which they typically dropped to pre-treatment levels. In the untreated control, IOB/SOB generally decreased over the course of the 2 year experiment. The

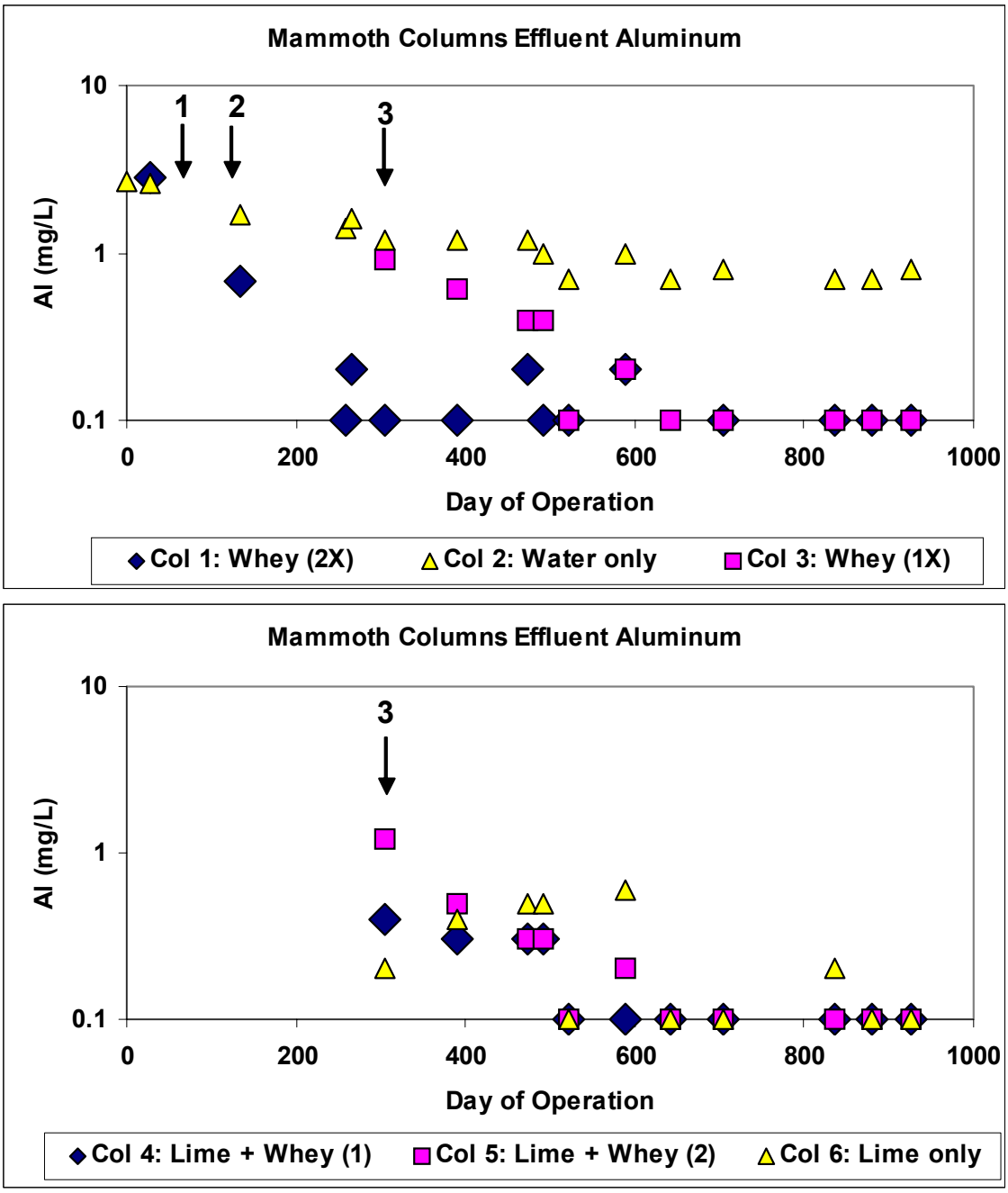

Figure 24. Mammoth column effluent aluminum during whey and lime addition experiments. 1: First whey addition to column 1 at day 56. 2: Second whey addition to column 1 at day 119. 3: Whey and/or lime addition to columns 3-6 at day 301.

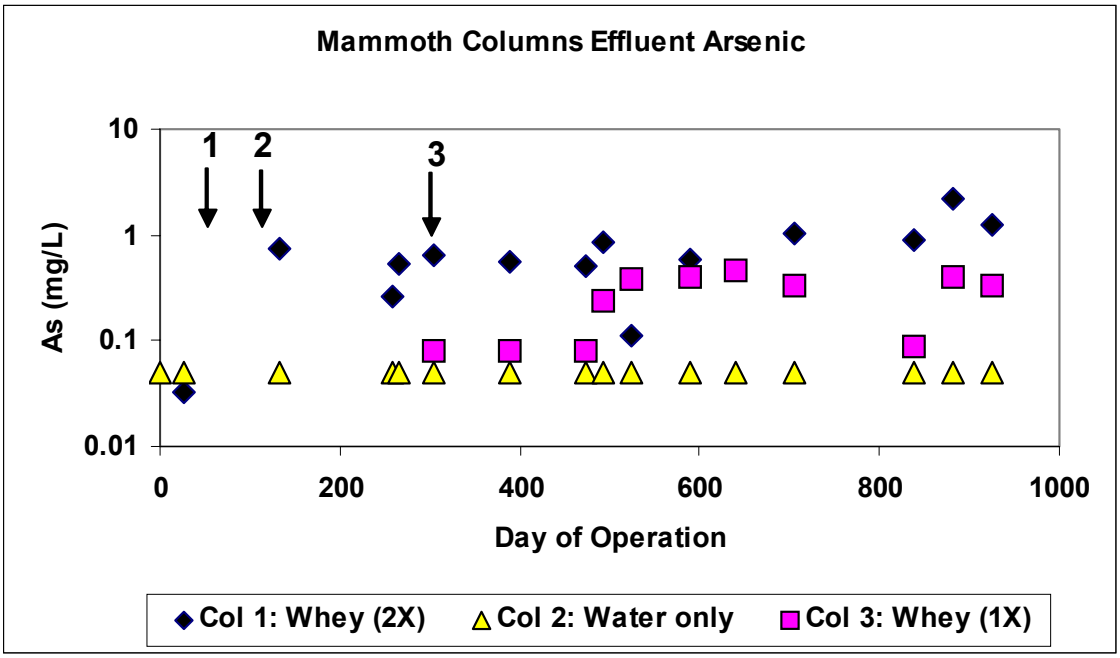

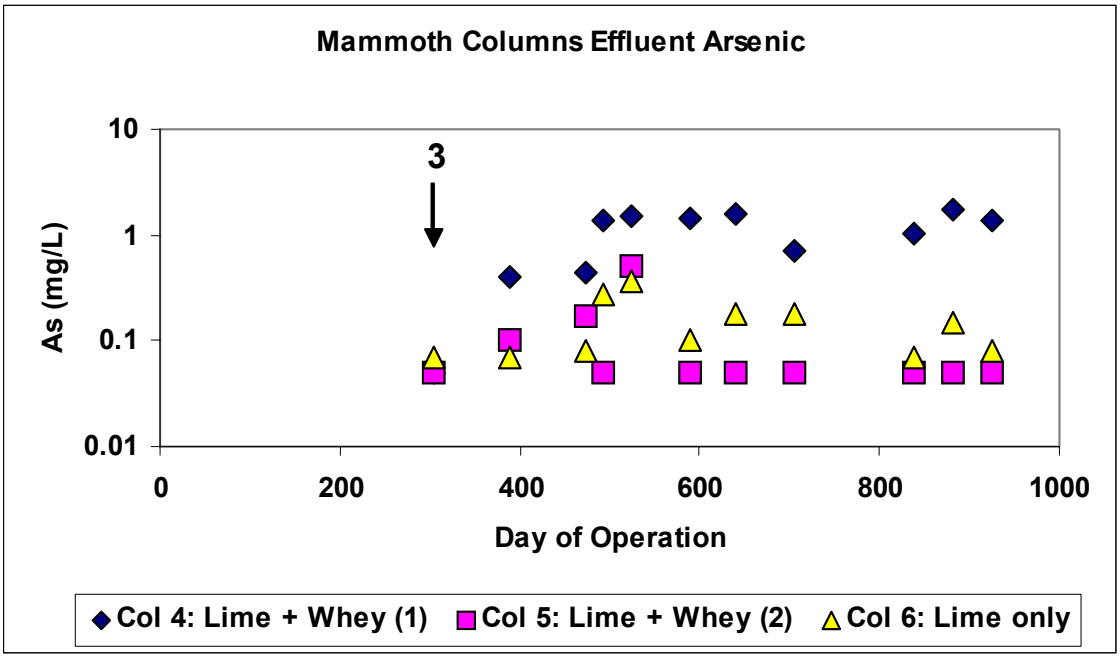

Figure 25. Mammoth column effluent arsenic during whey and lime addition experiments. 1: First whey addition to column 1 at day 56. 2: Second whey addition to column 1 at day 119. 3: Whey and/or lime addition to columns 3-6 at day 301.

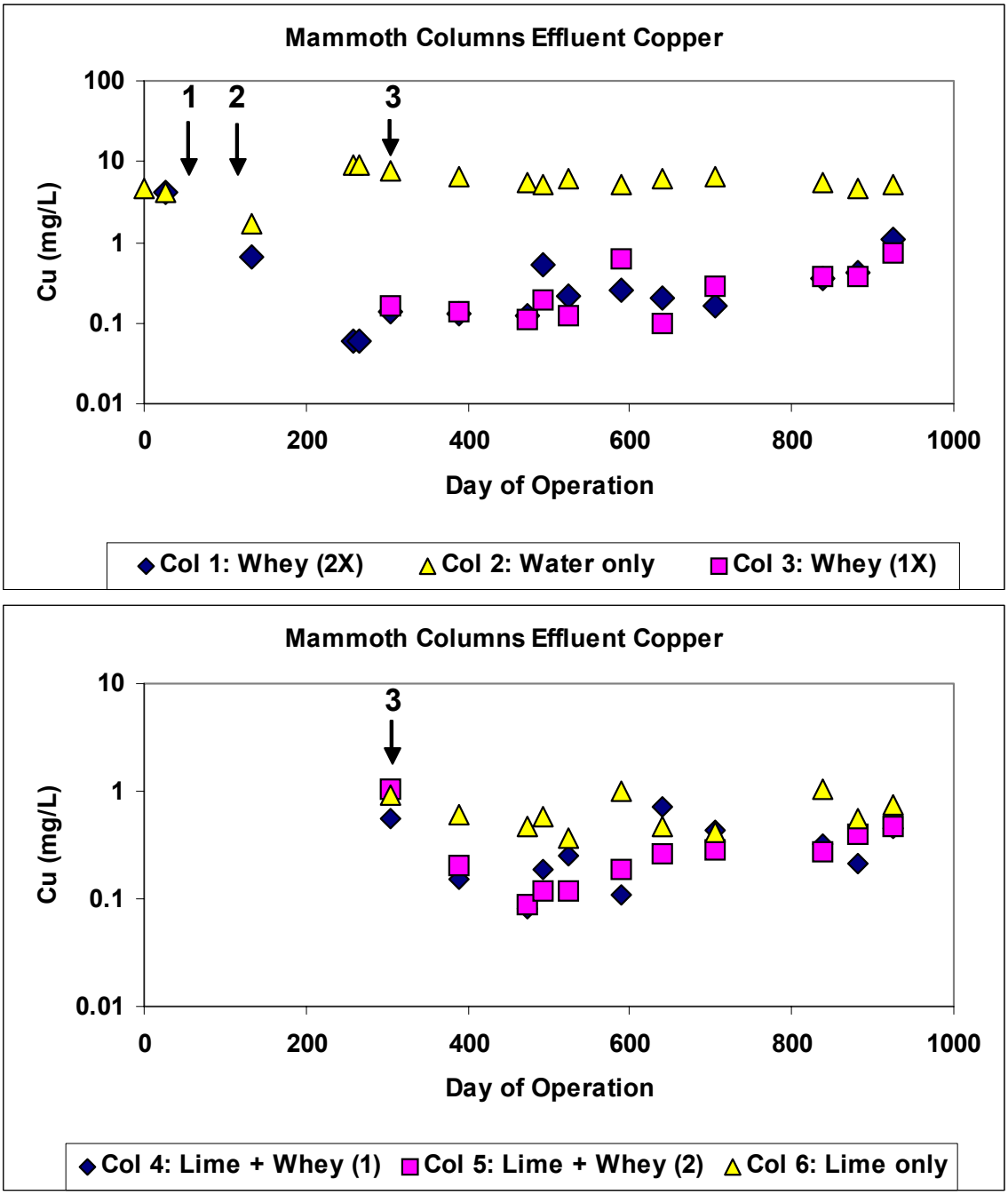

Figure 26. Mammoth column effluent copper during whey and lime addition experiments. 1: First whey addition to column 1 at day 56. 2: Second whey addition to column 1 at day 119. 3: Whey and/or lime addition to columns 3-6 at day 301.

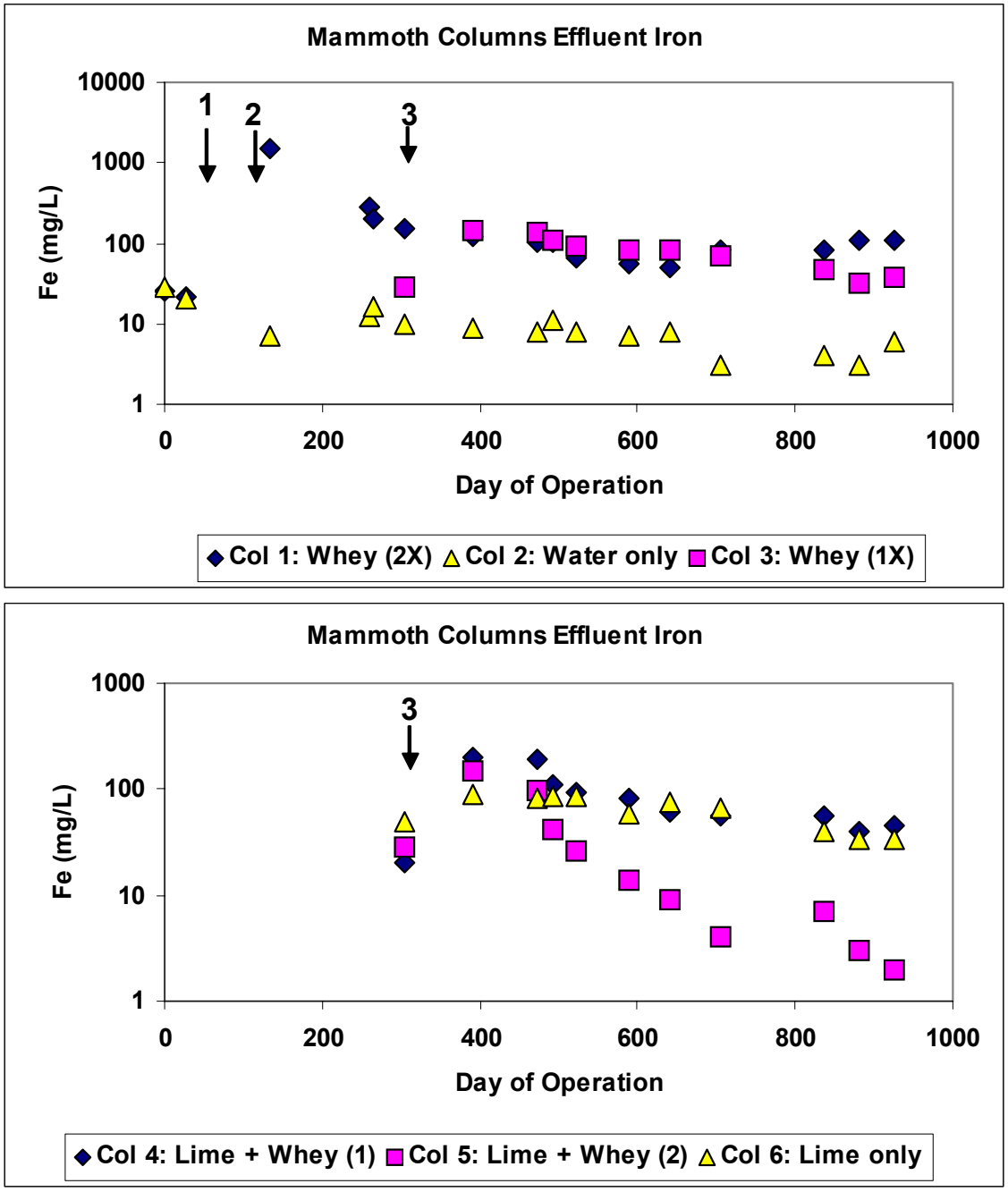

Figure 27. Mammoth column effluent iron during whey and lime addition experiments. 1: First whey addition to column 1 at day 56. 2: Second whey addition to column 1 at day 119. 3: Whey and/or lime addition to columns 3-6 at day 301.

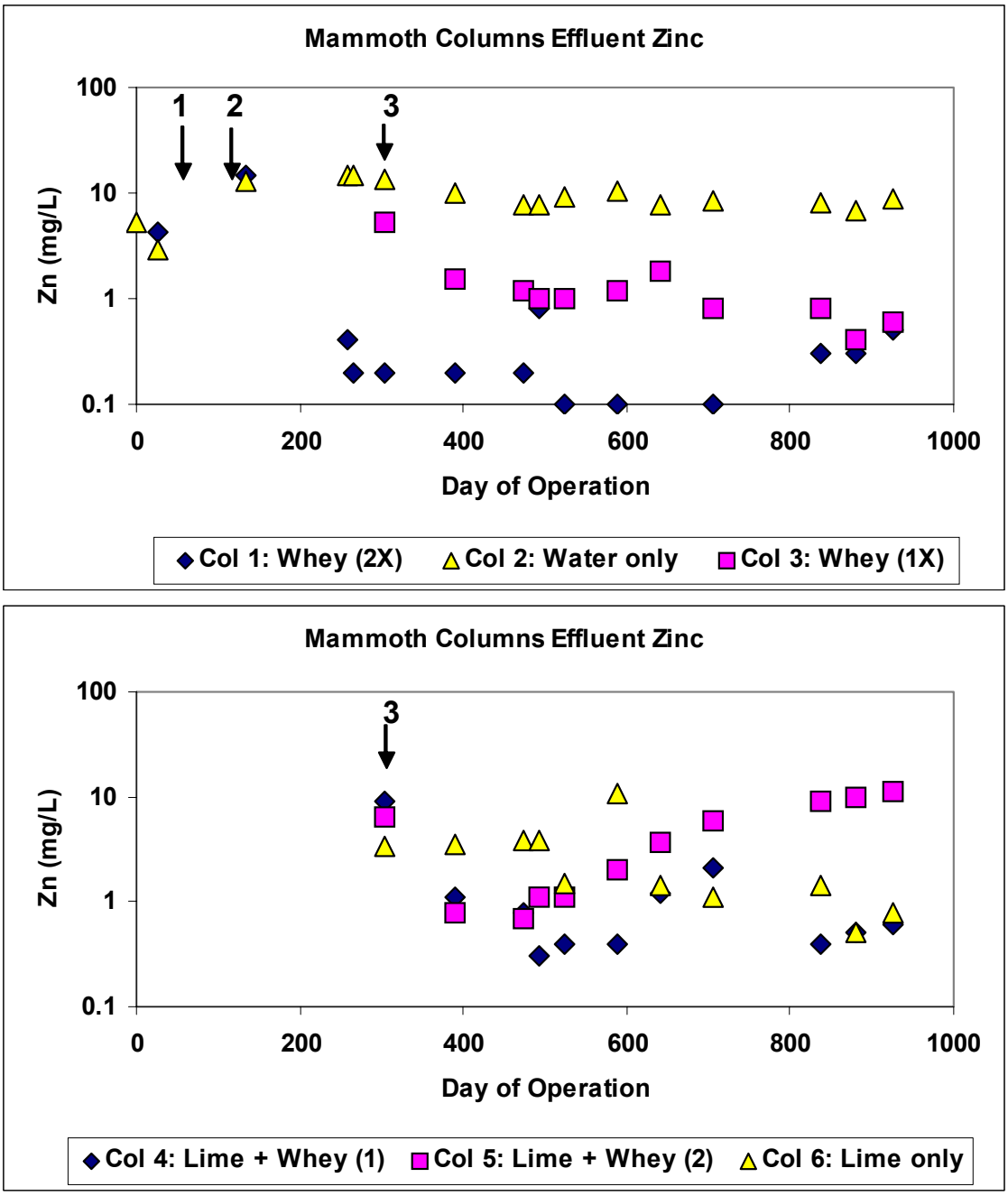

Figure 28. Mammoth column effluent zinc during whey and lime addition experiments. 1: First whey addition to column 1 at day 56. 2: Second whey addition to column 1 at day 119. 3: Whey and/or lime addition to columns 3-6 at day 301.

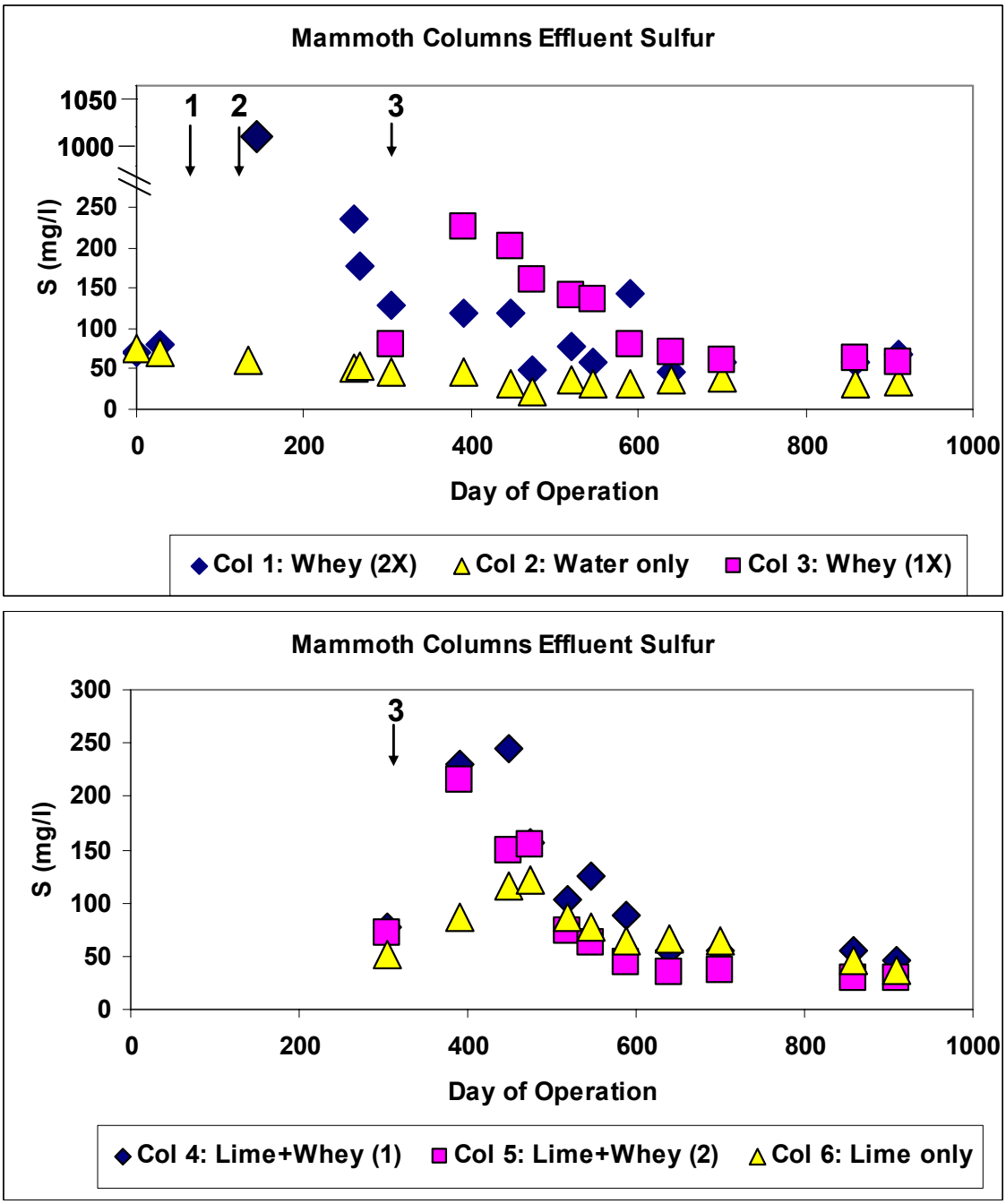

Figure 29. Mammoth column effluent sulfur during whey and lime addition experiments. 1: First whey addition to column 1 at day 56. 2: Second whey addition to column 1 at day 119. 3: Whey and/or lime addition to columns 3-6 at day 301.

opposite was true in the lime treated column, yet samples from this column remained well below the treated columns throughout the experiment.

Effluent SRB were stimulated approximately 2 orders of magnitude in column 1 by the two whey treatments, and remained elevated throughout the experiment (Figure 32). In column 3, the single whey treatment had an ephemeral effect on effluent SRB, which increased to a high of only 28 MPN/ml, and dropped to below detection quickly thereafter. Both whey + lime treated columns increased after treatment to 10^2-10^3 MPN/ml, whereas the lime only column increased only to 10 MPN/ml. SRB were initially measured in the water only control at 10 MPN/ml, but were undetectable after 250 days and remained so for the duration of the experiment.

Core samples taken from the Mammoth column receiving two whey treatments and from the water only control were analyzed for HPC, IOB/SOB, and SRB. Core samples were removed from depths of 5 cm, 35 cm, and 65 cm at day 0 prior to treatment and day 220 following 2 whey treatments. Heterotrophic bacteria were stimulated by whey treatments at the 5 cm depth, but were not affected at lower depths (Figure 33). IOB/SOB were measured at 10 MPN/g or under at day 0, but were present at 10^4-10^5 MPN/g in both treated and untreated columns after 220 days. SRB were evidently stimulated only at the 65cm depth in the treated column.

The attached microbial data corroborate observations from the effluent sampling for HPC and SRB. Attached community samples indicated HPC were stimulated in the top few centimeters of the treated column, but not in the deeper areas of the column. The effluent sample showed no apparent differences between columns 1 and 2, probably due

to the filtration effects of the HPC as they moved downward through the column. The effluent counts are more likely to accurately reflect deeper zone attached microbiology than that in the upper reaches of the columns. This conceptual model also explains the abundance of SRB in column 1 effluent, as SRB were found to be over 10 times as abundant at the 65cm depth in column 1 compared to column 2. The attached cell results for IOB/SOB would thereby predict similar effluent concentrations of these cells for both the treated and control columns, although they were 10 – 100 times as abundant in treated column effluent at day 200.

Overall, microbial data indicate an abundance of HPC in all columns. IOB/SOB were evidently stimulated in whey treated columns, but not the lime treated column. SRB were clearly stimulated by the dual whey treatment, and by the lime + whey treatment, but not by the lime-only treatment.

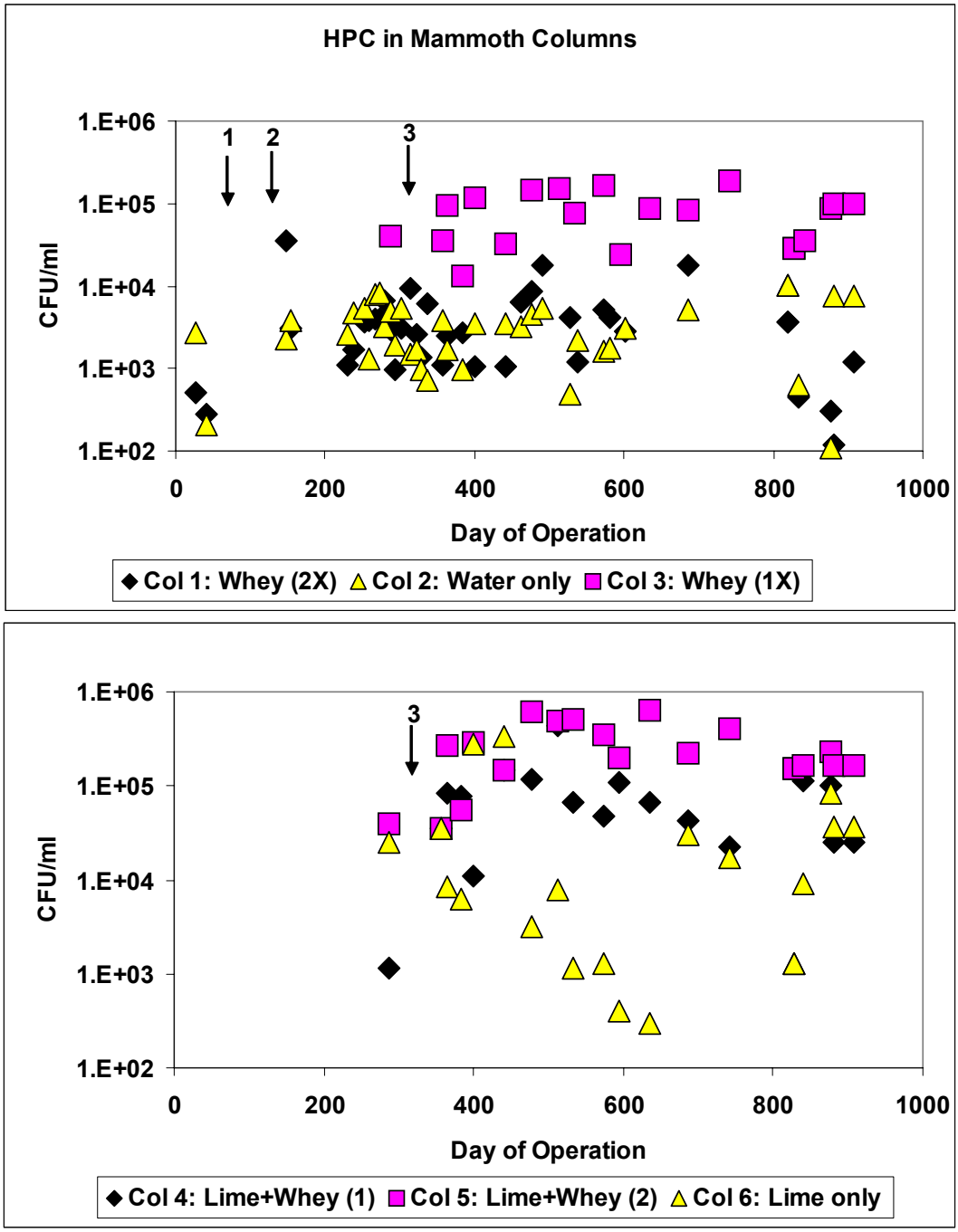

Figure 30. Mammoth column effluent HPC during whey and lime addition experiments. 1: First whey addition to column 1 at day 56. 2: Second whey addition to column 1 at day 119. 3: Whey and/or lime addition to columns 3-6 at day 301.

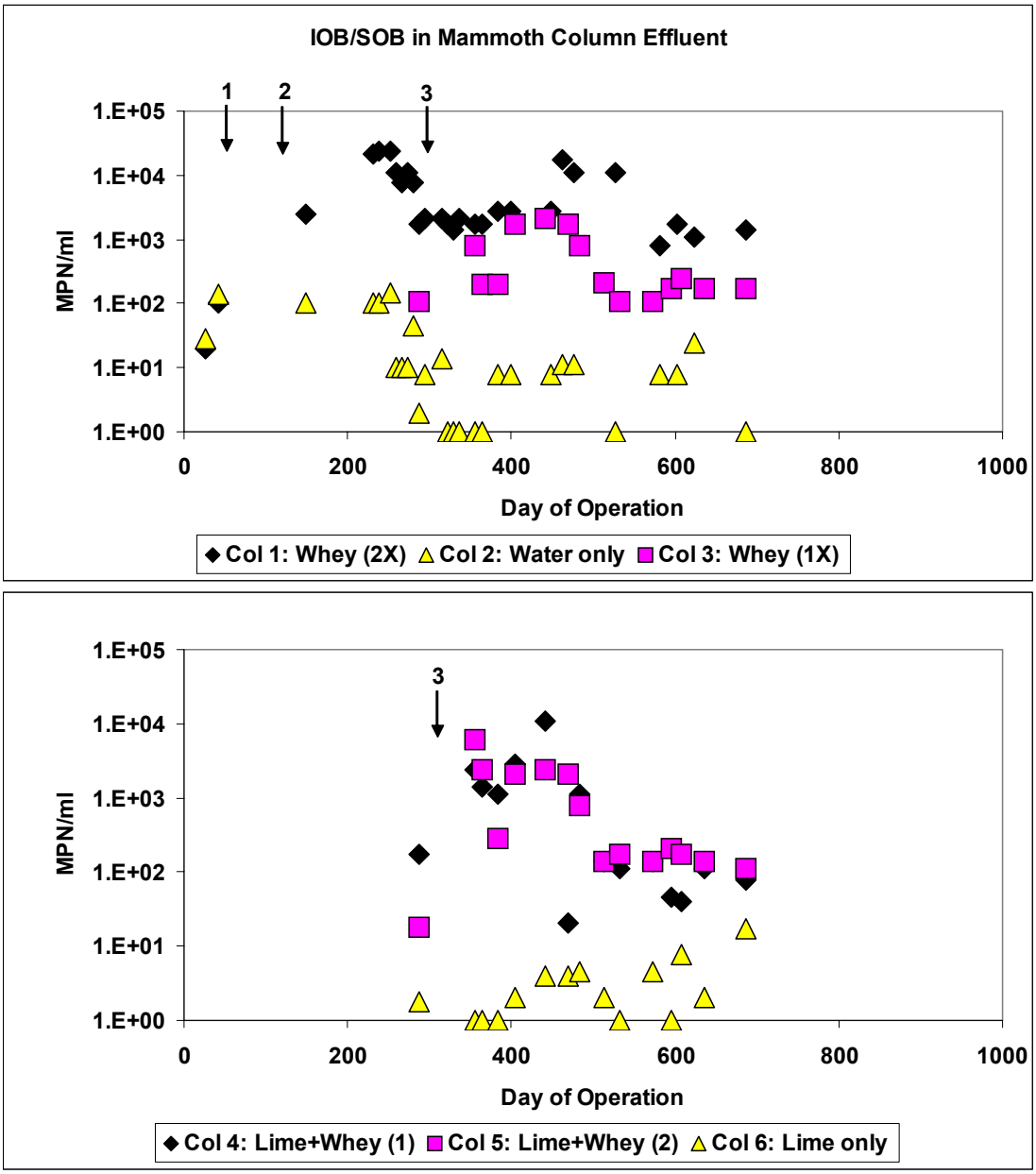

Figure 31. Mammoth column effluent IOB/SOB during whey and lime addition experiments. 1: First whey addition to column 1 at day 56. 2: Second whey addition to column 1 at day 119. 3: Whey and/or lime addition to columns 3-6 at day 301.

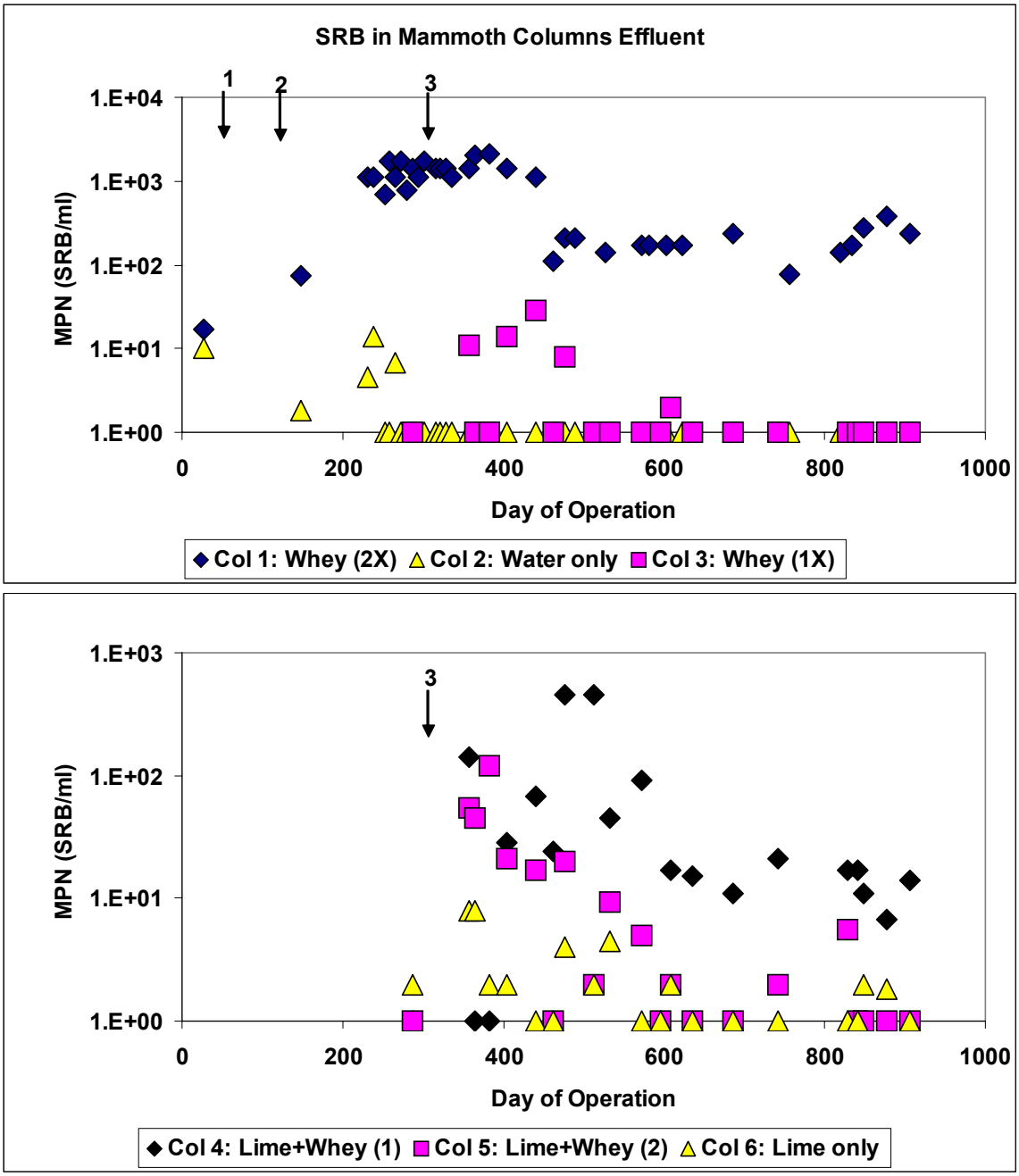

Figure 32. Mammoth column effluent SRB during whey and lime addition experiments. 1: First whey addition to column 1 at day 56. 2: Second whey addition to column 1 at day 119. 3: Whey and/or lime addition to columns 3-6 at day 301.

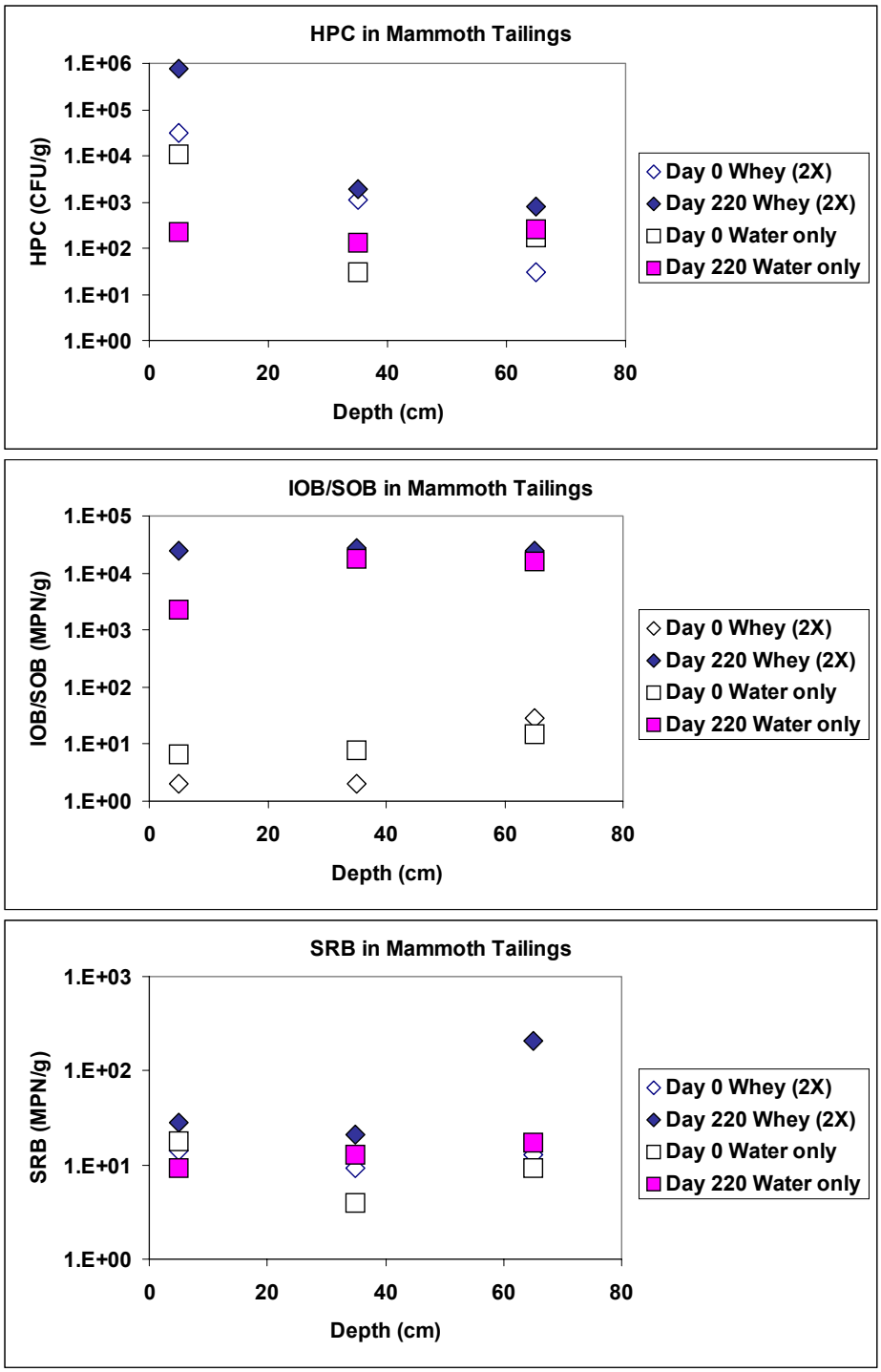

Figure 33. Mammoth column microbial colonization at various depths for the twice treated whey column (Whey 2X) and the water only control.

CHAPTER 5

DISCUSSION

General

Experimental results are discussed in a sequential manner similar to that in which they were presented in Chapter 4.

Mine Tailings Initial Conditions

Due to their differing levels of oxidation, sulfur content, and iron content, Fox Lake and Mammoth tailings represent significantly different environments for application of ARD control via dissolved organic carbon addition. The acid-generating capacity of Fox Lake tailings was over 150 times that of the Mammoth tailings. On a mass basis, sulfur and iron were present in Fox Lake tailings at an S:Fe ratio of 0.57:1, In the Mammoth tailings, this ratio was 0.16:1. Overall sulfur content was over ten times higher in Fox Lake tailings compared to Mammoth, whereas iron was only 3 times higher in Fox Lake tailings. Mammoth tailings contained slightly more oxygen than Fox Lake, and approximately 9 times as much silicon. These data suggest that the more highly weathered condition of the Mammoth tailings should be more conducive to the growth of non-acidophilic bacteria, and that organic carbon treatment should produce more rapid results in Mammoth columns. Interestingly, the Mammoth columns initially produced acidic, highly oxidized conditions more rapidly than Fox Lake (Tables 9 and 13), despite

the fact that populations of IOB/SOB were 1-2 orders of magnitude higher in Fox Lake tailings and dissolved sulfur was over 100 times greater in Fox Lake column effluent.

Fox Lake Column Molasses Addition Experiments

While effluent pH in both test columns initially responded in the predicted manner to repeated molasses treatments, it is evident that treatment efficacy diminished over time. In the first, second, and daily molasses treatments, effluent pH in TC1 rose at rates of 0.020 units/day, 0.055 units/day, and 0.024 units/day in the weeks following treatment. In TC2, only the first treatment resulted in an unequivocal pH increase (at a rate of 0.027 units/day) whereas the second treatment had no clear pH effect, and the daily treatment initially caused a steep decrease in pH at a rate of 0.096 units/day. Approximately 2 weeks into the daily addition period, TC2 effluent pH began to rise again, until the end of daily molasses addition. Effluent metals were generally higher in TC2 during this period, as was effluent sulfur. A striking difference between the test columns was effluent SRB, which remained undetectable in TC2 and the control column, but were enumerated at approximately 10^4 MPN/ml in TC1. Another interesting point is the relatively higher HPC counts in TC2 measured until midway through the daily addition period. The drop in TC2 HPC counts at this time coincided with the improvement in TC2 performance. Together, these data suggest that microbially catalyzed reactions may be responsible for performance differences between the test columns. Specifically, SRB activity in TC1 appears to contribute to differences in

effluent pH, iron, and sulfur between TC1 and TC2 during this period, and HPC activity evidently contributed to the poorer performance of TC2.

IOB/SOB were abundant in effluent from all columns throughout the molasses addition experiments, as were general heterotrophic bacteria. Other investigators (Bridge and Johnson, 1998; Johnson, 1998; Pronk et al., 1991a) have found overlap in these populations when describing mine tailings microflora. While organic carbon has been observed to inhibit the growth of obligate chemolithotrophs (Frattini, 2000), Johnson (2001b) has identified several members of the genus *Sulfobacillus* capable of both autotrophic and heterotrophic growth, depending on organic carbon availability. Some members of this genus are also capable of both ferrous iron oxidation and ferric iron reduction, depending on oxygen availability. Furthermore, it has been noted that heterotrophic bacterial iron reduction does not require strictly anoxic conditions, as was formerly believed. Johnson and McGinness (1991) noted an increase in ferric iron reduction under aerobic conditions by *Thiobacillus* and *Acidiphilium* isolates.

Prior to treatment, IOB/SOB populations were measured at higher levels than HPC in all columns. Following the first two treatments, populations of both bacterial types were of approximately equal abundance in each column, with the greatest numbers of both present in TC2 effluent. During the daily treatment period, IOB/SOB numbers continued to increase, while HPC dropped in both treated columns. This result is contrary to expectations, and suggests that IOB/SOB capable of heterotrophic growth during periods of abundant organic carbon may represent a large fraction of IOB/SOB in the test columns. The bacterial enumeration techniques used were not capable of

distinctly enumerating bacteria capable of both chemolithotrophy via iron- or sulfur-oxidation and heterotrophic populations, furthermore, it is likely that the HPC enumeration technique was not optimal for growth of heterotrophic iron/sulfur oxidizing bacteria. Therefore, IOB/SOB populations were likely not fully enumerated in HPC counts.

While effluent pH and ORP data corroborate the activity of SRB in TC1, it is interesting to note that effluent iron and sulfur were much less variable between the columns than pH and ORP. Both effluent iron and sulfur were 10-20% higher in TC2 than TC1 during molasses treatment, suggesting that SRB activity in TC1 was responsible for only modest reductions in effluent metals during this period. The effects of molasses treatment on pH and ORP in TC1 were more pronounced, with pH varying by approximately one unit between TC1 and TC2 following the daily addition period, and ORP varying by 250 mV between the test columns. In terms of both effluent Fe and S, the control column performed better than TC2 and similarly to TC1 until the final molasses addition. No SRB were measured in the control column effluent during this period (or ever during these experiments), suggesting that SRB activity in TC1 had little effect on Fe or S immobilization during this period.

The last molasses addition was performed approximately 100 days following the cessation of the daily addition period. Interestingly, this addition had no immediate benefit in either of the test columns, and in fact resulted in a marked drop in pH in both test columns approximately one month following treatment. pH dropped by approximately 1 unit in both test columns, and 0.5 units in the control column. Clearly,

any initial benefit gained from molasses treatment was absent during the final treatment. Indeed, the extended effects of both the daily addition and the final molasses treatment suggest a small initial pH increase followed by an overall increase in effluent acidity. This effect was much more pronounced in TC2, but was also observable in TC1. A conceptual model which accounts for this behavior is the stimulation of populations of IOB/SOB which are also capable of heterotrophic growth under carbon-rich conditions. Current research (Johnson, 1998; Johnson, 2001b) suggests these bacteria are present in many naturally occurring mine waste situations, although their differentiation from obligate heterotrophs and/or obligate IOB/SOB is problematic with conventional growth-based techniques.

Stability diagrams calculated using the effluent water chemistry conditions after the final molasses treatment indicate a high degree of similarity between the favored chemical phases in all three columns, despite pH and Eh differences. Conditions at this time (TC1 pH = 5.25, Eh = +100 mV; TC2 pH = 3.6, Eh = +260 mV; control column pH = 4, Eh = +320) favored aqueous phase sulfur (as SO_4^2) in all columns (Figures 34-37), while the stable Fe phase for TC1 was close to the equipotential lines between $CuFeSO_2$(s), FeOOH(s), and $FeSO_4$ (a). In TC2 and the control column, FeOOH(s) was the stable Fe phase, although conditions on both plots are close to the $CuFeO_2$ equipotential line. High effluent iron concentrations in all columns suggest that goethite and/or delafossite ($CuFeO_2$) either do not form, or form incompletely in TC1 and TC2 under the conditions present.

Distribution diagrams (Appendix A) drawn for the chemical conditions in all columns following the molasses addition experiments (day 222) illustrate how small changes in the Eh/pH conditions of the columns can have significant effects on metal solubility and precipitation of secondary mineral phases. These diagrams are perhaps more useful than Eh/pH stability diagrams because in the latter, only one controlling element can be listed and the importance of phases that do not contain the controlling element are lost. For example, it is clear that Eh/pH conditions at day 222 in the control column represent a borderline condition between the competing Fe phases $CuFeO_2$ and FeOOH (Figure 36). However, the distribution diagram must be reviewed to understand that if FeOOH predominates, then Cu will shift to aqueous $CuSO_4$.

The day 222 distribution diagrams generally corroborate the aqueous phase effluent metal and sulfur concentrations shown in Figure 6. These diagrams predict that conditions in TC1 are more conducive to secondary mineral formation for Al, Cu, and Zn than in TC2 or the control. Sulfur is predicted to remain aqueous in all columns while As is predicted to precipitate as zinc arsenate in all columns. The most abundant metal, Fe, was predicted to precipitate as FeOOH in both TC1 and the control, while remaining aqueous in TC2. In fact, effluent Fe concentrations were relatively high and very similar across the columns, again suggesting that goethite and delafossite are unable to form completely in under the conditions in the columns, perhaps due to slow formation kinetics relative to the column residence time.

Molasses Carbon/Oxygen Accounting

The total mass of molasses added to TC1 and TC2 in the first 250 days of operation was 690 g. Because molasses is approximately 63% organic matter (by weight) the total added organic matter was approximately 435 g. The most abundant sugar in molasses is sucrose ($C_{12}H_{22}O_{11}$), the oxidation of which proceeds via the reaction:

$$C_{12}H_{22}O_{11} \cdot H_2O + 12O_2 \rightarrow 12CO_2 + 12H_2O \qquad (22)$$

The mass ratio of oxygen:sucrose is 1.12:1, indicating that the total reducing power of the added molasses was 490 g O_2. Using the method of Elberling and Nicholson (1996) presented in Equation 18 and the parameters values identified in Table 4, the effective diffusion coefficient for oxygen can be calculated as approximately 2 x 10^{-6} m^2/s. Subsequent measurement of oxygen profiles within the columns indicated an absence of O_2 at 16-18" depth in both treated columns. The diffusive flux calculated using Fick's First Law (Equation 14) and these conditions is 0.28 mg cm^{-2} hr^{-1}. Applied over the 729 cm^2 column surface area, diffusive flux results in an estimated O_2 influx rate of 4.9 g d^{-1}. The total molasses reducing power added (490 g O_2 equivalent) would therefore theoretically consume the mass of oxygen diffusing into the columns over a 100 day period. The molasses additions were added over approximately 250 days, with results suggesting an appreciable decrease in acid production only in TC1.

Since no decrease in Fe production was noted in the test columns relative to the control, pyrite oxidation was likely similar among the columns. The influx of oxygen (4.9 g d^{-1}) is theoretically enough to oxidize 2.45 g d^{-1} Fe from pyrite, calculated by combining the biotic iron oxidation reaction (Equation 2) and the reaction for ferric iron

oxidation of pyrite (Equation 3). Fe was produced from all columns at a rate of approximately 2.6 g d^{-1} (calculated from 9000 mg L^{-1} Fe at a flowrate of 2 L per week), in close agreement with that which would be produced via the estimated oxygen diffusion rate.

As discussed earlier, the higher effluent pH in TC1 corroborates the observed SRB activity in this column. Catabolic SRB activity is described by the following stoichiometry for the metabolism of simple sugars (Okabe, 1992):

$$2CH_2O + SO_4^{2-} + H^+ \rightarrow H_2S + 2HCO_3^- \quad (23)$$

In the presence of dissolved metals, hydrogen sulfide generated in this reaction typically precipitates rapidly as metal sulfide as follows:

$$Me^{2+} + H_2S \rightarrow MeS\downarrow + 2H^+ \quad (24)$$

The combined result of these reactions is the generation of two moles of alkalinity and one mole of acidity. Thus the net result of metabolism of two moles of organic carbon and one mole of sulfur via SRB using a simple sugar carbon source is the generation of one mole of alkalinity.

Of the 435 g organic matter added during the molasses addition events, approximately 40%, or 170 g (approximately 14 moles), was organic carbon. If all added organic carbon had been oxidized via sulfate reduction, approximately 7 moles of alkalinity would have been generated, which would then neutralize a total of 7 moles H^+. The total proton production difference between TC1 and the control column after 250 days was 3.5 x 10^{-3} mol $[H^+]$ (calculated by the weekly pH readings and water addition rate). Alkalinity presumably generated via sulfate reduction in TC1 therefore accounted

for only approximately 0.05% of the added organic carbon. Furthermore, using a 1:1 ratio of [sulfur removed]:[alkalinity generated] and assuming sulfate reduction occurred at a rate sufficient to neutralize only 3.5 x 10^{-3} mol [H^+], the removal of sulfur from the aqueous phase would amount to only approximately 1.1 mg/L. The concurrent increase in pH in TC1 (relative to the control) without any evident effect of the treatment on Fe or S in TC1 effluent is therefore not inconsistent.

Although molasses addition favorably increased effluent pH in TC1 and favorably affected Al, Cu and Zn from this column, it had no evident effect on effluent Fe. Furthermore, molasses addition evidently increased acid, S, and production of some metals in TC2 due to the postulated enhancement of IOB/SOB populations evidently able to also grow heterotrophically. Because of this, experimentation with whey as an alternative dissolved organic carbon (DOC) source was initiated.

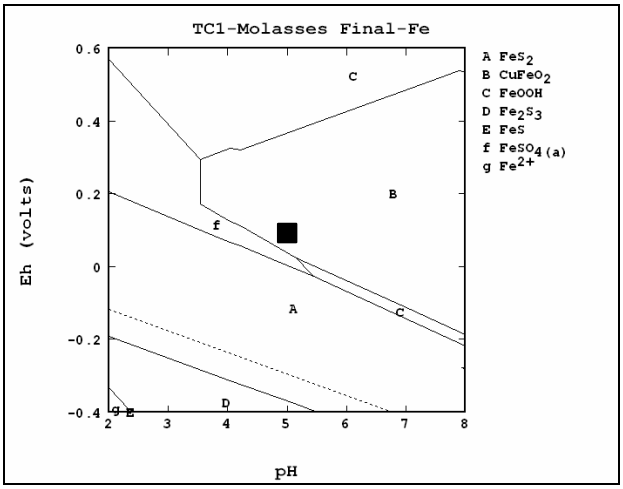

Figure 34. Stability diagram (Fe-controlled) for TC1 following molasses addition experiments. Black square indicates Eh-pH conditions.

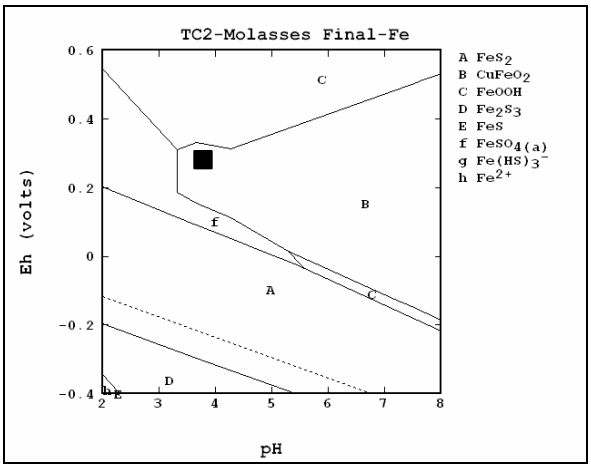

Figure 35. Stability diagram (Fe-controlled) for TC2 following molasses addition experiments. Black square indicates Eh-pH conditions.

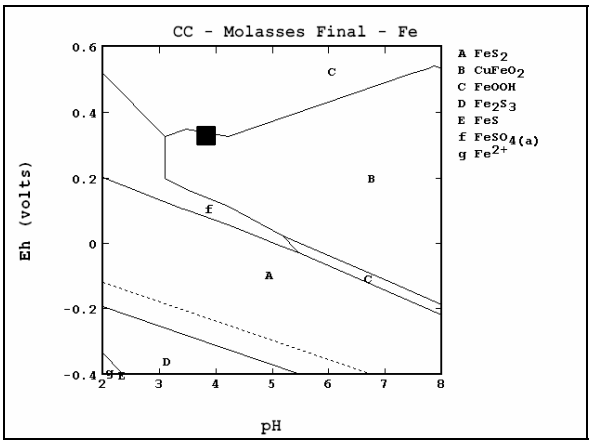

Figure 36. Stability diagram (Fe-controlled) for the control column following molasses addition experiments. Black square indicates Eh-pH conditions.

Fox Lake Column Whey and Methanol Addition Experiments

Whey treatment has been used in both laboratory and field situations as a method of generating reducing conditions through stimulation of heterotrophic growth (Barcelona and Xie, 2001) and as a direct stimulant of SRB (Christensen et al., 1996; Fauville et al.,

2004). Methanol has also been widely used as a direct SRB stimulant, and has proven an effective substrate for use in engineered bioreactors for AMD stream treatment (Tsukamoto and Miller, 1999). Whey and methanol were therefore used both separately and in tandem to assess their performance when applied to Fox Lake tailings.

Effect of Whey/Methanol Treatments on Effluent pH

Throughout the 1700+ days of operation of the columns, control column effluent pH trended downward at a rate of approximately 0.5 unit/yr. Immediately following the first whey addition on day 288, pH increased at a rate of 0.028 units/day and 0.038 units/day in TC1 and TC2, respectively. These rates of increase are in the range of those measured in TC1 during the first and second molasses additions. Similar rates of pH increase were measured in the second whey addition (0.027 units/day and 0.026 units/day in TC1 and TC2, respectively), however, pH response to the third whey treatment was less pronounced, particularly in TC1, where no response was observed. This may be due to TC1 having been at a relatively high pH (5.3) before this treatment. TC2 responded to the third whey treatment with a 0.019 unit/day rate of increase (starting pH = 2.8). These data highlight an important point regarding organic carbon treatment under these conditions; the maximum effluent pH achieved in these experiments was approximately 5.6 (observed in TC1 following the first and second whey additions). The fact that the third whey addition had no effect on TC1 effluent pH suggests that further increases beyond pH circa 5.6 may not be possible with limited duration organic carbon treatment under unsaturated tailing conditions.

In the three following treatments (methanol, whey + methanol, and the day 1503 whey treatment), the rate of pH increase in TC1 remained low, despite pre-treatment pH readings of 3.8-4.2 in all three cases. Methanol addition did appear to halt the pH decline in TC1, and the combined whey/methanol treatment caused a pH increase of 1 unit over 130 days, a rate of 0.008 units/day. TC2 responded better to these treatments; probably because the starting pH was significantly lower (2.15, 3.6, and 3.0, respectively). In TC2, a sustained increase of 0.008 units/day was observed for over 300 days following the combined treatment. pH increases to above 5 were not observed following any of these treatments, however. The day 1503 whey treatment increased test column pH at a rate of 0.005 units/day and in TC1 and 0.012 units/day in TC2. In both test columns, the maximum pH achieved was 4.5, again bolstering the observation of a maximum achievable pH using organic carbon treatment.

The "period of effect" (defined as the time from treatment to the time when effluent pH dropped to pre-treatment levels) varied between the treatments. For the first two whey treatments, this period was approximately 6 months in TC2, while in the third treatment it was almost a full year. Similar, albeit somewhat better, performance was observed in TC1 for the first 3 whey treatments, perhaps because the second and third treatments overlapped in their period of effect. Likewise, the methanol and whey + methanol treatments overlapped in effectiveness in both test columns. The period of effect of these treatments was approximately 500 days. Little synergistic pH effect could be discerned from the combined treatment of whey and methanol, and methanol alone was not as effective as whey in increasing pH. This is likely due to much lower total

organic carbon loading rates for methanol than whey (70 g methanol compared to 680 g whey), and because methanol has the propensity to inhibit bacterial growth under high concentrations.

A discussion of organic carbon concentration is helpful in comparing the whey and molasses treatments. During all 5 molasses treatments, a total of 180 g organic carbon was added over a period of 250 days. During whey treatment, 240 g organic carbon was added during each addition event; however, these events were spaced at 6-13 month intervals. Overall, the rate of organic carbon addition was 0.75 g/d for molasses and 0.88 g/d for whey and methanol. Though direct comparisons are difficult due to greater pH fluctuation during molasses treatment in TC2, it is apparent that the whey treatment effect was of longer duration than molasses in virtually all cases. In addition to the mass added, the treatment longevity also depends on the rate at which the organic carbon is consumed, and which populations consume it. Molasses was both consumed more rapidly and evidently stimulated non-ideal populations (in TC2) as compared to whey. Organic carbon mass additions and their implications for stimulation of various microbial populations will be discussed in a more quantitative manner in a later section.

Effect of Whey/Methanol Treatments on Effluent ORP

While effluent ORP in the test columns generally decreased following organic carbon addition, control column ORP rose at a mean rate of approximately 65 mV yr^{-1} throughout the whey/methanol addition period. However, as was the case for pH, the greater variability and overall poorer performance of TC2 relative to TC1 was apparent in ORP readings. TC1 effluent remained at less than -200 mV during the first three whey

additions, while that from TC2 dropped to between -100 mV and -150 mV immediately after treatment, but then rose to pre-treatment levels from 6-8 months following each treatment. These ORP fluctuations in TC2 mirrored the pH fluctuations described above. In TC1, however, ORP remained relatively stable and highly reducing during this period despite fluctuating pH. This is likely due to the higher SRB activity in TC1 at this time. The oxidation-reduction (redox) couples that influence ORP in this system are primarily iron and sulfur, both of which are affected by SRB activity. SRB metabolize SO_4^{-2} to H_2S, directly affecting the sulfur redox couple. Produced sulfide is also available to react with solution phase iron, reducing Fe^{+3} (if present) to Fe^{+2} and causing FeS precipitation.

During treatment with methanol, ORP dropped in TC2 but was unaffected in TC1, although it should be noted that ORP was already quite reducing in TC1. A similar lack of response for TC1 following methanol treatment was observed for pH (again, because it was already relatively high). When whey and methanol were added together, ORP from both test columns declined for approximately 5 months before rising again, in a manner coincident with pH changes (Figures 9 and 10) and similar to whey alone.

Comparison of ORP data with pH over the course of whey and methanol addition indicates the expected negative correlation, with variation between the columns. The correlation is highest in the control column followed by TC2, then TC1, as indicated by R^2 values for linear regression equations relating pH and ORP in the columns during this period (Figure 37). In TC1, where a small negative correlation exists (R^2=0.26), pH is generally not a good predictor of ORP, whereas in both TC2 (R^2=0.70) and the control column (R^2=0.83), variation between these parameters is more consistent. To understand

how this variation effects iron phases, it is useful to plot the pH-Eh data on predominance diagrams for each of the columns (note: Eh = ORP + 200 mV). The pH-Eh plot for TC1 during the whey and molasses addition experiments (Figure 38), indicates that effluent chemical conditions favored either solid pyrite (FeS_2) at lower Eh, or solution phase $FeSO_4$ at higher Eh. In contrast, TC2 effluent was evidently never stable for pyrite, but alternated between solid goethite, delafossite ($CuFeO_2$) and aqueous $FeSO_4$ (Figure 39). The control column effluent favored delafossite, and solid phase $FeSO_4$, by contrast (Figure 40). As discussed in the elemental composition study presented in Chapter 4, it is estimated that approximately half the iron present in the columns was initially in the form of pyrite, while approximately half existed as oxidized iron minerals such as goethite. Copper was initially present at approximately 300 mg/kg. SEM analysis suggested the presence of reduced Cu, such as chalcopyrite, however the concurrent presence of delafossite cannot be ruled out.

Conditions that favor goethite, delafossite or aqueous $FeSO_4$ would lead to the oxidation of pyrite (and chalcopyrite) and potential downgradient Fe (and Cu) mobilization. Pyrite oxidation in TC2 and the control column should therefore lead to higher aqueous phase Fe concentrations in these columns than in TC1. Interestingly, effluent iron concentrations in these experiments were similar for TC1and TC2, despite the obvious effluent Eh-pH differences shown in Figures 38 and 39. The reason for this is likely that the pH condition of the treated columns changes rapidly in the final several inches of the column (Figure 16). The conditions throughout much of TC1 (like TC2 and the control) are therefore not conducive to pyrite stability, but oxidation. While

secondary iron mineral formation occurs in the lower reaches of TC1 (and TC2, to a lesser extent), the residence time of fluid in this zone is likely not adequate to result in large-scale Fe reduction.

Some of the lowest pH readings in TC1 were observed at very low Eh (Figure 38). This is also true for TC2, but to a lesser extent. In TC1, this occurred circa days 280 and 500, immediately prior to the first and second whey additions. This corroborates a conceptual model wherein organic carbon addition enhances the growth of heterotrophic bacteria that may also be capable of iron (and sulfur) oxidation. While organic carbon is present, these bacteria grow heterotrophically, using either oxygen or Fe^{3+} as electron acceptor (Pronk and Johnson, 1992), but as organic carbon becomes limiting, they are capable of returning to chemolithotrophy, further oxidizing Fe^{2+} and S for energy. Under the conditions in TC1 and TC2, heterotrophic activity of these populations would limit acid production as iron and sulfur oxidation are inhibited following organic carbon treatment. The return to chemolithotrophic growth following organic carbon removal is associated with the drop in pH at the end of treatment efficacy. Overall effluent ORP remains low due to both limited oxygen influx capability and SRB activity deep within the columns. Both oxygen influx and microbial activity will be discussed further in later sections.

Effect of Whey/Methanol Treatments on Tailings Metals

Whey and, to a lesser extent, methanol treatment resulted in lower effluent dissolved metals for all metals assessed, however, results varied both between metals and

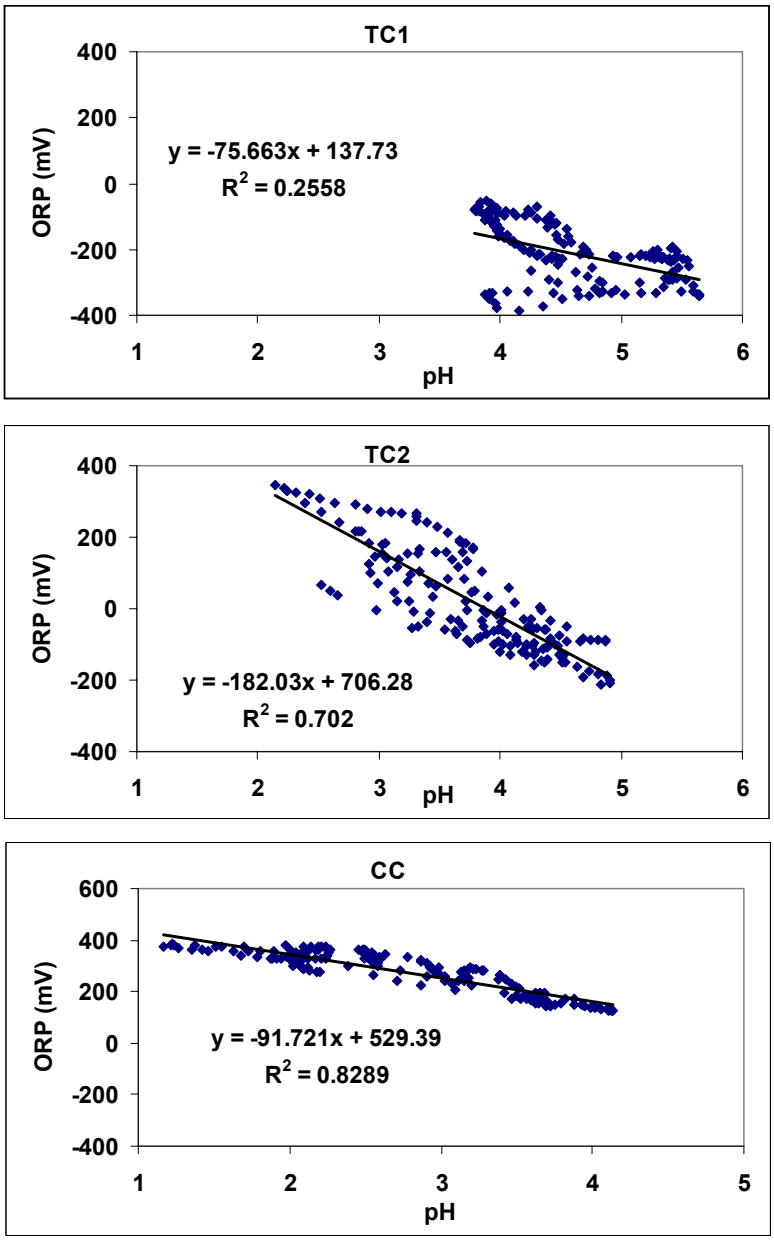

Figure 37. Correlation of effluent pH and ORP for Fox Lake columns during whey and methanol addition experiments.

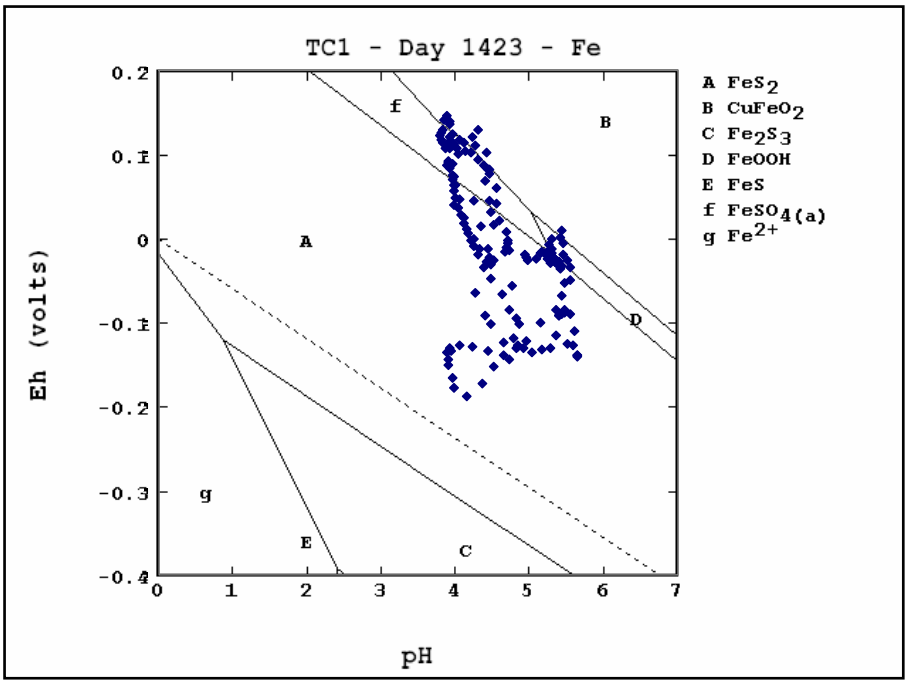

Figure 38. Iron predominance diagram for pH and Eh measurements from Fox Lake Test Column 1 during whey and methanol addition experiments.

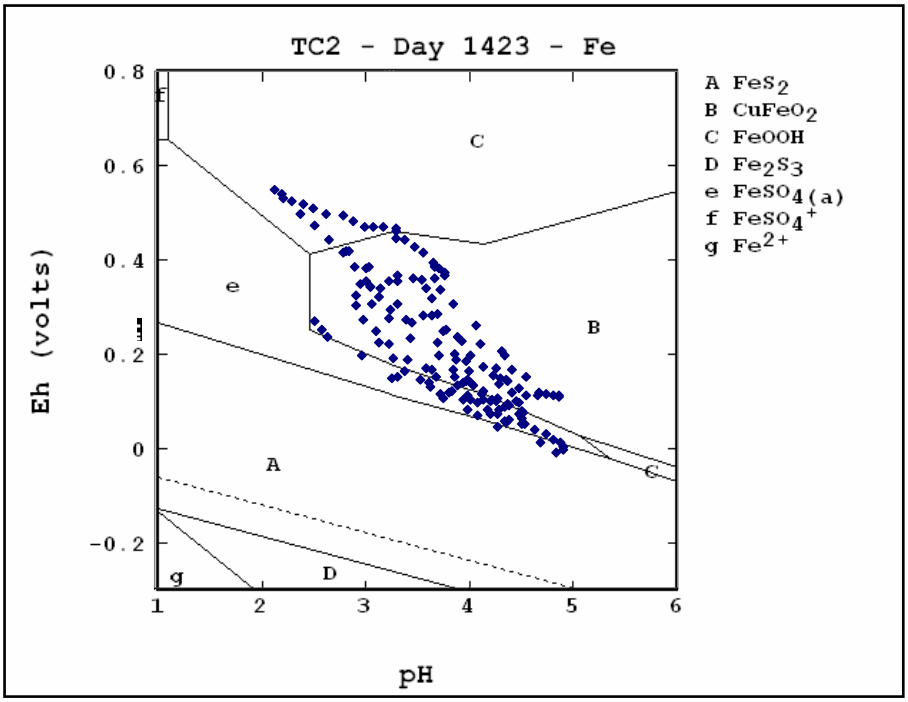

Figure 39. Iron predominance diagram for pH and Eh measurements from Fox Lake Test Column 2 during whey and methanol addition experiments.

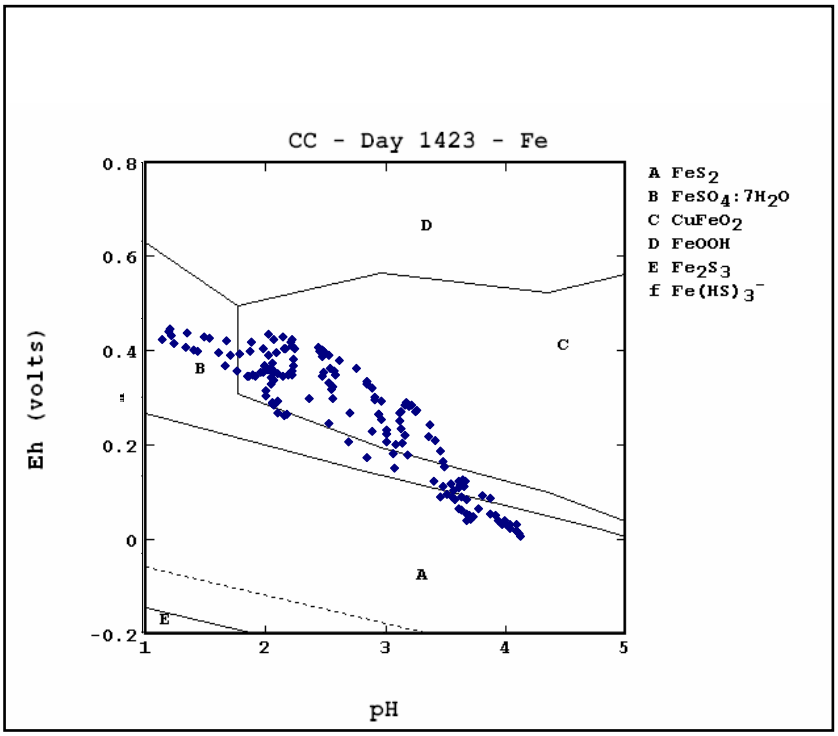

Figure 40. Iron predominance diagram for pH and Eh measurements from Fox Lake Control Column during whey and methanol addition experiments.

over time. In the case of aluminum, aqueous concentrations were observed to be very pH sensitive, as would be expected based on the phase distribution diagram (see Appendix A, TC1 – Day 824 – Al Distribution). This diagram predicts an abrupt transition from aqueous $Al(SO_4)_2^-$ to solid AlOOH predominance occurring at pH 4.9. In TC1, effluent Al was <5 mg/l when pH remained above this threshold, although when pH dropped below this, circa day 875, Al rose rapidly to >100 mg/l, as was observed in both the control column and TC2 throughout this time period. An ephemeral pH increase to above 4.9 observed following the whey + methanol addition caused a concurrent (and similarly ephemeral) drop in effluent Al in both test columns. As a result of this pH

dependence, aluminum responded well to whey treatment, particularly in TC1, however, the period of effect was less than 1 year, as indicated by the increase in TC1 effluent Al beginning circa day 800. Methanol treatment alone did not reduce Al concentrations in effluent from either column.

Arsenic presumably originated in Fox Lake tailings as arsenopyrite (FeAsS), orpiment (As_2S_3), or realgar (AsS), or a combination of all three. Oxidation of the tailings would result in the production of both arsenite as H_3AsO_3 (As(III)) and arsenate as H_3AsO_4 (As(V)). Arsenic mobility as a function of oxidation state is contrary to other metals tested, as its solubility and transport are typically enhanced under reducing conditions that favor arsenite (Macur et al., 2001). Arsenic mobility (both arsenite and arsenate) is controlled by sorption reactions with metal hydroxides (Raven et al., 1998). In the case of the Fox Lake tailings, iron hydroxides would be most significant. Arsenic mobility is also sensitive to pH, particularly at pH < 4, where increased As solubility occurs concurrently with the dissolution of ferrihydrite and iron (oxy)hydroxides to which the As is adsorbed (Raven et al., 1998). Aqueous arsenic in all column effluent matches closely with this model during whey and methanol treatment; where pH>4, As remains less than 2 mg/l, but under pH 4, effluent As increases with decreasing pH. The cyclic behavior of pH in TC2 effluent is reflected in effluent arsenic as well (Figure 11), with pH 4 acting as an approximate trigger point at which As levels in TC2 more closely resemble those in TC1 than in the control column (comparison of Figures 9 and 11).

Arsenic mobility is also sensitive to the activity of SRB, wherein produced sulfide reacts with both arsenite and arsenate to form the reduced sulfur-arsenic complexes

realgar, orpiment, or arsenopyrite (Thomson et al., 2001). Although SRB were measured in both test columns during whey and methanol treatment, effluent As is more highly correlated to pH than SRB numbers in both test columns, suggesting that arsenic performance is more highly influenced by iron mobility than SRB activity in this system. This would be expected based on the conceptual model of a relatively narrow SRB-active zone in the bottom few inches of each test column.

Effluent copper was evidently not effected by the first two whey treatments, but did show a reduction in both test columns following the third whey treatment and thereafter. The Cu predominance diagram suggests that the transition from solid to aqueous phases at pH 3-5 is heavily dependent on Eh (Figure 41) (see also Appendix A, Distribution Diagrams – Day 824). Whereas effluent from both test columns is well within the predominance range of chalcocite (Cu_2S) delafossite ($CuFeO_2$) and covellite (CuS), control column conditions favor aqueous $CuSO_4$. These conditions were prevalent through most of the whey-methanol treatment period (Figure 11) with the exception of a period circa day 1000 in TC2 when effluent Cu matched control column effluent. This coincided with the period whey effluent ORP from TC2 exceeded that from the control column.

Distribution diagrams (Eh controlled) for lead and zinc in column effluent at day 824 (Appendix A) corroborate effluent metals measurements. These diagrams indicate the predominance of solid phases in the test columns (PbS and $Zn_3(AsO_4)\cdot 2.5H_2O$) and solution phases ($PbSO_4(a)$ and $ZnSO_4/Zn^{2+}$) in the control. Figure 11 indicates the presence of some dissolved Pb and Zn in TC1 and TC2 effluent, however. It is likely that

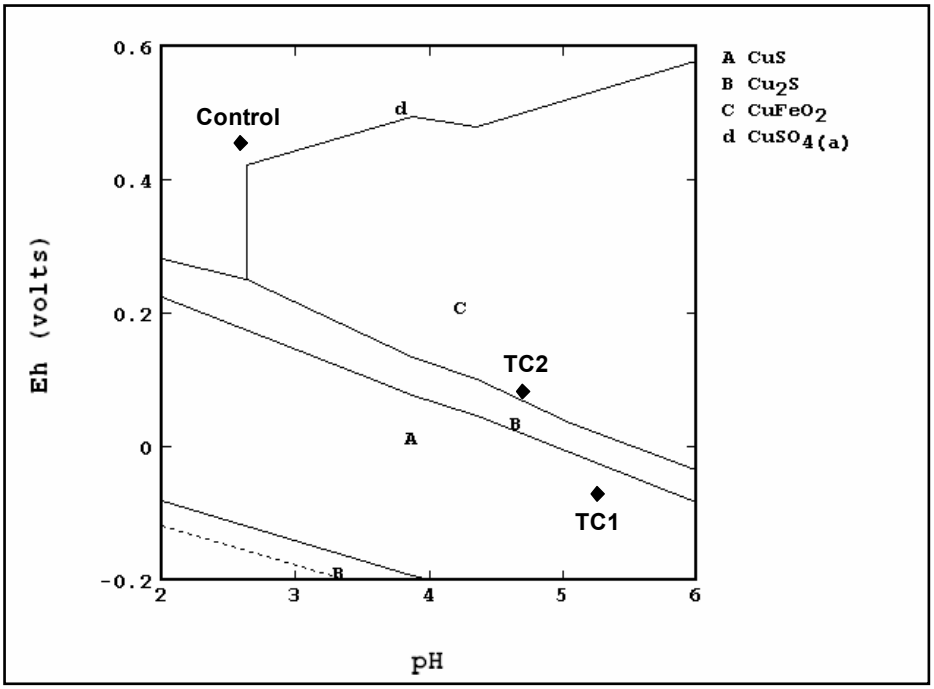

Figure 41. Predominance (Eh-pH) diagram for copper complexes in Fox Lake Column effluent following first 3 whey treatments. Eh-pH position of each column is indicated.

primary mineral dissolution occurs as Pb and Zn are present as iron- and/or manganese-containing minerals in the original tailings. Subsequent re-precipitation of galena or zinc arsenate therefore likely occurs, but column residence time limitations may prevent complete removal from the aqueous phase. This re-precipitation was observed in TC1 and TC2 for both Zn and to a lesser extent, Pb during solid phase sampling at day 1300 (Figure 42) as these metals increased in concentration at lower depths within the treated columns relative to the control.

Comparison of distribution diagrams drawn for day 824 (when the third whey treatment was at the height of its pH effectiveness) with those drawn for day 1056 (when column performance reached a post-treatment nadir) illustrates the differences in stable

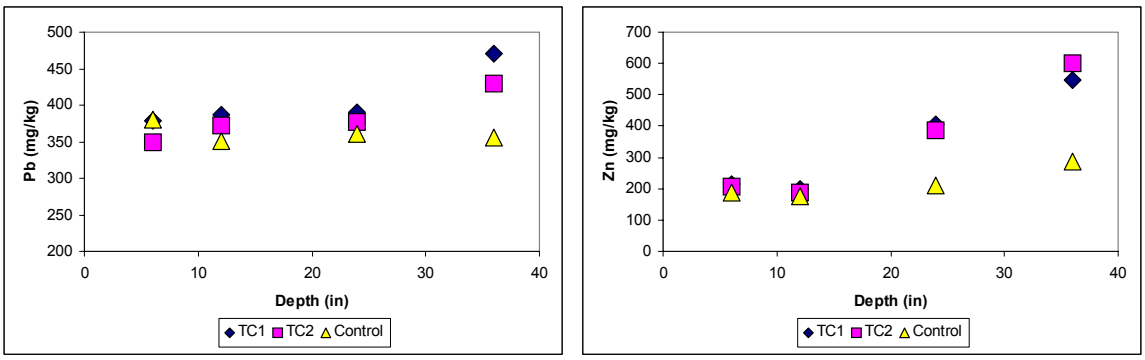

Figure 42. Solid phase concentration of Pb and Zn in columns as determined at day 1300.

metal phases caused by pH/Eh changes as treatment effectiveness wanes (Appendix A). Aluminum increased 3 orders of magnitude in TC1 between these time periods as a result of the loss of AlOOH stability under pH 5. The Fe increase in TC1 from 10,000 mg/L to 25,000 mg/L results from the +150 mV Eh shift causing the stable phase to shift from FeS_2 to $FeSO_4$(a). Similar increases are noted for Zn and S for TC1 and for As, Cu, and S in TC2. Collectively, the distribution diagrams illustrate the fine sensitivity between solid and solution phases for metallic species and S as a function of Eh and pH. The large changes in column effluent metal concentrations are consistent with this solubility data, except where, as previously hypothesized, the kinetics of mineral phase precipitation prevent secondary mineral formation due to insufficient residence time. The kinetics of secondary mineral precipitation are influenced by a variety of site specific factors, such as ionic strength, the availability of nucleation sites, the presence and activity of microorganisms, and the presence of organic matter, among others (Stumm and Morgan, 1981), and are therefore difficult to predict. Data collected in these

experiments, and modeling via STABCAL, suggest that for iron-containing secondary minerals, Fe-sulfides precipitate more readily than Fe-oxides. A review of solubility product constants for the most common initially formed sulfide (FeS) and oxide (amorphous FeOOH) helps to explain this observation. While the solubility product for FeS is 10^{-18}, that for (am) FeOOH is $10^{1.6}$, a difference of almost 20 orders of magnitude.

As discussed in the ORP section above, whey and methanol treatment resulted in lower effluent dissolved iron due to shifts in equilibrium to stable solid phases. Nonetheless, Fe was present at over 10,000 mg/l in the treated columns throughout most of the whey and methanol addition period. The total mass of iron (and S) produced in the whey/methanol addition period for each column is shown in Table 20. Dissolved organic carbon treatment during this period resulted in total Fe and S reductions of 50-60%. TC1 produced 7.5 kg less Fe and 6.2 kg less S than the control column during this period. TC2 produced 6.8 kg less Fe and 5.4 kg less S than the control.

Column	Fe (g)	% of control	S (g)	% of control
TC1	5568	43	4230	41
TC2	6290	48	5008	48
Control	13079		10439	

Table 20. Total mass of iron and sulfur produced from Fox Lake columns during whey and methanol addition period (day 288-1710).

Core samples taken for solid phase microbial enumeration indicated the presence of a black precipitate in the bottom 10 cm of each test column. Furthermore, SEM analysis confirmed the presence of greater levels of iron and sulfur in the test columns than in the control at the 36” depth (Figures 43 and 44). These data indicate the re-precipitation of iron sulfide solids. The stoichiometric ratio of these precipitates

predicted by the Fe and S removal data in Table 20 is $Fe_{0.69}S$ and $Fe_{0.72}S$ for TC1 and TC2, respectively. Other workers studying iron mineral re-precipitation in SRB-active mine tailings have found the Fe:S molar ratio of precipitated solids to vary from 0.59 to 1.15 (Fortin and Beveridge, 1997). Re-precipitated minerals with Fe:S ratios most closely matching those found in the Fox Lake tailings were found to be highly amorphous in structure, suggesting recent solidification. Because distribution diagrams indicated $CuFeO_2$ and FeOOH were likely to precipitate during much of the experimental period, it is likely that the actual Fe:S ratio of precipitated iron sulfide solids in the test columns was lower than the values calculated from Table 20, as some Fe likely precipitated as these oxidized minerals as well.

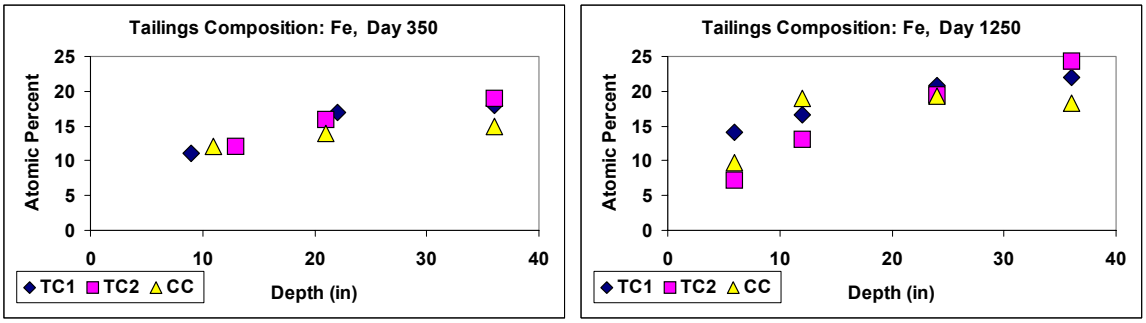

Figure 43. Iron composition of Fox Lake tailings at days 350 and 1250.

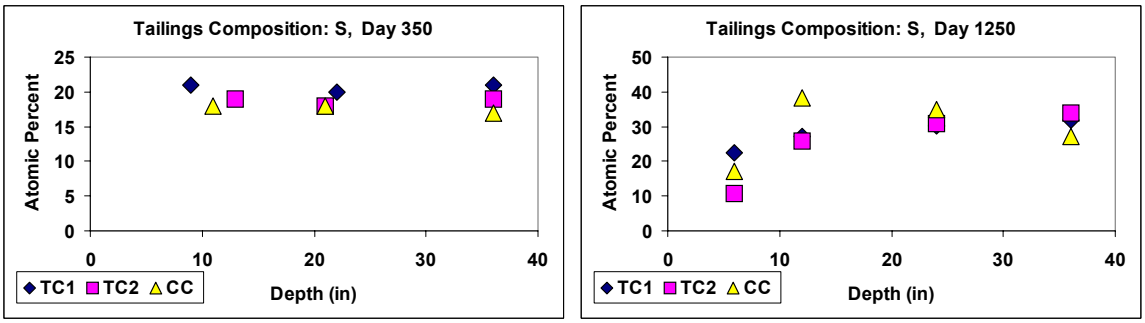

Figure 44. Sulfur composition of Fox Lake tailings at days 350 and 1250.

Effect of Whey/Methanol Treatments on Tailings Microbiota

While molasses treatment evidently did not stimulate SRB in TC2, whey treatment produced unequivocally greater populations of SRB in effluent from both test columns (Figure 13). The effects of methanol on SRB are more difficult to determine separately as methanol treatment followed over 2 years of whey treatment. Review of Figure 13 indicates no overall change in TC2 SRB levels, but a 1-2 log drop in TC1 SRB following methanol addition. Although methanol has been used extensively in both laboratory and field situations as substrate for SRB, in this case it was evidently not as effective as whey, or whey treatment had selected for SRB that could not respond to methanol. Additionally, methanol was added at a much lower concentration than whey, only 140 g total compared to 680 g whey per treatment. This may account for the downward trend in SRB observed circa day 1100 in TC1.

From the second whey addition forward, SRB levels in both test columns were well correlated with pH throughout the remainder of the experiment. This is illustrated for both test columns in Figures 45 and 46.

A cause-effect relationship appears to exists between higher pH levels and greater SRB numbers. Where pH > 4.5, effluent SRB are generally 10^3 MPN/ml or higher, whereas at pH < 4, SRB are generally less than 5 x10^2 MPN/ml. Effluent pH levels measured in both test columns were lower than those typically required for robust SRB growth (Postgate, 1984). Other workers have noted SRB growth under acidic conditions where a solid phase is present, but not in similarly acidic planktonic culture (Fortin et al.,

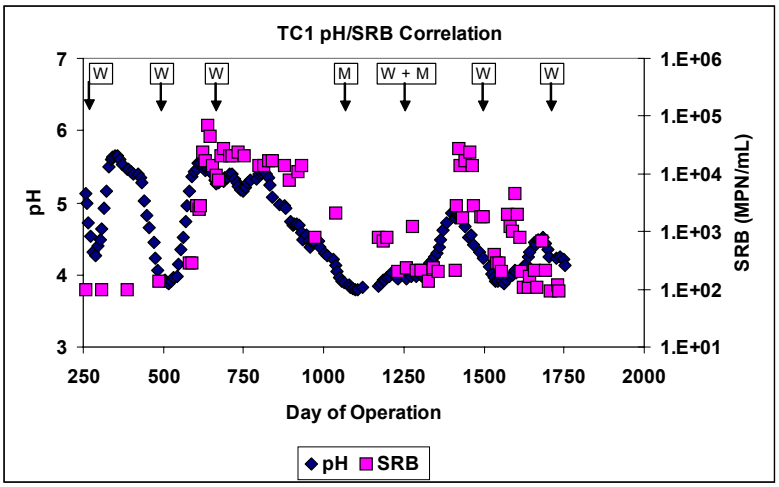

Figure 45. Effluent pH and SRB in TC1 during whey and methanol addition. "W" and "M" denote whey and methanol addition times, respectively.

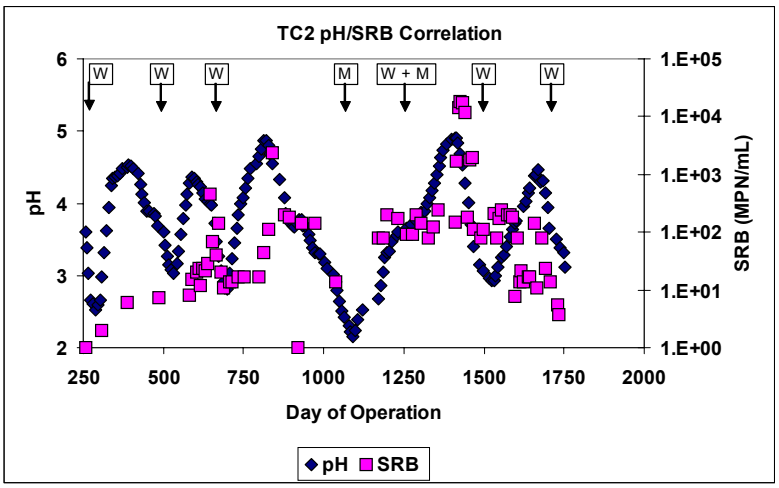

Figure 46. Effluent pH and SRB in TC1 during whey and methanol addition. "W" and "M" denote whey and methanol addition times, respectively.

1996). It is therefore likely that SRB both benefit from and facilitate pH increases in tailings effluent.

The stimulation of SRB via whey and methanol addition can be analyzed via a method of electron accounting proposed by Tsukamoto and Miller (1999). This method

relates the number of electrons produced in oxidation of various sources of organic carbon to the electron requirements for the reduction of H_2SO_4 to H_2S. Sulfate reduction to sulfide requires 8 electrons, while the reaction of methanol and a sugar-based carbon source (such as lactate, a large component of whey), respectively, produce electrons according to the following reactions:

$$H_2O + CH_3OH \rightarrow 6e^- + CO_2 + 6H^+ \quad (23)$$

$$H_2O + CH_2O \rightarrow 4e^- + CO_2 + 2H^+ \quad (24)$$

Therefore, the reaction of one mole carbon from methanol results in the reduction of 0.75 mole of sulfate, while the reaction of one mole of carbon from whey results in the reduction of 0.5 mole sulfate. During the whey/methanol addition period, a total of 4080 g whey and 140 g methanol was added to TC1 and TC2. Whey is approximately 35% organic carbon (as C) and methanol is 37.5% organic carbon (as C). Therefore, a total of 119 moles of C were added as whey and 4.4 moles C were added as methanol, accounting for a total of 63 moles S (2016 g). The decrease in S production from TC1 and TC2 during the whey/methanol addition period was 6.2 kg and 5.4 kg, respectively (Table 20), amounts well in excess of that predicted by electron accounting from organic carbon addition.

Alternatively, it is possible to asses the reducing power of the added whey and molasses via the stoichiometric oxygen demand, as was done in Equation 22 for molasses. In this case, the simplified stoichiometric equations for the oxidation of whey (lactate) and methanol are:

$$CH_2O + O_2 \rightarrow CO_2 + H_2O \quad (25)$$

$$CH_3OH + 1.5O_2 \rightarrow CO_2 + 2H_2O \quad (26)$$

The 119 and 4.4 moles organic carbon added from day 288-1710 during whey and methanol addition, respectively, would therefore consume 4032 g O_2 if oxidized according to equations 25 and 26. Oxygen influx (and CO_2 efflux) data for columns was collected periodically from day 1245 to day 1700. Some fluctuation in both values was observed over this period as a result of organic carbon treatment (Figure 15), however, these values were consistent enough to allow extrapolation of the average fluxes over the period from day 288 to day 1710 (from the first whey addition to the final whey addition). It is then possible to estimate the total mass of O_2 and CO_2 entering and exiting the columns via the air/tailings interface for this period. These estimates are shown in Table 21. It is at once clear that more than twice as much oxygen entered the test columns as can be accounted for through aerobic respiration of added organic carbon.

Column	Total Oxygen Influx (kg)	Total CO_2 Efflux (kg)
TC1	9.7	3.16
TC2	10.0	3.51
Control	11.2	-0.27*

Table 21. Estimated oxygen influx and carbon dioxide efflux from Fox Lake columns from day 288-1710 (* negative number reflects an influx of carbon dioxide into the control column).

Oxygen infiltrating the columns can be either consumed via biotic reactions or precipitate in mineral phases. The most likely oxygen-containing mineral precipitate in these tailings would be goethite (FeOOH), however, iron composition data (Figure 43) indicates a net loss of Fe in the aerobic zone of all columns. For the following calculations, all oxygen entering the columns was assumed to be microbially consumed. The simplified aerobic oxidation reaction presented in Equation 25 does not include the

anabolic (biomass generating) reaction. Using an estimated biomass yield of 0.45, and an estimated stoichiometric expression for biomass, the combined catabolic and anabolic reaction for whey is similar to that developed for simple sugars (Characklis and Marshall, 1990):

$$C_6H_{12}O_6 + 2.5O_2 + 0.7\ NH_3 \rightarrow 3.5\ CH_{1.4}O_{0.4}N_{0.2} + 2.5CO_2 + 4.6H_2O \qquad (27)$$

In this equation, six moles of organic carbon causes the consumption of 2.5 moles O_2 and the production of 2.5 moles CO_2. The 123 moles of added organic carbon would thereby cause the consumption of 52.5 moles (1680 g) O_2 and the production of 52.5 moles (2310 g) CO_2. The additional oxygen influx into the test columns, and the entire O_2 influx into the control column, is likely due to demand generated by the activity of autotrophic IOB/SOB.

The stoichiometry and kinetics of iron oxidizing bacteria, particularly *Acidithiobacillus ferrooxidans*, have been studied extensively over the past decades. The energy yield from iron oxidation has been reported as 6.5 kCal mol^{-1} (Lees et al., 1969), while 120 kCal is necessary to fix one mole organic carbon from CO_2 (Silverman and Lundgren, 1959). Assuming 100% efficiency, *A. ferrooxidans* would thus require the oxidation of over 18 moles Fe^{2+} for the assimilation of one mole of carbon. Significant variation has been reported in efficiency values for Fe^{2+} oxidation coupled to CO_2 uptake by *A. ferrooxidans* and other IOB, from 3% to 30%, with 10% as an average figure (Leduc and Ferroni, 1994; DiSpirito and Tuovinen, 1982).

The stoichiometric equation for the biotic oxidation of pyrite (Equation 2 from Chapter 2) predicts 4 moles ferrous iron reacting with one mole O_2. Using estimates of

the efficiency of carbon assimilation, as described above, of 3%, 10% and 30%, the expected mass ratio of carbon dioxide to oxygen can be calculated and compared to the control column gas flux data for these compounds (Table 22). The mass ratio of CO_2:O_2 for the control column, as calculated from the values in Table 22, is 0.030, the same as the ratio predicted for an efficiency of 10%. The observed oxygen and carbon dioxide influx into the control column therefore closely matches that which would be expected based on stoichiometric values reported in the literature.

Efficiency	Fe (mol)	Fe (g)	O_2 (mol)	O_2 (g)	CO_2 (mol)	CO_2 (g)	CO_2:O_2 (g/g)
100%	1	56	0.25	8	0.054	2.378	0.297
30%	1	56	0.25	8	0.016	0.714	0.089
10%	1	56	0.25	8	0.005	0.238	0.030
3%	1	56	0.25	8	0.002	0.071	0.009

Table 22. Predicted utilization of Fe, O_2, and CO_2 by iron oxidizing bacteria for various carbon assimilation efficiencies.

The stoichiometric ratio for Fe:O_2 predicted by Equation 2 and Table 22 is 56:8 or 7:1. Comparison of the values shown in Tables 20 and 21 for Fe produced and O_2 consumed for the control column show that the observed Fe:O_2 ratio was 1.2:1, far below that which would be expected if all influent oxygen oxidized Fe to the solution phase. The likely reason for this discrepancy is that effluent Eh-pH conditions favored the formation of insoluble oxidized iron minerals over much of the experiment, as predicted by Figure 40.

Stoichiometric comparisons for TC1 and TC2 are more complex because O_2 consumption and CO_2 production by heterotrophic organisms must be taken into account. A conceptual model that illustrates the complex interactions within the test columns is

shown in Figure 47. Exogenous organic carbon can be oxidized to CO_2 through the activity of aerobic heterotrophic organisms, which may be either obligately heterotrophic or capable of autotrophic and/or mixotrophic growth as well (see Table 1). Exogenous organic carbon may also be rendered to reduced carbon compounds under anoxic conditions. In the process of aerobic heterotrophic growth, some populations may concurrently oxidize Fe^{2+} and sulfur. Furthermore, obligately autotrophic organisms, such as *At. ferrooxidans* and *At. thiooxidans* continue to oxidize iron and sulfur, respectively, under aerobic conditions. Under anoxic conditions, some acidophiles are capable of coupling iron reduction to sulfur oxidation, as is illustrated for *At. ferrooxidans* below. These complementary and at times competing populations complicate microbial interactions in the test columns to the extent that any calculations with bulk measured parameters must necessarily be broad estimates, at best. However, analysis of added organic carbon, influx oxygen, produced CO_2, and effluent water chemistry can assist in quantifying the activity of various microbial populations in the test columns.

Unlike the control column, in which O_2 and CO_2 flux remained stable over time, both test columns experienced fluctuations in O_2 influx and CO_2 efflux as a result of whey treatment (Figure 15). Oxygen influx was depressed and CO_2 efflux was elevated for approximately 100 days following whey treatment, in approximate agreement with the 70 day nominal column residence time. The lowered oxygen influx immediately following whey treatment is probably a result of partially occluded pore spaces at the tailings surface due to biomass accumulation. Infiltration rates were measured both

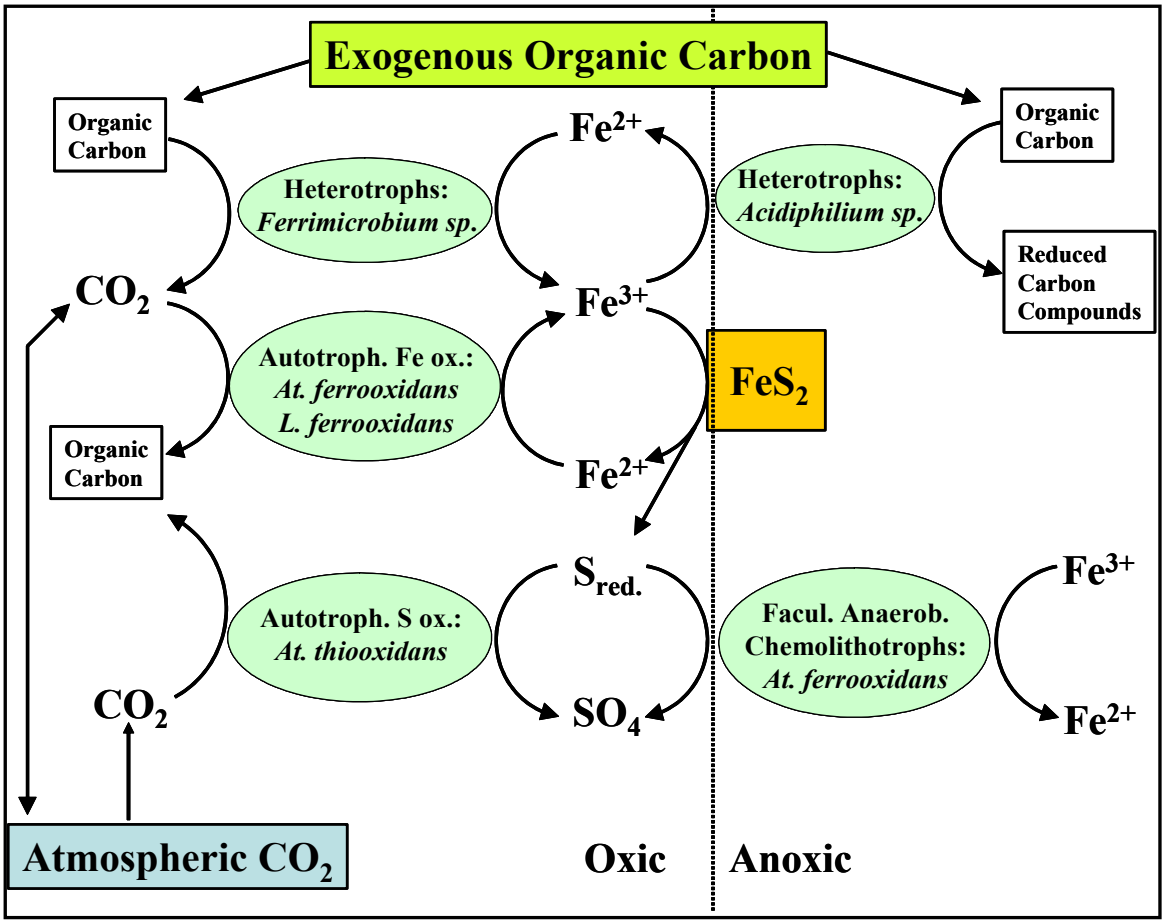

Figure 47. Schematic diagram representing exogenous carbon flow, CO_2 inputs, and bacterially catalyzed reactions in both oxic and anoxic environments. Bacterial species and genera shown are representative only, not inclusive.

before and after whey treatment as the time necessary for complete infiltration of the weekly water allotment. These data indicate that pretreatment rates were similar between the test columns and the control; however post-treatment infiltration rates were approximately 50% less in the fed columns. Visual inspection of the tailings surface indicated robust surface growth and the development of a crust-like layer in the top 1 cm

of tailings, which appeared immediately following treatment and gradually disappeared over several months.

Following whey treatment (Figure 15, circa day 1550), the rate of both O_2 flux into the test columns and CO_2 flux from the test columns was approximately 0.25 mg cm^{-2} hr^{-1}, an apparent O_2:CO_2 mass ratio of 1:1. The mass ratio of O_2:CO_2 for aerobic oxidation of whey is 0.73:1 (from Equation 27). If all influent oxygen were utilized according to this ratio, 0.34 mg cm^{-2} hr^{-1} effluent CO_2 would have been generated. The discrepancy between this theoretical value and the actual measurement is likely due to CO_2 demand from autotrophic organisms and possibly from abiotic demand exerted by the acidic pore water.

Immediately prior to the day 1503 whey treatment, the rate of O_2 flux into the test columns was approximately 0.45 mg cm^{-2} hr^{-1} while the CO_2 flux out of the test columns was approximately 0.04 mg cm^{-2} hr^{-1}. Using the approximate stoichiometric relationships between oxygen and CO_2 for both heterotrophic and autotrophic growth and the before- and after-whey gas flux data, it is possible to estimate the mass of each gas utilized (or produced) in each type of growth during each time period. In this method, the mass flux rate of both O_2 and CO_2 for each time period (before and after whey addition) is multiplied by the column surface area (729 cm^2) to calculate the hourly mass flux for each. The following equations are then solved for the four unknowns:

$$F_{O_2(T)} = R_{O_2(h)} + R_{O_2(a)} \tag{28}$$

$$F_{CO_2(T)} = R_{CO_2(h)} + R_{CO_2(a)} \tag{29}$$

$$0.73 = \frac{R_{O_2(h)}}{R_{CO_2(h)}} \tag{30}$$

$$33.6 = \frac{R_{O_2(a)}}{R_{CO_2(a)}} \tag{31}$$

where $F_{O2(T)}$ and $F_{CO2(T)}$ are the total flux of O_2 and CO_2 into the columns, $R_{O2(h)}$ and $R_{O2(a)}$ are the rates of consumption of oxygen via heterotrophic and autotrophic bioprocesses, respectively, and $R_{CO2(h)}$ and $R_{CO2(a)}$ are the rates of CO_2 consumption and production via heterotrophic and autotrophic bioprocesses, respectively. The constants 0.73 and 33.6 are the ratios of O_2:CO_2 in the heterotrophic and autotrophic reactions, respectively. Solving these equations before and after whey addition yields the following rate terms (Table 23).

Rate Term (mg/hr)	Before Whey Treatment	After Whey Treatment
$R_{O2(h)}$	33	133
$R_{O2(a)}$	295	49
$R_{CO2(h)}$	-45*	-183*
$R_{CO2(a)}$	8.8	1.4

Table 23. Estimated rates of oxygen and CO_2 consumption via heterotrophic and autotrophic bioprocesses in Fox Lake columns before and after whey treatment. *$R_{CO2(h)}$ appears as a negative value because CO_2 is produced rather than consumed in heterotrophic growth.

Not surprisingly, whey treatment increased the estimated rate of O_2 utilization and CO_2 production via heterotrophic reactions and decreased the estimated rate of autotrophic consumption of both gases. Autotrophic O_2 demand dropped over 80%, from 295 mg/hr before whey treatment to 49 mg/hr after treatment. Furthermore, autotrophic O_2 demand dropped from 90% of total oxygen demand before treatment to 27% of total demand after treatment. Organic carbon has been observed to inhibit the growth of

obligate iron oxidizing organisms when grown with obligate heterotrophs (Marchand and Silverstein, 2002). Additionally, iron oxidation among mixotrophic iron-oxidizing organisms has been shown to be inhibited in the presence of organic carbon, although growth still occurs (Frattini et al., 2000; Johnson et al., 2001b). The gas utilization rate data presented above is consistent with this pattern. Effluent IOB/SOB and HPC data (Figure 13) are also consistent with the observed gas flux data and the above interpretation during the period before and after the day 1503 whey addition.

Phylogenetic Analysis of Tailings Microbiota

Phylogenetic assessment of tailings microbiota prior to the day 1503 whey treatment identified many acidophilic genera commonly found in mine waste environments, as well as confirming the presence of several ecologically flexible, facultative anaerobes, mixotrophs, and heterotrophs. These data corroborate the effluent planktonic microbial data for most populations (Figure 13) and the solid-phase microbial data with respect to heterotrophic populations (Table 11) but appear to offer a more robust picture of tailings microbiology than the IOB/SOB and SRB data derived from solid-phase core sampling alone. In particular, phylogeny data shows the presence of *Desulfomaculum* or *Desulfosporosinus* at all levels in the control column, yet SRB were not detected in solid or liquid samples from this column. This may illustrate differences in presence versus activity among populations in an inhospitable environment. It is interesting to note that these SRB genera are noted spore formers and therefore potentially capable of survival in hostile conditions for extended periods of time (Suzuki et al., 2003).

The evident abundance of both *Sulfobacillus* and *Alicyclobacillus* at virtually all levels in the columns suggests that a robust mineral leaching environment exists under aerobic conditions, as both have been noted to enhance mineral dissolution in biomining operations (Bridge and Johnson, 1998; Rawlings, 2002). Of particular importance is the presence of *Sulfobacillus* sp. which, as indicated in Table 1, can grow autotrophically or heterotrophically and can both reduce Fe^{3+} and oxidize Fe^{2+}. The widespread occurrence of organisms with this metabolic diversity suggests that organic carbon addition is likely to stimulate metal dissolution and acidification unless oxygen can be continuously excluded from at least some portion of the water infiltration path and an active SRB population can be maintained. In the case of these column experiments, this was the case only in the lower 6-12" of the treated columns.

The ubiquity of members of the genus *Pantoea* among the columns suggests a widespread potential for dissimilatory Fe^{3+} reduction under anaerobic conditions. Members of this genus are also capable of reducing other oxidized metals, notably Cr(VI) and Mn (IV) using organic carbon as the electron donor (Francis et al., 2000). As a whole, the phylogenetic data suggest a substantial, varied, and persistent microbial community capable of adapting to changing chemical conditions. Not surprisingly, the energy inputs into the test columns have resulted in both more overall organisms and more genetic variation, yet even after over 4 years of operation with no organic carbon input, the control column also contains significant ecological diversity and potential for heterotrophic growth.

Phylogenetic assessment of the columns following whey treatment indicated that the overall banding pattern between pre- and post-treatment samples was similar, yet evidence is present of stimulation of IOB/SOB in the upper reaches of the columns, and SRB in the lower reaches of TC1 and TC2. The stimulation of *Sulfobacillus*-like organisms in the top zones of TC2 and the control column corroborates the conceptual model postulated previously, a system in which facultative, acidophilic heterotrophs in the upper column consume available organic carbon, but return to chemolithotrophy following its exhaustion. SRB are concurrently stimulated, but their ability to neutralize acid and metals production is highly variable, thus helping to explain the differences in TC1 and TC2 over the course of these experiments. Acid tolerant SRB are clearly stimulated in the fed columns, but a single whey treatment is evidently not adequate to invigorate populations in an already highly acidic system (e.g., the control column).

Several groups of organisms were relatively abundant prior to treatment (Table 14), but not identified in the post-treatment sample (Table 16). Members of the genus *Pantoea* (heterotrophic, facultative anaerobes) were found in every sample prior to treatment, but were evidently not present following whey addition. Interestingly, the band associated with *Pantoea* in Figure 17 (band 5) and the band associated with the equally ubiquitous *Alicyclobacillaceae* in the post-treatment sample (Figure 18, band 2) are evidently very nearly coincident. *Pantoea*, a group of anaerobic, dissimilatory metal-reducing organisms, would be expected to be enhanced by organic carbon treatment, not eliminated.

While an exhaustive study of tailings microbiota using DGGE analysis would greatly assist understanding site changes resulting from organic carbon treatment, such an analysis was not attempted here. For example, prior to treatment, bands identified as *L.ferrooxidans* and *At.ferroxidans*, two commonly studied IOB, were prominent in near-surface zones of TC1. These bacteria were not noted in the post treatment samples, however, the bands identified for both organisms (bands 1 and 2 in Figure 17), were also evidently present, but not sampled, in the post-treatment gel (Figure 18). In this study, time and resource limitations prevented the use of DGGE as an exhaustive community analysis tool; however, these results do confirm the presence of the expected heterotrophic Fe-oxidizers as well as diverse populations of SRB.

Fox Lake Treatment Summary

The various organic carbon treatments clearly had a beneficial effect in TC1 throughout these experiments. The effects of treatment in TC2, while less consistent and less favorable, nonetheless offer valuable insight into the possible response of uncontrolled microbial populations when provided with organic carbon stimulation. While beneficial pH, ORP and effluent metals effects on the order of 6-12 months following treatment were typical in TC1, results in TC2 were both difficult to predict and significantly less positive. Response differences were evident between the two test columns from very early in the molasses treatment period, and, while whey and/or methanol treatment evidently elicited more positive results in TC2, this column remained both more acidic and more oxidized than TC1. The phylogenetic analysis completed at the conclusion of these experiments bolsters earlier microbial sampling results in

indicating that this difference in behavior is coincident with a greater population of bacteria capable of both iron-oxidation and heterotrophic growth. Therefore, in addition to reporting the benefits of dissolved organic carbon treatment as a remedial measure, the results presented here also sound a note of caution regarding field application of this technology.

Mammoth Column Whey/Lime Addition Experiments

The total mass of whey added to the Mammoth columns was significantly less (on per gram of tailings basis) than that applied to the Fox Lake columns. Mammoth column 1 received a total of 0.006 g whey per g tailings, while columns 3, 4 and 5 received 0.003 g/g. The Fox Lake addition rate was 0.008 g/g for each whey addition. Despite this, the effects of these treatments on effluent pH lasted longer than with the Fox Lake columns. Clearly, the Mammoth tailings were more highly weathered than Fox Lake and contained lower concentrations of sulfidic mineral phases. The neutralization potential of the Mammoth tailings was 3 kg $CaCO_3$ per 1000 kg tailings whereas that for Fox Lake tailings was 469 kg $CaCO_3$ per 1000 kg tailings. The rate of acid generation from the Mammoth tailings, however, was similar to that of the Fox Lake tailings prior to treatment, and the ORP in Mammoth effluent was 200 mV higher than Fox Lake (probably as a result of the predominance of Fe(III) containing minerals).

Effect of Whey Addition

Effluent pH data for both the whey 2X (column 1) and whey 1X (column 3) treatments indicate the treatments reached their maximum effectiveness (in terms of pH

increase) approximately 250-300 days following addition, although the longevity of effect was far superior in the twice treated column. The effects of treatment can be quantitatively compared through analysis of the carbon added per gram of tailings in each case and the decrease in H^+ production (relative to the control column). In column 1, 0.006 g whey per g tailings reduced total effluent H^+ production by 2.9 mmol (78% of control) whereas in column 3, 0.003 g whey/g tailings produced a 2.2 mmol reduction (59% of control) in effluent H^+ over the course of the Mammoth experiment. The total H^+ production in the control column was 3.7 mmol. The diminishing effect with additional treatment is not unexpected, but would be difficult to predict *a priori*. For example, organic carbon additions to the Fox Lake columns suggested a threshold concentration of organic carbon must be met before significant benefit is achieved. At this point, insufficient data is available regarding mine tailings in general to predict what this organic carbon threshold will be for partially saturated tailings under active oxidation.

Predominance diagrams (Eh-pH) for columns 1 and 2 for effluent water chemistry conditions at day 300 of operation explain the high dissolved phase concentrations of Fe in column 1 relative to the control (column 2) (Figures 48 and 49). At pH 6 and Eh +100 mV, the predominant Fe and S equilibrium phases in column 1 effluent are $CuFeO_2$ (s) and SO_4^{2-}. Since Fe is initially present as both Fe(III) and S-containing Fe(II) minerals, the day 300 conditions favored iron dissolution (from goethite and S-containing minerals), subsequent Fe mobilization, and to some extent $CuFeO_2$ precipitation. In column 2 at pH 3.5 and Eh +600 mV, FeOOH (s) and SO_4^{2-} are the predominant phases.

Aqueous SO_4^{2-} is the predominant S phase in both columns, but conditions in column 1 require an Fe phase change and are much closer to equilibrium for aqueous Fe^{2+}. These differences in equilibrium phases explain the Fe:S ratio differences shown in Table 19 for columns 1 and 2. The Eh-pH plot for whey 1X column (column 3) at day 550 (250 days following whey treatment), indicates that the stable phases under the conditions present (pH 5.6, Eh +450 mV) are SO_4^{2-}(a) for sulfur and $CuFeO_2$ (s) for iron (Figure 50). Although these phases are similar to those predicted for column 1, the conditions in column 3 are much closer to the boundary for FeOOH, suggesting that goethite dissolution would likely be less under these conditions than in the column 1, but greater than in the control – a situation that corroborates the Fe:S ratio for column 3 shown in Table 19.

Although most iron was shown via EDS analysis to exist as oxidized mineral species in the original tailings, relatively high dissolved sulfate in all column effluent streams suggests the presence of reduced iron (pyrite and chalcopyrite) as well. Furthermore, no oxidized solid phase sulfur species are predicted to exist in the tailings below pH 5.9, where brochantite ($Cu_4SO_4(OH)_6$) forms in a narrow pH range (Figure 21). While other workers have noted oxidized sulfur-iron species in weathered tailings (e.g., jarosite, schwertmannite, and copiapite), these species are unlikely to account for significant phases in the Mammoth tailings due to both their propensity for grain cementation (Remolar et al., 2002; Blowes et al., 1991) and their typical formation through evaporation of mineral laden waters (efflorescence) (Nordstrom et al., 2000) – conditions which were not present at Mammoth. This suggests that sulfur mobilization

resulted from reduced (rather than oxidized) mineral dissolution. Given the preponderance of Fe over Cu, it is likely that the majority of sulfur existed as FeS, FeS_2, or Fe_2S_3 prior to treatment. If all sulfur in the columns was present as pyrite, for example, sulfur produced from columns 1, 2, and 3 would account for the concurrent dissolution of 6500 mg, 1291 mg, and 2196 mg Fe, respectively, from these columns. The actual Fe production was 7268 mg, 227 mg, and 1440 mg, respectively (Table 19). This indicates that sulfide mineral dissolution occurs in all columns, but significant re-precipitation of oxidized iron species accounts for the majority of iron mobilized in the non-fed control (column 2). In column 1 (whey 2X), more iron was produced than would be predicted from sulfur, suggesting oxidized Fe mineral dissolution as well. In column 3 (whey 1X), re-precipitation also appears to be occurring. This analysis suggests that very little, if any, iron is re-precipitated as Fe-sulfides in either treated column as a result of SRB activity. This is corroborated by visual observation of the clear polycarbonate columns, which, in the case of column 1, showed only a few discreet zones of obvious metal-sulfide precipitation, while no such zones appeared in column 3. SRB were nonetheless clearly present, particularly in column 1, yet predominance diagrams confirm that reduced iron species are not favored in either whey treated column.

Effluent SRB numbers were correlated with pH in column 1, reflecting the rapid increase following the addition of whey (Figure 51). In column 3, SRB were observed in column effluent only ephemerally – immediately following whey addition. It is therefore difficult to attribute the pH increase observed to SRB activity here. Relatively high levels of sulfur production (Table 19) suggest the activity of IOB/SOB, and their

presence was confirmed by measurement (Figure 31), and effluent ORP did not decrease significantly here. While SRB activity cannot be completely ruled out, part of the observed pH increase could be due to the dissolution of oxidized ferric minerals, such as FeOOH, which consumes protons based on the reaction:

$$FeOOH + 4H^{+} \rightarrow Fe^{3+} + 2H_2O \qquad (32)$$

Judging by the initial conditions in all columns, near-surface zone pH and Eh were both more acidic and more oxidizing than deeper zones, a condition which would favor FeOOH stability. Deeper in the columns (and in the effluent from both columns 1 and 3), conditions favor delafossite ($CuFeO_2$). Under such conditions FeOOH dissolution could occur. While delafossite precipitation from solution would theoretically produce protons at the same rate (on a per mole Fe reacted basis), high effluent iron indicates that all solution-phase iron did not precipitate. Furthermore, treated column effluent streams had virtually no Cu, while the control had 8 mg/l Cu, a condition that would result if delafossite precipitation were Cu limited.

Results from whey treatment in the Mammoth tailings compared to Fox Lake highlight differences in how the presence of oxidized Fe mineral phases affects the outcome of organic carbon addition. Effluent microbial and metals data indicates that reduced sulfide mineral phases dissolve in both cases as a result of IOB/SOB activity. However, the concurrent presence of oxidized secondary mineral phases adds another source of iron, which may dissolve more readily than primary phases under the more reducing Eh conditions caused by carbon addition. The result in the Mammoth whey treated columns was significantly more total Fe production as a result of treatment.

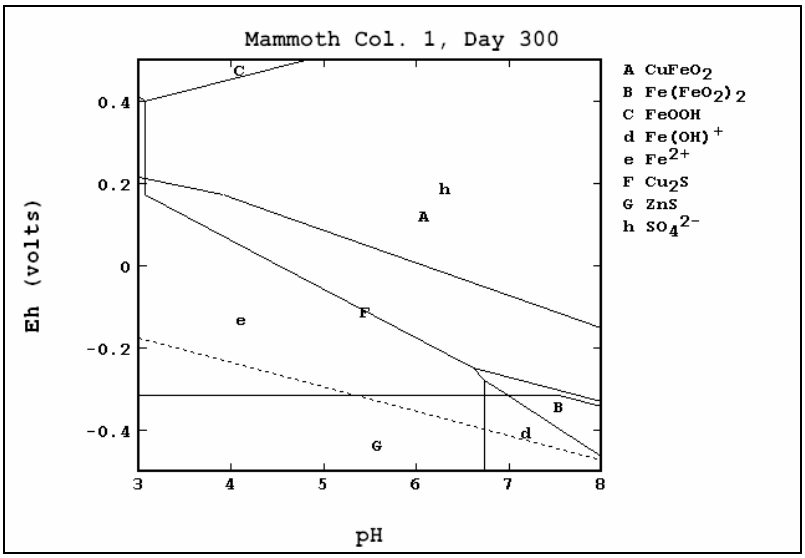

Figure 48. Predominance diagram for Mammoth Column 1, day 300, for Fe-containing minerals.

Effect of Lime Addition

The top-dressing of quicklime (CaO) was intended to provide neutralization to the top 10 cm of tailings to stimulate the growth of heterotrophic bacteria for oxygen exclusion from the tailings. When exposed to infiltrating water containing CO_2, quicklime neutralizes acid according to the following reactions:

$$CaO + H_2CO_3 \rightarrow CaCO_3 + H_2O \tag{33}$$

$$CaCO_3 + H_2SO_4 \rightarrow H_2CO_3 + CaSO_4 \tag{34}$$

One mol quicklime therefore neutralizes two moles of acidity, the resulting calcium cation reacting with sulfate to form calcium sulfate (anhydrite). On a mass basis, the 114 mg added CaO (1.9 mmol) in columns 4-6 was capable of neutralizing 3.8 mmol H^+. The capability of lime to fully neutralize column effluent is sensitive to pH, of course. At pH

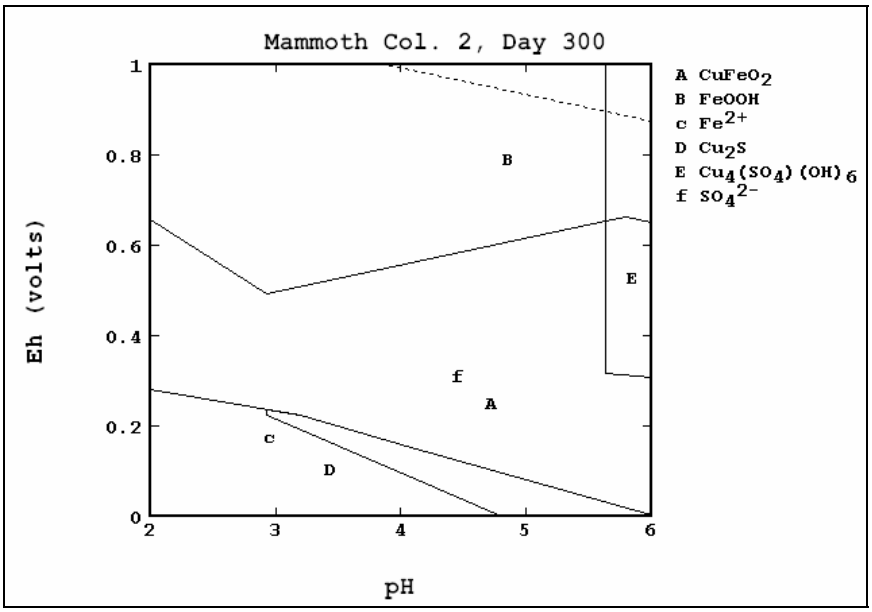

Figure 49. Predominance diagram for Mammoth Column 2, day 300, for Fe-containing minerals.

4 and a flowrate of 29 ml d^{-1}, 3.8 mmol H^+ would be produced from the Mammoth columns in 3.5 years, while at pH 3.5, the neutralization period drops to 14 months.

The apparent effect of the lime treatment can be determined by comparing the pH of the lime-only column (column 6) with the water-only control (column 2). Multiplication of the proton concentration difference between these columns by the flowrate indicates that over the operational time between day 300 and 900, column 6 produced approximately 0.0021 moles less H^+ (2.1 mmol) than column 2, accounting for approximately 55% of the neutralization capacity of the added lime.

Lime treatment was expected not just to neutralize acid in column effluent, but also to alter the microbial community that generates acid, in particular acting to inhibit the activity of IOB/SOB and stimulate heterotrophs. Neither effect was conclusively

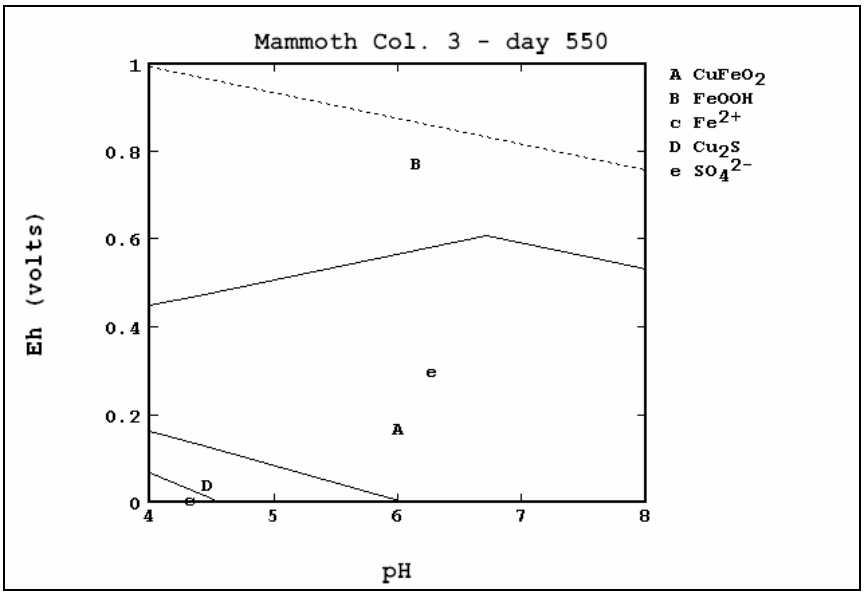

Figure 50. Predominance diagram for Mammoth Column 3, day 550.

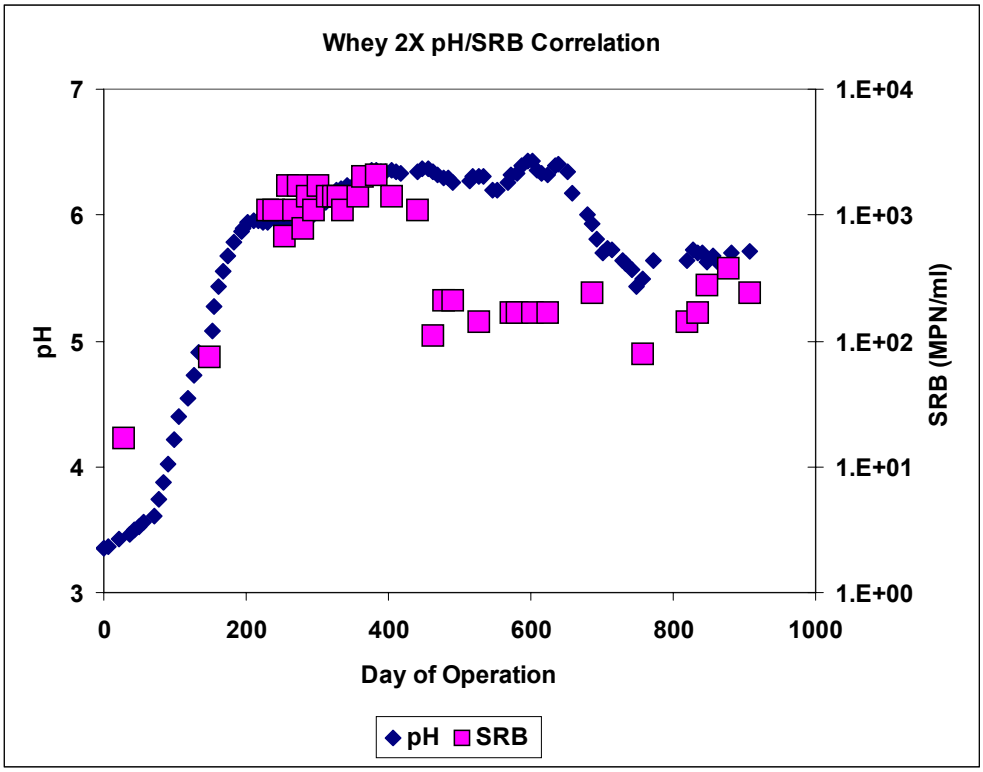

Figure 51. Effluent pH and SRB in Mammoth Column 1 (Whey 2X).

observed in column 6. Effluent IOB/SOB populations were similar to the water only control, while heterotrophic populations were among the lowest observed in any of the columns. It is likely that lime addition altered the ecology of the near surface tailings to the extent that microbial populations shifted away from the acidophilic autotrophs and heterotrophs adapted to site conditions at Mammoth. Such population shifts with pH have been noted for a variety of acidophilic organisms (Walsh and Mitchell, 1972; Edwards et al., 1999). Heterotrophic populations did recover approximately 1 year after lime treatment, just as pH dropped to pre-treatment levels (Figures 22 and 30).

SRB growth was evidently slightly more robust in the lime treated column than in the once-treated whey column, although neither of these treatments resulted in SRB levels appreciably above the water only control. Indeed, the pH response of these columns was almost identical, as were the concentrations of effluent metals. The only appreciable difference was in effluent ORP, which decreased in response to whey treatment but increased in the lime treated column.

Effect of Lime + Whey Addition

In terms of pH increases and ORP reduction, concurrent lime and whey addition was more effective than either lime or whey alone, but not as effective as the double whey treatment. Columns 4 and 5 each received a similar top dressing of CaO as column 6, and similar whey treatment as column 3. Although the pH and ORP response of the columns was initially similar, the aforementioned air leak in column 5 caused ORP levels to rise more than 300 mV over a 2 month period (while they remained relatively stable in column 4). The loss of treatment effectiveness was also evident in effluent pH, which

dropped more rapidly in column 5 than 4. The effect of combined treatment on pH in column 4 is quantified as a 64% reduction in effluent [H^+], compared to a 56% reduction in the lime only column, a 58% reduction in the whey 1X column, and a 78% reduction in the whey 2X column. This comparison suggests that the pH effect of the dual treatment was not additive.

In the case of HPC and IOB/SOB, concurrent lime and whey treatment did not result in significantly greater effluent microbial numbers than whey treatment alone. This was not the case for SRB, however, as both lime + whey columns achieved effluent SRB cell numbers 2 orders of magnitude higher than either the once-treated whey column or the lime-only column. This effect was ephemeral in column 5, however, due to the suspected air leak. These results suggest that whey application was more important in achieving high microbial numbers than lime, and that the effect of liming columns 4 and 5 was not as beneficial for pH control as the second whey treatment in column 1.

Mammoth Treatment Summary

Due to the effects of 80-100 years of weathering in a high-altitude climate, the Mammoth tailings contained relatively high concentrations of oxidized Fe-containing minerals at the outset of these experiments. The neutralization potential of these tailings was much less than that of the Fox Lake tailings, however, water application generated low pH rapidly in these columns. The effects of whey and lime treatment are illustrated by Eh-pH diagrams, which document the equilibrium Fe phase changes from goethite under the initial conditions to delafossite ($CuFeO_2$) in the treated columns. Although both are Fe(III) minerals, pH/Eh alteration clearly led to increased Fe mobilization in all

treated columns – both from reduced and oxidized Fe mineral forms. Low levels of effluent Cu in all treated columns strongly suggests that delafossite precipitation was Cu-limited, a condition that shifts the equilibrium Fe phase to either Fe^{2+} or FeOOH, the equipotential line dividing the two falling very close to the conditions in the treated columns. Because they obviously have the potential to mobilize Fe (and arsenic), the effectiveness of the Mammoth treatments must be weighed with consideration of the most important effluent consideration for a particular site.

Both whey and lime treatment increased pH, but the combination of the two was not as successful as two whey treatments. The whey and lime application rates (0.003 g/g for whey and 0.02 g/g for lime) resulted in very similar pH control effects whey applied independently, and offered perhaps important synergy when applied together – particularly with regard to enhanced SRB populations. Observation of overall microbial populations confirms that whey treatment results in greater populations of all organism types tested than lime treatment, and lime appeared somewhat inhibitory to IOB/SOB when applied alone.

Whether whey (alone or in combination with lime) can be applied economically at a site is a decision that must be made in consideration of many site specific factors such as location, tailings chemistry, rainfall, placement geometry, etc., as well as regulatory conditions. While specific site recommendations are beyond the scope of this document, this work has shown that whey can effectively control acidic drainage from weathered tailings for a period of 1-2 years, depending on the rate of application and the presence of concurrently applied neutralizing agents.

CHAPTER 6

CONCLUSIONS AND IMPLICATIONS

General

Acid rock drainage from mine tailings is rapidly accelerated by the activity of aerobic iron- and sulfur-oxidizing bacteria. Researchers and site managers have long recognized that the key to halting the cycle of iron oxidation in mine waste is the exclusion of oxygen from the bioactive zone in tailings. Furthermore, abatement and mitigation of acid rock drainage from mine tailings through the stimulation of specific microbial populations (e.g., SRB) has been proven effective in both laboratory and field situations. However, success has typically been achieved either through the use of engineered bioreactors which allow oxygen to be excluded from the reaction site, or via site controls which exclude oxygen, such as tailings flooding. Under both circumstances, site controls are implemented for the enhancement of SRB. This work took a broader perspective, and sought to stimulate both aerobic heterotrophic populations for the exclusion oxygen and SRB for the precipitation of solution phase metals as metal-sulfides.

Organic Carbon Choices

The organic carbon sources chosen for investigation were limited to those that were inexpensive and easily dissolved in water. Molasses, whey and methanol were chosen

for this study because they are easily dissolved in water, inexpensive, and can be readily applied to tailings surfaces with water handling equipment.

Molasses Treatment

Initial molasses treatments had the desired effect of increasing effluent pH and reducing ORP, however, the extent and longevity of this effect diminished with subsequent treatments. The behavior of the two test columns with regard to pH, ORP and microbial colonization differed significantly under molasses treatment. The better performing column (TC1) was consistently 1-1.5 pH units above TC2, and showed higher SRB and lower HPC counts. In TC2, the overall effect was of molasses addition on microbiota was evidently to stimulate populations of iron- and sulfur-oxidizing bacteria, ultimately leading to reduced pH and higher levels of produced metals. These conditions prevented the activity of SRB, as in the control column. Contrasting the performance of TC1 and TC2 illustrates both the variability that can occur with relatively uncontrolled (open) systems and the detrimental conditions that can result if initial organic carbon treatments stimulate microbial populations that are also capable of further acidification and metals leaching (e.g., heterotrophic IOB/SOB). Even in TC1 where molasses treatments were relatively effective, proton accounting indicated that only a small percentage (<1%) of the added organic carbon evidently contributed to the neutralization of excess protons via sulfate reduction.

While initially effective, molasses clearly lost its efficacy with repeated additions in both test columns. Although the first several molasses additions were not as concentrated as the subsequent whey treatments, the daily addition period did represent a

highly concentrated carbon dosing. Even under these conditions, molasses performance was diminishing in TC1 and clearly detrimental in TC2. Molasses was clearly not the optimal treatment in these studies.

Whey Treatment

Whey treatment was clearly capable of inhibiting acid production, decreasing oxidation and dissolved metals, and stimulating SRB in unsaturated mine tailings columns. The period of this effect was 6-12 months for the less weathered Fox Lake tailings, and up to 2 years for the more weathered (and hence less sulfide containing) Mammoth tailings. In the Fox Lake tailings, whey treatment was evidently not able to increase effluent pH to above 5.6, while in Mammoth, pH 6 was achieved. These studies suggest that there is a maximum pH above which further increases are not possible with organic carbon, and that this level is dependent on the treatment conditions. Certainly, the mineral content and ability of the tailings to generate acid is important, but also the physical system in which the tailings exist influences physical conditions, such as the rate of infiltration of water, air (oxygen) and CO_2 which in turn influences site microbiota. Therefore, the pH maxima determined here should not be applied directly to field situations. Furthermore, this work indicates that organic carbon treatment will probably not work well as a once-applied treatment. In the systems studied here, repeated applications were necessary. In temperate zone use of this technology, annual treatments could be engineered with proper site investigation.

An important point to be considered in using whey (or any organic carbon treatment) is the stimulation of detrimental bacterial populations. In the Fox Lake TC2,

whey treatment was evidently more effective than molasses in stimulating beneficial populations; however, detrimental populations were still activated by whey treatment in TC2. It is not possible to state if whey treatment would have been more effective in TC2 had these populations (e.g., heterotrophic IOB) not been stimulated by molasses, yet clearly they were not eliminated by whey addition. Demand exerted by autotrophic bacteria accounts for the majority of oxygen diffusing into both Fox Lake treated columns before whey addition, however this demand was temporarily reduced following treatment. Robust SRB growth was capable of rapidly increasing column pH in the bottom 6" of each column. Within this relatively small SRB-active zone, conditions for metals precipitation changed significantly, causing reductions in Al, Zn, Cu and Fe in TC1 and TC2.

Lime Treatment

The original purpose of lime was to stimulate the growth of non-acidophilic heterotrophic organisms in the near-surface zone of the treated columns. It did not accomplish this result, either alone or in combination with whey. However, lime treatment was beneficial. When used alone, lime applied the top surface of Mammoth tailings increased effluent pH, and appeared to have a somewhat inhibitory effect on IOB/SOB. However, the beneficial populations of SRB observed with whey treatment were not present with lime alone. The combination of whey and lime treatment (while not as successful as two whey treatments), nonetheless was more effective than whey alone in pH control and stimulating SRB populations. Depending on the expense of

application, these results suggest that liming in combination with whey treatment can be an effective means more rapidly generating the condition necessary for SRB growth.

Methanol Treatment

The concentration at which methanol becomes biocidal varies between microbial populations. Applied at a concentration of 7 g/L (0.7 %), methanol treatment had an inhibitory effect on oxygen consumption within the tailings, suggesting that aerobic bacterial activity was reduced following treatment. This may be a positive attribute of methanol addition if IOB/SOB activity is limited, yet SRB activity can be maintained. In this work, all bacterial types were less abundant in core samples following methanol treatment. Methanol has proven an effective AMD treatment in situations where engineering controls can both exclude oxygen and maintain a population of acclimated organisms. In open tailings systems, it would be difficult to fine tune methanol application to this extent unless it were continuously applied; a situation that would be both capital and maintenance intensive at remote mine locations. Combined treatment of whey and methanol did not result in apparent synergistic effects over whey treatment alone.

Literature Cited

Bacelar-Nicolau, P. and D.B. Johnson. 1999. Leaching of pyrite by acidophilic heterotrophic iron-oxidizing bacteria in pure and mixed cultures. Appl. Environ. Microbiol. 65:585-590.

Bagatto, G. and J.D. Shorthouse. 2000. Evaluation of municipal solid waste (MSW) compost as a soil amendment for acidic, metalliferous mine tailings. International Journal of Surface Mining, Reclamation and Environment. 14:205-214.

Barcelona, M.J. and G. Xie. 2001. In situ lifetimes and kinetics of a reductive whey barrier and an oxidative ORC barrier in the subsurface. Environ. Sci. Technol. 35:3378-3385.

Barros, M.E.C., D.E. Rawlings and D.R. Woods. 1984. Mixotrophic growth of a *T. ferrooxidans* strain. Appl. Environ. Microbiol. 47:593-595.

Benner, S.G., D.W. Blowes and C.J. Ptacek. 1997. A full-scale porous reactive wall for the prevention of acid mine drainage. Ground Water Monitoring Review. Fall 1997:99-107.

Benner, S.G., D.W. Blowes, W.D. Gould, R.B. Herbert Jr. and C.J. Ptacek. 1999. Geochemistry of a permeable reactive barrier for metals and acid mine drainage. Environ. Sci. Technol. 33:2793-2799.

Beveridge, T.J. 1981. Ultrastructure, chemistry and function of the bacterial cell wall. Int. Rev. Cytol. 72:229-317.

Beveridge, T.J., J.D. Meloche, W.S. Fyfe and R.G. Murray. 1983. Diagenesis of metals chemically complexed to bacteria: laboratory formation of metal phosphates, sulfides and organic condensates in artificial sediments. Appl. Environ. Microbiol. 45:1094-1108.

Beveridge, T.J., M.N. Hughes, H. Lee, K.T. Leung, R.K. Poole, I. Savvaidis, S. Silver and J.T. Trevors. 1997. Metal-microbe interactions: contemporary approaches. Advances in Microbial Physiology. 38:178-243.

Bigham, J.M, U. Schwertmann and G. Pfab. 1996. Influence of pH on mineral speciation in a bioreactor simulating acid mine drainage. Applied Geochemistry. 11:845-849.

Blenkinsopp, S.A., D.C. Herman, R.G.L. McCready and J.W. Costerton. 1992. Acidogenic mine tailings. Applied Biochem. Biotechnol. 34/35:801-809.

Blowes, D.W., E.J. Reardon, J.L. Jambor and J.A. Cherry. 1991. The formation and potential importance of cemented layers in inactive sulfide mine tailings. Geochimica et Cosmochimica Acta. 55:965-978.

Bond, P.L., G.K. Druschel and J.F. Banfield. 2000a. Comparison of acid mine drainage microbial communities in physically and geochemically distinct ecosystems. Appl. Environ. Microbiol. 66:4962-4971.

Bond, P.L., S.P. Smriga and J.F. Banfield. 2000b. Phylogeny of microorganisms populating a thick, subaerial, predominantly lithotrophic biofilm at an extreme acid mine drainage site. Appl. Environ. Microbiol. 66:3842-3849.

Bonnissel-Gissinger, P., M. Alnot, J.J. Ehrhardt and P. Behra. 1998. Surface oxidation of pyrite as a function of pH. Environ. Sci. Technol. 32:2839-2845.

Boon, M., M. Snijder, G.S. Hansford and J.J. Heijnen. 1998. The oxidation kinetics of zinc sulphide with *Thiobacillus ferrooxidans*. Hydrometallurgy. 48:171-186.

Brandl, H., R. Bosshard and M. Wegmann. 2001. Computer-munching microbes: metal leaching from electronic scrap by bacteria and fungi. Hydrometallurgy. 59:319-326.

Brenner, F.J. 2001. Use of constructed wetlands for acid mine drainage abatement and stream restoration. Water Science and Technology. 44:449-454.

Bridge, T.A. and D.B. Johnson. 1998. Reduction of soluble iron and reductive dissolution of ferric iron-containing minerals by moderately thermophilic iron-oxidizing bacteria. Appl. Environ. Microbiol. 64:2181-2186.

Brierley, C.L. 1978. Bacterial leaching. Critical Reviews in Microbiology. 6.207-262.

Brierley, C.L. and J.A. Brierley. 1996. Microbiology for the metal mining industry. In: C.J. Hurst, G.R. Knudsen, M.J. McInerney, M.V. Walter and L.D. Stetzenbach (eds.), Manual of Environmental Microbiology, pp. 830-841. ASM Press. Washington, D.C.

Briggs, P.H. 1996. Forty elements by inductively coupled plasma-atomic emission spectrometry, in Arbogast, B.F., ed., Analytical methods manual for the Mineral Resource Program, U.S. Geological Survey Open-File Report 96-525, p.77-94.

Brock, T.D. and J. Gustafson. 1976. Ferric iron reduction by sulfur- and iron-oxidizing bacteria. Appl. Environ. Microbiol. 32:567-571.

Bussiere, B., M. Aubertin and R.P. Chapuis. 2000. An investigation of slope effects on the efficiency of capillary barriers to control AMD. In: Proceedings from the Fifth

International Conference on Acid Rock Drainage, pp. 969-977. Society for Mining, Metallurgy, and Exploration, Inc. Littleton, CO.

Camper, A.K., M.W. LeChevallier, S.C. Broadaway, and G.A. McFeters. 1985. Evaluation of procedures to desorb bacteria from granular activated carbon. J. Microbiol. Methods. 3:187-198.

Chang, I.S., P.K. Shin and B.H. Kim. 2000. Biological treatment of acid mine drainage under sulfate-reducing conditions with solid waste materials as substrate. Water Research. 34:1269-1277.

Characklis, W.G. and K.C. Marshall. 1990. Biofilms. John Wiley & Sons, Inc. New York.

Christensen B., M. Laake and T. Lien. 1996. Treatment of acid mine water by sulfate-reducing bacteria; results from a bench scale experiment. Water Research. 30:1617-1624.

Cocos, I.A., G.J. Zagury, B. Clement and R. Samson. 2002. Multiple factor design for reactive mixture selection for use in reactive walls in acid mine drainage treatment. Water Research. 32:167-177.

Crundwell, F.K. 1988. The influence of electronic structure of solids on the anodic dissolution and leaching of semiconducting sulphide minerals. Hydrometallurgy. 21:155-190.

Cunningham, A.B., R.R. Sharp, R. Hiebert and G. James. 2003. Subsurface biofilm barriers for the containment and remediation of contaminated groundwater. Bioremediation J. 7(3-4):1-13.

Dakota Gasification Company. 2003. Methanol Material Safety Data Sheet. Beulah, ND.

Dave, N.K., T.P. Lim, D. Horne, Y. Boucher and R. Stuparyk. 1997. Water cover on reactive tailings and waste rock: laboratory studies of oxidation and metal relsase characteristics. In: Proceedings of the Fourth International Conference on Acid Rock Drainage, pp. 779-794. Vancouver, BC, Canada.

DiSpirito, A.A. and O.H. Tuovinen. 1982. Uranous ion oxidation and carbon dioxide fixation by *Thiobacillus ferrooxidans*. Arch. Microbiol. 133:28-32.

Douglas, S. and T.J. Beveridge. 1998. Mineral formation by bacteria in natural microbial communities. FEMS Microbiol. Ecol. 26:79-88.

Dugan, P.R. 1987. Prevention of formation of acid drainage from high-sulfur coal refuse by inhibition of iron- and sulfur-oxidizing microorganisms. II. Inhibition in "run of mine" refuse under simulated field conditions. Biotechnol Bioeng. 29:49-54.

Eaton, A.D., L.S. Clesceri and A.E. Greenberg. 1995. Standard Methods for the Examination of Water and Wastewater. Method 9240 D. American Public Health Association, Washington, D.C.

Edwards, K.J., T.M. Gihring and J.F. Banfield. 1999. Seasonal variation in microbial populations and environmental conditions in an extreme acid mine drainage environment. Appl. Environ. Microbiol. 65:3627-3632.

Edwards, K.J., P.L. Bond and J.F. Banfield. 2000a. Characteristics of attachment and growth of *Thiobacillus caldus* on sulphide minerals: a chemotactic response to sulphur minerals? Environ. Microbiol. 2:324-332.

Edwards, K.J., P.L. Bond, T.M. Gihring and J.F. Banfield. 2000b. An Archaeal iron-oxidizing extreme acidophile important in acid mine drainage. Science. 287:1796-1799.

El-Ammouri, E., P.A. Distin, S.R. Rao, J.A. Finch and K. Ngoviky. 2000. Treatment of acid mine drainage sludge by leaching and metal recovery using activated silica. In: Proceedings from the Fifth International Conference on Acid Rock Drainage, pp. 1087-1094. Society for Mining, Metallurgy, and Exploration, Inc. Littleton, CO.

Elberling, B. and R.V. Nicholson. 1996. Field determination of sulphide oxidation rates in mine tailings. Wat. Resources Research. 32:1773-1784.

Elberling, B., A. Schippers and W. Sand. 2000. Bacterial and chemical oxidation of pyritic mine tailings at low temperatures. J. Contaminant Hydrol. 41:225-238.

Elberling, B. and L.R. Damgaard. 2001. Microscale measurements of oxygen diffusion and consumption in subaqueous sulfide tailings. Geochimica et Cosmochimica Acta. 65:1897-1905.

Elliott, L.C.M., L. Liu and S.W. Stogran. 1997. Organic cover materials for tailings: do they meet the requirements of an effective long-term cover? In: Proceedings of the Fourth International Conference on Acid Rock Drainage. Vancouver, B.C., Canada. pp. 813-824.

Elliott, P., S. Ragusa and D. Catcheside. 1998. Growth of sulfate-reducing bacteria under acidic conditions in an upflow anaerobic bioreactor as a treatment system for acid mine drainage. Water Research. 32:3724-3730.

Elsetinow, A.R., M.A. Schoonen and D.R. Strongin. 2001. Aqueous geochemical and surface science investigation of the effect of phosphate on pyrite oxidation. Environ. Sci Technol. 35:2252-2257.

Evangelou, V.P. 1995. Pyrite oxidation and its control, p. 293. CRC Press. Boca Raton, FL.

Fauville, A., B. Mayer, R. Frommichen, K. Friese and J. Veizer. 2004. Chemical and isotopic evidence for accelerated bacterial sulfate reduction in acid mining lakes after addition of organic carbon: laboratory batch experiments. Chemical Geology. 204:325-344.

Ferris, F.G., W.S. Fyfe and T.J. Beveridge. 1991. Bacteria as nucleation sites for authigenic minerals. In: Diversity of Environmental Biogeochemistry. J. Berthelin (ed). Elsevier. New York. pp. 319-325.

Ferris, F.G. 1993. Microbial biomineralization in natural environments. Earth Science. 47:233-250.

Fletcher, M. (ed). 1996. Bacterial adhesion: molecular and ecological diversity, p. 1-24. Wiley-Liss, New York, NY.

Fortin, D., B. Davis, G. Southam and T.J. Beveridge. 1995. Biogeochemical phenomena induced by bacteria within sulfidic mine tailings. J. Indust. Microbiol. 14:178-185.

Fortin, D., B. Davis and T.J. Beveridge.1996. Role of *Thiobacillus* and sulfate-reducing bacteria in biocycling in oxic and acidic mine tailings. FEMS Microbiology Ecology. 21:11-24.

Fortin, D. and T.J. Beveridge. 1997. Microbial sulfate reduction within sulfidic mine tailings: formation of diagenetic Fe sulfides. Geomicrobiology Journal. 14:1-21.

Fowler, T.A. and F.K. Crundwell. 1998. Leaching of zinc sulfide by *Thiobacillus ferrooxidan*s: experiments with a controlled redox potential indicate no direct bacterial mechanism. Appl. Environ. Microbiol. 64:3570-3575.

Fowler, T.A. and F.K. Crundwell. 1999. Leaching of zinc sulfide by *Thiobacillus ferrooxidans*: bacterial oxidation of the sulfur product layer increases the rate of zinc sulfide dissolution at high concentrations of ferrous ions. Appl. Environ. Microbiol. 65:5285-5292.

Fowler, T.A., P.R. Holmes and F.K. Crundwell. 1999. Mechanism of pyrite dissolution in the presences of *Thiobacillus ferrooxidans*. Appl. Environ. Microbiol. 65:2987-2993.

Fowler, T.A., P.R. Holmes and F.K. Crundwell. 2001. On the kinetics and mechanism of the dissolution of pyrite in the presence of *Thiobacillus ferrooxidans*. Hydrometallurgy. 59:257-270.

Francis, C.A., A.Y. Obraztsova and B.M. Tebo. 2000. Dissimilatory metal reduction by the facultative anaerobe *Pantoea agglomerans* SP1. Appl. Environ. Microbiol. 66:543-548.

Frattini, C.J., L.G. Leduc and G.D. Ferroni. 2000. Strain variability and the effects of organic compounds on the growth of the chemolithotrophic bacterium *Thiobacillus ferrooxidans*. Antonie van Leeuwenhoek. 77:57-64.

Free, M.L., T. Oolman, S. Nagpal, and D.A. Dahlstroom. 1991. Bioleaching of sulfide ores – distinguishing between indirect and direct mechanisms. In: R.W. Smith and M. Misra (ed.), Mineral Bioprocessing. The Minerals, Metals and Materials Society, Warrendale, PA. p. 485-495.

Gatzweiler, R., S. Jahn, G. Neubert and M. Paul. 2000. Cover design for radioactive and AMD-producing mine waste in the Ronneburg area, Eastern Thuringia. Waste Management. 21:175-184.

Geesey, G.G. and L. Lang. 1989. Interactions between metal ions and capsular polymers, p. 325-357. In: T.J. Beveridge and R.J. Doyle (ed.), Metal ions and bacteria. John Wiley & Sons, New York, NY.

Gehrke, T., J. Telegdi, D. Thierry and W. Sand. 1998. Importance of extracellular polymeric substances from *Thiobacillus ferrooxidans* for bioleaching. Appl. Environ. Microbiol. 64:2743-2747.

Gonzalez-Toril, E., E. Llobet-Brossa, E.O. Casamayor, R. Amann, and R. Amils. 2003. Microbial ecology of an extreme acidic environment, the Tinto River. Appl. Environ. Microbiol. 69:4853-4865.

Guevremont, J.M., J. Bebie, A.R. Elsetinow, D.R. Strongin and M.A.A. Schoonen. 1998. Reactivity of the (100) plane of pyrite in oxidizing gaseous and aqueous environments: effects of surface imperfections. Environ. Sci. Technol. 32:3743-3748.

Gyure, R.A., A. Konopka, A. Brooks and W. Doemel. 1990. Microbial sulfate reduction in acidic (pH 3) strip-mine lakes. FEMS Microbiol. Ecol. 73:193-202.

Hahn, M.S., S. Willscher and G. Straube. 1993. Copper leaching from industrial wastes by heterotrophic microorganisms. In: A.E. Torma, J.E. Wey, V.L. Lakshamanan (eds.), Biohydrometallurgical Technologies, The Minerals, Metals & Material Society, Warrendale, pp. 99-108.

Hansford, G.S, and T. Vargas. 2001. Chemical and electrochemical basis of bioleaching processes. Hydrometallurgy. 59:135-145.

Harris, M.A. and M. Megharaj. 2001. The effects of sludge and green manure on hydraulic conductivity and aggregation in pyritic mine tailings materials. Environmental Geology. 41:285-296.

Harrison, A.P. 1984. The acidophilic *Thiobacilli* and other acidophilic bacteria that share their habitat. Ann. Rev. Microbiol. 38:265-292.

Herlihy, A.T. and A.L. Mills. 1985. Sulfate reduction in freshwater sediments receiving acid mine drainage. Appl. Environ. Microbiol. 49:179-186.

Holmes, P.R. and F.K. Crundwell. 1999. The kinetics of the oxidation of pyrite by ferric ions and dissolved oxygen: an electrochemical study. Geochimica et Cosmochimica Acta. 64:263-274.

Huang, X. and V.P. Evangelou. 1994. Suppression of pyrite oxidation by phosphate addition. In: Environmental Geochemistry of Sulfide Oxidation, C.N. Alpers and D.W. Blowes (eds). American Chemical Society. Washington D.C. pp. 562-573.

Johnson, D.B. 1998. Biodiversity and ecology of acidophilic microorganisms. FEMS Microbiol. Ecol. 27:307-317

Johnson, D.B. 1991. Diversity of microbial life in highly acidic, mesophilic environments. In: J. Berthelin (ed), Diversity of Environmental Biogeochemistry, p. 225-238. Elsevier Press, New York, NY.

Johnson, D.B. and S. McGinness. 1991. Ferric iron reduction by acidophilic heterotrophic bacteria. Appl. Environ. Microbiol. 57:207-211.

Johnson, D.B., M.A. Ghauri and M.F. Said. 1992. Isolation and characterization of an acidophilic, heterotrophic bacterium capable of oxidizing ferrous iron. Appl. Environ. Microbiol. 58:1423-1428.

Johnson, D.B. and F.F. Roberto. 1997. Heterotrophic acidophiles and their roles in the bioleaching of sulfide minerals. In: D.E. Rawlings (ed.), Biomining: Theory, Microbes and Industrial Processes. Springer-Verlag and Landes Bioscience. pp. 259-279.

Johnson, D.B., M.A. Dziurla and A. Kolmert. 2000. Novel approaches for bioremediation of acidic, metal-rich effluents using indigenous bacteria. In: Proceedings from the Fifth International Conference on Acid Rock Drainage, pp. 1209-1217. Society for Mining, Metallurgy, and Exploration, Inc. Littleton, CO.

Johnson, D.B. 2001a. Importance of microbial ecology in the development of new mineral technologies. Hydrometallurgy. 59:147-157.

Johnson, D.B. 2001b. Role of pure and mixed cultures of Gram-positive eubacteria in mineral leaching. In: Proceedings of the International Biohydrometallurgy Symposium, pp. 401-410. Ouro Preto, Minas Gerais, Brazil. Elsevier Science.

Johnson, D.B., N. Okibe and F.R. Roberto. 2003. Novel thermo-acidophilic bacteria isolated from geothermal sites in Yellowstone National Park: physiological and phylogenetic characteristics. Arch. Microbiol. 180:60-68.

Kelly, D.P. 1987. Sulphur bacteria first again. Nature. 326:830-833.

Kim, S.D., J.J. Kilbane, Jr. and D.K. Cha. 1999. Prevention of acid mine drainage by sulfate reducing bacteria: organic substrate addition to mine waste piles. Environmental Engineering Science. 16:139-145.

Kolmert, A. and D.B. Johnson. 2001. Remediation of acidic waste waters using immobilised, acidophilic sulfate-reducing bacteria. Journal of Chemical Technology and Biotechnology. 76:836-843.

Labrenz, M. and J.F. Banfield. 2004. Sulfate-reducing bacteria-dominated biofilms that precipitate ZnS in a subsurface circumneutral-pH mine drainage system. Microb. Ecol. 47:205-217.

Lan, Y., X. Huang and Z. Liu. 1999. Effect of $FePO_4$ film on the kinetics of pyrite oxidation. Environ. Chem. 18:52-56.

Lan Y., X. Huang and B. Deng. 2002. Suppression of pyrite oxidation by iron 8-hydroxyquinoline. Arch. Environ. Contam. Toxicol. 43:168-174.

Lane, D.J., A.P. Harrison, D. Stahl, B. Pace, S.J. Giovannoni, G.J. Olsen and N.R. Pace. 1992. Evolutionary relationships among sulfur- and iron-oxidizing eubacteria. J. Bacteriol. 174: 269-278.

Leathen, W.W., S.A. Braley, and L.D. McIntyre. 1953. The role of bacteria in the formation of acid from certain sulfuritic constituents associated with bituminous coal. II. Ferrous iron oxidizing bacteria. Appl. Microbiol. 1:65-68.

Leduc, L.G. and G.D. Ferroni. 1994. The chemolithotrophic bacterium *Thiobacillus ferrooxidans*. FEMS Microbiol. Rev. 14:103-120.

Leduc, D., L.G. Leduc and G.D. Ferroni. 2002. Quantification of bacterial populations indigenous to acidic drainage streams. Water, Air, and Soil Pollution. 135:1-21.

Lees, H., S.C. Kwok and I. Suzuki. 1969. The thermodynamics of iron oxidation by the ferrobacilli. Can. J. Microbiol. 15:43-46.

Lefebvre, R., D. Hockley, J. Smolensky and P. Gelinas. 2001. Multiphase transfer processes in waste rock piles producing acid mine drainage: 1: Conceptual model and system characterization. J. Contamin. Hydrol. 52:137-164.

Lewis, B.A., R.D. Gallinger and M. Wiber. 2000. Poirier site reclamation program. In: Proceedings from the Fifth International Conference on Acid Rock Drainage, pp. 959-968. Society for Mining, Metallurgy, and Exploration, Inc. Littleton, CO.

Li, M., L.J.J. Catalan and P. St-Germain. 2000. Rates of oxygen consumption by sulphidic tailings under shallow water covers – field measurements and modeling. In: Proceedings from the Fifth International Conference on Acid Rock Drainage, pp. 913-920. Society for Mining, Metallurgy, and Exploration, Inc. Littleton, CO.

Lizama, H.M., and I. Suzuki. 1991. Interaction of chalcopyrite and sphalerite with pyrite during leaching by *Thiobacillus ferrooxidans* and *Thiobacillus thiooxidans*. Can. J. Microbiol. 37:304-311.

Lyew, D. and J.D. Sheppard. 1997. Effects of physical parameters of a gravel bed on the activity of sulphate-reducing bacteria in the presence of acid mine drainage. J. Chem. Technol. Biotechnol. 70:223-230.

Macur, R.E., J.T. Wheeler, T.R. McDermott and W.P. Inskeep. 2001. Microbial populations associated with reduction and enhanced mobilization of arsenic in mine tailings. Environ. Sci. Tech. 35:3676-3682.

Marchland, E.A. and J. Silverstein. 2000. Remediation of acid rock drainage by inducing biological iron reduction. In: Proceedings from the Fifth International Conference on Acid Rock Drainage, pp. 1201-1207. Society for Mining, Metallurgy, and Exploration, Inc. Littleton, CO.

Marchand E.A. and J. Silverstein. 2002. Influence of heterotrophic microbial growth on biological oxidation of pyrite. Environ. Sci. Technol. 36:5483-5490.

Mullen, M.D., D.C. Wolf, F.G. Ferris, T.J. Beveridge, C.A. Flemming and G.W. Bailey. 1989. Bacterial sorption of heavy metals. Appl. Environ. Microbiol. 55:3143-3149

Morse, J.W. and T. Arakaki. 1993. Adsorption and coprecipitation of divalent metals with mackinawite (FeS). Geochimica et Cosmochimica Acta. 57:3635-3640.

Nicholson, R.V., R.W. Gillham, J.A. Cherry and E.J. Reardon. 1989. Reduction of acid generation in mine tailings through the use of moisture-retaining cover layers as oxygen barriers. Canadian Geotech. J. 26:1-8.

Nordstrom, D.K., C.N. Alpers, C.J. Ptacek and D.W. Blowes. 2000. Negative pH and extremely acidic mine waters from Iron Mountain, California. Environ. Sci. Technol. 34:254-258.

Okabe, S. 1992. Rate and stoichiometry of sulfate reducing bacteria in suspended and biofilm cultures. PhD Thesis. Montana State University, Bozeman, Montana.

Olson, G.J., T.R. Clark, T.I. Mudder and M. Logsdon. 2003. A novel approach for control and prevention of Acid Rock Drainage (ARD). In: Proceedings of the Sixth International Conference on Acid Rock Drainage, Cairns Australia.

Pronk, J.T., W.M. Meijer, W. Hazeu, J.P. van Dijken, P. Bos and J.G. Kuenen. 1991a. Growth of *Thiobacillus ferrooxidans* on formic acid. Appl. Environ. Microbiol. 57:2057-2062.

Postgate, J.R., 1984, The Sulphate-reducing Bacteria, 2nd Edition, 208 pp. Cambridge University Press, Cambridge.

Pronk, J.T., K. Liem, P. Bos and J.G. Kuenen. 1991b. Energy transduction by anaerobic ferric iron respiration in *Thiobacillus ferrooxidans*. Appl. Environ. Microbiol. 57:2063-2068.

Pronk, J.T and D.B. Johnson. 1992. Oxidation and reduction of iron by acidophilic bacteria. Geomicrobiology J. 10:153-171.

Raven, K.P., A. Jain and R.H. Loeppert. 1998. Arsenite and arsenate adsorption on ferrihydrite: kinetics, equilibrium, and adsorption envelopes. Environ. Sci. Technol. 32:344-349.

Rawlings, D.E. 2002. Heavy metal mining using microbes. Annual Rev. Microbiol. 56:65-91.

Reardon, E.J. and P.M. Moddle. 1985. Gas diffusion measurements on uranium mill tailings: implications to cover layer design. Uranium. 2:111-113.

Remolar, D.F., R. Amils, R.V. Morris and A.H. Knoll. 2002. The Tinto River basin: an analog for meridiani hematite formation on Mars? Lunar and Planetary Science XXXIII:1226-1227.

Robertson, J.D., G.A. Tremblay and W.W. Fraser. 1997. Subaqueous tailings disposal: a sound solution for reactive tailings. In: Proceedings of the Fourth International Conference on Acid Rock Drainage, pp. 1027-1041. Vancouver, BC, Canada.

Samuel, D.E., J.C. Sencindiver and H.W. Rauch. 1988. Water and soil parameters affecting the growth of cattails: pilot studies in West Virginia mines. In: Mine Drainage and Surface Reclamation. Vol I: Mine Water and Mine Waste, US Dept. of Interior, Bureau of Mines Information Circular 9183.

Sand, W., T. Gehrke, R. Hallmann and A. Schippers. 1995. Sulfur chemistry, biofilm, and the (in)direct attack mechanism – a critical evaluation of bioleaching. Appl. Microbiol. Biotechnol. 43:961-966.

Sand, W., T. Gehrke, P.G. Jozsa and A. Schippers. 2001. (Bio)chemistry of bacterial leaching – direct vs. indirect bioleaching. Hydrometallurgy. 59:159-175.

Schippers, A., R. Hallmann, S. Wentzien and W. Sand. 1995. Microbial diversity in uranium mine waste heaps. Appl. Environ. Microbiol. 61:2930-2935.

Schippers, A., P.G. Jozsa and W. Sand. 1998. Evaluation of the efficiency of measures for sulphidic mine waste mitigation. Appl. Microbiol. Biotechnol. 49:698-701.

Schippers, A. and W. Sand. 1999. Bacterial leaching of metal sulfides proceeds by two indirect mechanisms via thiosulfate or via polysulfides and sulfur. Appl. Environ. Microbiol. 65:319-321.

Schippers, A., P.G. Jozsa, Z.M. Kovacs, M. Jelea and W. Sand. 2001. Large-scale experiments for microbiological evaluation of measures for safeguarding sulfidic mine waste. Waste Management 21:139-146.

Schneegurt, M.A., J.C. Jain, J.A. Menicucci Jr., S.A. Brown, K.M. Kemner, D.F. Garofalo, M.R. Quallick, C.R. Neal and C.F. Kulpa Jr. 2001. Biomass byproducts for the remediation of wastewaters contaminated with toxic metals. Environ. Sci. Technol. 35:3786-3791

Schoonen, M.A.A. and H.L. Barnes. 1991. Reactions forming pyrite and marcasite from solution: II. via FeS precursors below 100ºC. Geochimica et Cosmochimica Acta. 55:1505-1514.

Schrenk, M.O., K.J. Edwards, R.M. Goodman, R.J. Hamers and J.F. Banfield. 1998. Distribution of *Thiobacillus ferrooxidans* and *Leptospirillum ferrooxidans*: implications for generation of acid mine drainage. Science. 279:1519-1522.

Sharp, T.R. 1999. Biological and geotechnical controls on CO_2 equilibria in free water wetlands. PhD Thesis, Department of Civil Engineering, Montana State University, Bozeman, Montana.

Shea, P. 2000. The U.S. Interior Department's abandoned mine lands program. In: Proceedings from the Fifth International Conference on Acid Rock Drainage, pp. 21-27. Society for Mining, Metallurgy, and Exploration, Inc. Littleton, CO.

Shelp, G.S., W. Chesworth and G. Spiers. 1995. The amelioration of acid mine drainage by an in situ electrochemical method –I. Employing scrap iron as the sacrificial anode. Appl. Geochem. 10:705-713.

Shoemaker, H.E., E. O. McLean and P. F. Pratt. 1961. Buffer methods for determining lime requirements of soils with appreciable amounts of extractable aluminum. Soil Science Society of America Proceedings. 25:274-277.

Shokes, T.E. and G. Moller. 1999. Removal of dissolved heavy metals from acid rock drainage using iron metal. Environ. Sci. Technol. 33:282-287.

Silverman, M.P. and D.G. Lundgren. 1959. Studies on the chemoautotrophic iron bacterium *Ferrobacillus ferrooxidans*. J. Bact. 77:642-647.

Silverman, M.P. and H.L. Ehrlich. 1964. Microbial formation and degradation of minerals. Adv. Appl. Microbiol. 6:181-183.

Simbahan, J., R. Drijber and P. Blum. 2004. Alicyclobacillus vulcanalis sp. nov., a thermophilic, acidophilic bacterium isolated from Coso Hot Springs, California, USA. ISJEM Papers in Press – Published online 19 March 2004 as http://dx.doi.org/10.1099/ijs.0.03012-0.

Singer, P.C. and W. Stumm. 1970. Acidic mine drainage: the rate determining step. Science. 167:1121-1123.

Smith, R. M., W.E. Grube, T. Arkle, and A. Sobek. 1974. Mine Spoil Potentials for Soil and Water Quality, U.S. Environmental Protection Agency, Cincinnati, Ohio, EPA-670/2-74-070.

Southam, G. and T.J. Beveridge. 1992. Enumeration of Thiobacilli within pH-neutral and acidic mine tailings and their role in the development of secondary mineral soil. Appl. Environ. Microbiol. 58:1904-1912.

Standard Methods for the Examination of Water and Wastewater, 20th Ed. 1998. American Public Health Association, American Water Works Association, Water Environment Federation. Washington, DC.

Stumm, W. and J.J. Morgan. 1981. Aquatic Chemistry, 2nd Edition. John Wiley and Sons. New York.

Sugio, T., C. Domatsu, O. MunakataT. Tano and K. Imai. 1985. Role of a ferric ion-reducing system in sulfur oxidation of *Thiobacillus ferrooxidans*. Appl. Environ. Microbiol. 49:1401-1406.

Sugio, T., K.J. White, E. Shute, D. Choate and R.C. Blake II. 1992. Existence of a hydrogen sulfide: ferric ion oxidoreductase in iron-oxidizing bacteria. Appl. Environ. Microbiol. 58:431-433.

Suzuki, I., D. Lee, B. Mackay, L. Harahuc and J.K. Oh. 1999. Effect of various ions, pH and osmotic pressure on oxidation of elemental sulfur by *Thiobacillus thiooxidans*. Appl. Environ. Microbiol. 65:5163-5168.

Suzuki, Y., S.D. Kelly, K.M. Kemner and J.F. Banfield. 2003. Microbial populations stimulated for hexavalent uranium reduction in uranium mine sediment. Appl. Environ. Microbiol. 69:1337-1346.

Thomson, B.M., D.S. Simonton and L.L. Barton. 2001. Stability of arsenic and selenium immobilized by *in situ* microbial reduction. In: Proceedings, 2001 Conference on Environmental Research, Kansas State University, pp. 17-26.

Tsukamoto, T.K. and G.C. Miller. 1999. Methanol as a carbon source for microbiological treatment of acid mine drainage. Water Research. 33:1365-1370.

Urrutia Mera, M., M. Kemper, R. Doyle and T.J. Beveridge. 1992. The membrane-induced proton motive force influences the metal binding ability of *Bacillus subtilis* cell walls. Appl. Environ. Microbiol. 58:3837-3844.

U.S. Water News. 1993. With or without reform, mining cleanup could cost $71 billion. Volume 10, October. U.S. Water News, Inc., Halstead KS.

Vigneault, B., P.G.C. Campbell, A. Tessier and R. DeVitre. 2001. Geochemical changes in sulfidic mine tailings stored under a shallow water cover. Water Research. 35:1066-1076.

Waksman, S.A. and J.S. Joffe. 1921. Acid production by a new sulfur oxidizing bacterium. Science. 53:216-219.

Walsh, F. and R. Mitchell. 1972. A pH-dependent succession of iron bacteria. Environ. Sci. Technol. 6:809-812.

Wang, F., P. Wang, M. Chen and X. Xiao. 2004. Isolation of extremophiles with the detection and retrieval of *Shewanella* strains in deep-sea sediments from the west Pacific. Extremophiles. 8:165-168.

Waybrant, K.R., C.J. Ptacek and D.W. Blowes. 2002. Treatment of mine drainage using permeable reactive barriers: column experiments. Environ. Sci. Technol. 36:1349-1356.

Webb, J.S., S. McGinness and H.M. Lappin-Scott. 1998. Metal removal by sulphate-reducing bacteria from natural and constructed wetlands. Journal of Applied Microbiology. 84:240-248.

Wenberg, G.M., F.H. Erbisch and M.E. Volin. 1971. Leaching of copper by fungi. Society of Mining Engineers Transactions. 250:207-212.

Wielinga, B., J.K. Lucy, J.N. Moore, O.F. Seastone and J.E. Gannon. 1999. Microbial and geochemical characterization of fluvially deposited sulfidic mine tailings. Appl. Environ. Microbiol. 65:1548-1555.

Ye, Z.H., J.W. Wong and M.H. Wong. 2000. Vegetation response to lime and manure compost amendments on acid lead/zinc mine tailings: a greenhouse study. Restoration Ecology. 8:289-295.

Zaluski, M., J. Trudnowski, M. Canty, and M.A. Harrington Baker. 2000. Performance of field bioreactors with sulfate-reducing bacteria to control acid mine drainage. In: Proceedings from the Fifth International Conference on Acid Rock Drainage, pp. 1169-1175. Society for Mining, Metallurgy, and Exploration, Inc. Littleton, CO.

APPENDICES

APPENDIX A

DISTRIBUTION DIAGRAMS

Distribution diagrams generated by STABCAL for pre-treatment conditions in Fox Lake columns. Diagrams show the solid and aqueous phases for major metals and sulfur with variation in Eh at pH 4.

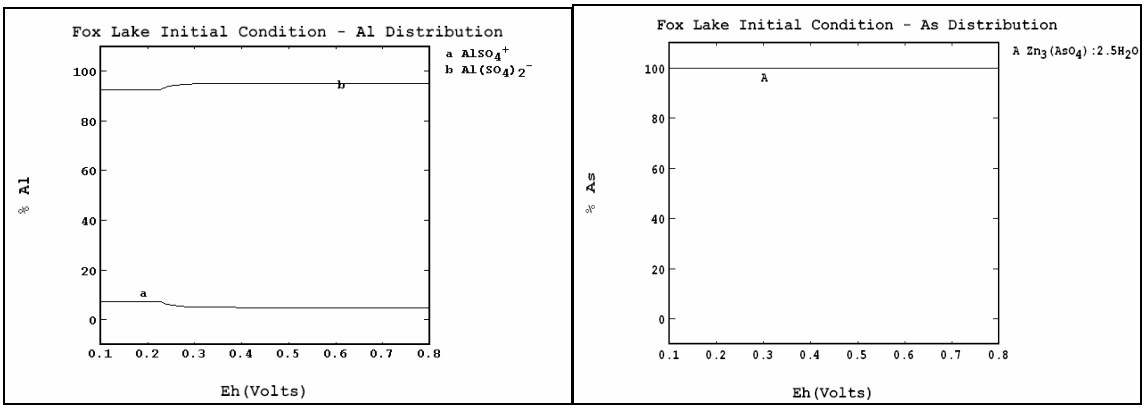

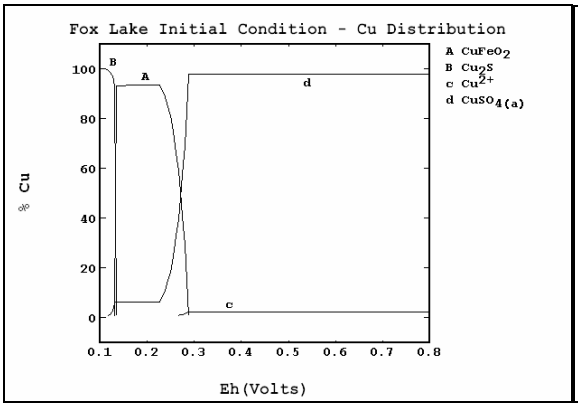

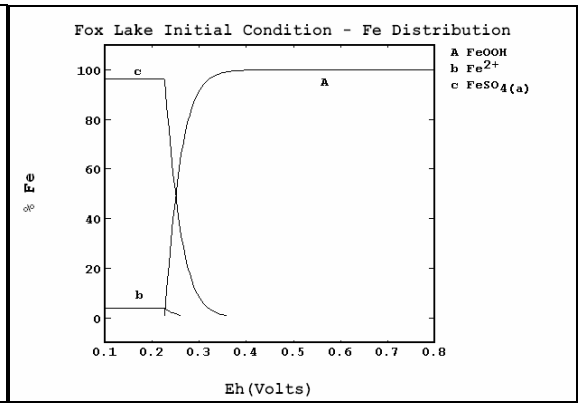

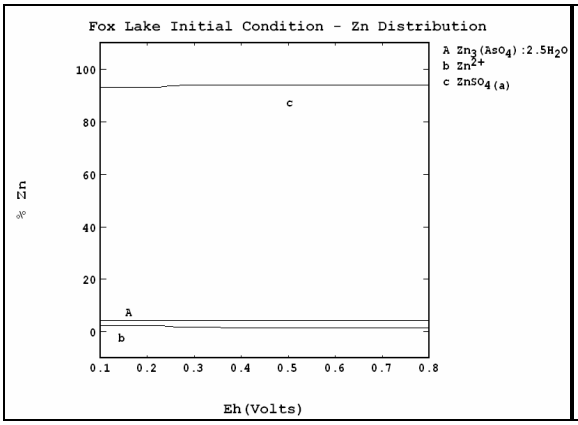

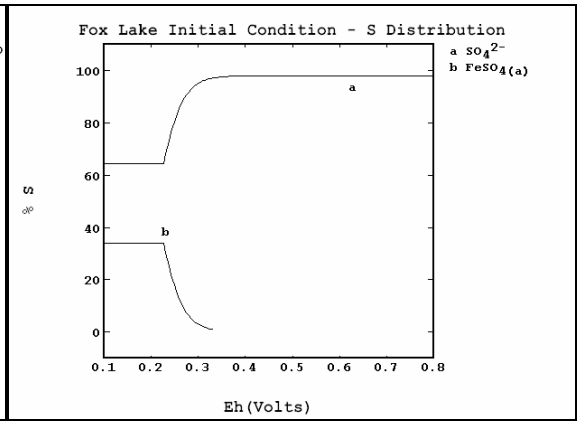

Distribution diagrams generated by STABCAL for conditions in Fox Lake TC1 at day 110. Diagrams show the solid and aqueous phases for major metals and sulfur with variation in Eh at pH 5. Measured Eh was +175 mV.

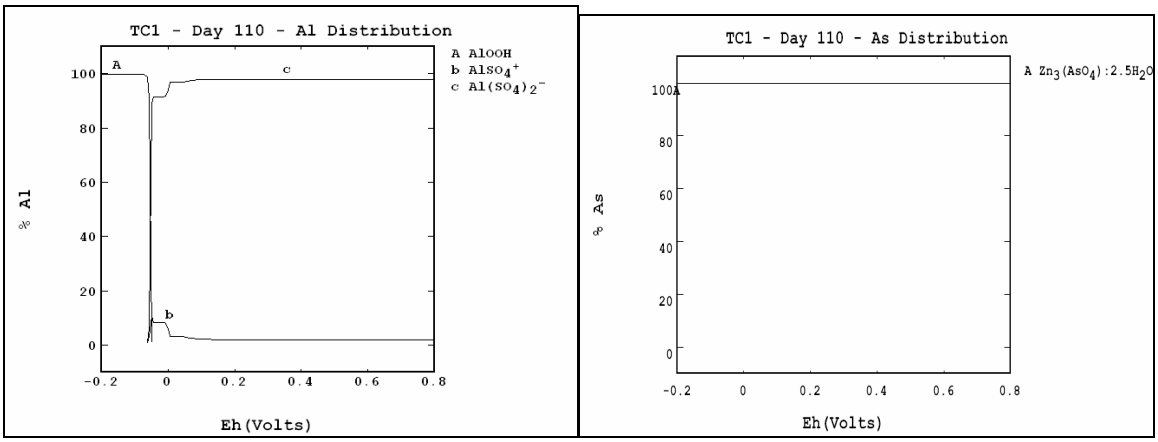

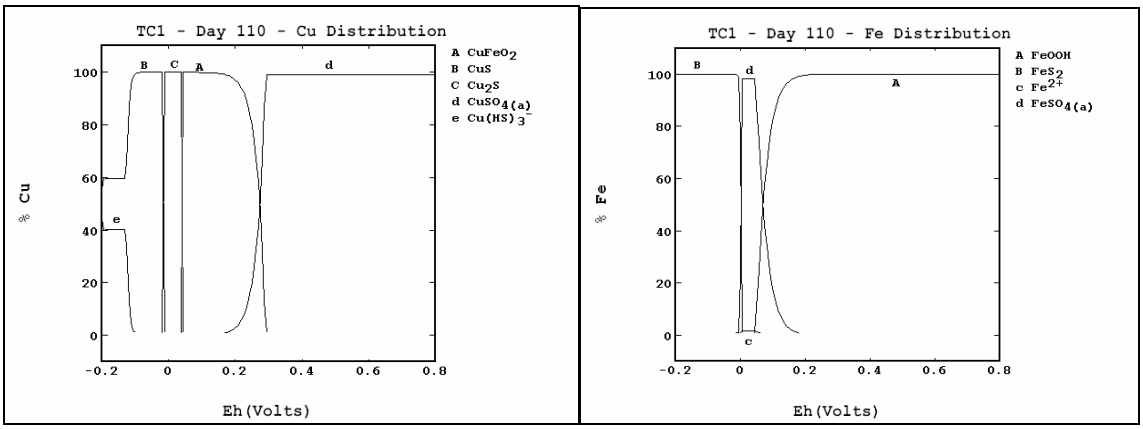

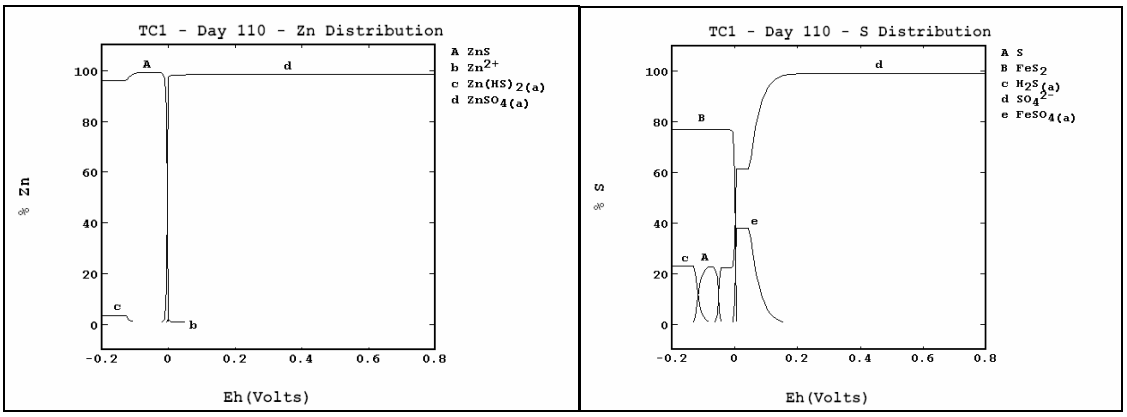

Distribution diagrams generated by STABCAL for conditions in Fox Lake TC2 at day 110. Diagrams show the solid and aqueous phases for major metals and sulfur with variation in Eh at pH 3.3. Measured Eh was +480 mV.

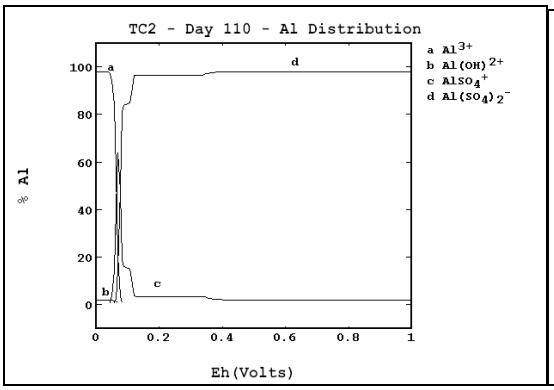

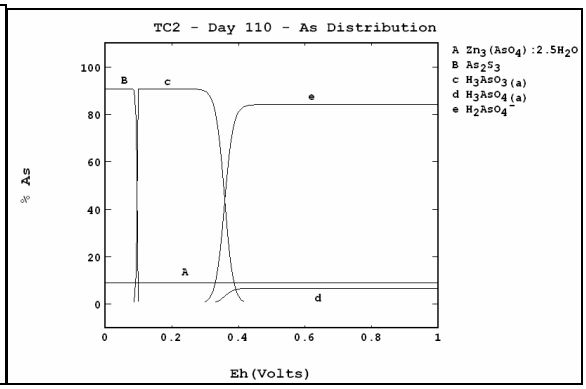

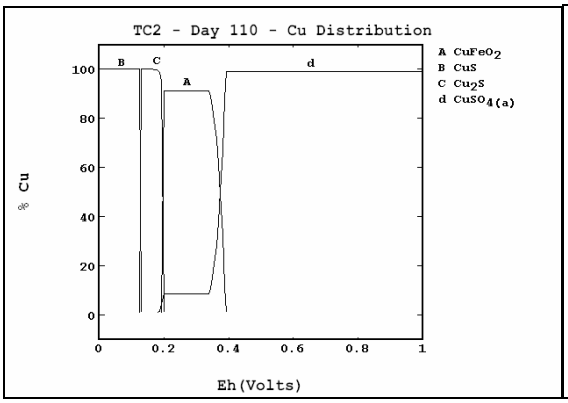

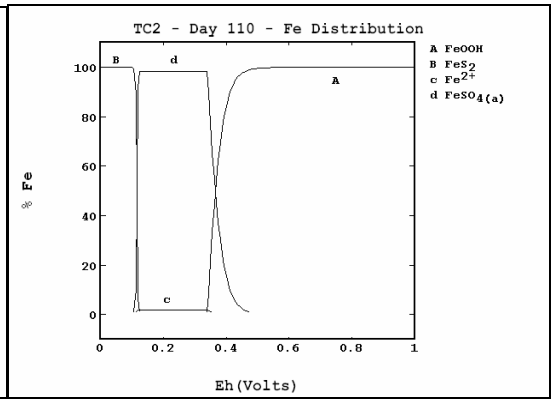

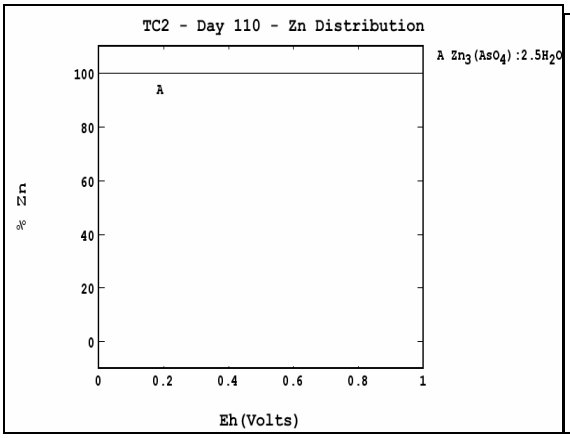

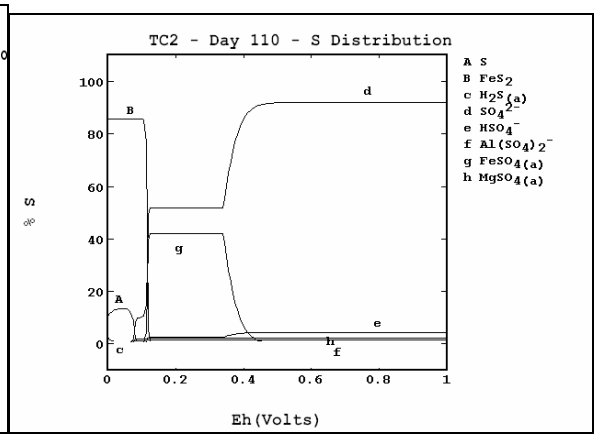

Distribution diagrams generated by STABCAL for conditions in Fox Lake Control Column at day 110. Diagrams show the solid and aqueous phases for major metals and sulfur with variation in Eh at pH 4.3. Measured Eh was +330 mV.

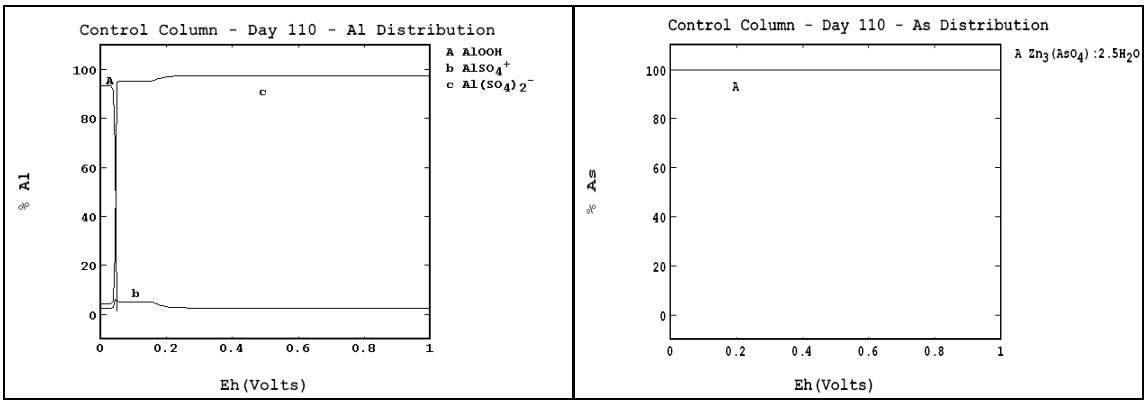

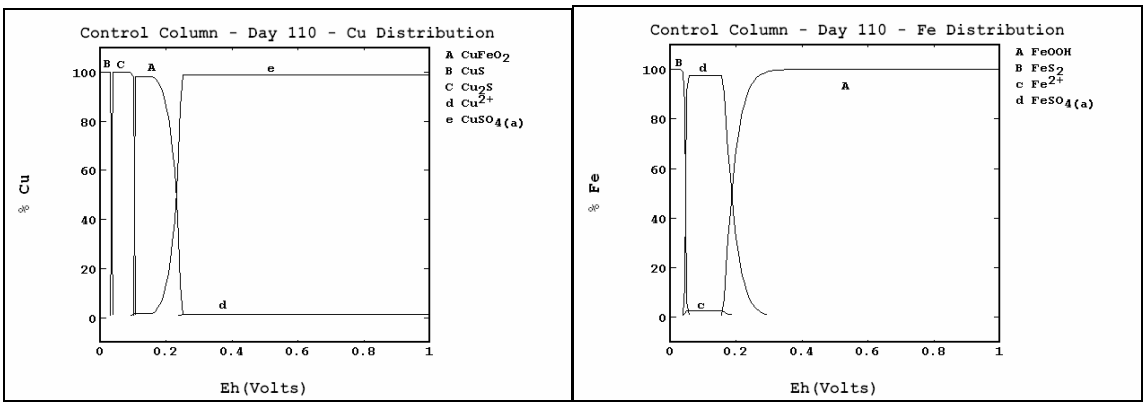

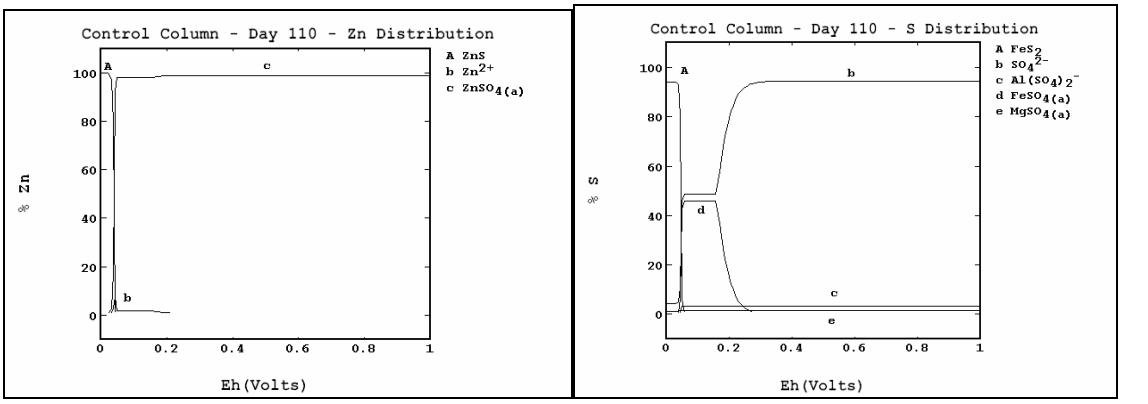

Distribution diagrams generated by STABCAL for conditions in Fox Lake column TC1 (day 222 of operation), pH 5.25, Eh +100 mV.

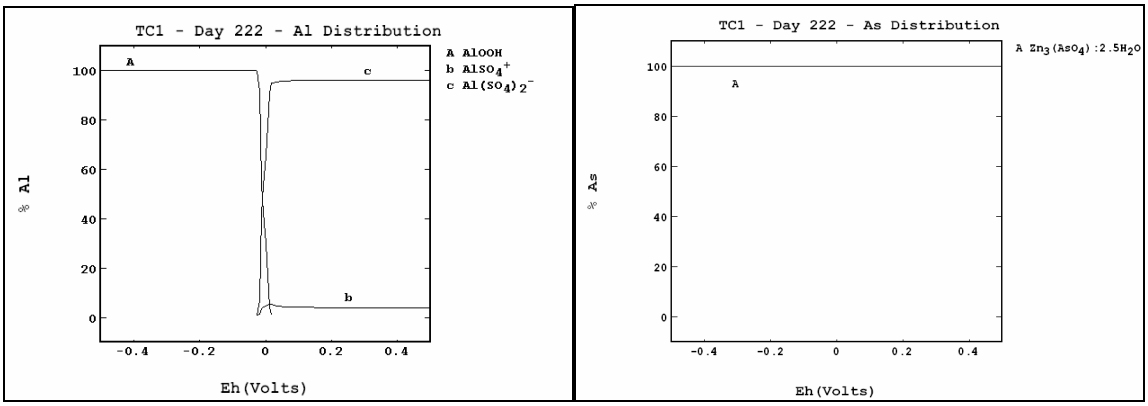

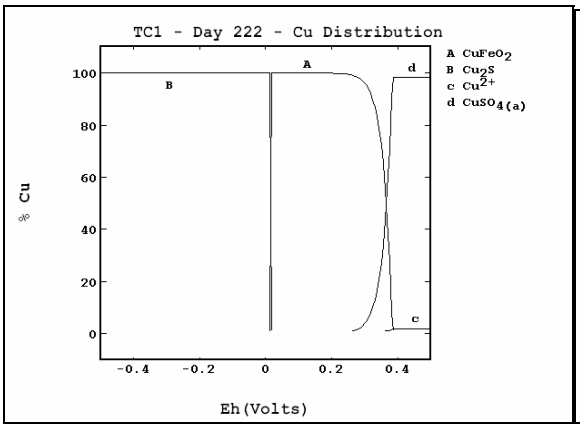

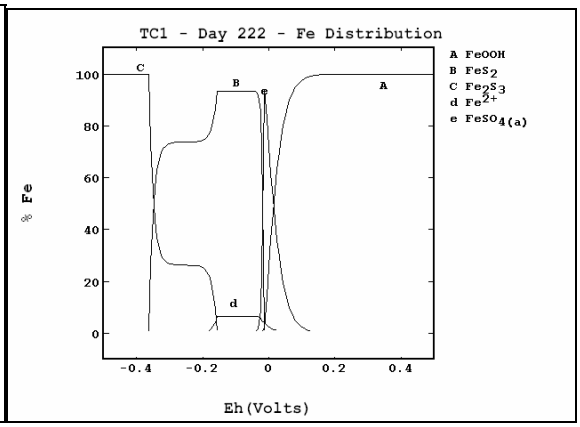

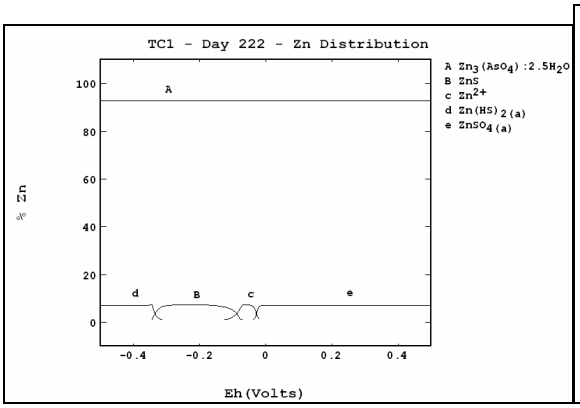

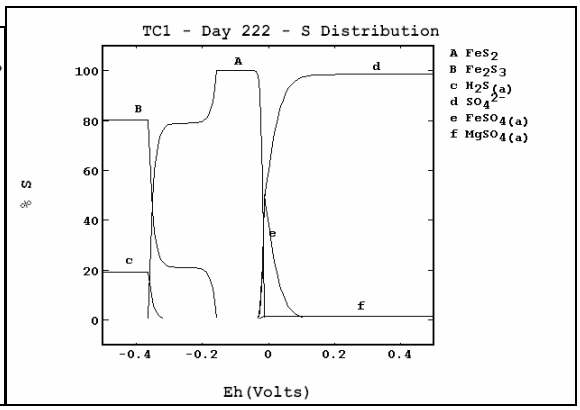

Distribution diagrams generated by STABCAL for conditions in Fox Lake column TC2 (day 222 of operation), pH 3.6, Eh +260 mV.

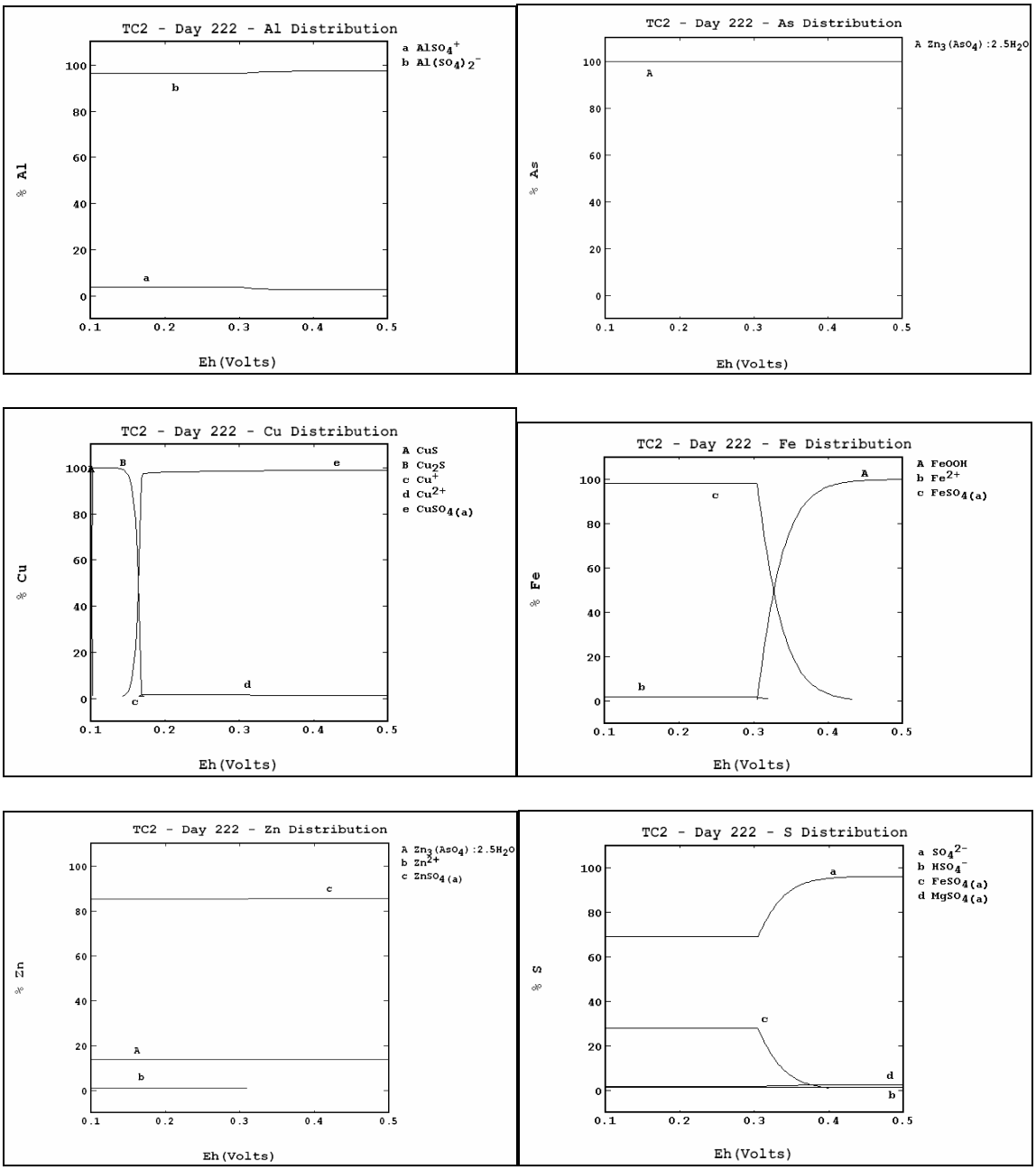

Distribution diagrams generated by STABCAL for conditions in Fox Lake control column (day 222 of operation), pH 4, Eh +320 mV.

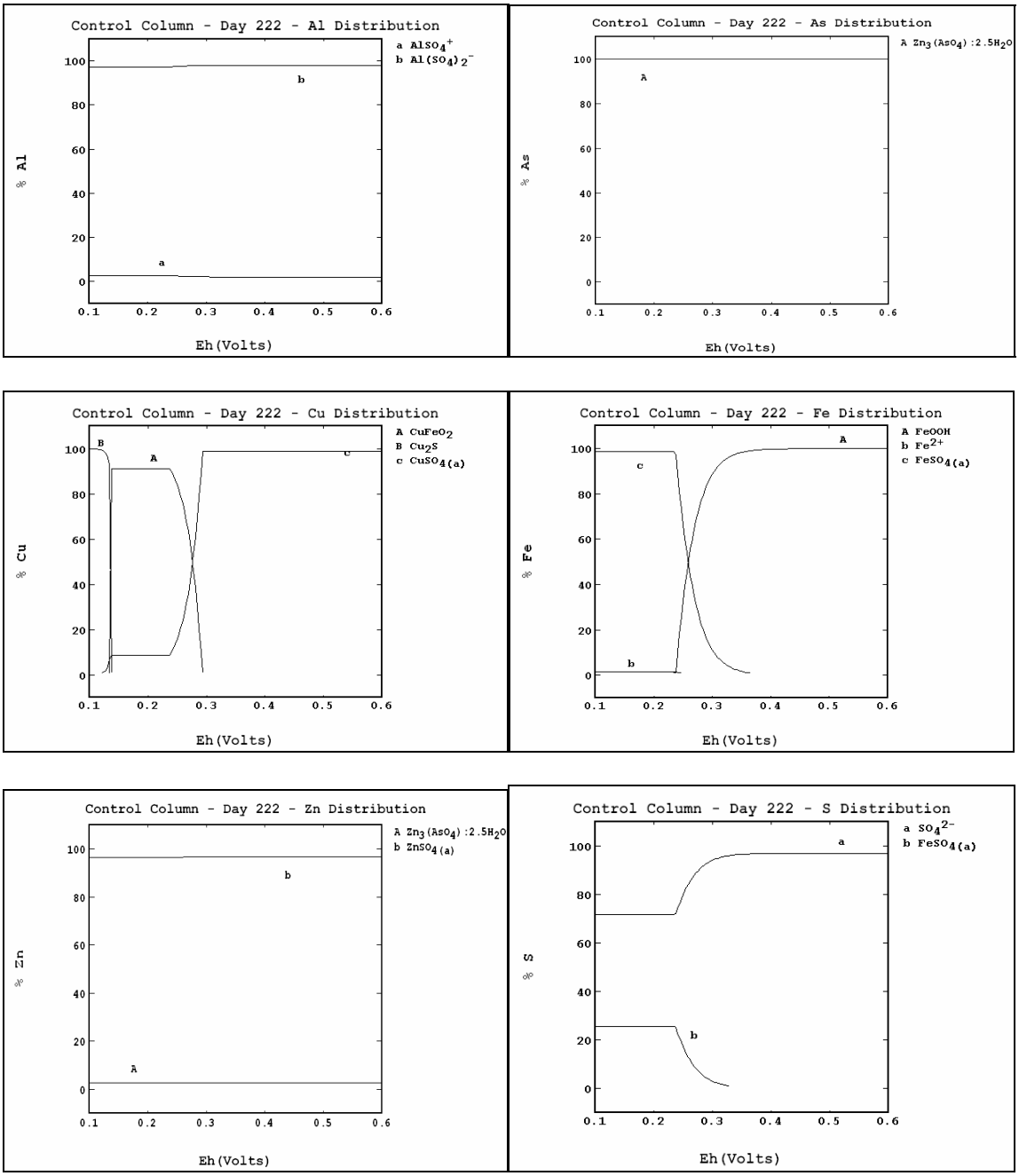

Distribution diagrams generated by STABCAL for conditions in Fox Lake column TC1 (day 824 of operation), pH 5.3, Eh = -50 mV.

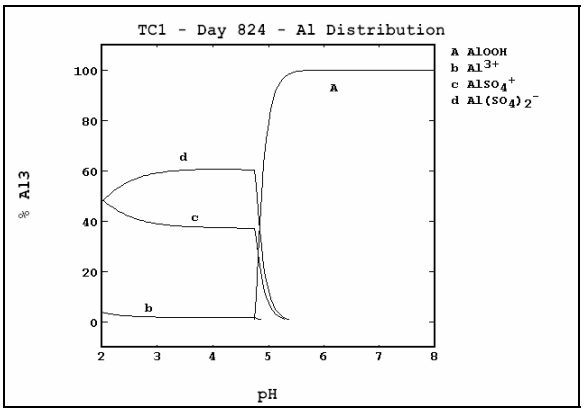

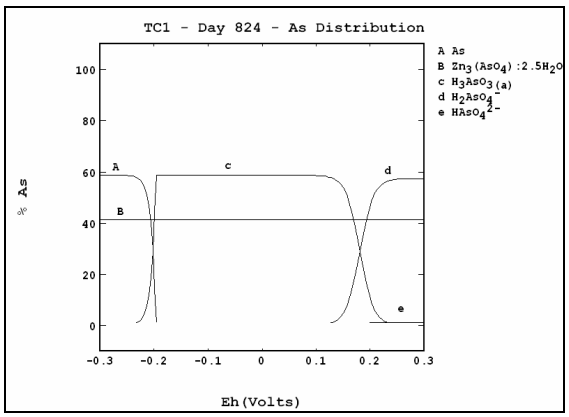

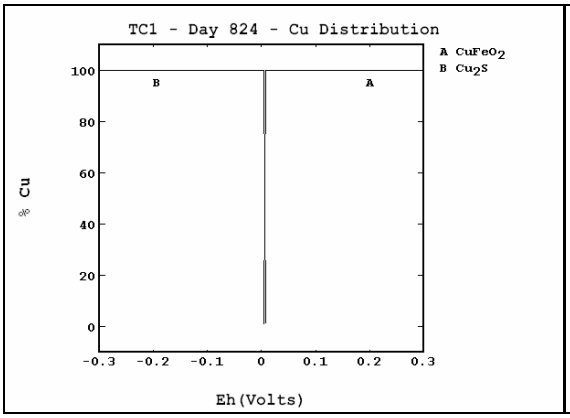

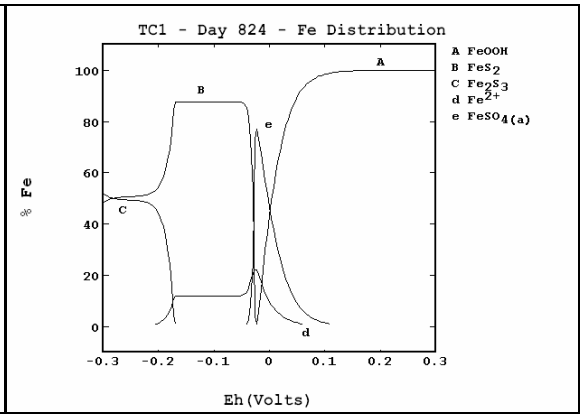

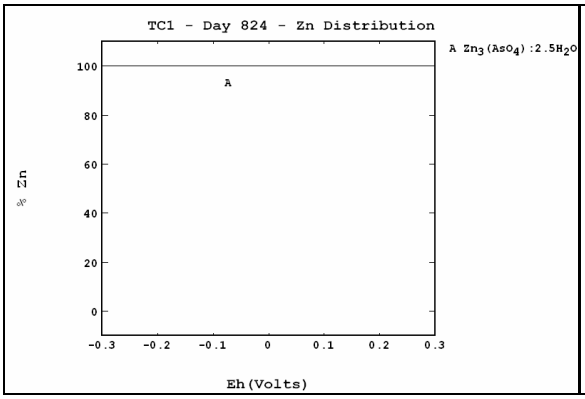

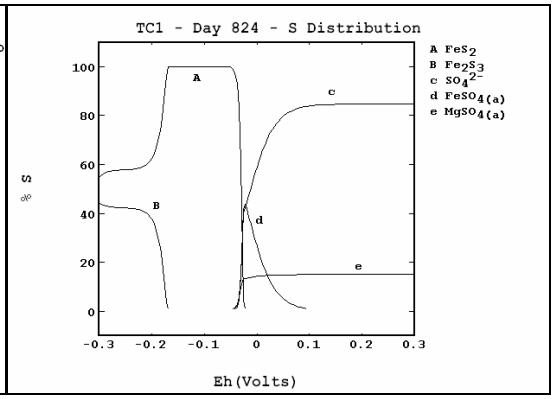

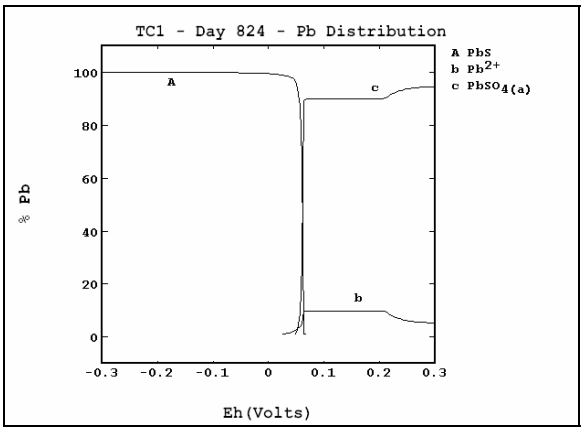

Distribution diagrams generated by STABCAL for conditions in Fox Lake column TC2 (day 824 of operation), pH 4.8, Eh = +100 mV.

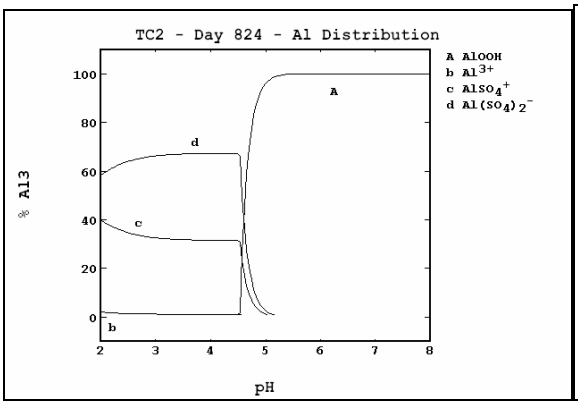

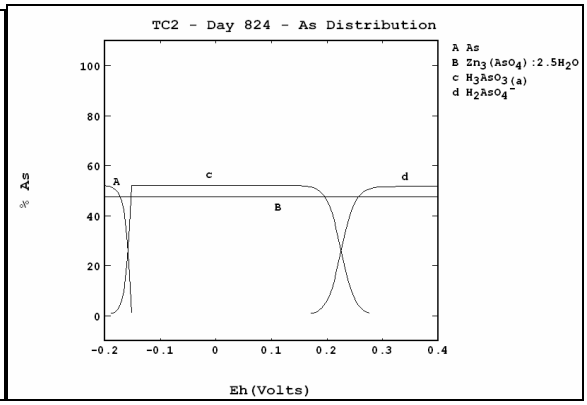

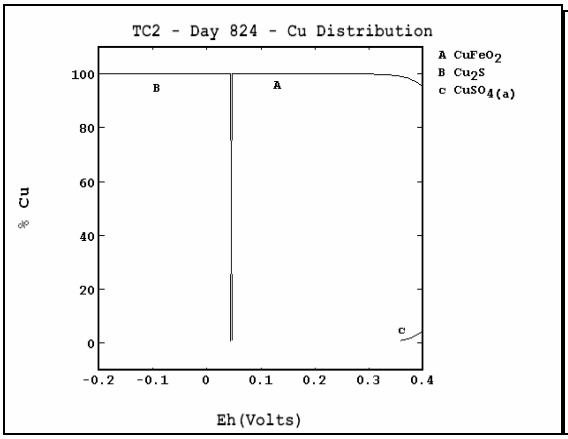

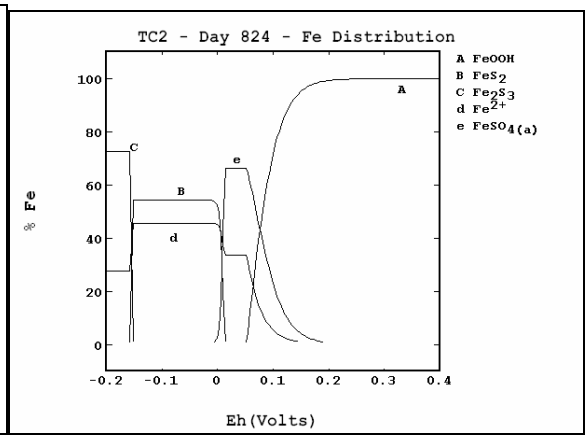

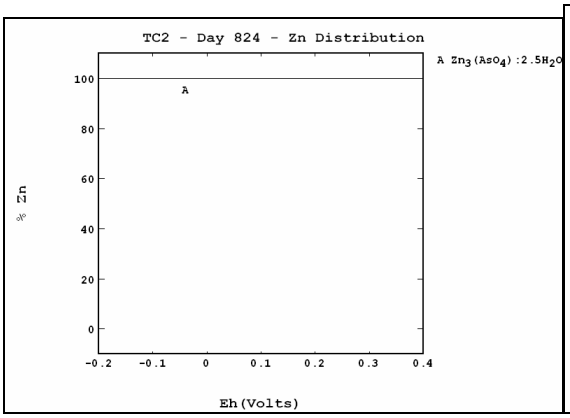

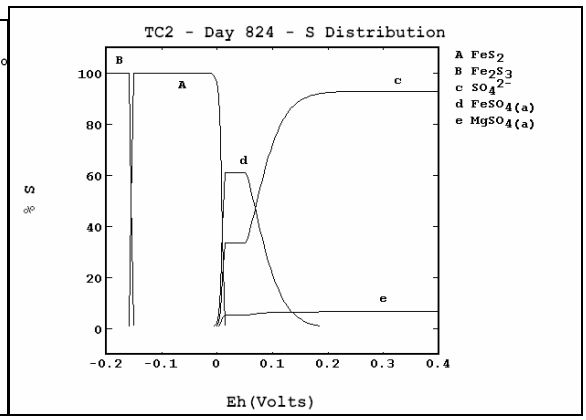

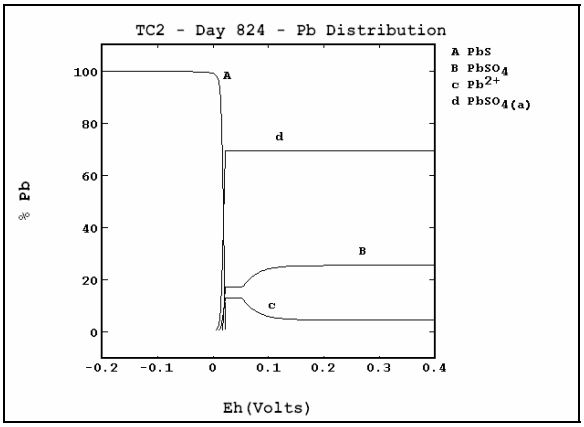

Distribution diagrams generated by STABCAL for conditions in Fox Lake control column (day 824 of operation), pH 2.6, Eh = +450 mV.

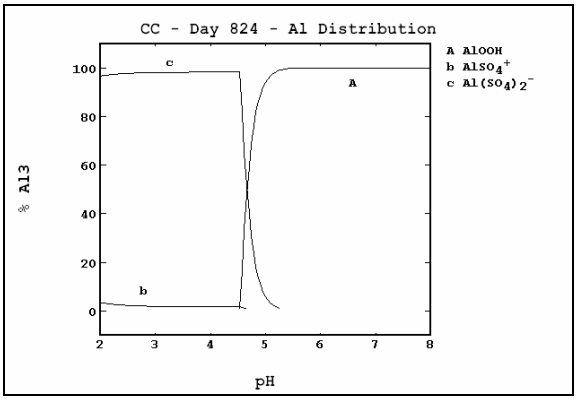

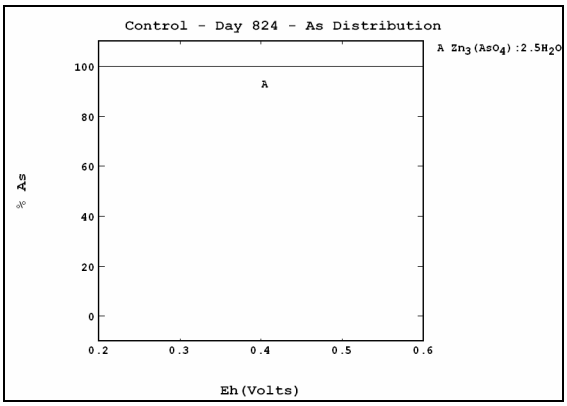

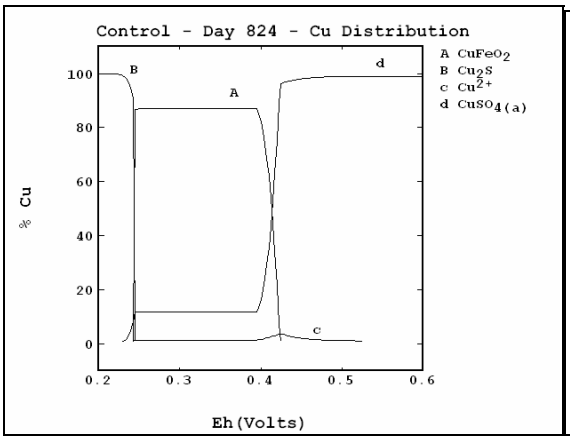
Control - Day 824 - Cu Distribution
A CuFeO2
B Cu2S
c Cu2+
d CuSO4(a)
% Cu
Eh(Volts)

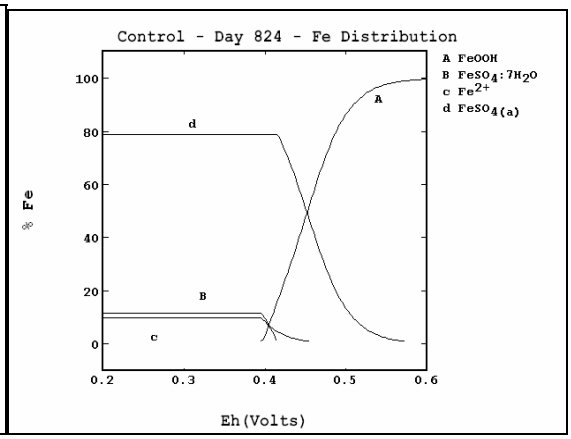
Control - Day 824 - Fe Distribution
A FeOOH
B FeSO4:7H2O
c Fe2+
d FeSO4(a)
% Fe
Eh(Volts)

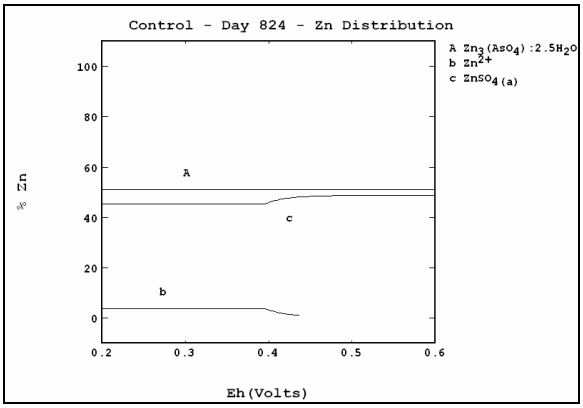
Control - Day 824 - Zn Distribution
A Zn3(AsO4):2.5H2O
b Zn2+
c ZnSO4(a)
% Zn
Eh(Volts)

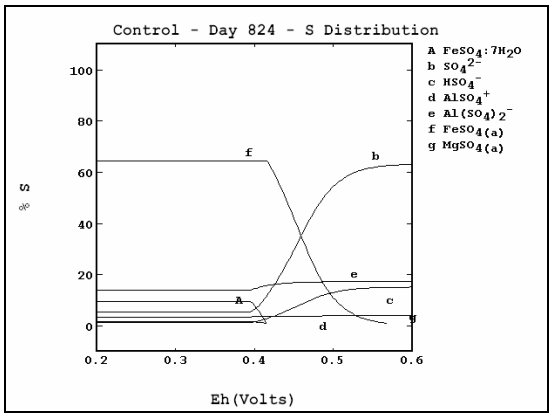
Control - Day 824 - S Distribution
A FeSO4:7H2O
b SO42-
c HSO4-
d AlSO4+
e Al(SO4)2-
f FeSO4(a)
g MgSO4(a)
% S
Eh(Volts)

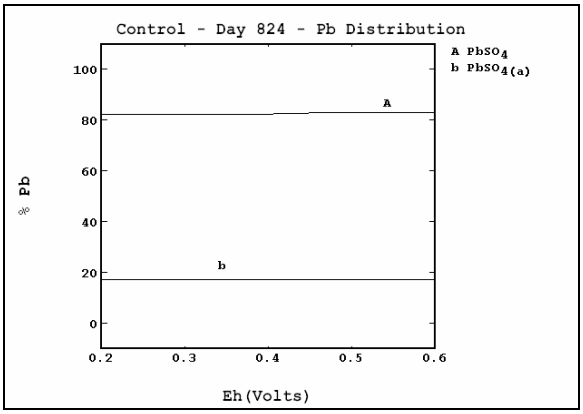
Control - Day 824 - Pb Distribution
A PbSO4
b PbSO4(a)
% Pb
Eh(Volts)

Distribution diagrams generated by STABCAL for post-treatment conditions in Fox Lake column TC1 (day 1056 of operation), pH 4, Eh = +100 mV.

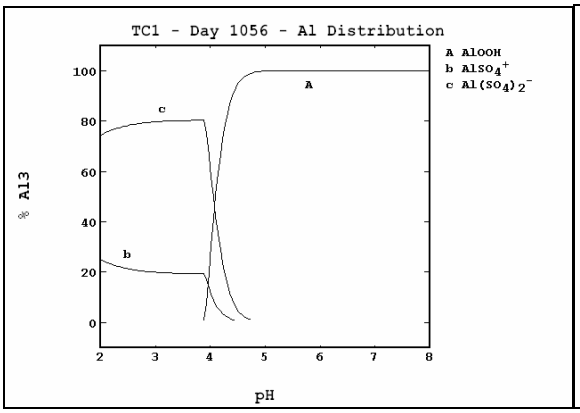

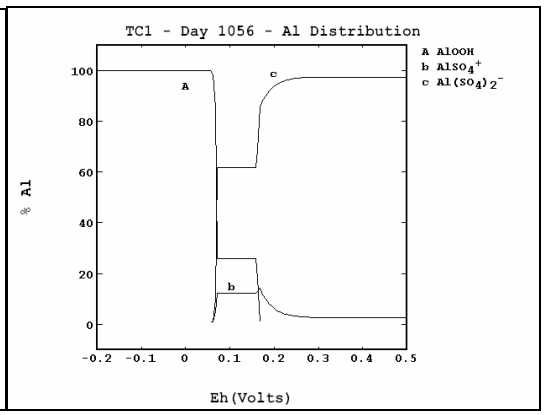

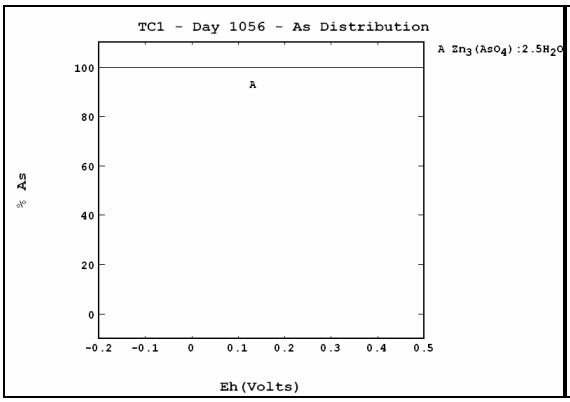

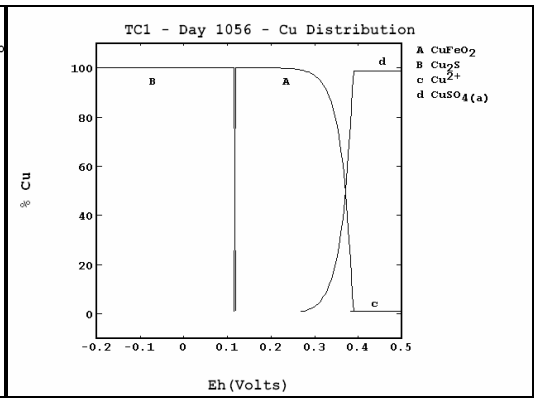

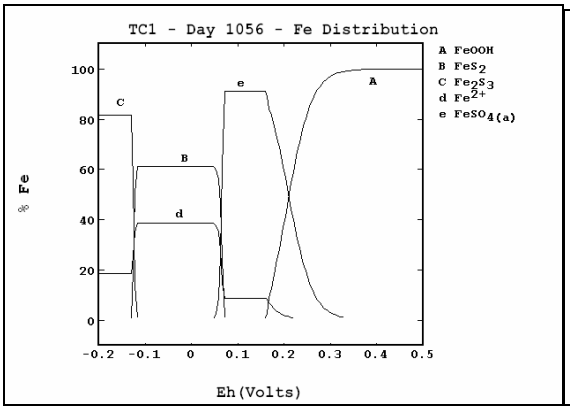

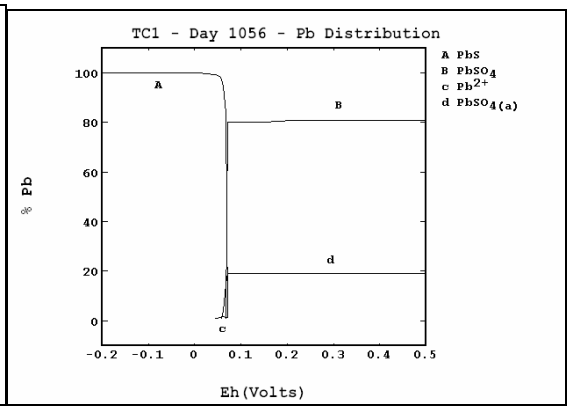

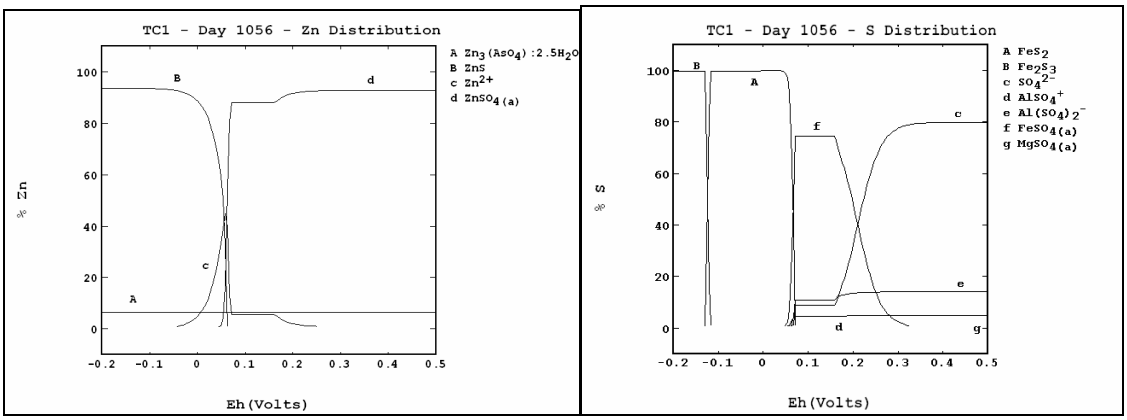

Distribution diagrams generated by STABCAL for post-treatment conditions in Fox Lake column TC2 (day 1056 of operation), pH 2.4, Eh= +500 mV.

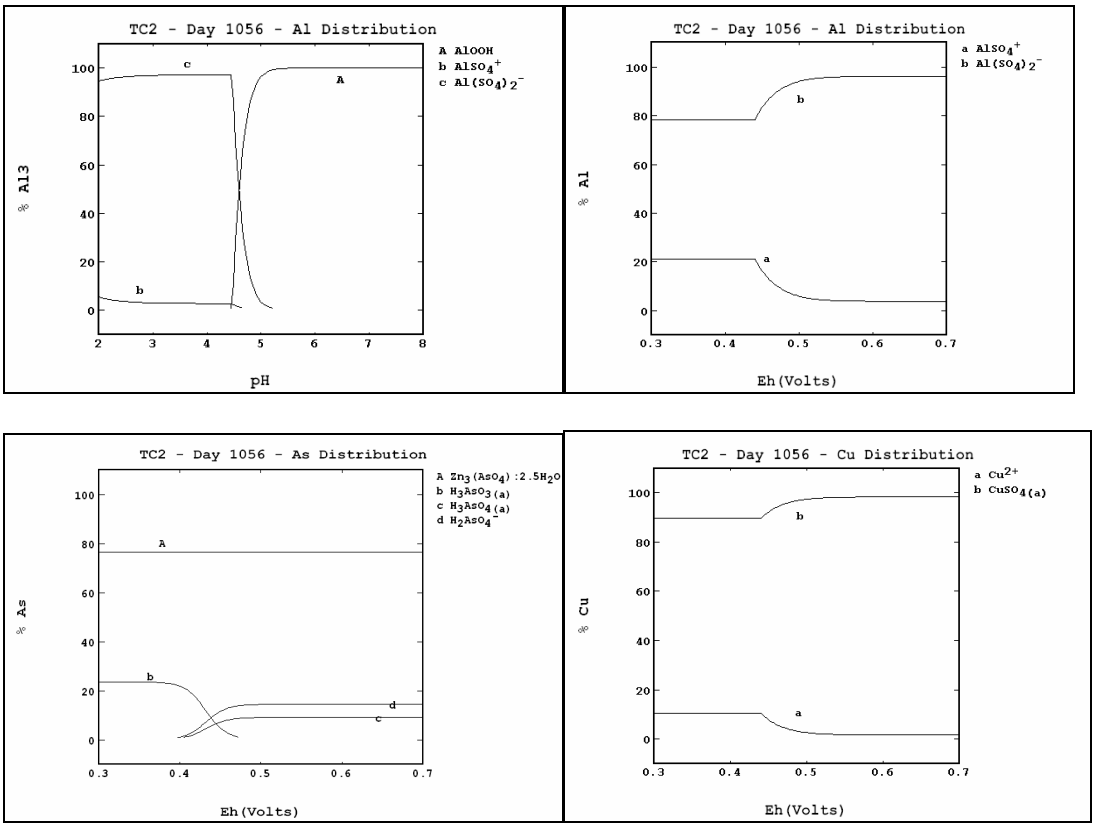

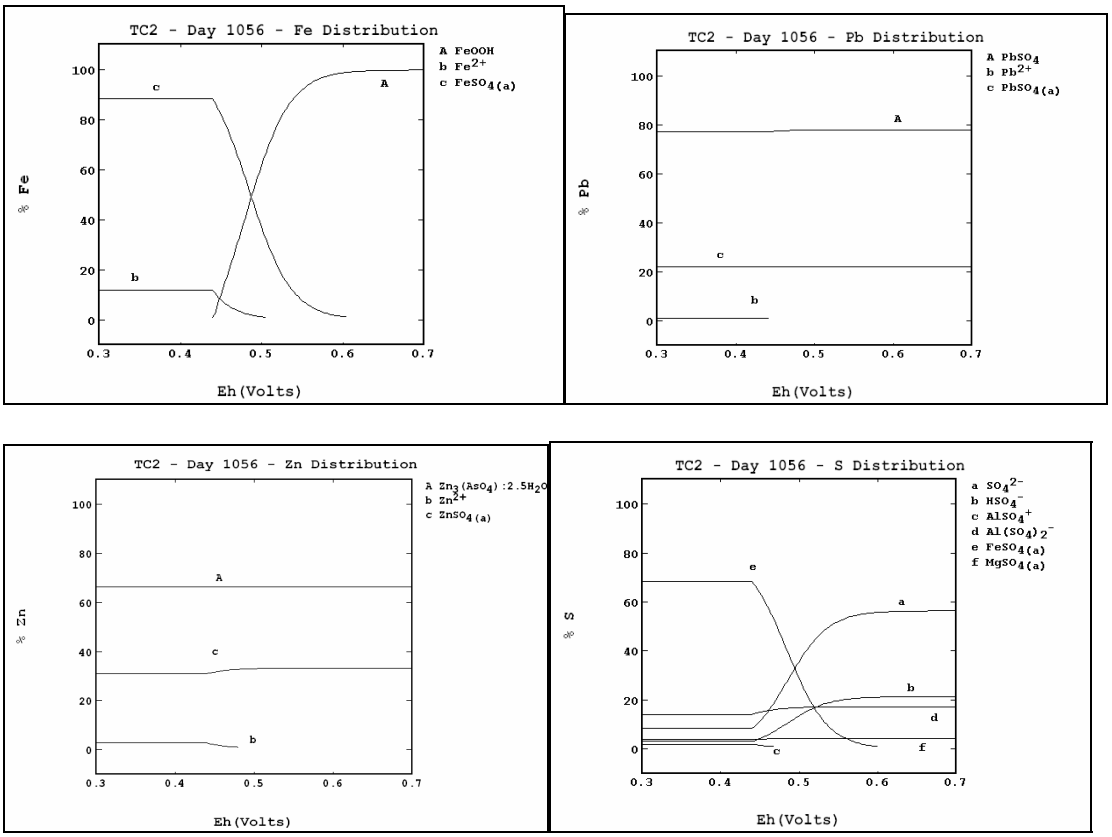

Distribution diagrams generated by STABCAL for post-treatment conditions in Fox Lake control column (day 1056 of operation), pH 2.4, Eh= +450 mV.

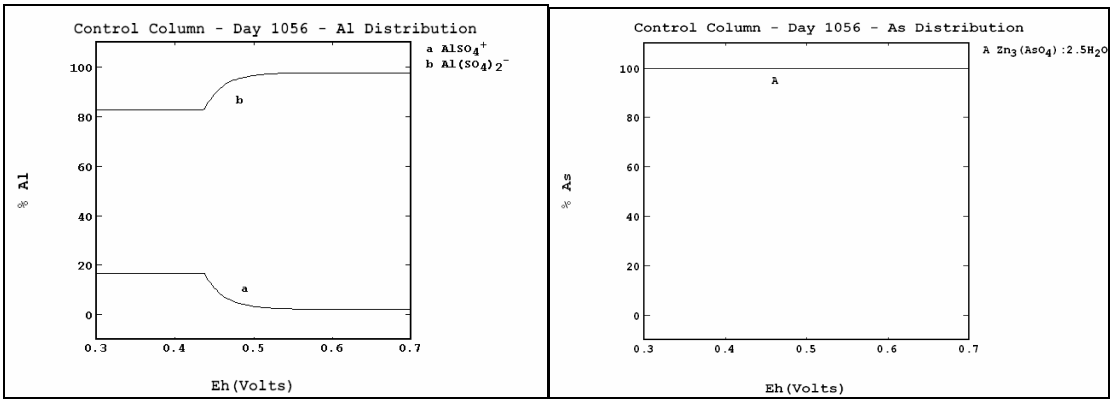

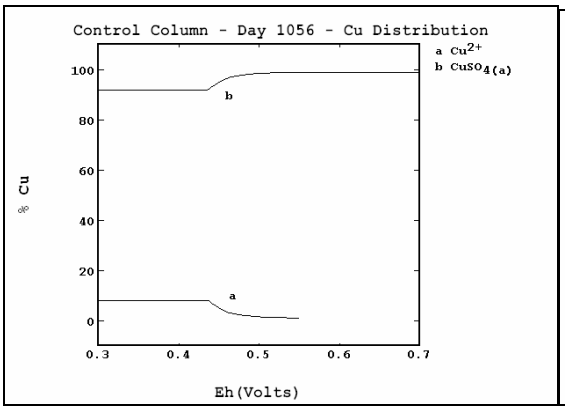
Control Column - Day 1056 - Cu Distribution
a Cu^{2+}
b $CuSO_4(a)$
% Cu
Eh(Volts)

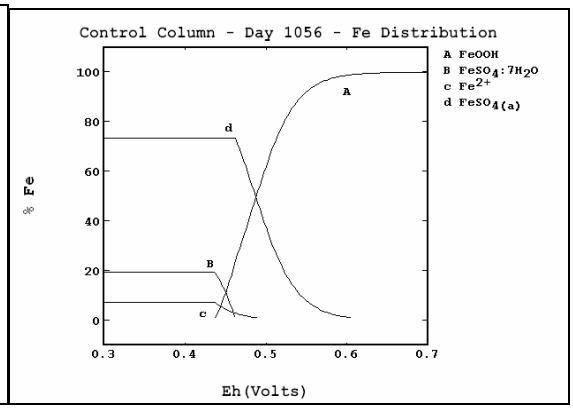
Control Column - Day 1056 - Fe Distribution
A FeOOH
B $FeSO_4:7H_2O$
c Fe^{2+}
d $FeSO_4(a)$
% Fe
Eh(Volts)

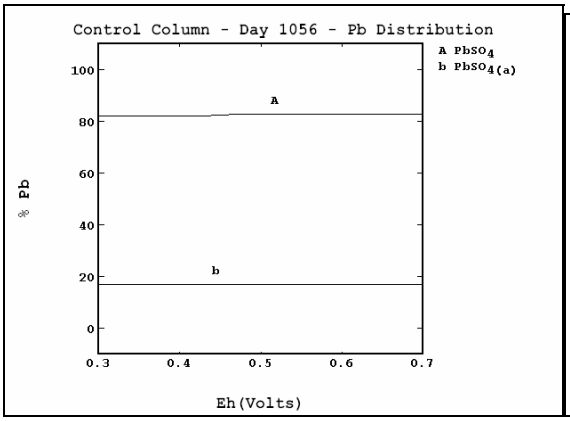
Control Column - Day 1056 - Pb Distribution
A $PbSO_4$
b $PbSO_4(a)$
% Pb
Eh(Volts)

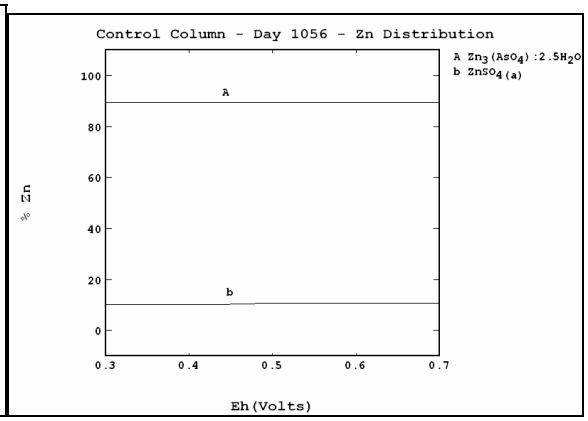
Control Column - Day 1056 - Zn Distribution
A $Zn_3(AsO_4):2.5H_2O$
b $ZnSO_4(a)$
% Zn
Eh(Volts)

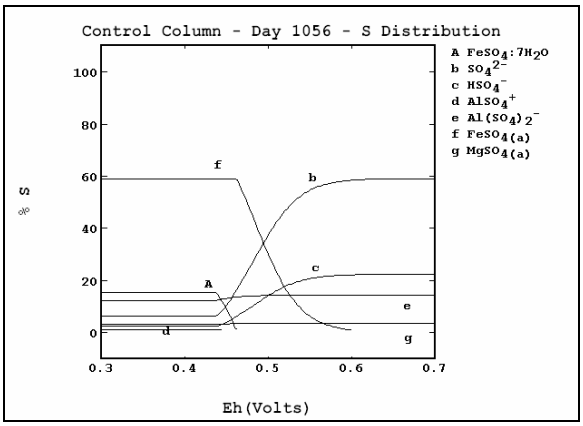
Control Column - Day 1056 - S Distribution
A $FeSO_4:7H_2O$
b SO_4^{2-}
c HSO_4^-
d $AlSO_4^+$
e $Al(SO_4)_2^-$
f $FeSO_4(a)$
g $MgSO_4(a)$
% S
Eh(Volts)

Distribution diagrams generated by STABCAL for pre-treatment conditions in Mammoth columns (day 56 of operation).

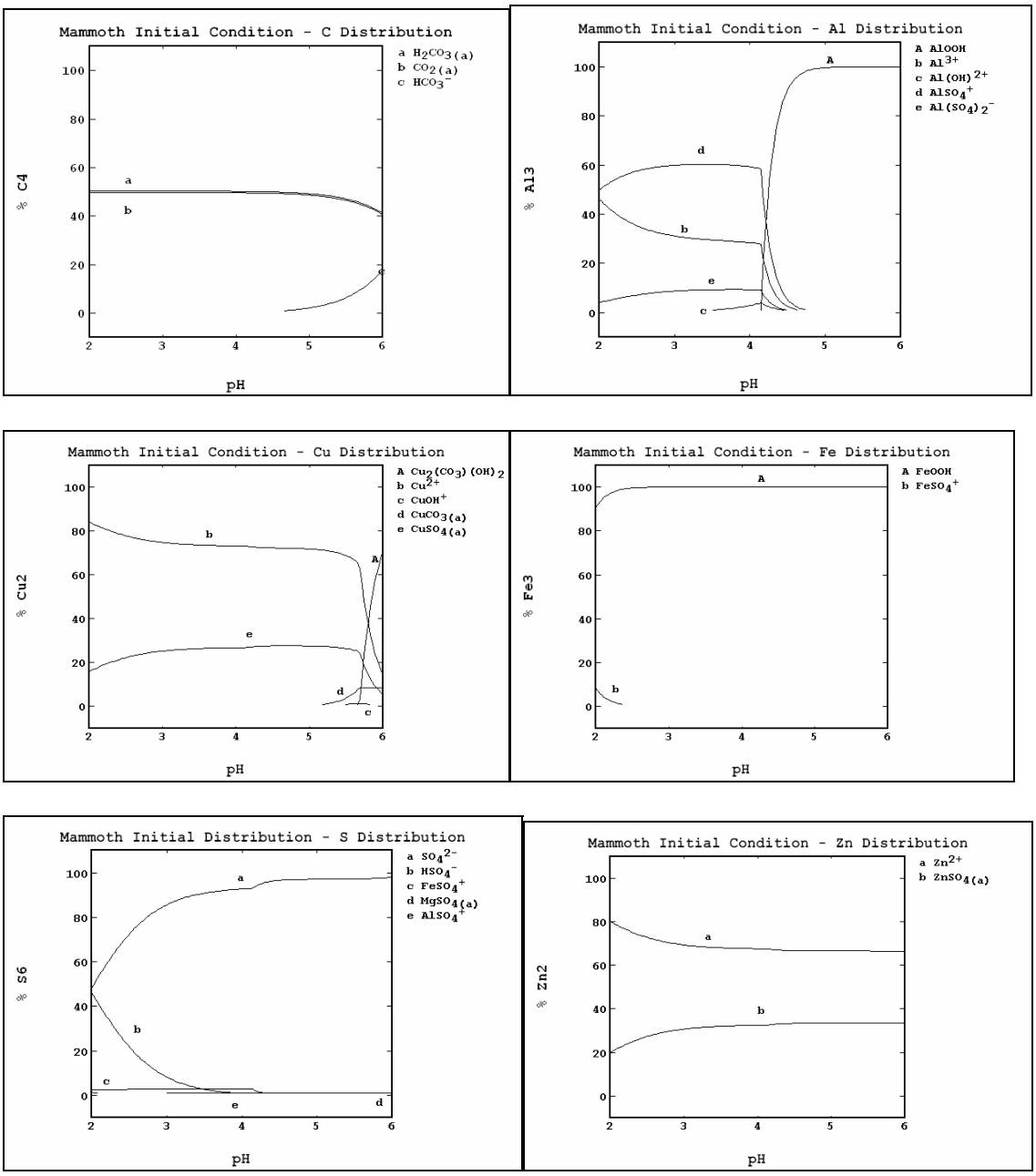

Distribution diagrams generated by STABCAL for post-treatment conditions in Mammoth column 1 (day 300 of operation).

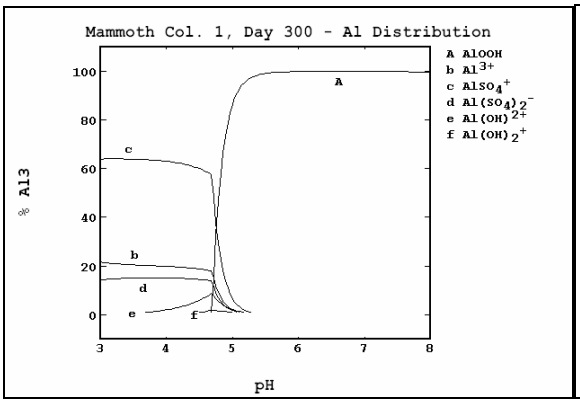

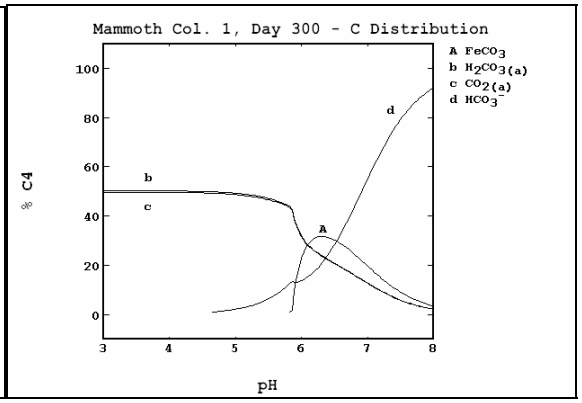

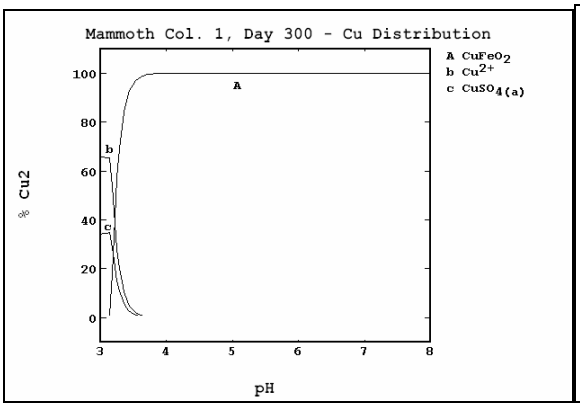

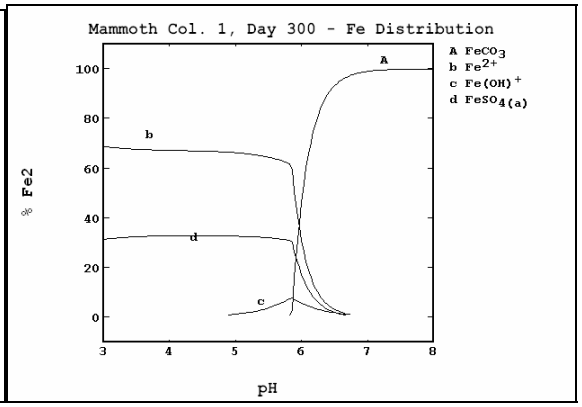

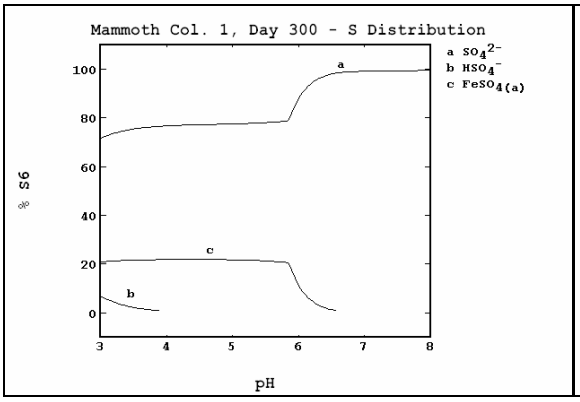

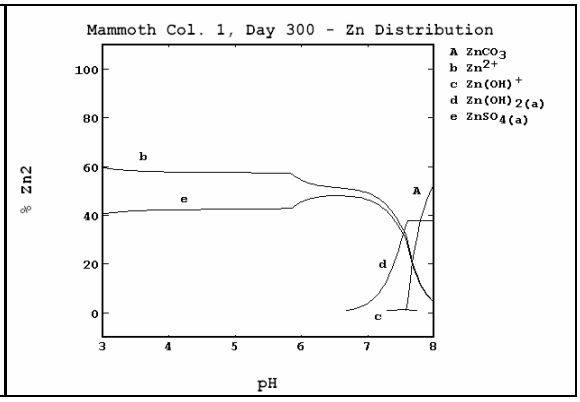

Distribution diagrams generated by STABCAL for conditions in Mammoth column 2 (day 300 of operation).